Enhanced Numerical Techniques for Time Domain Electromagnetic Analysis[†]

I. J. Craddock

October 1995

[†]A thesis submitted to the University of Bristol in accordance with the requirements for the degree of Doctor of Philosophy in the Faculty of Engineering, Department of Electrical and Electronic Engineering.

Abstract

With the ever increasing exploitation of the electromagnetic spectrum in a number of fields, including communications, comes an increasing need to understand electromagnetic phenomena. Modern electromagnetic analysis is numerical in nature and employs computers to solve Maxwell's equations of electromagnetism and, while numerical methods, such as the FDTD algorithm, are well established, there are always limitations to their application since computational resources are always finite. In order to reduce the computational demands of the algorithms, and hence widen their applicability, it is necessary to continually examine the nature of the methods and find ways in which they can be improved and enhanced. The aim of this thesis is therefore to derive and demonstrate new or enhanced time domain numerical methods for electromagnetic analysis. Various enhancements are considered, including the use of the near far transform to efficiently determine the far fields of a structure, the use of system identification to reduce the overheads associated with the time domain analysis of resonant structures and, most significantly, the inclusion of *a priori* knowledge of field behaviour in the algorithm. Each of these techniques is described and the accuracy of the results is evaluated by comparison against a suitable theoretical or measured set of data. In the case of including *a priori* knowledge of the field behaviour in the algorithm, detailed consideration is given in particular as to how this may have a detrimental effect on the stability of the method and how such an effect may be avoided. By examination of the properties of a new numerical method (the SFDTD technique) a better understanding of the stability issue is attained and a technique for guaranteeing the stability of the established FDTD method is produced. Finally, consideration of the relationship between the stability properties of the FDTD method and the principles of finite element analysis yields a new, interesting and extremely valuable understanding of the well known FDTD technique.

to
Bridget

Acknowledgements

I would like to express my gratitude to all the people who have made completion of this thesis possible. In particular I would like to thank Professor Joe McGeehan for the opportunity of undertaking a Ph.D. at Bristol and for his support and encouragement over the years.

I am also most grateful to my supervisor, Dr. Chris Railton, whose profound understanding of electromagnetics I have found to be matched by patience, approachability and enthusiasm.

I have very much enjoyed working as part of the Centre for Communications Research (CCR) and am indebted to all its members, past and present. I would especially like to acknowledge Nick Pothecary, Steve Meade, Paul Turner, Liz Daniel, Dave Shorthouse, Ted Ridgway Watt, Dominique Paul, Lizhaung Ma, Geoff Hilton, Wyc Slingsby and Nishan Canagarajah.

Outside the CCR a number of people have given their time to discuss aspects of this thesis, I would like to thank in particular Dick Clements and Gordon Reece (Department of Engineering Mathematics, Bristol), Andy Wathen, Yves Tourigny and Tony Humphries (Department of Mathematics, Bristol), John Schneider (Washington State University) and Kane Yee (Lockheed Palo Alto).

Financial support, for which I am extremely grateful, has been provided by EPSRC and DRA Malvern. At DRA Malvern Andy Hume, Mike Dean, Greg Ball and Paul Fletcher have been closely involved in my work and I have benefited greatly from their contributions.

Thanks to my family for their unfailing love and support and to my friends, particularly those – Chris, Nick, Steve and Paul – who have advised me on the content of this thesis and with whom I have shared the ups and downs of research work over the last 3 years.

Author's Declaration

Unless otherwise acknowledged, the content of this thesis is the original and sole work of the author. No portion of the work in this thesis has been submitted by the author in support of an application for any other degree or qualification, at this or any other university or institute of learning. The views expressed in this thesis are those of the author, and not necessarily those of the University of Bristol.

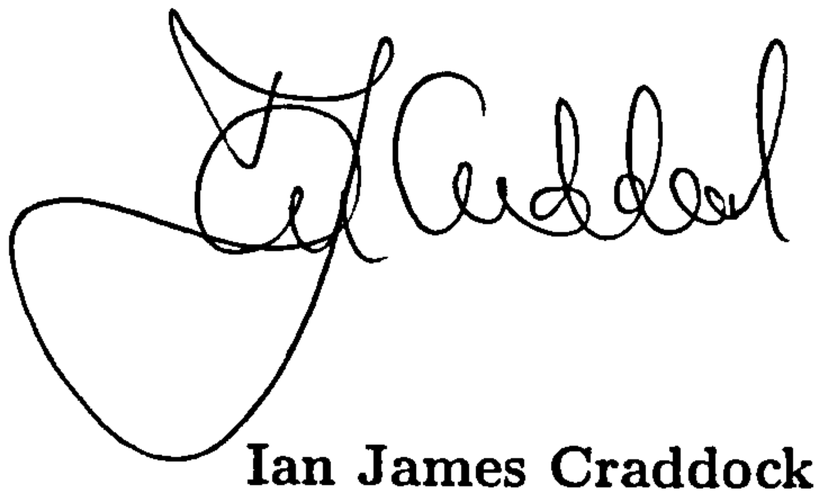

Ian James Craddock

Copyright

Contents

List of Figures

List of Tables

List of Symbols and Notation

Notation:

$\mathbf{a}$, $\mathbf{A}$	Any matrix (possibly a vector)
$\mathbf{A}^T$	Transpose of $\mathbf{A}$
$\mathbf{a} \cdot \mathbf{b}$	Dot (scalar) product between two vectors $\mathbf{a}$ and $\mathbf{b}$
$\mathbf{a} \times \mathbf{b}$	Cross (vector) product between two vectors $\mathbf{a}$ and $\mathbf{b}$
∂_a	Differentiation of function with respect to variable a
∇a	Gradient of scalar function a
$\nabla \cdot \mathbf{a}$	Divergence of vector function $\mathbf{a}$
$\nabla \times \mathbf{a}$	Curl of vector function $\mathbf{a}$
$< \cdot, \cdot >$	Inner product
$\Re\mathrm{e}$	Real part
$\Im\mathrm{m}$	Imaginary part
$\lvert \cdot \rvert$	Magnitude function
$\lVert \cdot \rVert$	Vector norm
$\lvert\lvert\lvert \cdot \rvert\rvert\rvert$	Matrix norm

Symbols

π	Pi
μ, ϵ	Permeability and permittivity
c	Speed of wave propagation
$\mathbf{i}$, $\mathbf{j}$, $\mathbf{k}$	Cartesian unit vectors
Δ	Space step
Δ_x, Δ_y, Δ_z	Space steps in x, y and z directions
Δ_t	Time step

List of Abbreviations

ABC	Absorbing Boundary Condition
CFD	Computational Fluid Dynamics
DSI	Discrete Surface Integral
FCT	Flux Corrected Transport
FDTD	Finite Difference Time Domain
MFV	Modified Finite Volume
PML	Perfectly Matched Layer
RBC	Radiating Boundary Condition
RLS	Recursive Least Squares
SDM	Spectral Domain Method
SFDTD	Second-order Finite Difference Time Domain
TLM	Transmission Line Matrix

List of Publications

Published/In Press

I. J. Craddock and C. J. Railton, "Derivation and application of a passive equivalent circuit for FDTD," *Microwave and Guided Wave Letters*, vol. 6, Jan. 1996. In press.

I. J. Craddock and C. J. Railton, "Analysis of curved and angled surfaces on a Cartesian mesh using a novel finite difference time domain algorithm," *IEEE Transactions on Microwave Theory and Technique*, vol. MTT-43, Oct. 1995. In press.

C. J. Railton and I. J. Craddock, "Analysis of general 3D PEC structures using an improved CPFDTD algorithm" *Electronics Letters*, vol. 31, pp. 1753–1754, Sept. 1995.

C. J. Railton, I. J. Craddock, and J. B. Schneider, "Improved locally distorted CPFDTD algorithm with provable stability," *Electronics Letters*, vol. 31, pp. 1585–1586, Aug. 1995.

I. J. Craddock and C. J. Railton, "A novel finite difference algorithm incorporating correction coefficients for curved structures," in *Proceedings of the 24$^{\text{th}}$ European Microwave Conference*, vol. 2, pp. 1536–1540, Sept. 1994.

I. J. Craddock, P. G. Turner, and C. J. Railton, "Reducing the computational overhead of the near field transform through system identification," *Electronics Letters*, vol. 30, pp. 1609–1610, Sept. 1994.

I. J. Craddock and C. J. Railton, "Application of the FDTD method and a full time domain near field transform to the problem of radiation from a PCB," *Electronics Letters*, vol. 23, pp. 2017–2018, Nov. 1993.

Submitted

C. J. Railton, I. J. Craddock, and J. B. Schneider, "The analysis of general 2D PEC structures using a modified CPFDTD algorithm," *IEEE Transactions on Microwave Theory and Technique.* Submitted.

C. J. Railton and I. J. Craddock, "A modified CPFDTD algorithm for the analysis of arbitrary 3D PEC structures," *IEEE Transactions on Microwave Theory and Technique.* Submitted.

Chapter 1

Introduction

1.1 Introduction

Historically, changes in technology have always transformed society and *vice-versa*. During the last few decades advances in telecommunications and computer technology (referred to collectively as information technology) have been widely seen as transforming developed economies around the world from industrial to so-called *information* societies [1–3]. While the future effects of this transformation on society as a whole are difficult to foresee [4, 5], it is certain that the production, storage and dissemination of information is, and will continue to be, of increasing importance to economic competitiveness [6, 7].

One of the key technologies in an information society is the means of information exchange. Various methods of exchange can be identified, however all means of modern communication rely on the modulation of electromagnetic waves – whether these waves are radio-, micro- or even light-waves and broadcast around the world through the atmosphere or transmitted along a cable from one fixed point to another.

An electromagnetic wave is an intangible phenomenon that propagates at extremely high speed through space. These waves are normally described in terms of their frequency (measured in cycles per second, or Hz) and form a continuous spectrum from less than 1 Hz to greater than 10^{24} Hz. Waves of similar frequencies have broadly similar properties in terms of how they propagate and how their presence is detected and, as a result, are usually grouped together into frequency bands. The most common subdivisions of the electromagnetic spectrum are identified in figure 1.1.

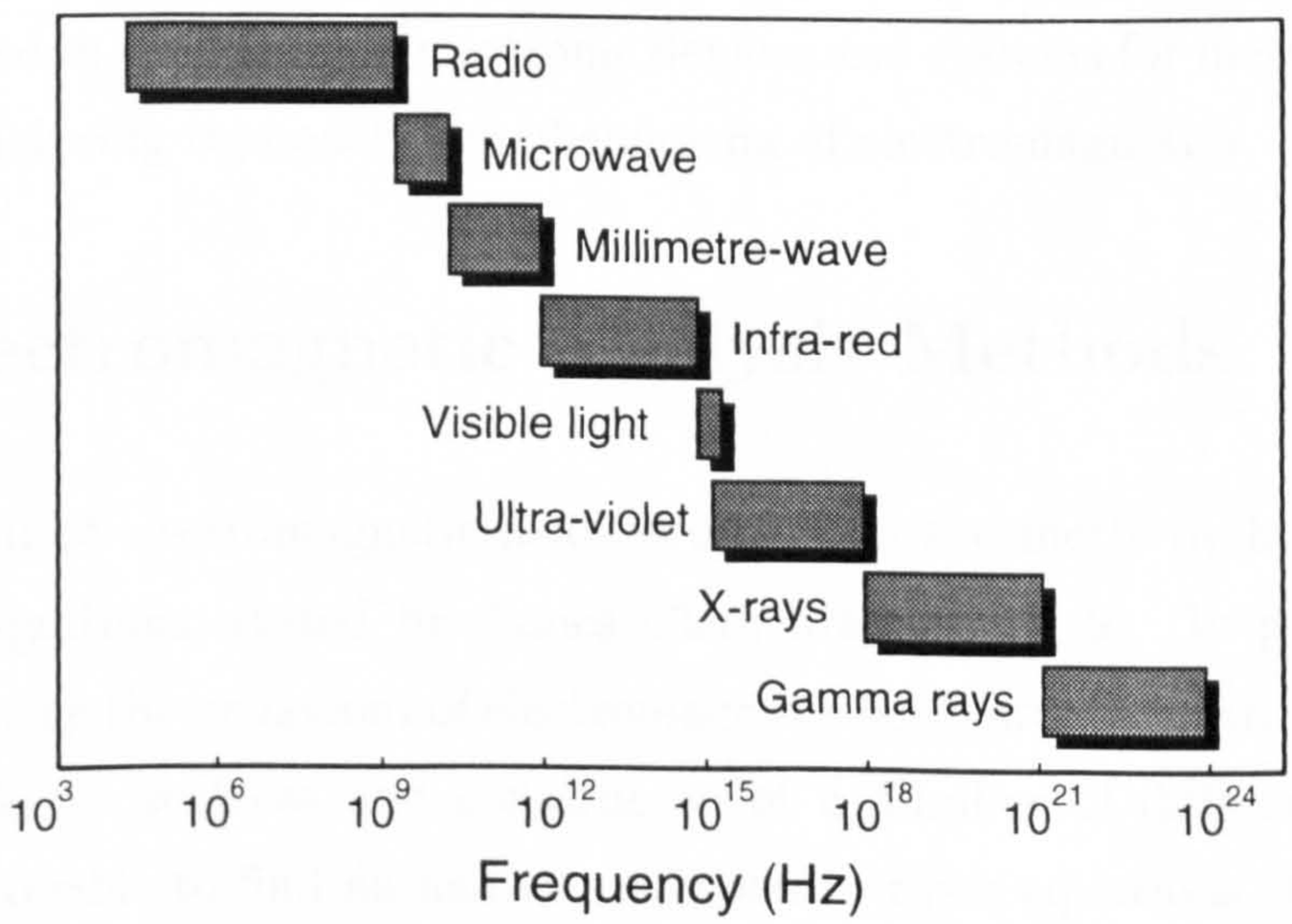

Figure 1.1: The electromagnetic spectrum

In general, knowledge of an electromagnetic wave is gained indirectly from its interaction with an intermediary object; the most obvious example of this phenomenon is the interaction of waves between about 4×10^{14} and 7.5×10^{14} Hz with pigment-containing cells in the human retina – waves in this frequency band are known as 'visible light'.

With the ever-increasing demand for voice and data transmission comes a demand for electromagnetic bandwidth; the lower frequency bands are already heavily used and are limited in the amount of spectrum they can provide. Historically therefore, communication systems have moved upwards in frequency to less used bands with more available bandwidth. There are also advantages, in terms of frequency re-usage, to be gained by operating cellular-type systems at frequencies in the microwave and millimetre wave regions where a line-of-sight path predominates for wave propagation.

So it is that while in 1912, at the Radiotelegraph Conference in London, frequencies above 3 MHz were considered useless [7, chapter 6], current cellular mobile telephone services operate in Europe at frequencies around 900 MHz and the latest generation of services (the DCS1800 system) operates at 1.8 GHz. There are many proposals to exploit even higher operating frequencies for systems such as Wireless Local Area Networks which are envisaged as operating at up to 60 GHz [8]. System design at such high frequencies creates considerable technical challenges.

While at low frequencies the complex theories of electromagnetics can be simplified to straightforward circuit theory, as operating frequencies move upwards into the microwave and millimetre-wave region and circuit dimensions shrink, there becomes a pressing need in the design of electronic devices and systems for methods of analysis capable of analysing rigorously the phenomena of electromagnetics.

1.2 Electromagnetic Analysis Methods

The behaviour of electromagnetic fields is described succinctly by Maxwell's partial differential equations, stated by James Clerk Maxwell in [9]. In general however, when considering the behaviour of electromagnetic fields around a structure consisting of many different surfaces and constructed of a number of different materials, it becomes impossible to find an analytic solution to these equations. In these cases a *numerical* algorithm of some sort is often employed; the algorithm itself is derived

from Maxwell's equations and provides an entirely numerical solution to the problem; the development of these numerical techniques is considered in the following sections.

1.2.1 A Brief History of Numerical Methods for Differential Equations

Many phenomena of engineering and science, including electromagnetics, are described in terms of partial differential equations. Some of these phenomena (such as steady state temperature distributions) are essentially equilibrium problems and are described by elliptic differential equations. Many others are propagation phenomena (such as the transient propagation of heat through a medium) and give rise to either parabolic or hyperbolic differential equations (Maxwell's equations being of the latter type) [10, chapter 1].

Using numerical methods, such as finite difference techniques, to solve differential equations is a well established idea whose origin can be traced back to Euler [11]. It was not until the turn of the twentieth century however that serious attempts were made to apply the methods to solving problems of realistic complexity. Runge [12] in 1908 was probably the first to compute a finite difference solution to a two-dimensional system, followed closely by Richardson [13] in 1910.

An interesting example of the problems associated with the numerical solution of differential equations is provided by the work of the remarkable Quaker scientist Lewis Fry Richardson (1881–1953) [14]. One of Richardson's many and varied interests was meteorology and, while stationed in France during the First World War as a volunteer member of the Friends' Ambulance Unit, he performed the first numerical weather 'forecast'.

Richardson derived a finite difference method for the solution of the differential equations of atmospheric motion and with only a slide rule he performed the reams of calculations required for a six hour forecast in his rest periods over an interval of six weeks. During the Battle of Champagne the results were sent to the rear where they were lost for several months before, fortunately for Richardson, being rediscovered under a coal heap – eventually being published in 1922 [15].

Richardson's valiant attempt, described by a contemporary reviewer as an 'enterprise ... of almost quixotic boldness' [16], was doomed to failure through inaccurate initial

data. His estimate that 64,000 human 'computers' would be required to predict the weather, using his method, *as fast as the weather itself evolved* resulted in numerical methods in meteorlogy being shunned for the next thirty years. A second reason for Richardson's failure was that his algorithm was numerically unstable [17] – as will be demonstrated by chapters 4, 5 and 6 of this thesis, instability remains a problem with numerical algorithms today.

Happily however, Richardson lived long enough to correspond with researchers who, in 1949, employed a numerical model similar to Richardson's own on ENIAC – now widely considered the world's first true digital computer [18]. These experiments with ENIAC, which was capable of performing around 5000 additions per second, began the modern era of numerically based methods of weather prediction and indeed opened the door to the application of numerical methods in many other fields.

Digital computers have now made numerical techniques practical methods for solving the partial differential equations arising in areas of science and engineering as diverse as meteorology [17], structural mechanics [19] and electromagnetics [20].

1.2.2 Numerical Modelling Methods in Electromagnetics

During the 1950's and early 1960's, computers were expensive and not widely available; their application in electromagnetics during this period was, as a result, somewhat limited [21, 22].

In the mid 1960's however Kane Yee was working at the Lawrence Livermore National Laboratory, studying finite difference methods for the analysis of water waves [23]. In the process of learning to use the computer at the laboratory he sought a simple example to program and, having had some previous experience of electromagnetics, attempted a finite difference solution of Maxwell's equations.

After a short period of trial and error Yee arrived at an algorithm which employed a staggered spatial discretisation to achieve centered differencing of all the field derivatives (described in section 2.6.2). Yee published this method (initially applied only in two spatial dimensions due to the limited computational facilities of the time) in [24] and returned to the study of water waves.

The Yee method received little attention, due to its relatively large computational requirements, until the mid 1970's, when the first application of the full three-

dimensional method was presented [25]. As computers increased in capability and decreased in price the Yee algorithm became more popular as workers in the area became attracted by its generality, elegant simplicity and ease of implementation; it is now widely refered to as *the* Finite Difference Time Domain or 'FDTD' method.

1.3 Applications of the Yee Algorithm

An indication of the rising interest in the Yee FDTD method is given by table 1.1 which shows, for each year, the number of journal papers in the BIDS ISI[1] database which include the phrase 'Finite Difference Time Domain' (and derivatives) in their title.

Year	Number of Papers
1984	1
1985	1
1986	4
1987	7
1988	10
1989	11
1990	21
1991	31
1992	51
1993	60
1994	116
Total	313

Table 1.1: Number of papers on the Yee method

At the University of Bristol's Centre for Communications Research, a Computational Electromagnetics group has been lead since 1986 by Dr. Chris Railton. Since the beginning of that time development of the FDTD algorithm has taken a high priority and has encompassed many of the major areas of FDTD research:

- Incorporation of numerical boundary conditions [26].
- Analysis of dispersive waveguides. [27].

[1]Bath Information and Data Services; index supplied by Institute for Scientific Information.

- Analysis of antenna structures [28].
- Use of FDTD models for medical imaging [29].
- Combined thermal and electromagnetic models for microwave heating [30].
- Inclusion of *a priori* knowledge of field behaviour in FDTD [31].

The author's main area of study has been into the inclusion of *a priori* knowledge into the FDTD algorithm and is described by chapters 4, 5 and 6. In addition research has been undertaken into near field transformation methods and characterisation of resonant devices (see chapter 3).

1.4 Summary and Thesis Overview

In this chapter it has been shown that in the field of communications technology, electromagnetic phenomena have a fundamental rôle. The solution of the partial differential equations which describe these phenomena is therefore important in the design of communications systems and is anticipated to become increasingly so in the future as these systems move ever higher in operating frequency.

The solution of partial differential equations is commonly achieved by a numerical method. Use of these techniques entails thousands (millions or even billions) of calculations and, while pioneers in the area produced solutions by hand, it was not until the advent of the digital computer that numerical methods became practical and useful techniques in many areas of science and engineering.

In the next chapter some of the numerical methods commonly used in electromagnetic analysis are introduced with particular attention being given to those methods which operate in the time domain. The chapter concludes by considering in more detail the properties of the FDTD algorithm [24] introduced earlier in this chapter.

The FDTD method has many attractive features which have resulted in its current high level of popularity; the computational demands of the method are however considerable, particularly when the domain to be analysed is electrically large and when the spatial resolution required is high. Chapters 3, 4, 5 and 6 discuss methods for avoiding or ameliorating these drawbacks.

Section 1.4 : Summary and Thesis Overview

Chapter 3 presents a near field transformation which may be used to characterise the fields at electrically large distances from a structure without utilising a correspondingly large computational volume. Additionally in this chapter a technique for reducing the overheads entailed in the time domain analysis of resonant devices is considered.

In chapter 4 methods for reducing the required spatial resolution of the FDTD method are discussed; the advantages and disadvantages of one particular technique – the 'correction factor' method – are considered in some detail.

Chapters 5 and 6 consider a number of correction factor schemes and present new results pertaining to the use of these and related formulations in FDTD and other difference algorithms. Chapter 6 concludes by presenting a new formulation of the popular FDTD method and considers the implications of this for the future development and extension of FDTD.

This thesis concludes with chapter 7 which reiterates some of the major findings of previous chapters and suggests potentially rewarding directions for future investigation.

References

[1] R. Finnegan, G. Salaman, and K. Thompson, *Information Technology: Social Issues.* Hodder and Stoughton, 1987.

[2] D. Bell, *The Coming of Postindustrial Society.* Penguin, 1974.

[3] A. Toffler, *The Third Wave.* Pan, 1980.

[4] D. Lyon, *The Information Society - Issues and Illusions.* Polity Press, 1988.

[5] Group of Experts on Social Aspects of New Technologies, *New Technologies in the 1990's: A Socio-Economic Strategy.* OECD, 1988.

[6] P. Jowett and M. Rothwell, *The Economics of Information Technology.* Macmillan Press, 1986.

[7] M. Paetsch, *Mobile Communications in the US and Europe: Regulation, Technology and Markets.* Artech House, 1993.

[8] A. Santamaria and F. Lopez-Hernandez, *Wireless LAN Systems.* Artech House, 1994.

[9] J. C. Maxwell, *A Treatise on Electricity and Magnetism.* Dover Publications, 3 ed., 1954. Work originally published in 1873.

[10] W. F. Ames, *Numerical Methods for Partial Differential Equations.* Thomas Nelson and Sons, 1969.

[11] L. Euler, *Institutiones Calculi Integralis.* St. Petersberg, 1768.

[12] C. Runge *Zeitschrift fur Mathematik und Physik*, vol. 56, p. 225, 1908.

[13] L. F. Richardson, "The approximate arithmetical solution by finite differences of physical problems involving differential equations, with an application to the stresses in masonry dams," *Philosophical Transactions*, vol. A210, pp. 307–357, 1910.

[14] O. M. Ashford, *Prophet - or Professor? The Life and Work of Lewis Fry Richardson.* Adam Hilger Ltd, Bristol, 1985.

[15] L. F. Richardson, *Weather Prediction by Numerical Process.* Cambridge University Press, 1922. Re-printed in 1965 by Dover Publications.

[16] S. Chapman, "Review: Weather Prediction by Numerical Process," *Quarterly Journal of the Royal Meteorological Society*, vol. 40, pp. 285–286, 1922.

[17] S. L. Hess, *Theoretical Meteorology.* Holt Rinehart and Winston, 1959.

[18] J. G. Charney and A. Eliasson, "A numerical method for predicting the perturbations of the middle latitude westerlies," *Tellus*, vol. 1, no. 2, pp. 38–54, 1949.

[19] I. Holand and K. Bell, *Finite Element Methods in Stress Analysis.* TAPIR, 1969.

[20] M. A. Morgan, *Progress in Electromagnetics Research: Finite Element and Finite Difference Methods in Electromagnetic Scattering.* Elsevier, 1990.

[21] E. M. Kennaugh, *Multipole Field Expansions and their use in Approximate Solution of Electromagnetic Scattering Problems.* PhD thesis, Dept. of Electrical Engineering, Ohio State University, 1959.

[22] R. J. Garbacz, "Electromagnetic scattering from radially inhomogenous spheres," *Proceedings of the IEEE/IRE*, p. 1837, Aug. 1962.

[23] K. S. Yee, May 1995. Private Communication.

[24] K. S. Yee, "Numerical solution of initial boundary value problems involving Maxwell's equations in isotropic media," *IEEE Transactions on Antennas and Propagation*, vol. AP-14, pp. 302–307, May 1966.

[25] A. Taflove and M. E. Brodwin, "Numerical solution of electromagnetic scattering problems using the time-dependent Maxwell's equations," *IEEE Transactions on Microwave Theory and Techniques*, vol. MTT-23, pp. 623–630, Aug. 1975.

[26] C. J. Railton, E. M. Daniel, D. L. Paul, and J. P. McGeehan, "Optimised absorbing boundary conditions for the analysis of planar circuits using the finite difference time domain method," *IEEE Transactions on Microwave Theory and Techniques*, vol. MTT-40, pp. 290–297, Feb. 1993.

[27] D. L. Paul, N. M. Pothecary, and C. J. Railton, "Calculation of the dispersive characteristics of open dielectric structures by the finite difference time domain method," *IEEE Transactions on Microwave Theory and Techniques*, vol. MTT-42, pp. 1207–1212, July 1994.

[28] G. Hilton, C. Railton, G. Ball, A. Hume, and M. Dean, "FDTD analysis of a printed dipole antenna," in *Proc. 9th International Conference on Antennas and Propagation*, pp. 72–75, Apr. 1995.

[29] C. Ni, M. P. Robinson, R. H. Johnson, A. W. Preece, J. L. Green, N. M. Pothecary, and C. J. Railton, "Non-invasive *in vivo* measurement of tissue permittivity," in *2nd International Scientific Meeting on Microwaves in Medicine*, (Rome), Oct. 1993.

[30] L. Ma, N. M. Pothecary, and C. J. Railton, "Finite difference time domain modelling of domestic microwave ovens," in *Proc. Microwave and High Frequency (Gotenborg)*, 1993. 1:11.

[31] C. J. Railton, "An algorithm for the treatment of curved metallic laminas in the finite difference time domain method," *IEEE Transactions on Microwave Theory and Techniques*, vol. MTT-41, pp. 1429–1438, Aug. 1993.

Chapter 2

Numerical Techniques for Electromagnetic Analysis

2.1 Introduction

With a history of around 30 years the number of numerical electromagnetic analysis techniques is extremely large and ever increasing. Even textbooks, for example [1, 2], on the subject are only able to describe a small selection of methods in any detail. It is then beyond the scope of this thesis to introduce a representative range of methods.

While acknowledging the difficulty of introducing all the various analysis techniques, it is necessary to put the work described by later chapters of this thesis into context. To this end, this chapter sets out to describe the two main families of rigorous numerical electromagnetic analysis methods, namely the Integral and Differential techniques. Attention will be paid to the strengths and weaknesses of each family as a whole and how the nature of the problem to be solved makes some methods more attractive than others.

Having thus summarised the wide range of available electromagnetic analysis methods one important set of techniques is examined in greater detail. This particular set are those Differential methods which operate in the time domain; after examining a number of time domain Differential methods the Finite Difference Time Domain (FDTD) algorithm (introduced in chapter 1) becomes the main focus of attention toward the end of the chapter and indeed throughout the remainder of this thesis.

2.2 Differential and Integral Solutions

Electromagnetic phenomena are described by Maxwell's equations [3]; in most practical circumstances an analytic solution to these equations is unavailable and attention must be given to the numerical analysis of the situation.

A large proportion of rigorous numerical electromagnetic analysis methods can be described as falling into one of two broad classes. In both classes the solution is obtained by a discretisation process; in the first Maxwell's differential equations are solved directly and in the second an integral (or integro-differential) equation is first derived from Maxwell's equations – and it is this integral equation which is subsequently solved. The members of the first class are accordingly described as being *Differential* methods and those of the second as *Integral* methods.

Maxwell's curl equations in an isotropic medium are:

$$\begin{aligned} \nabla \times \mathbf{E} &= -\mu \partial_t \mathbf{H} \\ \nabla \times \mathbf{H} &= \epsilon \partial_t \mathbf{E} + \mathbf{J} \end{aligned} \tag{2.1}$$

where μ and ϵ are electrical properties of the medium, $\mathbf{E}$ and $\mathbf{H}$ are the electric and magnetic field intensities (in Vm^{-1} and Am^{-1} respectively) and $\mathbf{J}$ is the conduction current density with units Am^{-2}.

It is common practice to assume a sinusoidal time-dependence for the fields and thus, in the frequency domain, equations (2.1) become:

$$\begin{aligned} \nabla \times \mathbf{E} &= -j\omega\mu \mathbf{H} \\ \nabla \times \mathbf{H} &= j\omega\epsilon \mathbf{E} + \mathbf{J} \end{aligned} \tag{2.2}$$

where ω is the angular frequency in radians s^{-1}.

An alternative approach to solving Maxwell's equations directly is to derive an Integral form which is commonly written:

$$\mathbf{E}^s(\mathbf{r}) = \int \mathbf{G}(\mathbf{r}, \mathbf{r}') \mathbf{J}(\mathbf{r}') d\mathbf{r}' \tag{2.3}$$

$\mathbf{E}^s(\mathbf{r})$ is the scattered field set up by $\mathbf{J}(\mathbf{r}')$ and $\mathbf{G}$ is a dyadic Green's function which describes the influence of an infinitesimal current at $\mathbf{r}'$ on the field at point $\mathbf{r}$.

A incident field term $\mathbf{E}^i$ is usually introduced (unless a solution is sought only for the eigenvalues of the problem [1, p.91]) and boundary conditions enforced to give an equation which is of the general *form* of:

$$\mathbf{E}^i(\mathbf{r}) = -\int \mathbf{G}(\mathbf{r}, \mathbf{r}') \mathbf{J}(\mathbf{r}') d\mathbf{r}' \tag{2.4}$$

The precise form of equation (2.4) will depend on many features of the problem – whether for example the field under consideration is indeed the electric field (it could equally well be $\mathbf{H}$ [1, p.89]) and on the type of boundary conditions imposed. Equation (2.4) does however serve to illustrate the general features of the Integral methods.

It is worth noting that both the Differential (2.1)-(2.2) and the Integral forms (2.4) can be rearranged to be expressed as:

$$\mathcal{L}\mathbf{x} = \mathbf{y} \tag{2.5}$$

where $\mathbf{x}$ is the unknown function, $\mathbf{y}$ is a known term and $\mathcal{L}$ is a dyadic operator. It is not surprising then that, despite the very different compositions of the Differential and Integral methods, the solution for the unknown $\mathbf{x}$ usually proceeds via a similar process [1, chapter 2] – this consists of expressing the unknown as a weighted sum of known functions $\sum \mathbf{x}_i(\mathbf{r})\mathbf{a}_i$ where the unknowns are now the coefficients $\mathbf{a}_i$.

The solution process adopted here for solving the general operator equation (2.5) is the Weighted Residual Method (WRM) (although other approaches are possible – notably the variational formulation [4, chapter 4]). As noted in [5] when applied to integral equations in electromagnetics the method has historically been known as the Method of Moments (or MoM) elsewhere the method is widely known as the Finite Element Method (or FEM).

2.3 Integral Methods

2.3.1 Solution of Integral Equations

The integral equation (2.4) may be written:

$$\mathcal{L}\mathbf{J}(\mathbf{r}') = \mathbf{E}^i(\mathbf{r}) \tag{2.6}$$

and the unknown current distribution $\mathbf{J}$ expanded as a series of N known diagonal dyadic basis functions $\mathbf{J}_i$ (also known as expansion or interpolation functions) weighted by N unknown coefficient vectors, $\mathbf{a}_i$ such that:

$$\sum_{i=1}^{N} \mathcal{L}\mathbf{J}_i(\mathbf{r}')\mathbf{a}_i \approx \mathbf{E}^i(\mathbf{r}) \tag{2.7}$$

the equality of equation (2.6) has been replaced by the approximate equality since in general the left and right sides of equation (2.7) can not be equal for all $\mathbf{r}$ except in trivial cases. The approximate equality may be replaced with an equality by requiring that the equality be enforced only in an average sense for each basis function. To do this a set of N testing (sometimes known as weighting) functions, $\mathbf{w}_j$, is introduced:

$$\left\langle \mathbf{w}_j(\mathbf{r}), \sum_{i=1}^{N} \mathcal{L}\mathbf{J}_i(\mathbf{r}')\mathbf{a}_i \right\rangle = \left\langle \mathbf{w}_j(\mathbf{r}), \mathbf{E}^i(\mathbf{r}) \right\rangle \qquad \forall j \tag{2.8}$$

where $< a, b >$ represents a suitably defined inner product between a and b whose properties are given by [6, definition 5.1.3].

This may be written in matrix notation:

$$\begin{pmatrix} < \mathbf{w}_1, \mathcal{L}\mathbf{J}_1 > & \cdots & < \mathbf{w}_1, \mathcal{L}\mathbf{J}_N > \\ \vdots & \ddots & \\ < \mathbf{w}_N, \mathcal{L}\mathbf{J}_1 > & & < \mathbf{w}_N, \mathcal{L}\mathbf{J}_N > \end{pmatrix} \begin{pmatrix} \mathbf{a}_1 \\ \vdots \\ \mathbf{a}_N \end{pmatrix} = \begin{pmatrix} < \mathbf{w}_1, \mathbf{E}^i > \\ \vdots \\ < \mathbf{w}_N, \mathbf{E}^i > \end{pmatrix} \tag{2.9}$$

or, for brevity:

$$\mathbf{La} = \mathbf{e} \tag{2.10}$$

where $\mathbf{L}$ is the matrix of inner products (in a frequency domain analysis often called the impedance matrix), $\mathbf{a}$ is the unknown coefficient vector and $\mathbf{e}$ is the vector of inner products with the excitation field $\mathbf{E}^i$.

The value of $\mathbf{a}$ can be found in principle by inverting $\mathbf{L}$ in which case a solution is obtained simply for any given $\mathbf{e}$. The approach more normally taken (since it involves less computation) is to solve for one particular $\mathbf{e}$ by employing any suitable algorithm for the solution of linear equations [7].

2.3.2 Choice of Basis and Testing Functions

The usual procedure when choosing both the basis and testing functions ($\mathbf{w}_j$ and $\mathbf{J}_i$ above) is to choose simple functions that are each only non-zero over one small part of the problem space. This is not a necessary feature of the solution method although it is common practice and implied here by the use of the term 'finite element' to describe the solution method. (It might be argued that the fact that basis functions may have entire domain support mitigates in favour of the 'Method of Moments' appellation to describe the above solution procedure. The modern solution of electromagnetic problems in geometrically complex domains however makes the use of entire domain functions the exception rather than the rule).

These functions must be linearly independent [8, p.7] and are frequently chosen to be low order piecewise polynomials. Figure 2.1 illustrates two piecewise polynomials of unity amplitude, the first being a piecewise constant centred on $x = 2$ the second a piecewise linear function centered on $x = 4$.

An important consideration when choosing the basis functions is to select functions that will naturally fit the expected distribution of $\mathbf{J}$ [1, p.82]. This is particularly important when the current variation is expected to be predominately influenced by a singularity (such as that present at a corner or edge) [9].

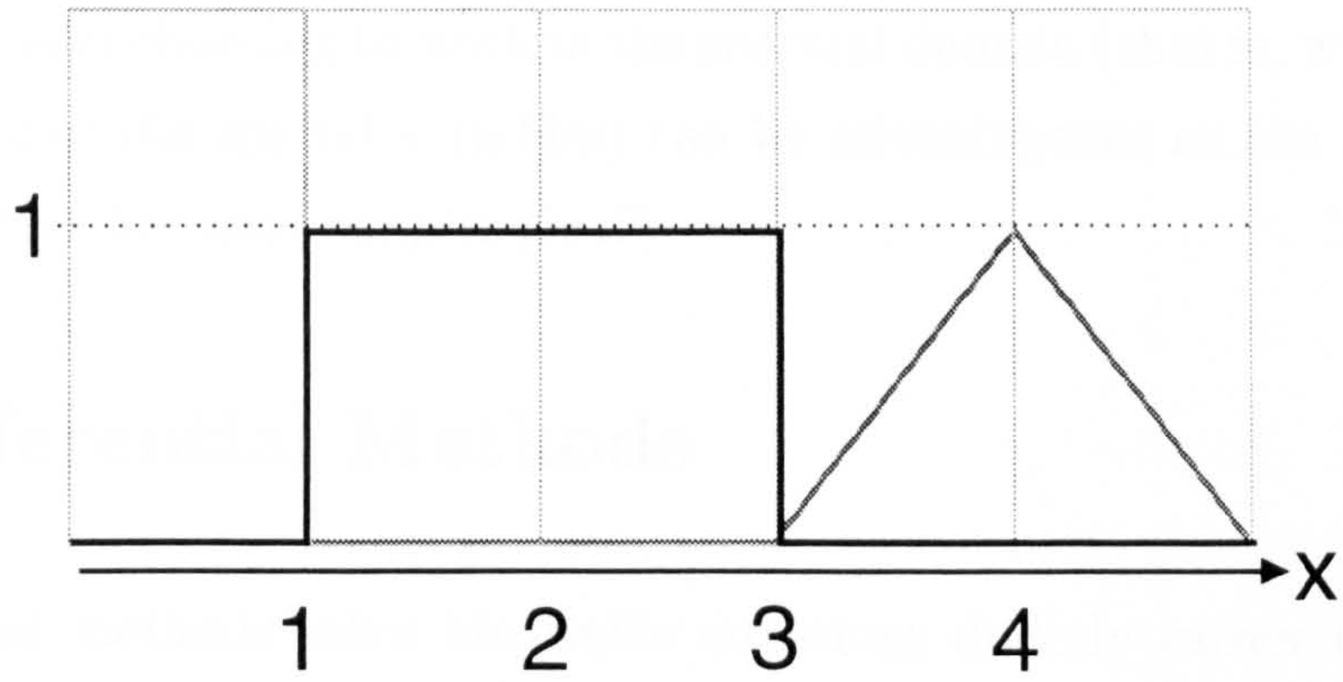

Figure 2.1: Piecewise polynomials of low order

The test and basis function sets need not be identical; this is however a common choice and usually leads to particularly well-behaved methods, often described as Galerkin techniques [8, p.7], where reciprocity is guaranteed [1, p.95].

A second common choice is to use Dirac delta functions [10] as the weighting functions, in this case the inner products in (2.9) become trivial and the result is known as a point-matching or collocation method where the left and right hand sides of (2.7) are simply set equal to each other at N points.

2.3.3 Features of the Integral Methods

While there are many different Integral methods, the fact that they all share the same basic formulation results in the fact that they have a number of common properties:

- A Greens function $\mathbf{G}(\mathbf{r}, \mathbf{r}')$ must be derived by analytic means.
- The Greens function will only be applicable for a particular class of problem.
- The Greens function will implicitly include the conditions at the boundary of the problem domain.
- In many cases $\mathbf{J}$ will only exist on a given surface [2, chapter 6].
- The final matrix equation (2.9) will not be sparse [11, p.426].

Many different variations are possible on the general method given above depending on the choice of solution domain and the choice of basis and test functions.

- The frequency domain is usually preferred to the time domain.

- In some cases choosing to work in the spectral domain (that is, with the Fourier transform of the spatial variables) can be advantageous as the formulation of the problem becomes simpler [9, 12].

2.4 Differential Methods

The Differential methods solve Maxwell's equations directly rather than solving a related integral equation. Just as for the Integral methods a solution to the equation is usually approached via a finite element procedure.

2.4.1 Solution of Differential Equations

Commencing with Maxwell's equations in operator form:

$$\mathcal{L}\mathbf{v}(\mathbf{r}) = \rho(\mathbf{r}) \tag{2.11}$$

where $\mathcal{L}$ is a differential operator, $\mathbf{v}$ is an amalgamated vector of $\mathbf{E}$ and $\mathbf{H}$ and ρ is a known source term.

Expanding $\mathbf{v}$ as a series of basis functions $\mathbf{v}_i$ and introducing testing functions $\mathbf{w}_j$ yields:

$$\begin{pmatrix} < \mathbf{w}_1, \mathcal{L}\mathbf{v}_1 > & \cdots & < \mathbf{w}_1, \mathcal{L}\mathbf{v}_N > \\ \vdots & \ddots & \\ < \mathbf{w}_N, \mathcal{L}\mathbf{v}_1 > & & < \mathbf{w}_N, \mathcal{L}\mathbf{v}_N > \end{pmatrix} \begin{pmatrix} \mathbf{a}_1 \\ \vdots \\ \mathbf{a}_N \end{pmatrix} = \begin{pmatrix} < \mathbf{w}_1, \rho > \\ \vdots \\ < \mathbf{w}_N, \rho > \end{pmatrix} \tag{2.12}$$

which is of exactly the same form as (2.9) and again may be written succinctly:

$$\mathbf{La} = \mathbf{e} \tag{2.13}$$

which may be solved in principle by any suitable method.

2.4.2 Choice of Basis and Testing Functions

Just as in the solution of an Integral problem, low-order piecewise polynomials of finite support are usually chosen for the test and basis functions. This choice is particularly appropriate for the Differential methods because the resulting matrix equation will be sparse and is thus well suited for solution by algorithms such as the conjugate gradient method [13].

Once again the choice of a point-matching procedure (as described in the Integral case) is a popular one. This procedure generally results in simple, low-order and often explicit schemes that have much in common with the well established finite difference methods (see for example section 2.6.2) [14].

Efficient techniques are again often achieved by choosing basis functions which will fit the expected field distribution closely. This is particularly important when the field at a point (such as at the tip of a cone or the edge of an acute-angled wedge) is known to be singular [4, p.173].

A problem that arises frequently from the choice of basis functions is that of the generation of spurious solutions [4, p.164]. These spurious solutions are generally attributed to the lack of enforcement of the divergence condition ($\nabla \cdot \mathbf{E} = 0$ and $\nabla \cdot \mathbf{H} = 0$ in a source free region) and are a major cause of inaccuracy.

The problem of spurious solutions has received much attention in the literature and a common solution has been the inclusion of a penalty term in the problem formulation [15]. An alternative and increasingly popular method is the use of vector or edge elements [4, chapter 8] which will be discussed briefly in the context of time domain Differential formulations in section 2.6.3.5.

2.4.3 Features of the Differential Methods

Once again there are features common to this family of methods:

- Little or no analytic work is required to achieve a solution since a Greens function is not required.
- These methods can be applied to a wide range of structures.
- The discretised unknowns are the field variables which exist throughout space. Thus the number of unknowns is proportional to the volume of the problem [11, p.6].
- The final matrix equation (2.12) will be sparse if reasonable choices are made for test and basis functions.
- Appropriate open or closed boundary conditions need to be explicitly imposed on the method.

There is also a choice of solution domains:

- There is no advantage to be gained by utilising the spectral domain, the spatial domain is therefore the usual choice.
- Either a time or frequency domain formulation can be chosen.

While the finite element procedure described above (section 2.4.1) is widely used to produce a solution in a Differential method, there are alternative ways of approaching this solution and some of these will be described later in this chapter. It is worth noting, however, that these alternative methods bear many similarities to the finite element formulation and in some cases can be shown to produce identical algorithms to a finite element procedure (see for example section 2.6.2).

2.5 Integral and Differential Methods Compared

As described in the preceding sections it is the use of a Greens function which fundamentally separates the Integral and Differential approaches; this function is of great assistance as it includes the relevant boundary conditions and frequently reduces the problem to a surface rather than volume based one. At the same time however the necessity of producing the Greens function analytically is a severe limitation as these functions are only available in a limited number of cases. Even when a Greens function has been derived it may not be closed form and the necessary integrations in (2.9) may be problematic [1, chapter 3].

The Differential methods are popular when the problem is inherently volumetric (ie does not consist entirely of perfectly conducting surfaces or infinitesimally thin wires) and when an analysis tool is required which is capable of treating a wide range of structures, regardless of whether they have a known Greens function.

Considerable attention has been paid to combining the Differential and Integral methods in such a way as to eliminate their respective disadvantages while retaining their advantageous features. These hybrid methods are commonly referred to as Finite Element Boundary Integral techniques and have been applied to both two and three dimensional problems [16, 17].

2.5.1 Time Domain Analysis

In many situations a time domain solution is attractive since the structure's behaviour over a wide band of frequencies is available and an inspection of time domain results may yield information about the response of a structure that is not apparent from a frequency domain analysis.

A time domain solution can be achieved by both Integral and Differential methods. Integral methods have been employed in the time domain with some success, for example [18], but have not achieved a very high level of acceptance, partly due it would seem, to concerns about long term stability [19, 20]. The use of time domain Differential methods however is widespread and has a history in electromagnetics of some 30 years. Accordingly the rest of this chapter is concerned only only with this class of techniques.

2.6 Time Domain Differential Methods

In general a finite element solution to a four dimensional problem will require the use of finite elements in all four dimensions (including time) but in fact the finite element concept is normally avoided in the time dimension. This is because finite elements are normally viewed as a solution to a boundary value problem and the temporal behaviour of a solution is not usually bounded. Instead a 'marching in time' procedure is adopted for the solution and a finite difference expression is commonly used to obtain the temporal variation of the solution.

2.6.1 The Time Domain Finite Element Formulation

As described above, a slightly different approach from that described in section 2.4.1 is usually taken when considering time-dependent finite element solutions. Maxwell's curl equations in the time domain and a Cartesian coordinate system are:

$$\nabla \times \mathbf{E}(t,x,y,z) = -\mu \partial_t \mathbf{H}(t,x,y,z) \tag{2.14}$$

$$\nabla \times \mathbf{H}(t,x,y,z) = \epsilon \partial_t \mathbf{E}(t,x,y,z) \tag{2.15}$$

where for simplicity the conduction current $\mathbf{J}$ has been neglected.

Both $\mathbf{E}$ and $\mathbf{H}$ are expanded as a set of N weighted dyadic basis functions:

$$\begin{aligned}\sum_{i=1}^{N} \nabla \times \mathbf{E}_i(x,y,z)\mathbf{e}_i(t) &= -\mu \sum_{i=1}^{N} \mathbf{H}_i(x,y,z)\partial_t \mathbf{h}_i(t) \\ \sum_{i=1}^{N} \nabla \times \mathbf{H}_i(x,y,z)\mathbf{h}_i(t) &= \epsilon \sum_{i=1}^{N} \mathbf{E}_i(x,y,z)\partial_t \mathbf{e}_i(t)\end{aligned} \tag{2.16}$$

where the basis functions $\mathbf{E}_i, \mathbf{H}_i$ are assumed to be functions of space only and it is the coefficients $\mathbf{e}_i, \mathbf{h}_i$ that include the temporal variation.

An inner product with a set of N testing functions $\mathbf{u}_j, \mathbf{w}_j$ is introduced for each expression:

$$\left\langle \mathbf{u}_j(x,y,z), \sum_{i=1}^{N} \nabla \times \mathbf{E}_i(x,y,z) \right\rangle \mathbf{e}_i(t) = -\mu \left\langle \mathbf{u}_j(x,y,z), \sum_{j=1}^{N} \mathbf{H}_i(x,y,z) \right\rangle \partial_t \mathbf{h}_i(t) \qquad \forall j \tag{2.17}$$

$$\left\langle \mathbf{w}_j(x,y,z), \sum_{i=1}^{N} \nabla \times \mathbf{H}_i(x,y,z) \right\rangle \mathbf{h}_i(t) = \epsilon \left\langle \mathbf{w}_j(x,y,z), \sum_{j=1}^{N} \mathbf{E}_i(x,y,z) \right\rangle \partial_t \mathbf{e}_i(t) \qquad \forall j \tag{2.18}$$

writing this in matrix form yields:

$$\begin{aligned}&\begin{pmatrix} < \mathbf{u}_1, \nabla \times \mathbf{E}_1 > & \cdots & < \mathbf{u}_1, \nabla \times \mathbf{E}_N > \\ \vdots & \ddots & \\ < \mathbf{u}_N, \nabla \times \mathbf{E}_1 > & & < \mathbf{u}_N, \nabla \times \mathbf{E}_N > \end{pmatrix} \begin{pmatrix} \mathbf{e}_1 \\ \vdots \\ \mathbf{e}_N \end{pmatrix} \\ &= -\mu \begin{pmatrix} < \mathbf{u}_1, \mathbf{H}_1 > & \cdots & < \mathbf{u}_1, \mathbf{H}_N > \\ \vdots & \ddots & \\ < \mathbf{u}_N, \mathbf{H}_1 > & & < \mathbf{u}_N, \mathbf{H}_N > \end{pmatrix} \partial_t \begin{pmatrix} \mathbf{h}_1 \\ \vdots \\ \mathbf{h}_N \end{pmatrix}\end{aligned} \tag{2.19}$$

and:

$$\begin{aligned}&\begin{pmatrix} < \mathbf{w}_1, \nabla \times \mathbf{H}_1 > & \cdots & < \mathbf{w}_1, \nabla \times \mathbf{H}_N > \\ \vdots & \ddots & \\ < \mathbf{w}_N, \nabla \times \mathbf{H}_1 > & & < \mathbf{w}_N, \nabla \times \mathbf{H}_N > \end{pmatrix} \begin{pmatrix} \mathbf{h}_1 \\ \vdots \\ \mathbf{h}_N \end{pmatrix} \\ &= \epsilon \begin{pmatrix} < \mathbf{w}_1, \mathbf{E}_1 > & \cdots & < \mathbf{w}_1, \mathbf{E}_N > \\ \vdots & \ddots & \\ < \mathbf{w}_N, \mathbf{E}_1 > & & < \mathbf{w}_N, \mathbf{E}_N > \end{pmatrix} \partial_t \begin{pmatrix} \mathbf{e}_1 \\ \vdots \\ \mathbf{e}_N \end{pmatrix}\end{aligned} \tag{2.20}$$

these equations are usually written more briefly as:

$$\mathbf{K}_1\mathbf{e}(t) = \mathbf{M}_1\partial_t\mathbf{h}(t) \tag{2.21}$$

$$\mathbf{K}_2\mathbf{h}(t) = \mathbf{M}_2\partial_t\mathbf{e}(t) \tag{2.22}$$

$\mathbf{M}_1, \mathbf{M}_2$ are traditionally known as 'mass' matrices and $\mathbf{K}_1, \mathbf{K}_2$ are called 'stiffness' matrices [21].

The temporal derivative is commonly replaced by an approximation such as a centred finite difference where:

$$\partial_t\mathbf{h}(t) = \frac{\mathbf{h}(t+0.5\Delta_t) - \mathbf{h}(t-0.5\Delta_t)}{\Delta t} \tag{2.23}$$

with Δ_t being a small time interval called the 'time-step'. This yields:

$$\mathbf{M}_1\frac{\mathbf{h}(t+0.5\Delta_t) - \mathbf{h}(t-0.5\Delta_t)}{\Delta_t} = \mathbf{K}_1\mathbf{e}(t) \tag{2.24}$$

$$\mathbf{M}_2\frac{\mathbf{e}(t+\Delta_t) - \mathbf{e}(t)}{\Delta_t} = \mathbf{K}_2\mathbf{h}(t+0.5\Delta_t)(t) \tag{2.25}$$

giving:

$$\mathbf{M}_1\mathbf{h}(t+0.5\Delta_t) = \mathbf{M}_1\mathbf{h}(t-0.5\Delta_t) + \Delta_t\mathbf{K}_1\mathbf{e}(t) \tag{2.26}$$

and:

$$\mathbf{M}_2\mathbf{e}(t+\Delta_t) = \mathbf{M}_2\mathbf{e}(t) + \Delta_t\mathbf{K}_2\mathbf{h}(t+0.5\Delta_t) \tag{2.27}$$

which, given that initial values are known, provides an update scheme for $\mathbf{e}$ and $\mathbf{h}$. This method is widely used and often described as the 'leap-frog' technique.

It is desirable to make the mass matrices $\mathbf{M}_1, \mathbf{M}_2$ diagonal, in which case $\mathbf{h}(t+0.5\Delta_t)$ and $\mathbf{e}(t+\Delta_t)$ can be found explicitly from the previous values. If the mass matrices are non-diagonal the algorithm is implicit and a set of simultaneous equations must be solved in order to update each element of $\mathbf{h}$ and $\mathbf{e}$. A diagonal mass matrix may result from the use of low order basis and test functions or from a 'mass lumping' scheme, where the mass matrices are approximately diagonalised [22, 23].

This section has demonstrated how the finite element concept is usually applied to the time domain Maxwell's equations. It is clear that a number of different algorithms may result from employing the above procedure, depending on:

- The choice of basis functions.
- The choice of test functions.
- The method used to approximate the ∂_t operator.
- Whether or not mass lumping is employed.

In the following sections a number of time domain Differential methods will be considered, most of which are examples of the time domain finite element method with various choices for these four points.

2.6.2 Finite Difference Time Domain Methods

Various methods are traditionally derived by the application of finite difference approximations to the derivatives in Maxwell's equations – the most popular of these methods being the Finite Difference Time Domain (FDTD) or Yee algorithm, first proposed by Yee in 1966 (see chapter 1) [24]. This method places the field unknowns in a spatial mesh built up of unit cells.

The vector field components are associated with the edges of the unit cells as shown by figure 2.2; this meshing scheme is usually referred to as 'staggered' in reference to the fact that no two field components occupy the same position in space.

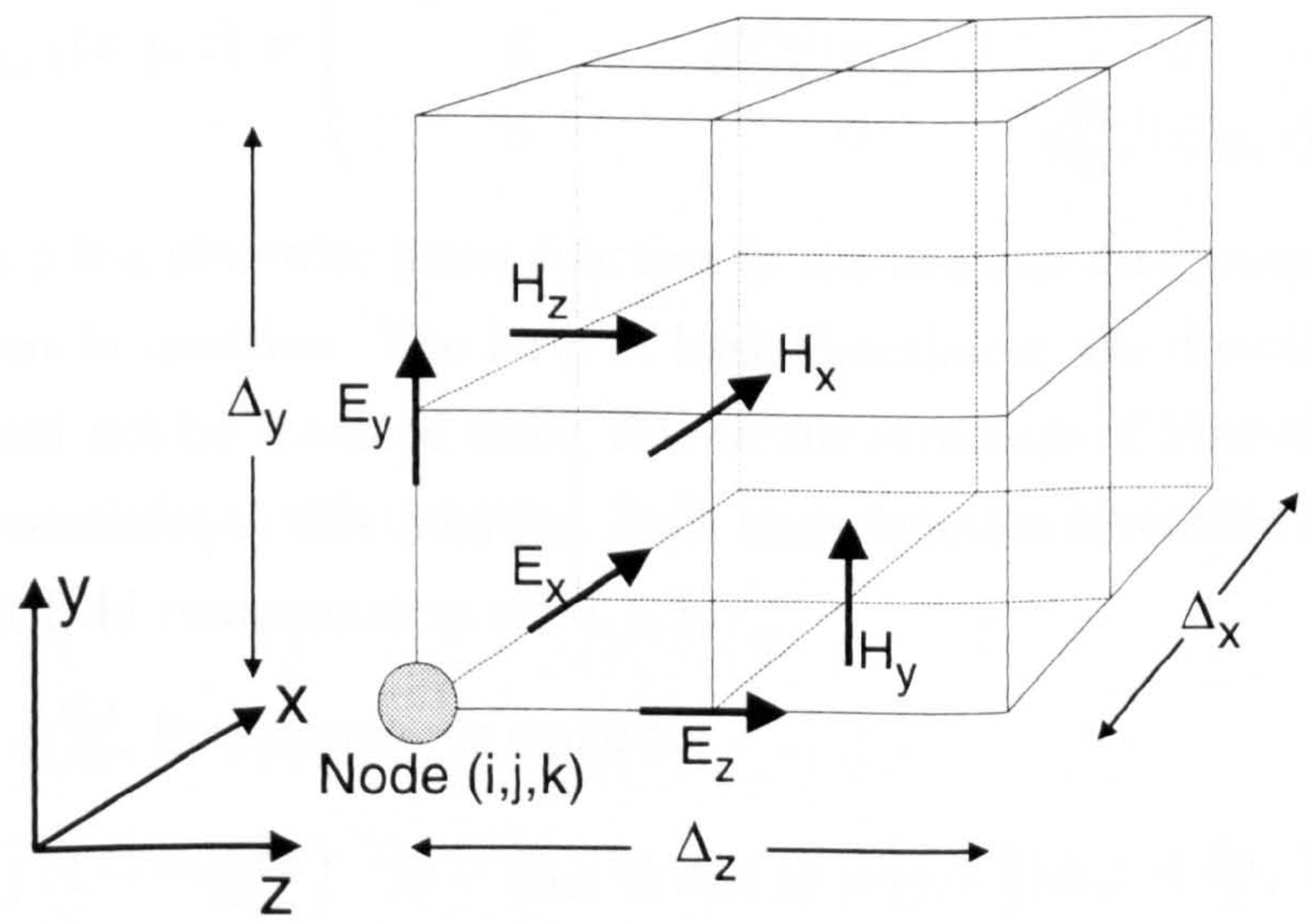

Figure 2.2: The FDTD unit cell (showing unit cell dimensions).

While the normal approach to deriving the FDTD algorithm is to replace the partial derivatives in Maxwell's equation with centred difference expressions, yielding an

explicit finite difference algorithm, it is also possible to view the FDTD method as a special case of the finite element procedure described in section 2.6.1. This is a useful approach since it introduces an element concept for FDTD (utilised in section 4.5.2 and in subsequent chapters) and emphasizes the commonality between a number of analysis methods.

Introducing for convenience a slightly modified notation for the enumeration of the basis and testing functions:

$$\mathbf{E}(x,y,z) = \sum_{i=1}^{N_x}\sum_{j=1}^{N_y}\sum_{k=1}^{N_z} \mathbf{E}_{i,j,k}(x,y,z)\mathrm{e}_{i,j,k}(t) \tag{2.28}$$

$$\mathbf{H}(x,y,z) = \sum_{i=1}^{N_x}\sum_{j=1}^{N_y}\sum_{k=1}^{N_z} \mathbf{H}_{i,j,k}(x,y,z)\mathrm{h}_{i,j,k}(t) \tag{2.29}$$

where N_x, N_y and N_z are the number of unit cells in the x, y and z directions respectively and:

$$\mathbf{E}_{i,j,k}(x,y,z) = \begin{pmatrix} \phi^{(E_x)}_{i,j,k}(x,y,z) & 0 & 0 \\ 0 & \phi^{(E_y)}_{i,j,k}(x,y,z) & 0 \\ 0 & 0 & \phi^{(E_z)}_{i,j,k}(x,y,z) \end{pmatrix} \tag{2.30}$$

$$\mathbf{H}_{i,j,k}(x,y,z) = \begin{pmatrix} \phi^{(E_x)}_{i,j,k}(x,y,z) & 0 & 0 \\ 0 & \phi^{(E_y)}_{i,j,k}(x,y,z) & 0 \\ 0 & 0 & \phi^{(E_z)}_{i,j,k}(x,y,z) \end{pmatrix} \tag{2.31}$$

Each function ϕ is a piecewise linear function in the two axis directions normal to the field component in question. The form of basis function in the direction of the field component need not be specified since, due to the structure of Maxwell's equations, the result is insensitive to this quantity. Each basis function is centred on the position of the relevant field component in cell i,j,k.

The function $\phi^{(E_y)}_{i,j,k}$, for example, is equal to:

$$\begin{cases} \left(1-\frac{|x-i\Delta_x|}{\Delta_x}\right)\left(1-\frac{|z-k\Delta_z|}{\Delta_z}\right) & |x-i\Delta_x| \le \Delta_x,\ |y-(j+\frac{1}{2})\Delta_y| \le \frac{\Delta_y}{2},\ |z-k\Delta_z| \le \Delta_z \\ 0 & \text{otherwise} \end{cases} \tag{2.32}$$

This basis function is depicted by figure 2.3 – only the variation in the z direction is indicated.

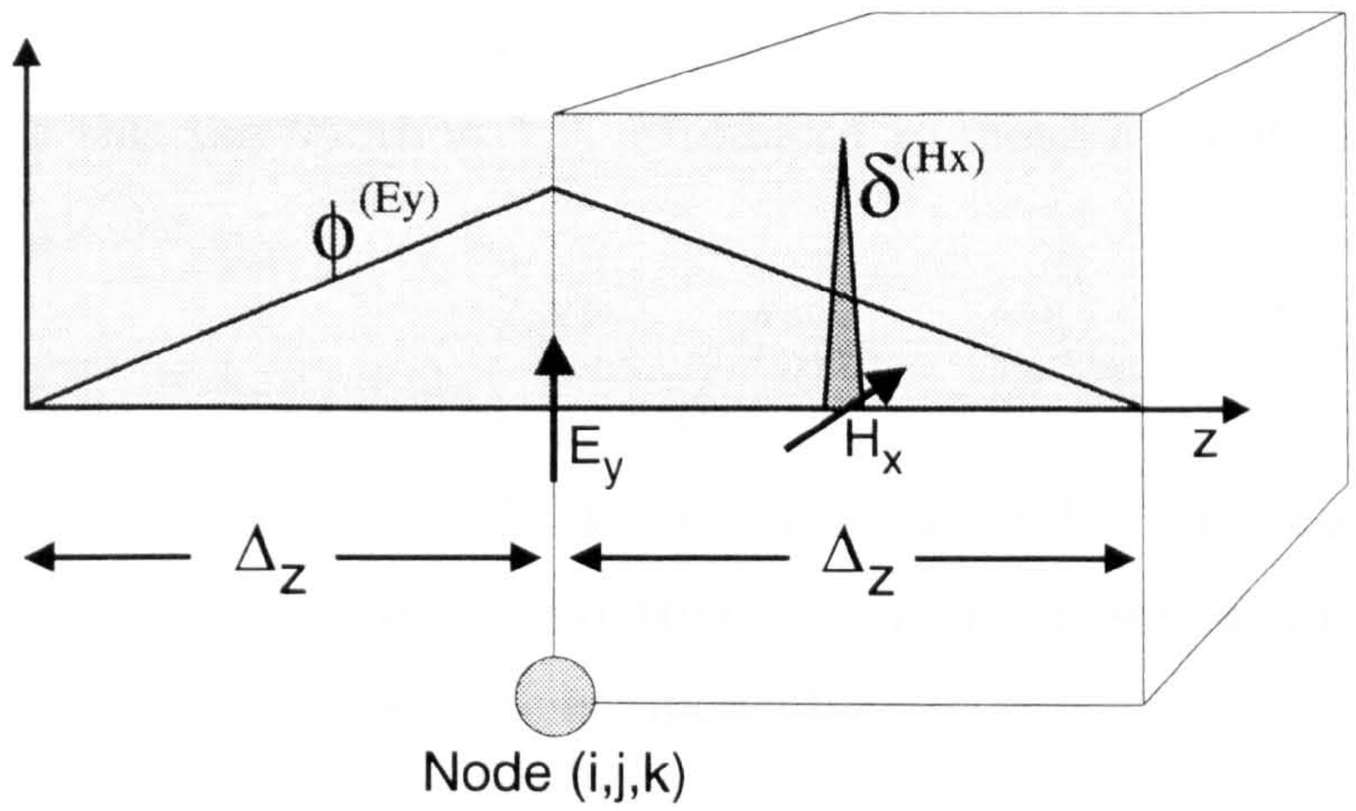

Figure 2.3: Basis function $\phi^{(E_y)}$ and test function $\delta^{(H_x)}$ shown as a function of z only.

For the testing functions Dirac delta functions [10] are employed, thus:

$$\mathbf{w}_{i,j,k}(x,y,z) = \begin{pmatrix} \delta_{i,j,k}^{(E_x)}(x,y,z) & 0 & 0 \\ 0 & \delta_{i,j,k}^{(E_y)}(x,y,z) & 0 \\ 0 & 0 & \delta_{i,j,k}^{(E_z)}(x,y,z) \end{pmatrix} \tag{2.33}$$

$$\mathbf{u}_{i,j,k}(x,y,z) = \begin{pmatrix} \delta_{i,j,k}^{(H_x)}(x,y,z) & 0 & 0 \\ 0 & \delta_{i,j,k}^{(H_y)}(x,y,z) & 0 \\ 0 & 0 & \delta_{i,j,k}^{(H_z)}(x,y,z) \end{pmatrix} \tag{2.34}$$

each Dirac delta is only non-zero at the position of the indicated field component (the test function $\delta^{(H_x)}$ is indicated by the 'spike' in figure 2.3).

To show how these basis and test functions lead to the FDTD method consider only the evaluation of the time derivative of one component of a given vector coefficient, for example $\partial_t h_{x_{i,j,k}}$ – the coefficient associated with the H_x component in the unit cell i, j, k.

It can be shown that the only non-zero terms involved in computing $\partial_t h_{x_{i,j,k}}$ are:

$$\left\langle \delta_{i,j,k}^{(H_x)}, \phi_{i,j,k}^{(H_x)} \right\rangle \partial_t h_{x_{i,j,k}}(t) = \frac{1}{\mu} \left\langle \delta_{i,j,k}^{(H_x)}, \left(\partial_z \left\{ \phi_{i,j,k}^{(E_y)} e_{y_{i,j,k}}(t) + \phi_{i,j,k+1}^{(E_y)} e_{y_{i,j,k+1}}(t) \right\} \right.\right.$$
$$\left.\left. -\partial_y \left\{ \phi_{i,j,k}^{(E_z)} e_{z_{i,j,k}}(t) + \phi_{i,j+1,k}^{(E_z)} e_{z_{i,j+1,k}}(t) \right\} \right) \right\rangle \tag{2.35}$$

The inner products evaluate straightforwardly to give:

$$\partial_t h_{x_{i,j,k}}(t) = \frac{1}{\mu} \left(\frac{e_{z_{i,j,k}}(t) - e_{z_{i,j+1,k}}(t)}{\Delta_y} + \frac{e_{y_{i,j,k+1}}(t) - e_{y_{i,j,k}}(t)}{\Delta_z} \right) \tag{2.36}$$

where the terms in the brackets are recognisable as centred difference approximations to the derivatives ∂_y and ∂_z.

The final step is to replace the time derivative $\partial_t h_{x_{i,j,k}}(t)$ with a difference approximation. To do this the notation ^{n} is introduced to mean a point in time given by $t = n\Delta_t$. This yields:

$$h^{n+1}_{x_{i,j,k}} = h^n_{x_{i,j,k}} + \Delta_t \left(\frac{e^{n+0.5}_{z_{i,j,k}} - e^{n+0.5}_{z_{i,j+1,k}}}{\Delta_y} + \frac{e^{n+0.5}_{y_{i,j,k+1}} - e^{n+0.5}_{y_{i,j,k}}}{\Delta_z} \right) \tag{2.37}$$

This expression is the standard FDTD update equation for the field component h_x (barring some slightly non-standard notation). Similar expressions can be derived for the remaining magnetic and electric components.

It has been shown that the Yee FDTD algorithm is in fact a particular case of a time domain finite element technique. Point matched piecewise linear basis functions are employed in space and a centered finite difference employed in time yielding a fully explicit algorithm (since the mass matrices are diagonal).

There are a number of other time domain Differential techniques which result from the use of spatial finite differences and these are briefly described in the following sections.

2.6.2.1 FDTD in Non-Cartesian Coordinates

FDTD is usually derived assuming a Cartesian coordinate system, as shown above, however this results in poor characterisation of bodies such as the cylinder shown in figure 2.4 since it must be approximated in the FDTD method by a 'staircase' of some description. This approximation is extremely undesirable [25, 26] and is discussed further in section 4.1.

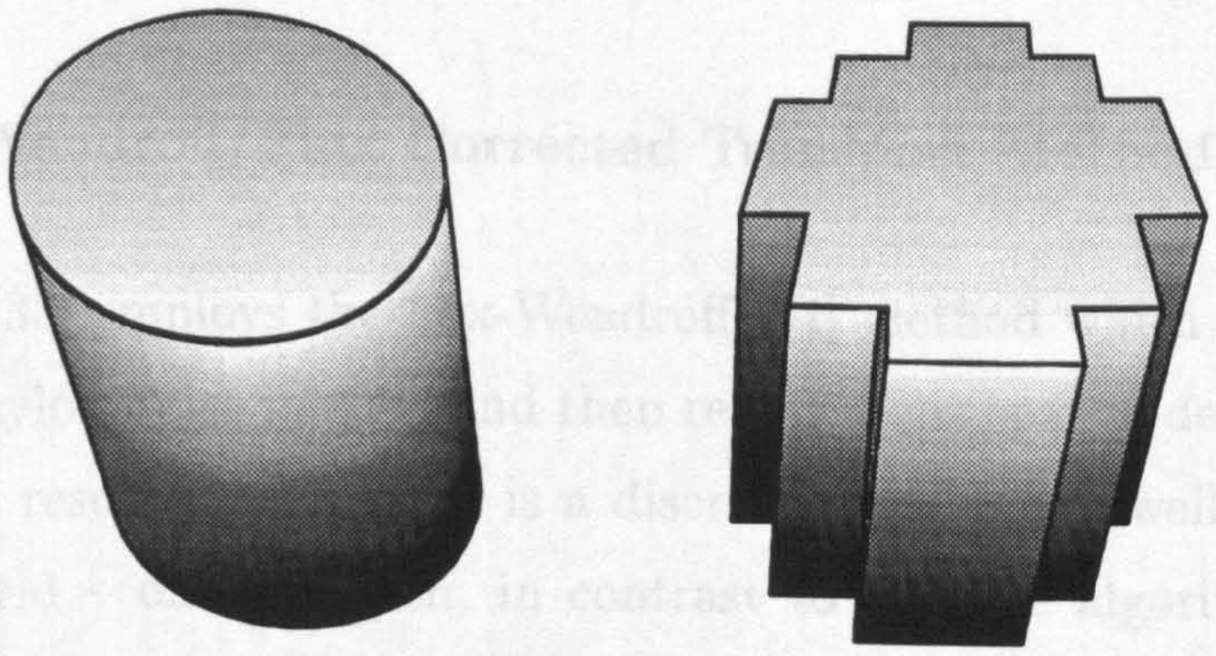

Figure 2.4: (i) Cylindrical body and (ii) its representation by a staircase.

For some structures the problem may be overcome by deriving FDTD in orthogonal curvilinear coordinates such as the circular-cylindrical [27] or spherical [28] systems.

The FDTD mesh will then be able to characterise the object without employing a staircase.

This approach is obviously limited however as for the majority of structures it is not possible to choose an orthogonal coordinate system which conforms to an arbitrary set of boundaries.

2.6.2.2 Non-orthogonal FDTD

The generalisation of FDTD to a non-orthogonal coordinate system enables the treatment of arbitrarily shaped objects and was originally presented in [29] with subsequent investigations by [30, 31]. This generalisation however requires double the amount of computer storage and three times as much computation per unit cell in the algorithm [31].

An extension to the idea was proposed in [32] where several overlapping FDTD methods are employed. A non-orthogonal FDTD algorithm is employed where necessary to characterise curved bodies and the standard (more efficient) FDTD technique is employed elsewhere. The field data is interpolated between the algorithms at their interfaces.

Restricting the use of the conformal method to a small proportion of the problem space obviously provides considerable computational savings over employing it throughout the problem and simplifies the generation of the non-orthogonal mesh. The authors do mention however some stability problems with this technique which require careful selection of the interpolation procedure.

2.6.2.3 Lax-Wendroff/Flux Corrected Transport Method

This algorithm [33] employs the Lax-Wendroff [34] method which expands the field variables in a Taylor series in time and then replaces the spatial derivatives by finite differences. The resulting algorithm is a discretisation of Maxwell's equations on a non-staggered grid – one in which, in contrast to the Yee algorithm, all the field components are defined at the same points in each unit cell.

The Lax-Wendroff method is shown to be more dispersive than FDTD and as a result the Flux Corrected Transport (FCT) technique (widely used in fluid dynamics [35]) is employed to reduce the dispersion of the algorithm – resulting in a method which

is actually less dispersive than FDTD.

While this method involves considerably more computations per time step than the Yee method, the authors contend that a less dense mesh may be employed and that the non-staggered mesh allows better characterisation of curved surfaces than FDTD (c.f. chapter 5).

2.6.2.4 Discussion of the Finite Difference Methods

The finite difference techniques are popular in electromagnetics as they are explicit, direct solutions of Maxwell's equations. The Yee method (FDTD) is particularly popular as, due to its application on an orthogonal mesh, its computational overheads are relatively modest.

As has been shown, other finite difference based methods have been proposed which offer advantages over FDTD (particularly in their handling of non-rectilinear geometries) however these generally impose considerable extra computational overheads and, for that reason, they have yet to supplant the original FDTD method.

2.6.3 Finite Element Time Domain Methods

Some attempts have been made to derive time domain methods from a purely finite element point of view. These methods' principal advantage over FDTD is that curved (or angled) structures may generally be modelled without the staircase approximation as a result of the application of more flexible basis and test functions.

2.6.3.1 Point Matched Method of Cangellaris *et al.*

In [36] a time domain finite element method in two dimensions is proposed which employs isoparametric (bilinear) basis functions over quadrilateral mesh elements. This mesh is able to conform locally to the shape of the object being modelled thus reducing the overhead of storing and generating a full conformal mesh. Dirac delta test functions are employed and the time derivative is approximated by the leap frog scheme as in FDTD; the resulting algorithm is therefore explicit. The extension to three dimensions is described in principle by [37] as being to employ hexahedral mesh elements.

2.6.3.2 Finite Element Methods of Madsen *et al.*

Similar two-dimensional methods to those of [36] were investigated in [38]. In this paper the Galerkin formulation is employed (the test and basis function sets are identical). Such a formulation would normally result in implicit algorithms but mass-lumping renders the algorithms explicit.

Various choices of basis functions were considered for both **E** and **H** however the paper concludes that the Modified Finite Volume (MFV) method [39] also presented in the paper possesses superior accuracy to the finite element methods. The MFV and related methods are described in section 2.6.4.

2.6.3.3 Penalty Method of Lynch *et al.*

A three dimensional finite element formulation is described in [22]. The approach taken is to eliminate the magnetic field **H** from Maxwell's equations to give the double curl equation:

$$\nabla \times \frac{1}{\mu} \nabla \times \mathbf{E} = -\epsilon \partial_{tt} E \tag{2.38}$$

The finite element solution of this equation is known to suffer from spurious modes [40] consequently a form of penalty term (as mentioned in section 2.4.2) is introduced to ameliorate these effects.

The choice of basis and test functions is taken to be Galerkin's and a lumping technique is required to render the scheme explicit; the second order time derivative is approximated by the standard centred difference:

$$\partial_{tt}\mathbf{E}(t) = \frac{\mathbf{E}(t+\Delta_t) - 2\mathbf{E}(t) + \mathbf{E}(t-\Delta_t)}{\Delta_t^2} \tag{2.39}$$

2.6.3.4 Taylor-Galerkin Method of Ambrosiano *et al.*

In [41] the Taylor-Galerkin method is described which is capable of solving Maxwell's equations on an unstructured mesh. This method is very similar to the Lax Wendroff finite difference technique (section 2.6.2.3) except that a Galerkin finite element approach replaces the spatial difference operator, resulting in an implicit algorithm that requires an iterative solution technique at each time step.

As discussed in the context of the finite difference method the Lax Wendroff scheme has the disadvantage that it is fairly dispersive. As a solution to this the FCT method [35] is again utilised. The results given are for two dimensions although the technique generalises to three.

2.6.3.5 Edge Element Methods

A new type of basis function for vector fields has been described in the literature [42, 43] [4, chapter 8]; these 'edge' element basis functions are associated (as their name suggests) with the edge quantities in a mesh rather than the vertex values. The basis functions impose only the tangential continuity of field across element and material interfaces and have been shown to be less susceptible to the problem of spurious solutions [44].

Recently these functions have begun to be used in time domain finite element formulations. In [45] edge elements are used for the basis functions; collocation and the leap frog method yield an explicit solution method for which good accuracy is reported. Instability is mentioned as a problem however and it is suggested that an implicit scheme may be needed to remove this drawback; such a scheme is employed in [46] where the test and basis function sets are identical, giving an implicit, Galerkin, formulation.

2.6.3.6 Discussion of Finite Element Time Domain Methods

In this section a number of time domain methods based on the finite element technique have been described. Due to the use of more complex basis- (and sometimes test-) functions these methods are all capable of handling non-rectilinear structures in a more rigorous fashion than the standard Yee FDTD method.

While an analysis of the computational overheads of all these techniques is not presented here it is well known that both computation time and memory use will increase over that required by FDTD. A particularly dramatic increase in computational requirements results when the algorithms become implicit.

2.6.4 Finite Volume Methods

In Computational Fluid Dynamics (CFD) so-called finite volume methods are widely used. These methods can in many cases be viewed as as finite element methods with element test functions – in other words each test function is unity over a given volume called the 'unit cell' [47]. The resulting algorithms usually result in an integration over the volume of this unit cell.

The finite volume concept of integrating around the unit cell is useful since a global coordinate system is not, as such, required. The finite volume techniques can thus be applied on very irregular grids which do not conform to any particular coordinate system and can therefore be used to characterise curved and angled bodies.

2.6.4.1 Finite Volume-Like Methods

In [39] Madsen *et al.* describe a three dimensional algorithm called the Modified Finite Volume (MFV) capable of solving Maxwell's equations on a non-orthogonal mesh. The algorithm conveniently specialises to the FDTD method when applied on an orthogonal mesh and thus, by applying non-orthogonal cells only where necessary, the computational overheads associated with the non-orthogonal treatment may be minimised. A similar technique is investigated by Holland in [48].

The MFV algorithm was reported to suffer from late-time instability however [39] and so a related algorithm, the Discrete Surface Integral (DSI) method [49], has been proposed. The DSI method has been successfully applied to a range of structures without reported stability problems [50] on a non-orthogonal mesh (see figure 2.5).

The computational overheads associated with the DSI method are considerable, with about 5 times as many operations needed at each iteration and large amounts of storage required for the vector description of the mesh. Like the MFV technique though, the DSI method on an orthogonal mesh reduces to the FDTD method and so the computational costs may be considerably reduced by employing only a locally conforming mesh.

The efficiency of the DSI method on a locally non-orthogonal mesh and the fact that, like the FDTD method but unlike many finite element methods, the method is charge (divergence) preserving, are major considerations in favour of the DSI method [49].

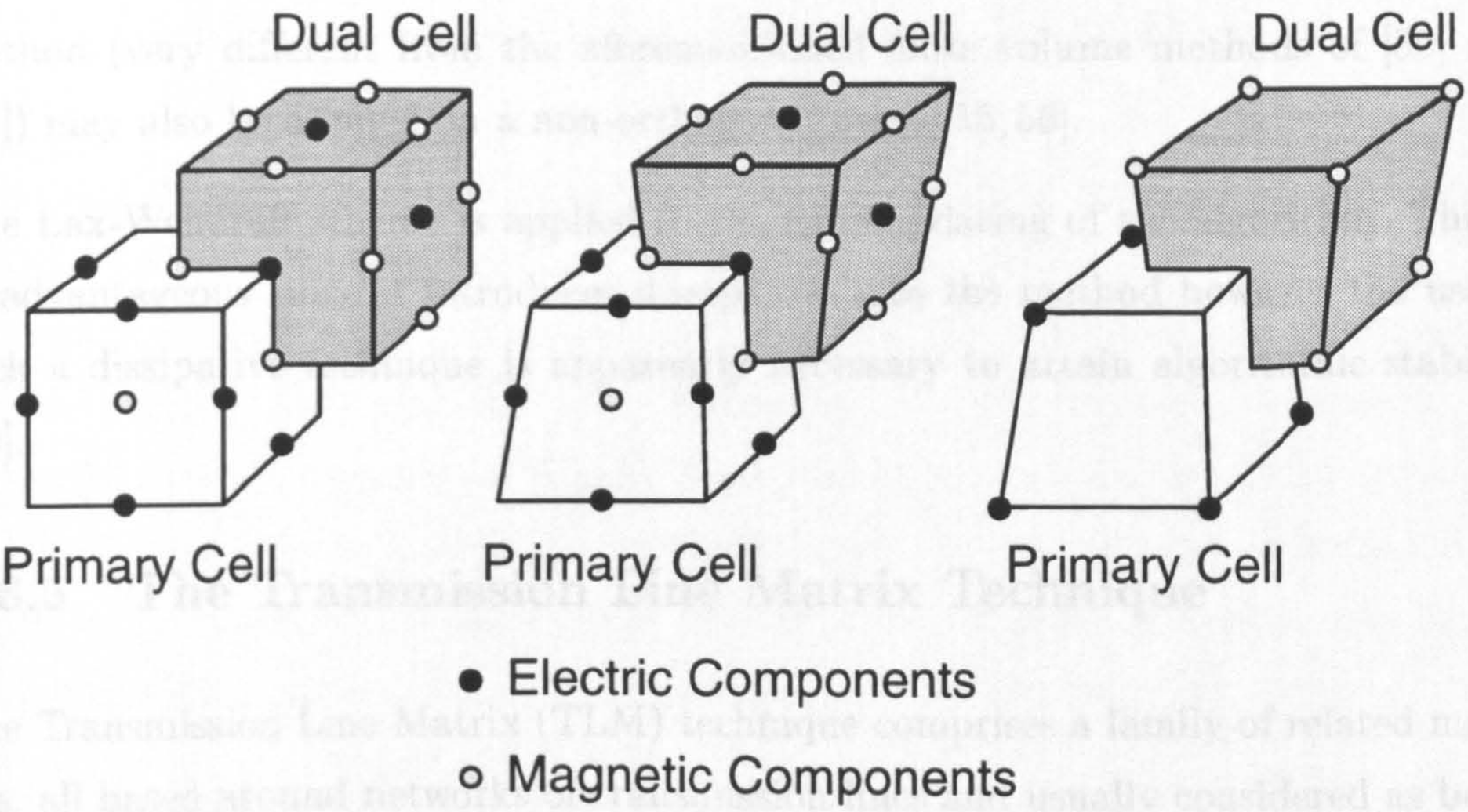

Figure 2.5: Unit cells of (i) FDTD (ii) DSI/MFV (iii) Finite volume method of [51].

The conformal FDTD method of [32], described in section 2.6.2.2, utilises several orthogonal and non-orthogonal FDTD algorithms and interpolates field values between them as necessary. In [51] a finite volume algorithm is used in the non-orthogonal region in preference to the non-orthogonal FDTD technique. This finite volume method renders the interpolation procedure more straightforward since (unlike FDTD, MFV and DSI) it places the unknown fields at the vertices of the unit cells – as shown by figure 2.5).

This hybrid method has been used to characterise several curved structures with far greater accuracy than FDTD [51–53]. Mitigating against the algorithm is the fact that computation time is reported as being of the order of four times greater than that of FDTD and the memory requirements are increased by more than a factor of two [52].

While the above techniques seem to offer the possibility of generalising FDTD to arbitrarily shaped bodies their disadvantages include generally increased demands on computation and storage, complexity of mesh generation and concerns over stability [39, 51, 52, 54].

2.6.4.2 Upwind approach of Shankar *et al.*

An approach inspired by work in CFD is to cast Maxwell's equations in a conservation form and to apply so-called 'upwind' techniques. This 'Time Domain Finite Volume'

method (very different from the aforementioned finite volume methods of [50] and [51]) may also be applied on a non-orthogonal mesh [55, 56].

The Lax-Wendroff scheme is applied to the time updating of the algorithm. This is disadvantageous since it introduces dissipation into the method however the use of such a dissipative technique is apparently necessary to attain algorithmic stability [49].

2.6.5 The Transmission Line Matrix Technique

The Transmission Line Matrix (TLM) technique comprises a family of related methods, all based around networks of transmission lines and usually considered as being based on Huygens' principle rather than Maxwell's equations. The original TLM method was described in two spatial dimensions in 1971 [57] and subsequently in three in 1974 [58].

A number of TLM methods exist, with the two most popular techniques being the original expanded node method (ExpN) [58] and the newer symmetrical condensed node technique (SCN) [59, 60]. The SCN method is usually considered as being of slightly better accuracy than the ExpN model [61] at the expense of a small increase in computational effort – recent contributions suggest however that the the newer method may suffer from larger errors in some circumstances [62].

An alternative technique is the so-called Bergeron Method [63] which employs a spatial network having many similarities with the expanded node TLM network; its authors have indeed described the method as a 'refined TLM technique' [64].

While the TLM methods seem quite distinct from the other time domain Differential methods discussed in this chapter (being not usually derived from Maxwell's equations) these are included here as they have many features in common with the other techniques; recent publications have shown for example that the various TLM methods can, like FDTD, be derived from a finite element approach [65, 66]. The relationship between ExpN TLM and FDTD in particular has long been a subject for debate [67, 68] – some authors describe the methods as 'formally equivalent' [69] with the TLM technique being the less efficient of the two.

2.7 Further Aspects of the Yee FDTD Method

In section 2.6.2 it was shown that the FDTD method can be viewed as a particular instance of the time domain finite element solution of Maxwell's equations. The method is popular since the algorithm is explicit (the mass matrices are diagonal) and the storage and computation requirements for each unit cell are modest. The principle disadvantage of the standard method is its poor treatment of structures which do not conform to FDTD's orthogonal grid – to date no alternative algorithm has been proposed which can counter this drawback without incurring considerable computational overheads (see the discussion earlier in this chapter).

In this section some of the practical aspects of implementing the FDTD method to model inhomogeneous bodies are introduced. For a more detailed introduction to the FDTD method the reader is referred to [70] and [71].

2.7.1 Spatial Discretisation

As previously discussed, the FDTD method proceeds by dividing the modelled volume into a mesh of unit cells. The algorithm solves for each of the 6 field components in each unit cell at each time iteration. It is clear then that it is desirable to keep the number of unit cells and the number of time steps at a minimum if the computational demands of the algorithm are not to become excessive.

The dimensions of the unit cells in the x, y and z directions are throughout this thesis denoted as Δ_x, Δ_y and Δ_z (and when direction is not of interest the symbol Δ will be used). In practice the maximum size of the unit cells is limited by geometrical detail around a structure and by the requirement for wavelength resolution otherwise.

A heuristic criterion often applied for wavelength resolution is:

$$\Delta < \frac{c_0}{10 f_{\text{highest}} \sqrt{\epsilon_r}} \tag{2.40}$$

where f_{highest} is the the highest frequency of interest. If this limit is broken then numerical dispersion and anisotropy will become significant as a result of the piece-wise linear basis functions no longer being a sufficiently good description of the field variation. This is illustrated by figure 2.6.

In practice however the problem will contain geometrical detail and in this case the unit cell dimension will have to be small enough to resolve the features of the object

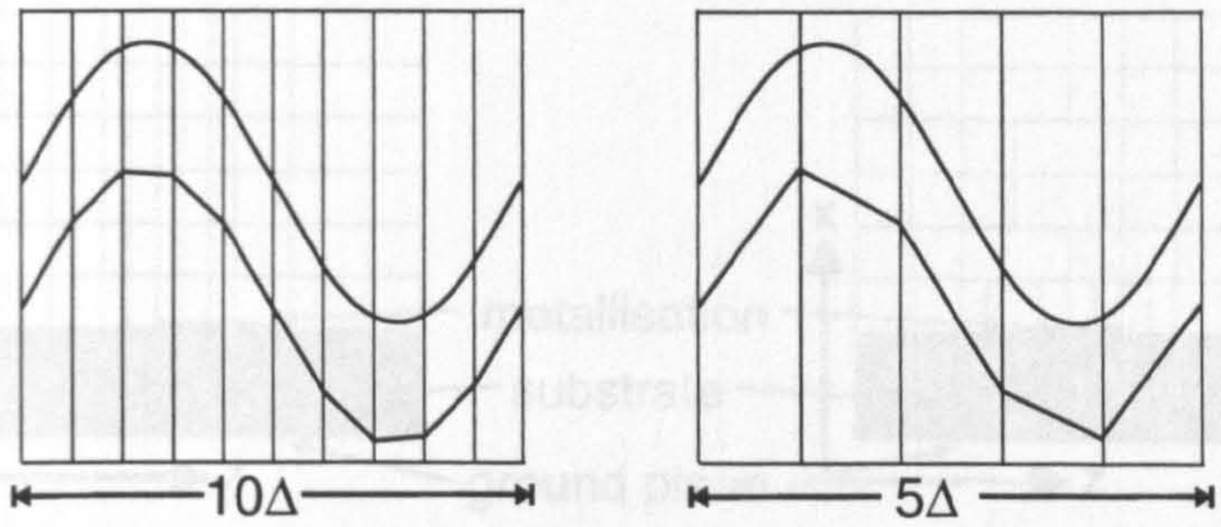

Figure 2.6: Sine wave and its piecewise linear representation on meshes with resolutions $\Delta = \lambda/10$ and $\Delta = \lambda/5$.

and model the surrounding field variation. This is often a more stringent criterion for Δ than the straightforward requirement for wavelength resolution.

In general FDTD can be applied on a uniform mesh (where $\Delta_x = \Delta_y = \Delta_z = \Delta$), on an axis uniform mesh (where $\Delta_x \neq \Delta_y \neq \Delta_z$) and on an axis graded mesh (where Δ_x, Δ_y and Δ_z are functions of space). These three cases are illustrated (in two dimensions) by figure 2.7.

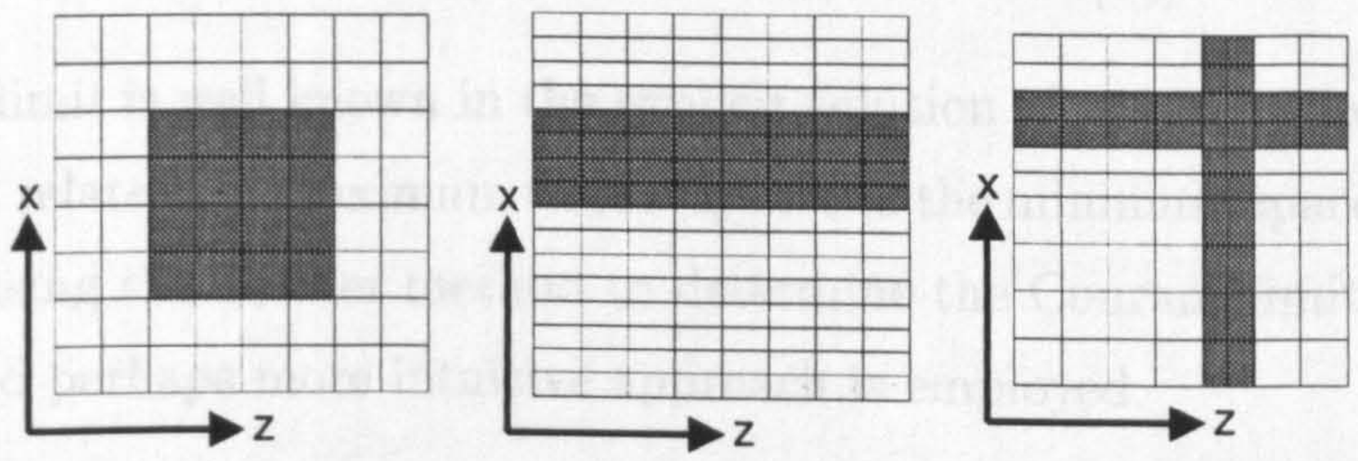

Figure 2.7: (i) Uniform, (ii) axis uniform and (iii) axis graded meshes.

The axis graded mesh is useful since, when a small geometrical feature must be described, the fine discretisation need not be employed everywhere else also. The graded mesh is not ideal however since some unnecessary refinement will almost certainly be introduced, as shown for the case of discretising a microstrip in figure 2.8 – a more satisfactory scheme would be the completely local refinement also shown by figure 2.8, achieving such a refinement however is not straightforward [72, 73].

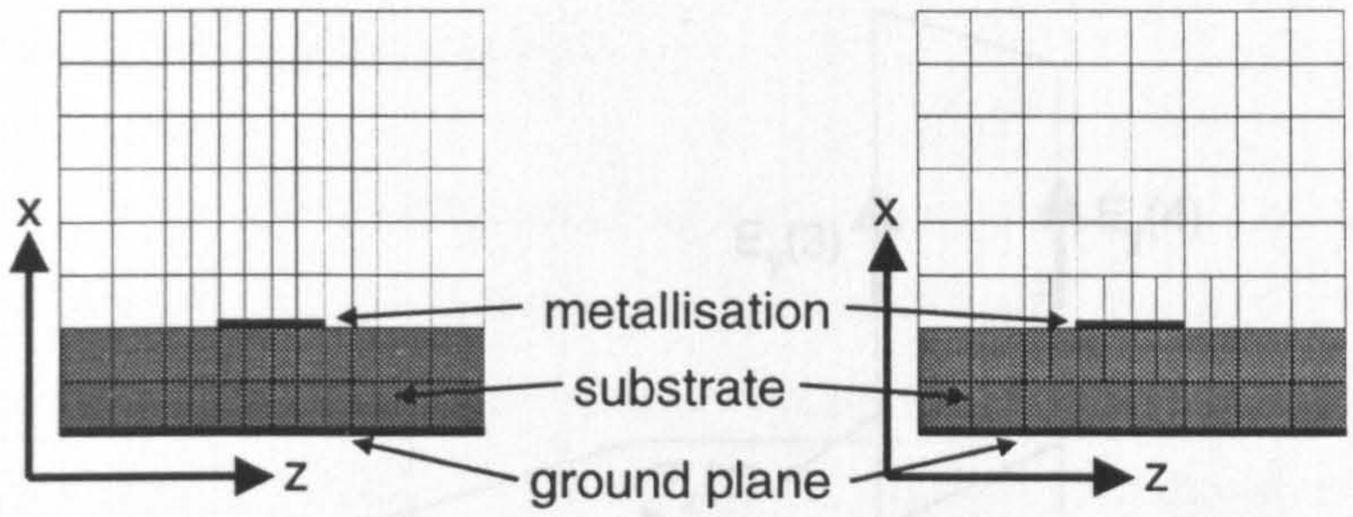

Figure 2.8: Microstrip cross-section with (i) Graded mesh (ii) Locally refined mesh.

2.7.2 The Time Step

The issue of the size of the time step Δ_t might also be thought to be one of sufficient sampling, thus:

$$\Delta_t < \frac{1}{10 f_{\text{highest}}} \tag{2.41}$$

in fact it is well known that the value of time step will usually have to be considerably smaller than this value, due to the so-called Courant limit [74].

The Courant limit is well known in the explicit solution of propagation problems [75, chapter 4] and relates the maximum time step size to the minimum space step. Instead of, as usual, using the Fourier method to determine the Courant limit for FDTD an instructive and perhaps more intuitive approach is employed.

Figure 2.9 shows the FDTD unit cell once more. The Courant limit arises because, while the speed of an electromagnetic wave is fixed by Maxwell's equations, the speed at which a FDTD numerical solution can propagate in the mesh is limited to a speed where the solution travels one node in any *axis direction* every iteration.

It is clear, then, that considering a wave travelling along the z axis in figure 2.9 the FDTD solution will travel from $E_y(1)$ to $E_y(2)$ in a time Δ_t. Thus the speed of the numerical solution in the z direction is Δ/Δ_t which must obviously be greater than c if the numerical solution is to be able to keep up with the real one.

The worse case however is to consider a wave travelling diagonally from $E_y(1)$ to $E_y(4)$. The numerical solution will take a minimum of three time steps to travel this distance (passing via $E_x(1)$ and $E_y(3)$ say). The actual distance travelled is $\sqrt{3}\Delta$ so the effective speed is $\sqrt{3}\Delta/3\Delta_t$ thus it can be seen that:

$$\Delta_t \leq \frac{\Delta}{\sqrt{3}c} \tag{2.42}$$

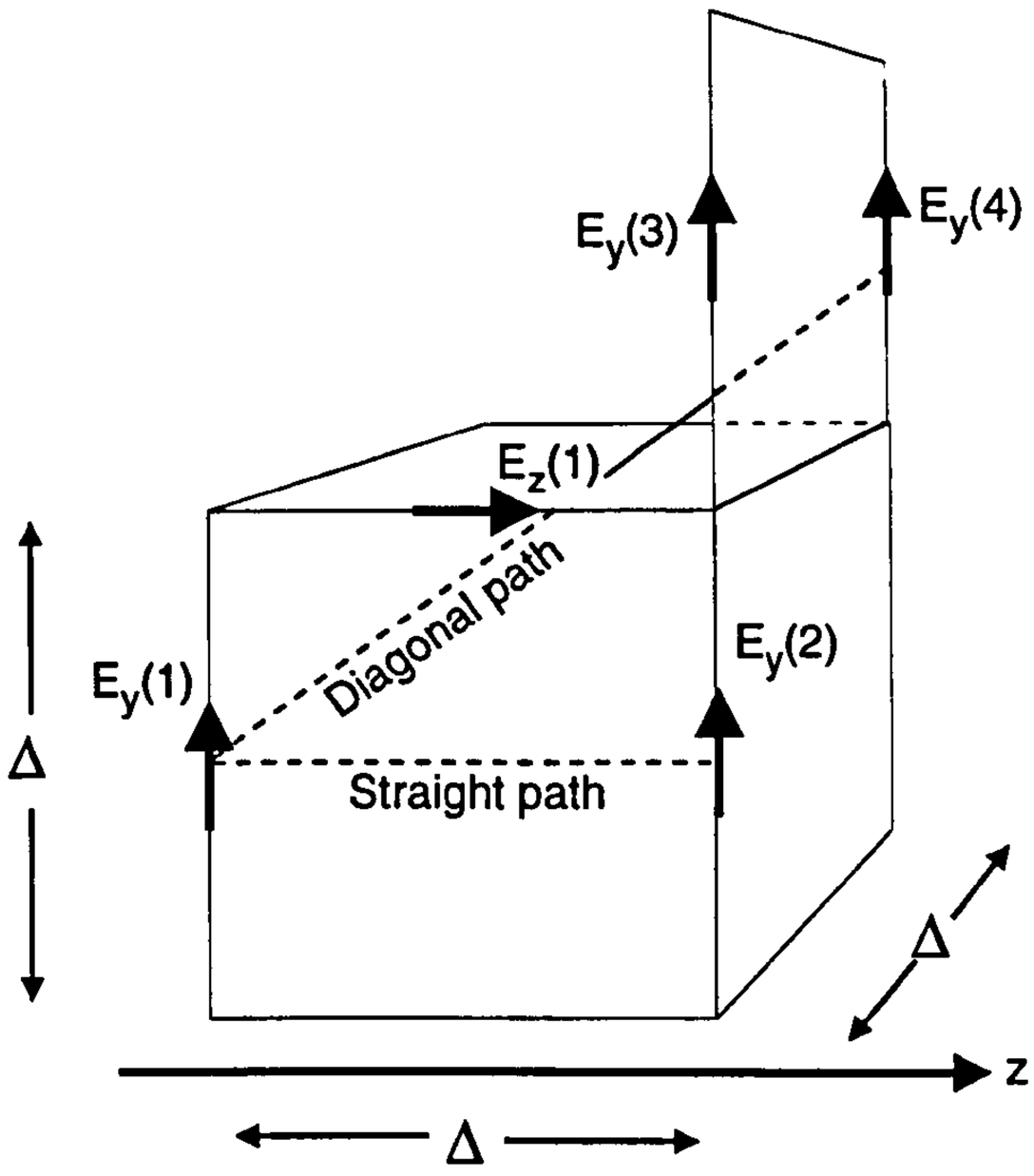

Figure 2.9: Illustration of Courant stability limit for FDTD

which is the Courant limit for FDTD with a uniform mesh.

At first sight this does not seem to impose too severe a limit on the FDTD time step; it is straightforward to show that with $\Delta \approx \lambda/10$ the time step will give $10\sqrt{3}$ (about 17) samples per cycle rather than the 10 that would be expected. The real difficulty comes however when it is considered that Δ will be the smallest cell width in the problem space and will be dictated by the size of the smallest geometrical feature (usually much smaller than $\lambda/10$) – resulting in a FDTD algorithm with perhaps several hundred time steps per cycle.

The Courant condition applies equally well to any other explicit solution to a propagation problem. From chapter 1 it is recalled that Richardson's computation of a solution to the equations of atmospheric motion suffered from instability; the root cause of this phenomenon was that the atmospheric equations that Richardson set out to solve were so general as to include sound waves which travel at over 600 miles an hour. These phenomena have no significant rôle in the far slower process of weather evolution and are neglected in modern numerical weather models in order to satisfy the Courant criterion without introducing a very small time step. Richardson's time step, chosen from the point of view of sufficient sampling, was insufficiently small and instability was the unfortunate result.

2.7.3 Boundary Conditions

As discussed in section 2.4.3 Differential methods require boundary conditions to be imposed on the solution (whereas the boundary conditions are implicit in the Integral methods). In some cases the problem to be analysed can be bounded by Perfectly Electrically Conducting (PEC) walls and this condition is easily implemented by FDTD.

In many cases however the object being modelled exists in free space and the computational domain of the Differential method (in this case FDTD) must be bounded in such a way as to allow energy to be radiated from the modelled object without being reflected back at it. This type of boundary condition is widely known as a Radiating Boundary Condition (RBC) and its implementation in FDTD has been the subject of considerable research [76].

Various approaches have been taken to implement an RBC for FDTD. The most obvious technique is to 'line' the FDTD boundary with some sort of electrically lossy material in order that the radiating energy may be absorbed (this type of boundary is sometimes known as an ABC or 'Absorbing Boundary Condition') – examples of the use of this technique can be found in [77] and [78] (the latter including magnetic loss terms in addition to the electric losses).

Rather than introduce fictitious lossy layers into the FDTD algorithm most boundary conditions apply discrete approximations based on a discretisation of a one-way wave operator [70, 79]. The most popular boundary condition for use with FDTD has probably been the so-called Mur first order boundary described in [80], this condition provides usually adequate absorption of radiated energy, particularly when the energy is normally incident upon the boundary.

A recent development has been the concept of a 'Perfectly Matched Layer' (PML) which, it has been shown, can result in extremely low levels of reflection [81]. This technique, like those of [77] and [78] relies upon the use of an absorbing layer but extends the concept considerably to yield extremely low levels of reflection (potentially of the order of -80dB [82]). This new method introduces some computational overhead over the Mur first order method [83].

In general the implementation of a RBC will be a trade-off between the tolerable level of reflected waves and the computational overhead in implementing the condition.

In some applications the results obtained are not particularly sensitive to reflected energy – in which case a simple first order Mur condition may be adequate, in others the computational effort involved in implementing a more sophisticated technique may well be justified.

2.7.4 Further Modelling Considerations

In the above discussion some of the most fundamental aspects of the Yee FDTD method have been introduced; namely the spatial mesh, the time step and its relation by means of the Courant limit to the unit cell size, and the boundary conditions.

A host of other factors must be considered when implementing a FDTD method, among which the excitation (or source), the treatment of dielectric interfaces and the transformation of time domain results to the frequency domain could numbered. For a discussion of these issues see, for example, [70] and [71].

2.8 Summary

It has been seen in this chapter that a wide range of numerical electromagnetic analysis techniques can be divided into Integral methods (those which solve an integral or integro-differential equation involving a Greens function) and Differential methods (which are applied directly to Maxwell's differential equations).

Consideration has been given in particular to the time domain Differential methods and how these may be implemented using the finite element or similar procedures. The merits of a reasonably comprehensive cross section of published finite element, finite difference, finite volume and transmission line matrix techniques have been considered and it has been shown that the properties of the Yee FDTD method [24] make it an attractive method for time domain analysis.

Alternative methods to the Yee algorithm have mostly been proposed to counter FDTD's poor treatment of curved objects. These proposed methods are generally not as computationally efficient as the standard FDTD algorithm (and indeed may not even be explicit).

It is the FDTD method that will be the main focus of the rest of this thesis and therefore the examination of numerical methods has been concluded by consideration

of the Yee FDTD method in more detail. The important concepts of the spatial discretisation, the time step and the boundary conditions have all been introduced.

References

[1] T. Itoh, *Numerical Techniques for Microwave and Millimeter-Wave Passive Structures.* John Wiley and Sons, 1989.

[2] J. J. H. Wang, *Generalised Moment Methods in Electromagnetics.* John Wiley and Sons, 1991.

[3] J. C. Maxwell, *A Treatise on Electricity and Magnetism.* Dover Publications, 3 ed., 1954. Work originally published in 1873.

[4] J. Jin, *The Finite Element Method in Electromagnetics.* John Wiley and Sons, 1993.

[5] M. A. Morgan, "Finite methods," in *Progress in Electromagnetics Research 2 - Finite Element and Finite Difference Methods in Electromagnetic Scattering* (M. A. Morgan, ed.), Elsevier Science Publishing, 1990.

[6] R. A. Horn and C. A. Johnson, *Matrix Analysis.* Cambridge University Press, 1985.

[7] J. R. Westlake, *A Handbook of Numerical Matrix Inversion and Solution of Linear Equations.* Prentice Hall, 1968.

[8] R. F. Harrington, *Field Computation by Moment Methods.* IEEE Press, 1993. Originally published by MacMillan Publishing Company.

[9] S. A. Meade and C. J. Railton, "Efficient implementation of the spectral domain method including precalculated corner basis functions," *IEEE Transactions on Microwave Theory and Techniques*, pp. 1678–1684, Sept. 1994.

[10] R. F. Hoskins, *Generalised Functions.* Ellis Horwood Limited, 1979.

[11] K. Umashankar and A. Taflove, *Computational Electromagnetics.* Artech House, 1993.

[12] R. H. Jansen, "The spectral domain approach for microwave integrated circuits," *IEEE Transactions on Microwave Theory and Techniques*, vol. MTT-33, pp. 1043–1056, Oct. 1985.

[13] M. R. Hestenes, *Conjugate Direction Methods in Optimisation.* Springer Verlag, 1980.

[14] G. D. Smith, *Numerical Solution of Partial Differential Equations: Finite Difference Methods.* Oxford University Press, 2 ed., 1978.

[15] B. M. A. Rahman and J. B. Davies, "Penalty function improvement of waveguide solution by finite elements," *IEEE Transactions on Microwave Theory and Techniques*, vol. MTT-32, pp. 922–928, Aug. 1984.

[16] B. H. McDonald and A. Wexler, "Finite element solution of unbounded field problems," *IEEE Transactions on Microwave Theory and Techniques*, vol. MTT-20, pp. 841–847, Dec. 1972.

[17] J. M. Jin and J. L. Volakis, "A finite element boundary integral formulation for scattering by three dimensional cavity backed apertures," *IEEE Transactions on Antennas and Propagation*, vol. AP-39, pp. 97–104, Jan. 1991.

[18] S. M. Rao and D. R. Wilton, "Transient scattering by conducting surfaces of arbitrary shape," *IEEE Transactions on Antennas and Propagation*, vol. AP-39, pp. 56–61, Jan. 1991.

[19] B. P. Rynne, "Stability and convergence of time marching methods in scattering problems," *IMA Journal of Applied Mathematics*, vol. 35, no. 3, pp. 297–310, 1985.

[20] B. P. Rynne and P. D. Smith, "Stability of time marching methods for the electric field integral equation," *Journal of Electromagnetic Waves and Applications*, vol. 4, no. 12, pp. 1181–1205, 1990.

[21] W. L. Wood, *Practical Time Stepping Schemes.* Clarendon Press, 1990.

[22] D. R. Lynch and K. D. Paulsen, "Time domain integration of the Maxwell equations on finite elements," *IEEE Transactions on Antennas and Propagation*, vol. AP-38, pp. 1933–1942, Dec. 1990.

[23] K. H. Huebner, *The Finite Element Method for Engineers.* John Wiley and Sons, 1975.

[24] K. S. Yee, "Numerical solution of initial boundary value problems involving Maxwell's equations in isotropic media," *IEEE Transactions on Antennas and Propagation*, vol. AP-14, pp. 302–307, May 1966.

[25] A. C. Cangellaris and D. B. Wright, "Analysis of the numerical error caused by the stair-stepped approximation of a conducting boundary in FDTD simulations of electromagnetic phenomena," *IEEE Transactions on Antennas and Propagation*, vol. AP-39, pp. 1518–1525, Oct. 1991.

[26] R. Holland, "Pitfalls of staircase meshing," *IEEE Transactions on Electromagnetic Compatibility*, vol. EMC-35, pp. 434–439, Nov. 1993.

[27] R. Holland and J. R. Hill, "Self consistent atmospheric EMP coupling in three dimensions," *IEEE Transactions on Nuclear Science*, vol. NS-23, pp. 1283–1293, Dec. 1976.

[28] R. Holland, "THREDS: A finite difference time domain EMP code in 3D spherical co-ordinates," *IEEE Transactions on Nuclear Science*, vol. NS-30, pp. 4592–4595, Dec. 1983.

[29] R. Holland, "Finite difference solutions of Maxwells equations in generalised non-orthogonal coordinates," *IEEE Transactions on Nuclear Science*, vol. NS-30, pp. 4589–4591, Dec. 1983.

[30] M. Fusco, "FDTD algorithm in curvilinear coordinates," *IEEE Transactions on Antennas and Propagation*, vol. AP-38, pp. 76–89, Jan. 1990.

[31] P. H. Harms, J.-F. Lee, and R. Mittra, "A study of the nonorthogonal FDTD method versus the conventional FDTD technique for computing resonant frequencies of cylindrical cavities," *IEEE Transactions on Microwave Theory and Techniques*, vol. MTT-40, pp. 741–746, Apr. 1992.

[32] K. S. Yee, J. S. Chen, and A. H. Chang, "Conformal finite difference time domain (FDTD) with overlapping grids," *IEEE Transactions on Antennas and Propagation*, vol. AP-40, pp. 1068–1075, Sept. 1992.

[33] S. R. Omick and S. P. Castillo, "A new finite difference time domain algorithm for the accurate modeling of wide band electromagnetic phenomena," *IEEE Transactions on Electromagnetic Compatibility*, vol. EMC-35, pp. 215–222, May 1993.

[34] P. D. Lax and B. Wendroff, "Systems of conservation laws," *Communications in Pure and Applied Mathematics*, vol. 13, pp. 217–237, May 1960.

[35] S. T. Zalesak, "Fully multidimensional flux corrected transport algorithms for fluids," *Journal of Computational Physics*, vol. 31, pp. 335–362, June 1979.

[36] A. C. Cangellaris, C. Lin, and K. K. Mei, "Point matched time domain finite element methods for electromagnetic radiation and scattering," *IEEE Transactions on Antennas and Propagation*, vol. AP-35, pp. 1160–1173, Oct. 1987.

[37] A. C. Cangellaris, "Time domain finite methods for electromagnetic wave propagation and scattering," *IEEE Transactions on Magnetics*, vol. MAG-27, pp. 3780–3785, Sept. 1991.

[38] N. K. Madsen and R. W. Ziolkowski, "Numerical solution of Maxwell's equations in the time domain using irregular nonorthogonal grids," *Wave Motion*, vol. 10, no. 6, pp. 583–596, 1988.

[39] N. K. Madsen and R. W. Ziolkowski, "A 3 dimensional modified finite volume technique for Maxwell's equations," *Electromagnetics*, vol. 10, no. 1–2, pp. 147–161, 1990.

[40] D. R. Lynch and K. D. Paulsen, "Origin of vector parasites in numerical Maxwell solutions," *IEEE Transactions on Microwave Theory and Techniques*, vol. MTT-39, pp. 383–394, Mar. 1991.

[41] J. J. Ambrosiano, S. T. Brandon, R. Lohner, and C. R. DeVore, "Electromagnetics via the Taylor Galerkin finite element method on unstructured grids," *Journal of Computational Physics*, vol. 110, pp. 310–319, Feb. 1994.

[42] J. C. Nedelec, "Mixed finite elements in R^3," *Numerische Mathematik*, vol. 35, pp. 315–341, 1980.

[43] A. Bossavit and J. C. Verite, "A mixed FEM-BIEM method to solve 3-D eddy current problems," *IEEE Transactions on Magnetics*, vol. MAG-18, pp. 431–435, Mar. 1982.

[44] A. Bossavit, "Solving Maxwell's equations in a closed cavity and the question of spurious modes," *IEEE Transactions on Magnetics*, vol. MAG-26, pp. 702–705, Mar. 1990.

[45] G. Mur, "A mixed finite element method for computing three dimensional time domain elactromagnetic fields in strongly inhomogenous media," *IEEE Transactions on Magnetics*, vol. MAG-26, pp. 674–677, Mar. 1990.

[46] J.-F. Lee, "WETD – a finite element time domain approach for solving Maxwell's equations," *IEEE Microwave and Guided Wave Letters*, vol. 4, pp. 11–13, Jan. 1994.

[47] W. K. Morton and E. Suli, "Finite volume methods and their analysis," *IMA Journal of Mathematical Analysis*, vol. 11, no. 2, pp. 241–260, 1991.

[48] R. Holland, V. P. Cable, and L. C. Wilson, "Finite volume time domain (FVTD) techniques for EM scattering," *IEEE Transactions on Electromagnetic Compatibility*, vol. EMC-33, pp. 281–294, Nov. 1991.

[49] N. K. Madsen, "Divergence preserving discrete surface integral methods for Maxwell's curl equations using non-orthogonal unstructured grids," *RIACS Technical Report*, pp. 147–161, Feb. 1992.

[50] N. K. Madsen, "Divergence preserving discrete surface integral methods for Maxwell's curl equations using non-orthogonal unstructured grids," *Journal of Computational Physics*, vol. 119, pp. 34–45, 1995.

[51] K. S. Yee and J. S. Chen, "Conformal hybrid finite difference time domain and finite volume time domain," *IEEE Transactions on Antennas and Propagation*, vol. AP-42, pp. 1450–1455, Oct. 1994.

[52] K. S. Yee and J. S. Chen, "Hybrid finite difference time domain and finite volume time domain in solving Maxwell's equations," in *ACES 1995 Conference Proceedings*, Mar. 1995.

[53] B. Singh and A. C. Marvin, "Hybrid finite volume finite difference time domain modelling of curved surfaces," *Electronics Letters*, vol. 31, pp. 352–353, Mar. 1995.

[54] K. S. Yee, "Ten years of evolution of the FDTD-like conformal techniques," in *ACES 1995 Conference Proceedings*, Mar. 1995.

[55] V. Shankar, W. F. Hall, and A. H. Mohammadian, "A time domain differential solver for electromagnetic scattering problems," *Proceedings of the IEEE*, vol. 77, pp. 709–720, May 1989.

[56] A. H. Mohammadian, V. Shankar, and W. F. Hall, "Application of the time domain finite volume method to some radiation problems in two and three dimensions," *IEEE Transactions on Magnetics*, vol. MAG-27, pp. 3841–3844, Sept. 1991.

[57] P. B. Johns and R. L. Beurle, "Numerical solution of 2 dimensional scattering problems using a transmission line matrix," *Proceedings of the IEE*, vol. 118, pp. 1203–1208, Sept. 1971.

[58] S. Akhtarzad and P. B. Johns, "Solution of 6-component electromagnetic fields in three space dimesions and time by the TLM method," *Electronics Letters*, vol. 10, pp. 535–537, Dec. 1974.

[59] P. B. Johns, "New symmetrical condensed node for three dimensional solution of electromagnetic wave problems by TLM," *Electronics Letters*, vol. 22, pp. 162–164, Jan. 1986.

[60] P. B. Johns, "A symmetrical condensed node for the TLM method," *IEEE Transactions on Microwave Theory and Techniques*, vol. MTT-35, pp. 370–377, Jan. 1987.

[61] R. Allen, A. Mallik, and P. B. Johns, "Numerical results for the symmetrical condensed TLM node," *IEEE Transactions on Microwave Theory and Techniques*, vol. MTT-35, pp. 378–382, Apr. 1987.

[62] M. Celuch-Marcysiak and W. K. Gwarek, "On the effect of bilateral dispersion in inhomogenous symmetrical condensed node scattering," *IEEE Transactions on Microwave Theory and Techniques*, vol. MTT-42, pp. 1069–1073, June 1994.

[63] N. Yoshida, I. Fukai, and J. Fukuoka, "Transient analysis of two-dimensional Maxwell's equations by Bergeron's method," *IECE Transactions Japan*, vol. J62-B, pp. 511–518, June 1979.

[64] T. Shibata, T. Hayashi, and T. Kimura, "Analysis of microstrip circuits using a three dimensional full wave electromagnetic field analysis in the time domain," *IEEE Transactions on Microwave Theory and Techniques*, vol. MTT-36, pp. 1064–1070, June 1988.

[65] P. Russer and M. Krumpholtz, "The Hilbert space formulation of the TLM method," *International Journal of Numerical Modelling: Electronic Networks, Devices and Fields*, vol. 6, pp. 29–45, Feb. 1993.

[66] M. Krumpholtz and P. Russer, "A field theoretical derivation of TLM," *IEEE Transactions on Microwave Theory and Techniques*, vol. MTT-42, pp. 1660–1668, Sept. 1994.

[67] P. B. Johns, "On the relationship between the TLM and finite difference method for Maxwell's equations," *IEEE Transactions on Microwave Theory and Techniques*, vol. MTT-35, pp. 60–61, Jan. 1987.

[68] W. K. Gwarek, "Comments on: On the relationship between the TLM and finite difference method for Maxwell's equations," *IEEE Transactions on Microwave Theory and Techniques*, vol. MTT-35, pp. 872–873, Sept. 1987.

[69] M. Celuch-Marcysiak and W. K. Gwarek, "Formal equivalence and efficiency comparison of the FDTD, TLM and SN methods in application to microwave CAD programs," in *21st European Microwave Conference Proceedings*, vol. 1, pp. 199–204, 1991.

[70] A. Taflove and K. R. Umashankar, "The finite difference time domain method for numerical modeling of electromagnetic wave interactions with arbitrary structures," in *Progress in Electromagnetics Research 2 - Finite Element and Finite Difference Methods in Electromagnetic Scattering* (M. A. Morgan, ed.), Elsevier Science Publishing, 1990.

[71] K. S. Kunz and R. J. Luebbers, *The Finite Difference Time Domain Method for Electromagnetics*. CRC Press, 1993.

[72] S. S. Zivanovic, K. S. Yee, and K. K. Mei, "A subgridding method for the time domain finite difference method to solve Maxwell's equations," *IEEE Transactions on Microwave Theory and Techniques*, vol. MTT-39, pp. 471–479, Mar. 1991.

[73] D. T. Prescott and N. V. Shuley, "A method for incorporating different sized cells into the finite difference time domain analysis technique," *IEEE Microwave and Guided Wave Letters*, vol. 2, pp. 434–436, Nov. 1992.

[74] R. Courant, K. Friedrichs, and H. Lewy, "Über die partiellen Differenzengleichungen der mathematischen Physik," *Mathematische Annalen*, vol. 100, pp. 32–74, 1928.

[75] W. F. Ames, *Numerical Methods for Partial Differential Equations.* Thomas Nelson and Sons, 1969.

[76] C. J. Railton, E. M. Daniel, D. P. Paul, and J. P. McGeehan, "Optimized absorbing boundary-conditions for the analysis of planar circuits using the finite-difference time-domain method," *IEEE Transactions on Microwave Theory and Techniques*, vol. MTT-41, pp. 290–297, Feb. 1993.

[77] A. Taflove and M. E. Brodwin, "Numerical solution of steady state electromagnetic scattering problems using the time dependent Maxwell's equations," *IEEE Transactions on Microwave Theory and Techniques*, vol. MTT-23, pp. 623–630, Aug. 1975.

[78] A. Reineix and B. Jecko, "Analysis of microstrip patch antennas using the finite difference time domain technique," *IEEE Transactions on Antennas and Propagation*, vol. AP-37, pp. 1361–1369, Nov. 1989.

[79] B. Engquist and A. Majda, "Absorbing boundary conditions for the numerical simulation of waves," *Mathematics of Computation*, vol. 31, pp. 629–651, July 1977.

[80] G. Mur, "Absorbing boundary conditions for the finite difference approximation of the time domain elecromagnetic field equations," *IEEE Transactions on Electromagnetic Compatibility*, vol. EMC-23, pp. 377–382, Nov. 1981.

[81] J.-P. Berenger, "A perfectly matched layer for the absorption of electromagnetic waves," *Journal of Computational Physics*, vol. 114, no. 2, pp. 185–200, 1994.

[82] C. E. Reuter, R. M. Joseph, E. T. Thiele, D. S. Katz, and A. Taflove, "Ultra-wideband absorbing boundary condition for termination of waveguiding structures in FDTD simulations," *IEEE Microwave and Guided Wave Letters*, vol. 4, pp. 344–346, Oct. 1994.

[83] D. S. Katz, E. T. Theile, and A. Taflove, "Validation and extension to three dimensions of the Berenger PML boundary condition for FDTD meshes," *IEEE Microwave and Guided Wave Letters*, vol. 4, pp. 268–270, Aug. 1994.

Chapter 3

Near Field Transformation and System Identification

3.1 Introduction

Various practical aspects of the FDTD method were introduced in section 2.7. It was shown (see section 2.7.1) that, in order to minimise the computational overheads of the algorithm, the number of unit cells used to discretise the computational volume should be kept to a minimum. This implies that:

i . The unit cell dimensions should be as large as possible (means for ensuring this are discussed in chapters 4, 5 and 6).

ii . The computational volume should be as small as possible.

The size of the computational volume must be sufficient to encompass the structure of interest, additionally however if the fields are required at points some distance from the structure then the volume must extend to these points. In the case of evaluating the far field of an scatterer or antenna for example, it follows from (ii) above that this is extremely undesirable; the structure may have dimensions of less than one wavelength however the computational volume is required to extend a distance of at least ten wavelengths in order to evaluate the far fields. Such a dramatic increase in the size of the computational volume would in most circumstances make the analysis impractical.

This chapter describes a technique (known as a near to far transform) which can extrapolate the near fields into the far zone. By employing a transform of this kind the FDTD algorithm need only be used to calculate the near fields (those adjacent to the structure) and thus the determination of the far field, accomplished by the extrapolation of these near fields, no longer requires a large computational volume. An implementation of this transform is described and its accuracy when applied to a relatively complex structure is evaluated. The time domain near far transform given here is based on [1, 2] and its implementation was a continuation of work described in [3, chapter 6].

A third cause of large computational overheads in FDTD (and indeed any time domain method) is the treatment of highly resonant structures. In the analysis of these structures the transient response decays only slowly to a point where it may be considered complete and, as a result, the number of required algorithm iterations may become large. Section 3.6.1 describes and applies one method which is capable of

reducing the number of iterations needed to characterise a resonant object.

3.2 The Near Far Transformation

In order to develop a method for transforming the FDTD-calculated near fields to the far field, the equivalence principle is be employed. This principle states that the fields exterior to a closed surface S are unchanged if the fields inside S are set to zero and equivalent electric and magnetic currents $\mathbf{J}_{\text{eq}}$ and $\mathbf{M}_{\text{eq}}$ flow on S with the values:

$$\begin{aligned} \mathbf{J}_{\text{eq}}(\mathbf{r}', t) &= \hat{\mathbf{n}}(\mathbf{r}') \times \mathbf{H}_s(\mathbf{r}', t) \\ \mathbf{M}_{\text{eq}}(\mathbf{r}', t) &= -\hat{\mathbf{n}}(\mathbf{r}') \times \mathbf{E}_s(\mathbf{r}', t) \end{aligned} \tag{3.1}$$

where $\hat{\mathbf{n}}$ is the unit vector normal to S at $\mathbf{r}'$ and $\mathbf{E}_s$ $\mathbf{H}_s$ are the fields on S [4]. This situation is illustrated by figure 3.1.

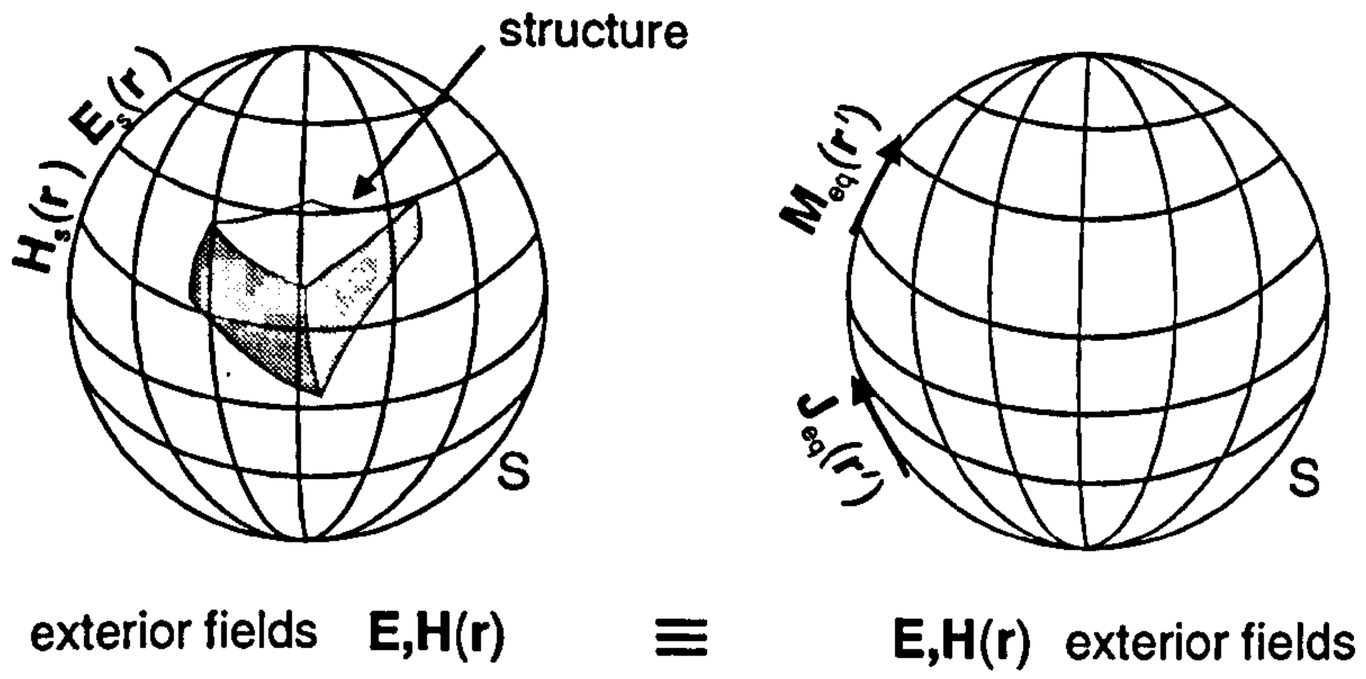

Figure 3.1: Equivalence principle.

In order to determine the far field at a point $\mathbf{r}$ (called an 'observation point') external to S, the retarded vector potentials $\mathbf{A}$ and $\mathbf{F}$:

$$\begin{aligned} \mathbf{A}(\mathbf{r}, t) &= \frac{1}{4\pi} \int_S \frac{\mathbf{J}_{\text{eq}}(\mathbf{r}', t - \tau)}{|\mathbf{r} - \mathbf{r}'|}\, dS \\ \mathbf{F}(\mathbf{r}, t) &= \frac{1}{4\pi} \int_S \frac{\mathbf{M}_{\text{eq}}(\mathbf{r}', t - \tau)}{|\mathbf{r} - \mathbf{r}'|}\, dS \end{aligned} \tag{3.2}$$

are used, where $\tau = |\mathbf{r} - \mathbf{r}'|/c$. In the far field the attenuation factor $|\mathbf{r} - \mathbf{r}'|^{-1}$ can be considered equal to $|\mathbf{r}|^{-1}$ and taken outside of each integral giving:

$$\begin{aligned} \mathbf{A}(\mathbf{r}, t) &= \frac{1}{4\pi|\mathbf{r}|} \int_S \mathbf{J}_{\text{eq}}(\mathbf{r}', t - \tau)\, dS \\ \mathbf{F}(\mathbf{r}, t) &= \frac{1}{4\pi|\mathbf{r}|} \int_S \mathbf{M}_{\text{eq}}(\mathbf{r}', t - \tau)\, dS \end{aligned} \tag{3.3}$$

In order to find the actual fields **E** and **H** at **r**, expressions (9) and (10) of [2] may be employed:

$$E_\theta(\mathbf{r},t) = -\frac{1}{\epsilon}\partial_t A_\theta(\mathbf{r},t) + \frac{1}{c}\partial_t F_\phi(\mathbf{r},t)$$
$$E_\phi(\mathbf{r},t) = -\frac{1}{\epsilon}\partial_t A_\phi(\mathbf{r},t) - \frac{1}{c}\partial_t F_\theta(\mathbf{r},t) \tag{3.4}$$

The results (3.4) and (3.3) give the spherical components of the electric far field at $(\mathbf{r},t)$ as produced by the equivalent currents on S at $(\mathbf{r}',t-\tau)$. Given that the equivalent currents may be produced from the tangential fields on the surface using (3.1), this provides the required means of transforming FDTD results into the far field.

3.3 Transformation Implementation

The transformation described above must be implemented in terms of the discrete field quantities of the FDTD model and this may be achieved as follows:

3.3.1 Equivalent Current Calculation

If a surface S is envisaged, enclosing the elements of the FDTD problem, the equivalent currents $\mathbf{M_{eq}}$ and $\mathbf{J_{eq}}$ can be evaluated from the tangential fields to the surface where it intersects each FDTD unit cell (equation (3.1)). Due to the staggered FDTD spatial discretisation however (see figure 2.2) the tangential **E** and **H** components are not defined on the same plane, additionally the two tangential components of each field are not located at the same points. As a result the electric field components must be interpolated in four directions and the magnetic components in two (as shown for E_x and H_z in figure 3.2) to yield tangential field values at the centre of each Yee cell.

3.3.2 Integral Evaluation

The use of equation (3.1) and the averaging procedure of section 3.3.1 above provides one equivalent electric and magnetic current sample for each FDTD cell on the surface. The integrals at time t in equations (3.3) are formed by multiplying each equivalent current sample by the area of the FDTD cell (e.g. $\Delta_A = \Delta_x\Delta_z$ in figure 3.2) containing the current, applying the time delay τ, and summing the results

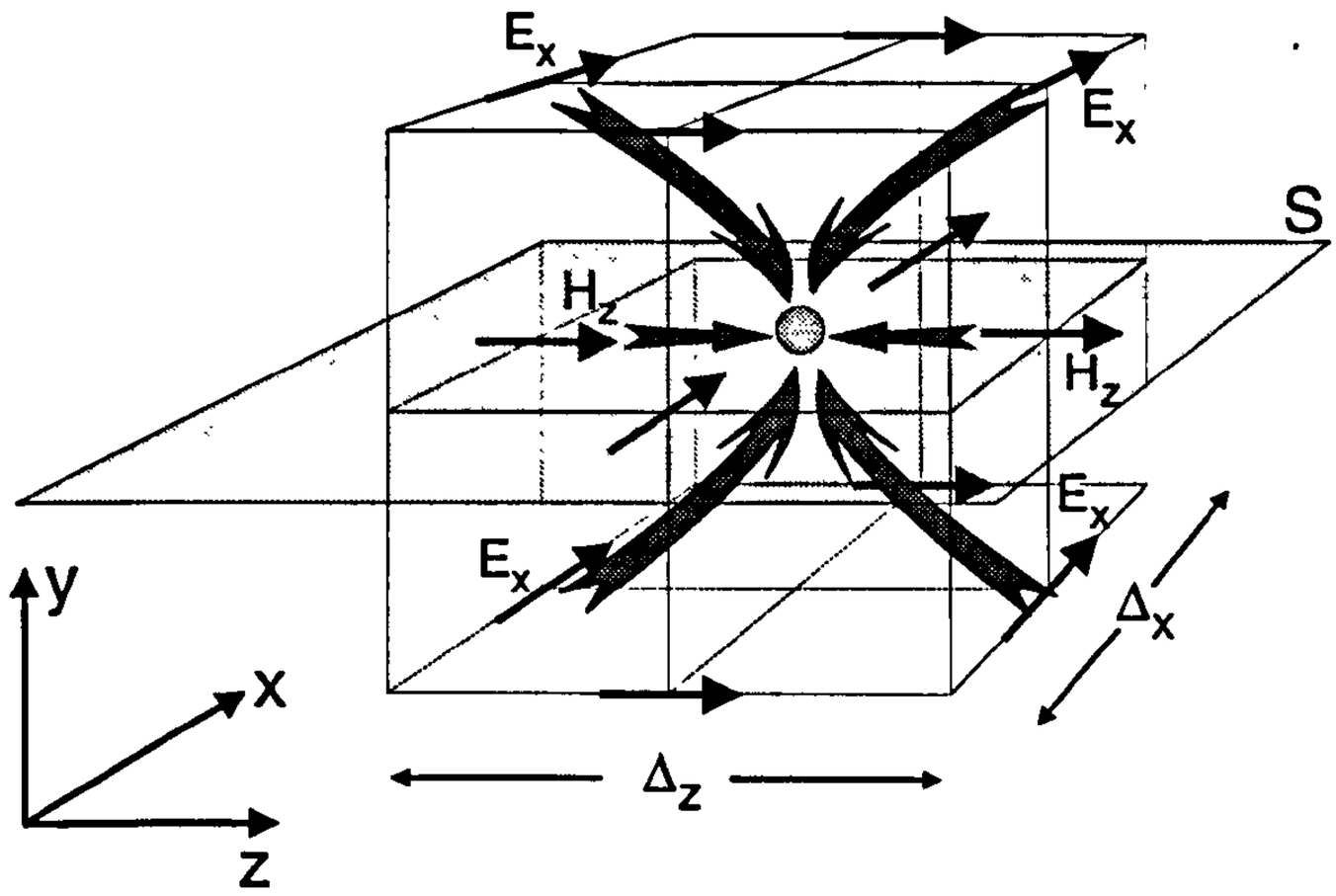

Figure 3.2: Averaging process employed for evaluation of tangential fields on S.

together. Since τ (the delay associated with the path $\mathbf{r}' \rightarrow \mathbf{r}$) is a function of the position of point $\mathbf{r}'$, a scheme must be devised whereby the influence of each current element contributes to the far field at the correct point in time [1].

A further complication occurs since the current calculated from the FDTD data at time $n\Delta_t$ is a constant between times $n\Delta_t$ and $(n+1)\Delta_t$, and contributes over a period of time ($n\Delta_t + \tau$ to $(n+1)\Delta_t + \tau$) to the far field integral. The far field, however, must be calculated at discrete points in time $m\Delta_t$ so, unless the time delay τ is an integer number of time steps (i.e. $\tau = (m-n)\Delta_t$) an interpolation method is required.

An illustration of the calculation routine is provided by figure 3.3. Here, only three currents are considered, one current ($\mathbf{M}_2$) being a distance $|\mathbf{r} - \mathbf{r}'| = c\Delta_t$ from the far field point, the two others being $|\mathbf{r} - \mathbf{r}'| = 1.5c\Delta_t$ distant. The contribution from each current is added into a time sequence at the appropriate point. In the case of $\mathbf{M}_2$ its influence arrives at the beginning of time 'bin' 3, for $\mathbf{M}_1$ and $\mathbf{M}_3$, though, the contribution arrives 'across' two bins. In this case half the contribution will be added to time bin 3, and half to bin 4.

Once the contributions from currents all across the surface have been added to the integral in the above fashion the far field values can be calculated using backward difference approximations of the time derivatives in equation (3.4).

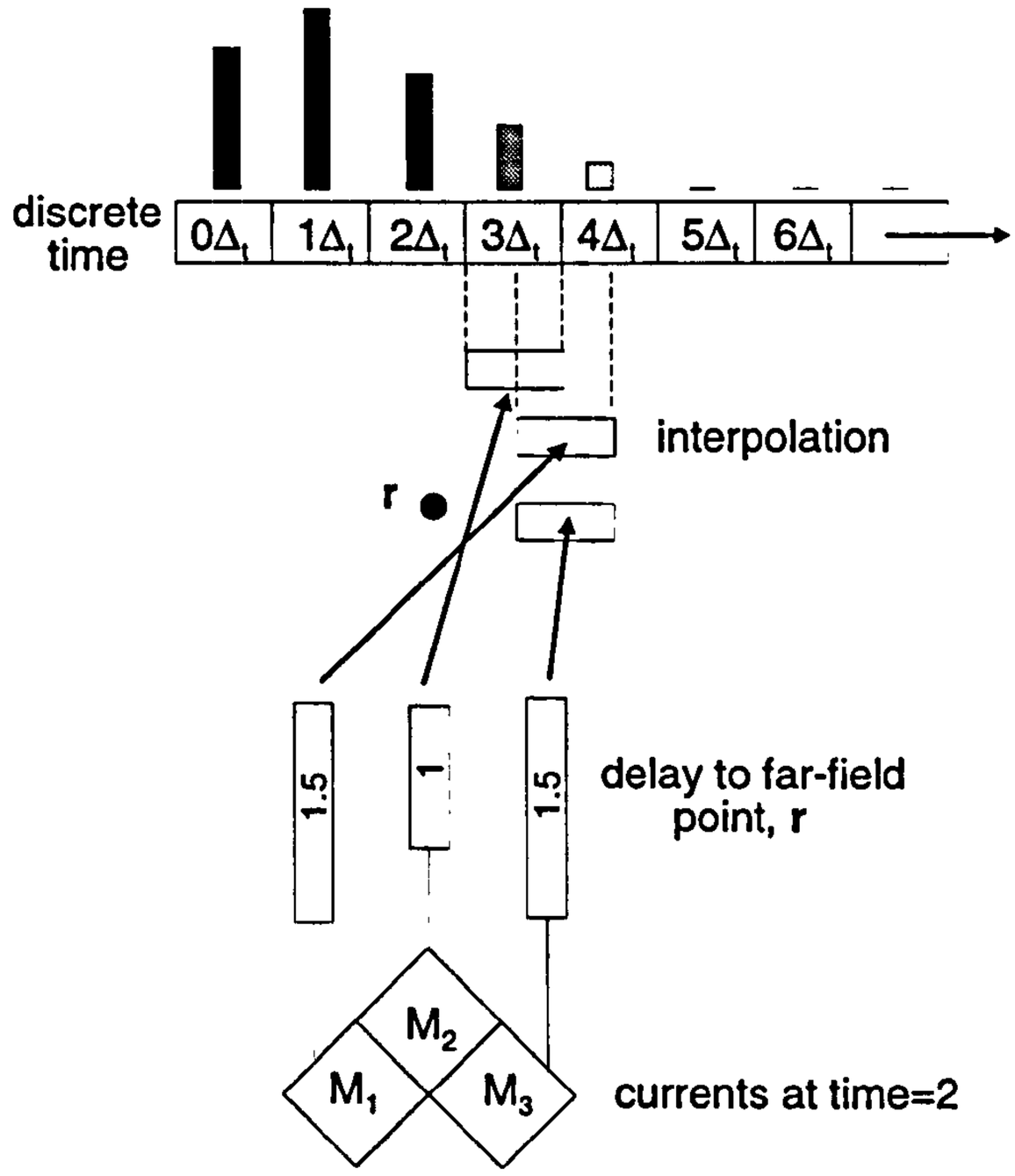

Figure 3.3: Transform calculation.

3.3.3 The Skip Value

The integral calculation described above need not be performed at every FDTD time step and in fact is usually performed once every K FDTD iterations, where K is an integer value called the 'skip value'. For greatest accuracy it is desirable that the equivalent currents $\mathbf{M_{eq}}$ and $\mathbf{J_{eq}}$ are calculated and transformed every FDTD iteration (i.e. $K = 1$), since this results in the full frequency spectrum available to the FDTD algorithm being used for the transform and minimises the error resulting from the time bin interpolation process described in section 3.3.2. This approach unfortunately also maximises the computational overhead associated with the transform.

3.3.4 Including a Ground Plane

The functions (3.3) assume that all the field sources are enclosed in S and that the equivalent currents radiate in free space. Many devices however, including antennas, operate in conjunction with an electrically large ground plane therefore unless the entire ground plane can be contained within the FDTD model (which is unlikely) S cannot enclose it.

As a solution to this problem a second surface S' may be envisaged supporting the images of the equivalent currents $\mathbf{M}_{eq}$ and $\mathbf{J}_{eq}$, $\mathbf{M}'_{eq}$ and $\mathbf{J}'_{eq}$ as in figure 3.4.

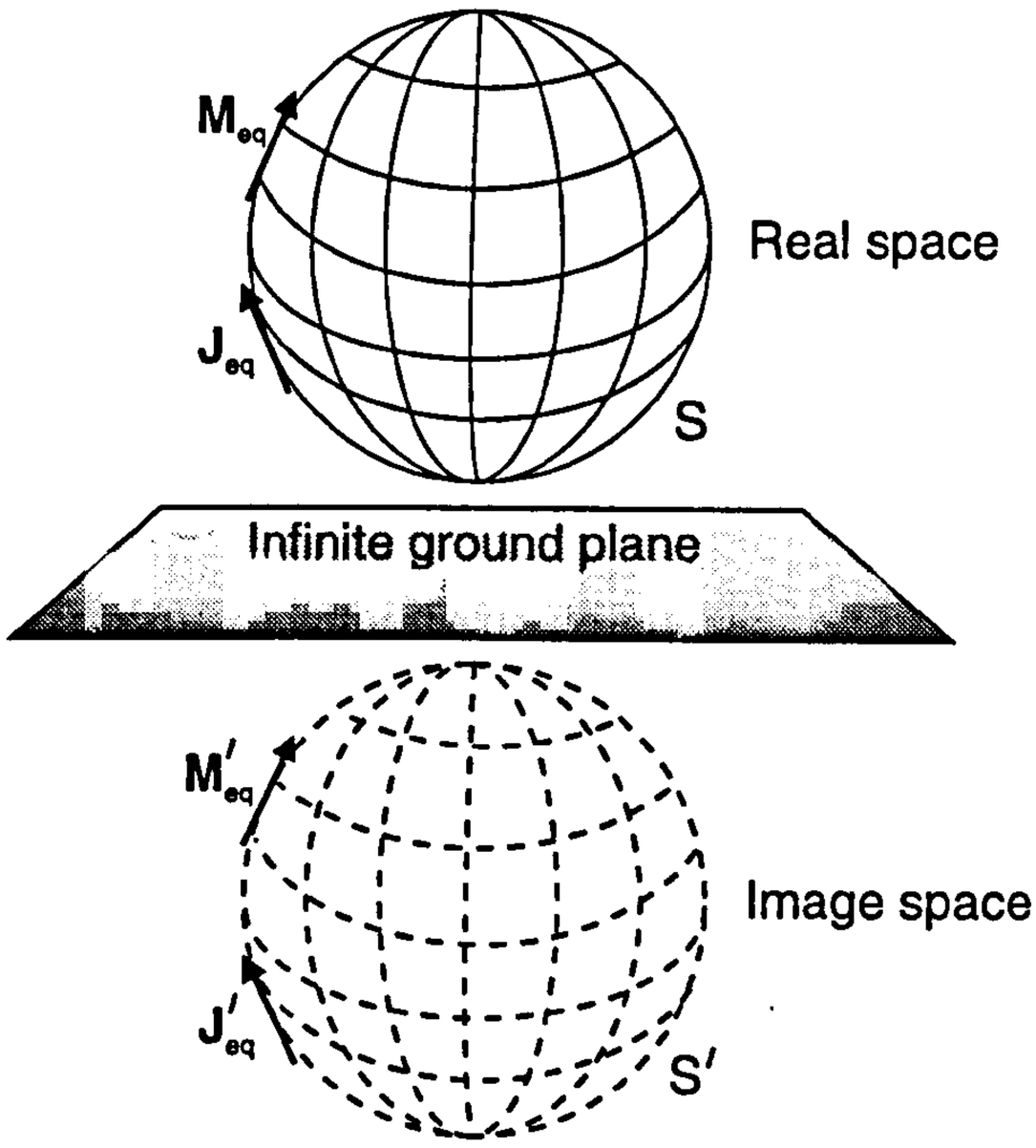

Figure 3.4: Image solution to the ground plane problem.

By transforming the additional image currents to the far field point, the effect of the large ground plane is included without the need to enclose it in S. This obviously introduces a degree of approximation however as the image theory assumes that the ground plane is infinite in extent whereas in practice it is only electrically large (see the following example).

3.4 Validation of the Transform

While time domain near field transforms for the Yee algorithm have been known for about 5 years, applications have not been particularly widespread and mostly restricted to scattering from simple structures at one or two angles [1, 2].

In this section the time domain transform described above is used to determine the radiation pattern of a printed dipole antenna. This application is quite a challenging one for the near far transform as the object in question is relatively complex (resulting in an FDTD model of 76×30×70 unit cells) and, in order to determine the pattern with reasonable angular resolution, a large number of observation points is required.

The antenna is shown in figure 3.5; a narrow piece of substrate (permittivity $\epsilon_r = 10$) passes through a hole in a metallic backplane. On one face of the substrate a feed is defined and on the reverse side the ground plane is etched away to form the two arms of a dipole. The dipole is a broad band element and is designed for use between approximately 8 and 12 GHz.

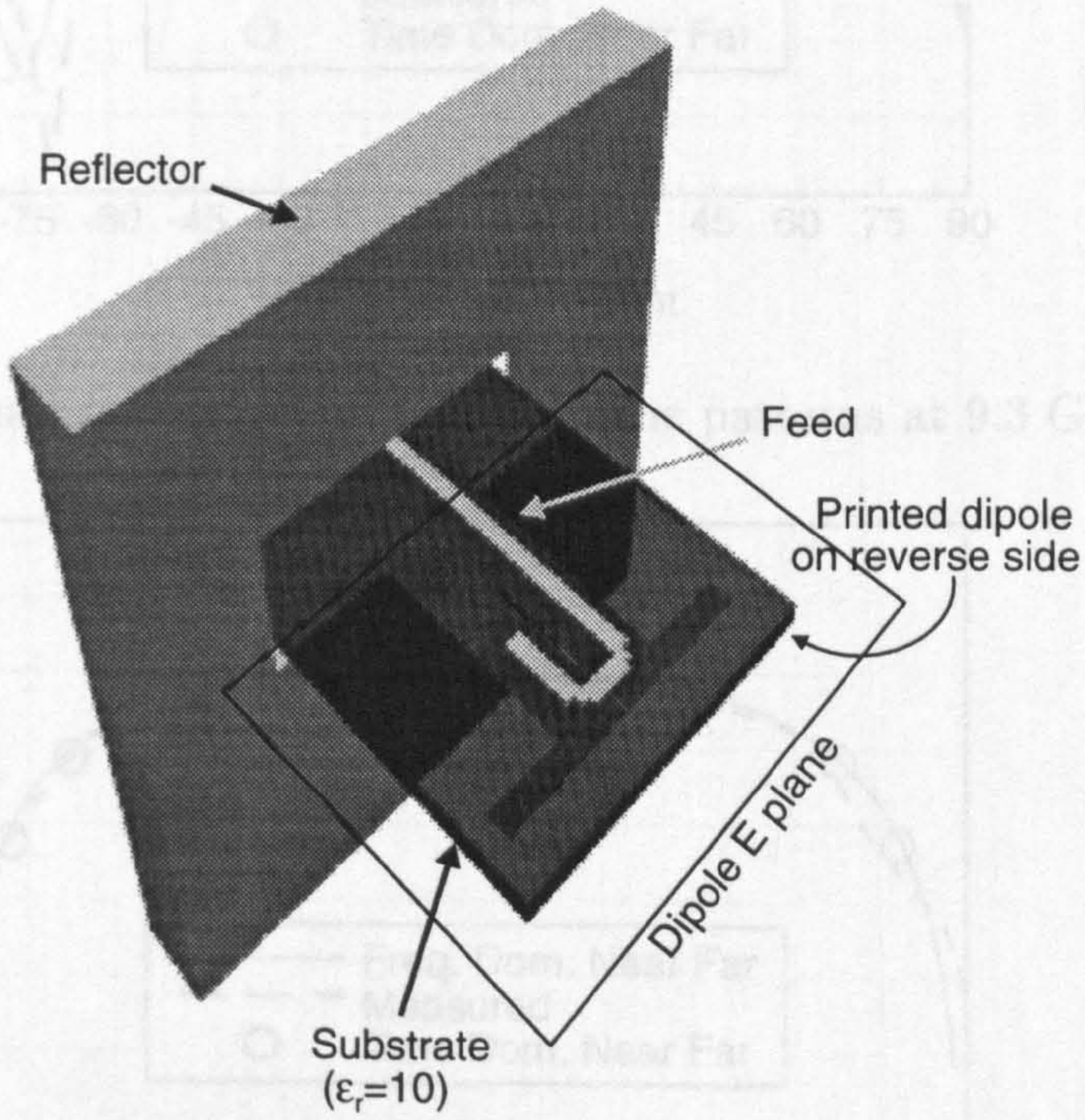

Figure 3.5: Printed dipole antenna.

A rectangular extrapolation surface was defined around five sides of the printed dipole and the ground plane was assumed to be infinite; the image method described in section 3.3.4 was used to include the effect of the ground plane on the far fields. 21 observation points were placed in the antenna's E and H-planes, giving an average angular resolution of approximately 15°, this being sufficient to determine the general features of the antenna's radiated field pattern; very narrow nulls, for example, might not however be detected.

Validation of the time domain near far transform can be achieved by comparison with an independently implemented and well tested frequency domain transform [5–7] and, at 9.3 GHz, measured results obtained in the Centre for Communications Research's anechoic chamber by Dr. S. A. Meade. Figures 3.6 and 3.7 show the co-polar E- and H-plane radiation patterns at 9.3 GHz, figures 3.9 and 3.8 show the patterns at 10 GHz.

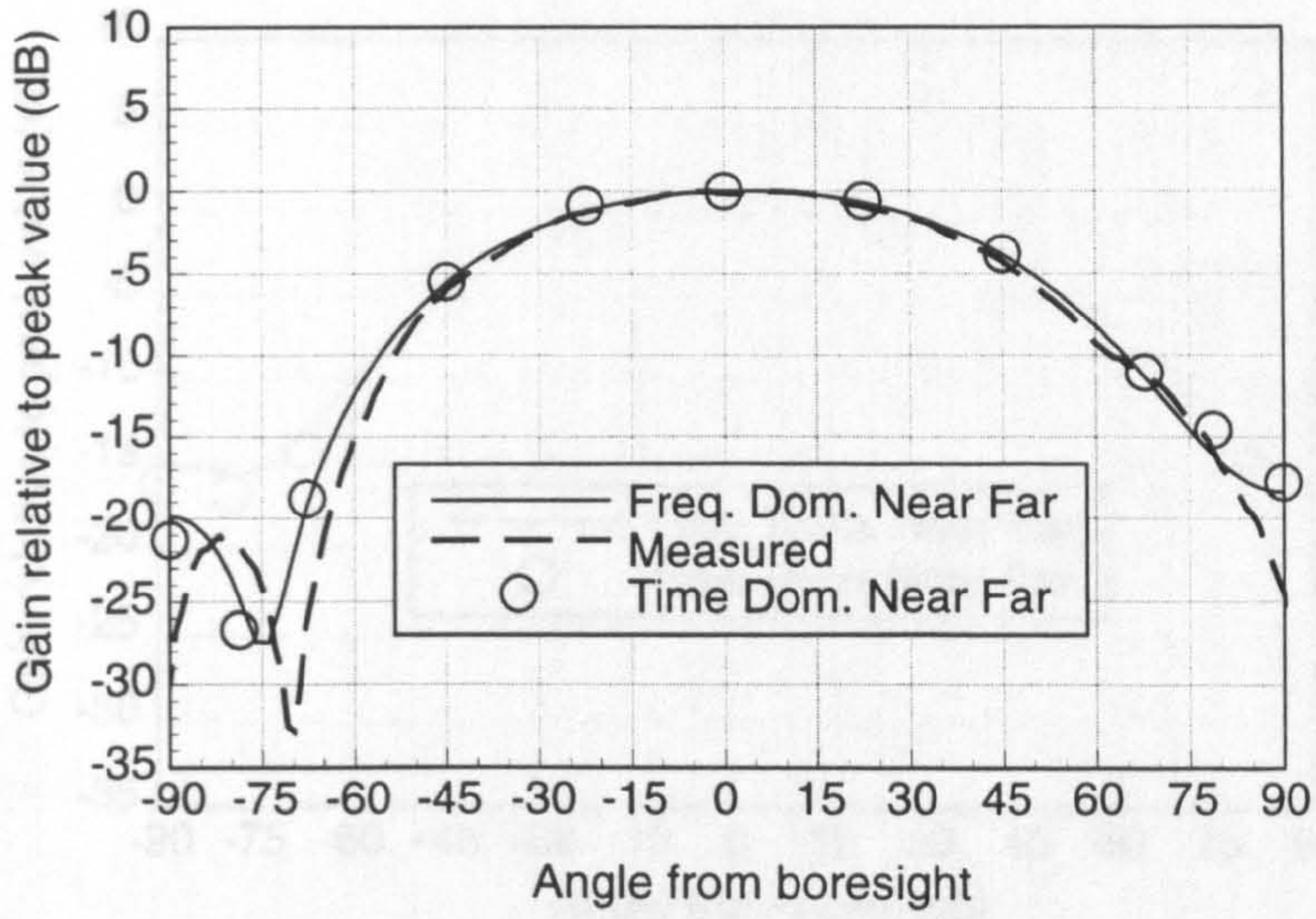

Figure 3.6: Measured and theoretical E-plane patterns at 9.3 GHz.

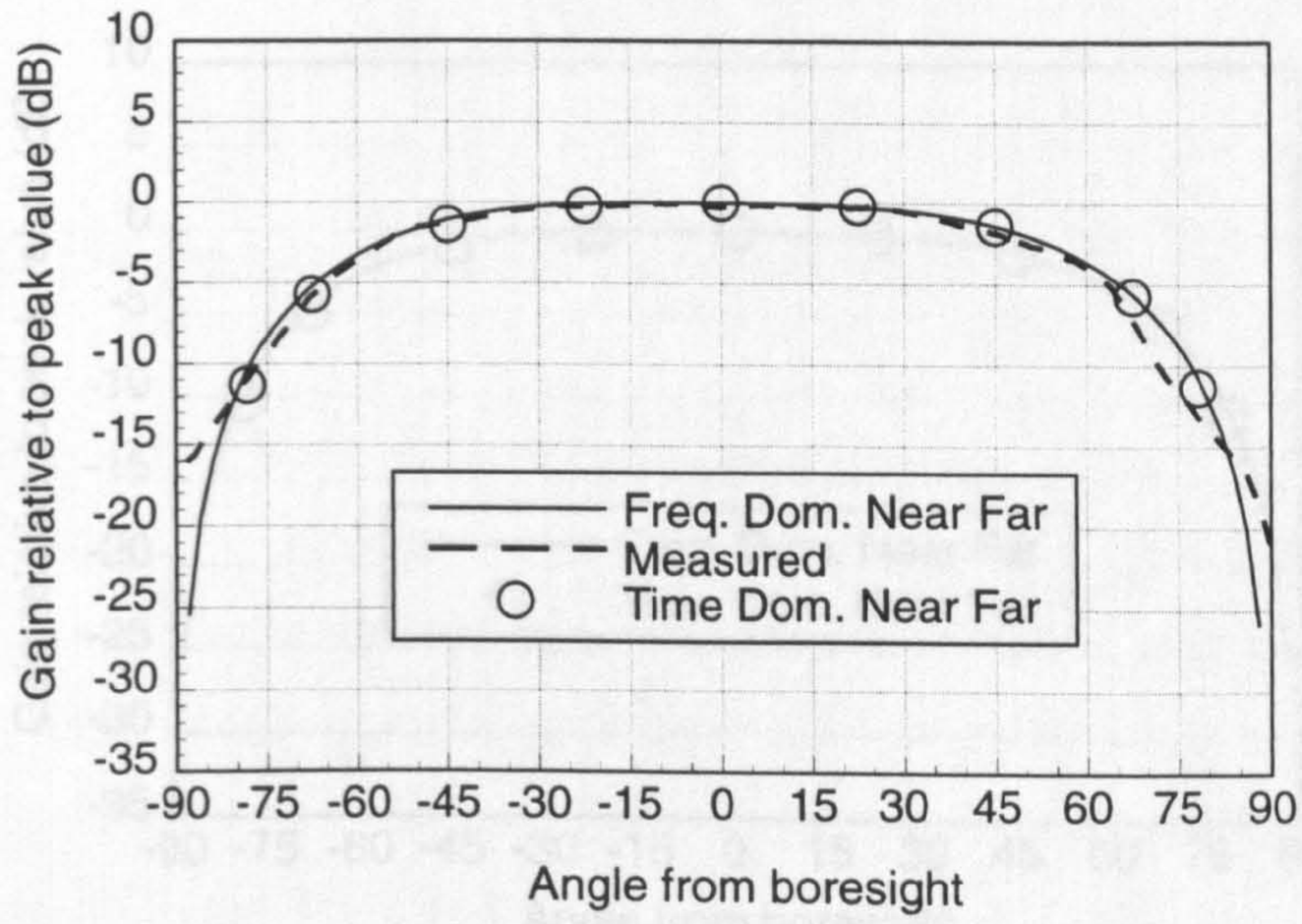

Figure 3.7: Measured and theoretical H-plane patterns at 9.3 GHz.

Both sets of theoretical data (the frequency domain and the time domain transforms) are in extremely close agreement and in turn at 9.3 GHz they both agree well with the measured data. The only regions of difference between the theoretical and the measured patterns are in the endfire region ($\pm$ 90°) and can be attributed to the assumption that the ground plane is infinite in extent (see section 3.3.4) – the effects of this assumption are particularly clear at 90° in the H-plane results where the infinite ground plane requires the theoretical co-polar field levels to be precisely zero.

The great advantage of the time domain near far transform over the frequency domain version is that it provides a characterisation of the device over a very wide band from just one execution of the algorithm. This fact is illustrated by figure 3.10 which plots

Figure 3.8: Theoretical E-plane patterns at 10 GHz.

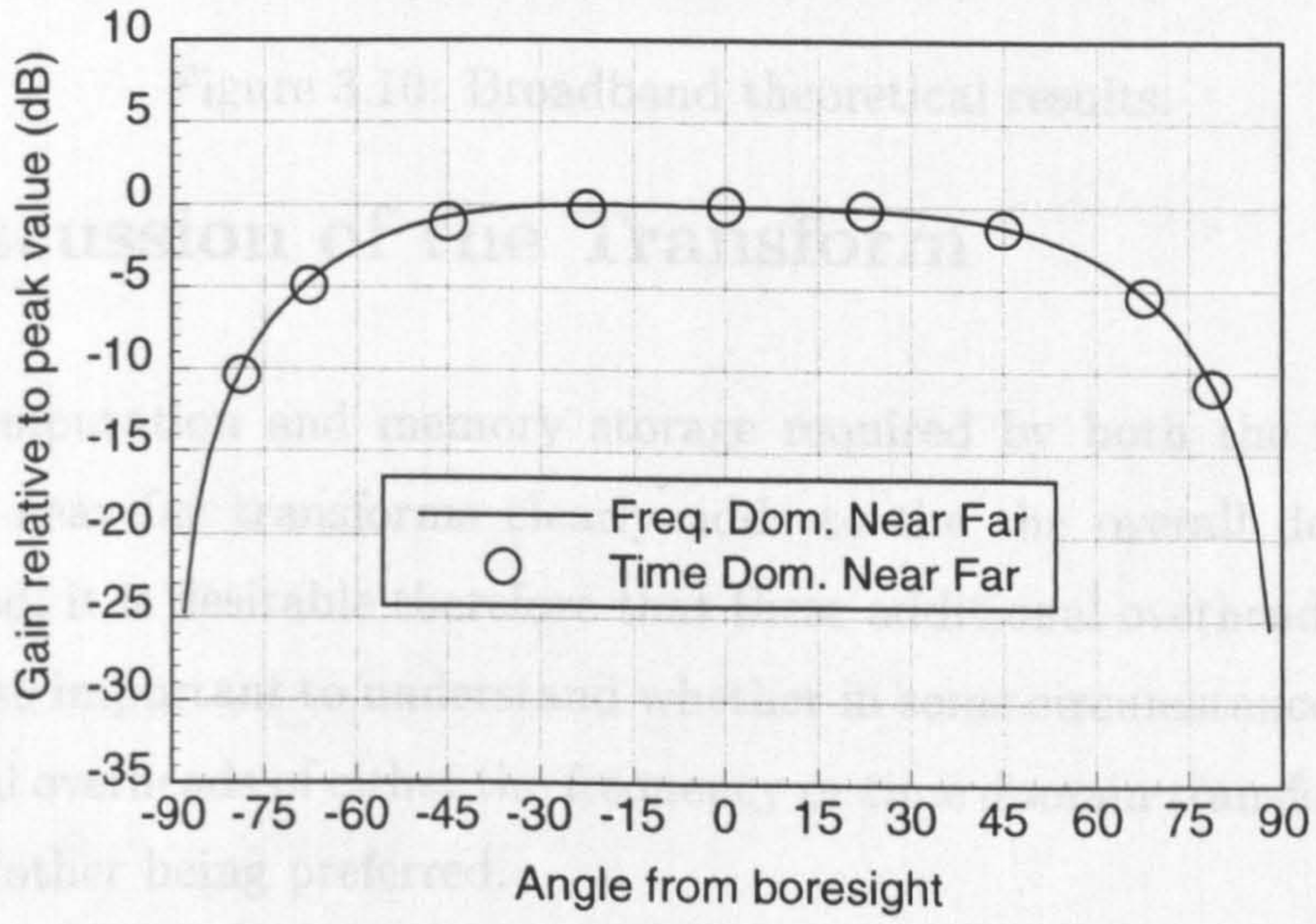

Figure 3.9: Theoretical H-plane patterns at 10 GHz.

the E-plane radiation characteristic of the dipole against frequency at four angles.

Various observations about the behaviour of the antenna can be made by inspecting figure 3.10; the antenna radiates strongly between about 8 and 10 GHz and the E-plane null at about 75^o is present over the whole of this band – lessening in depth as the frequency approaches 10 GHz (see figure 3.8). Away from the 8 to 10 GHz band the antenna develops nulls in the boresight direction.

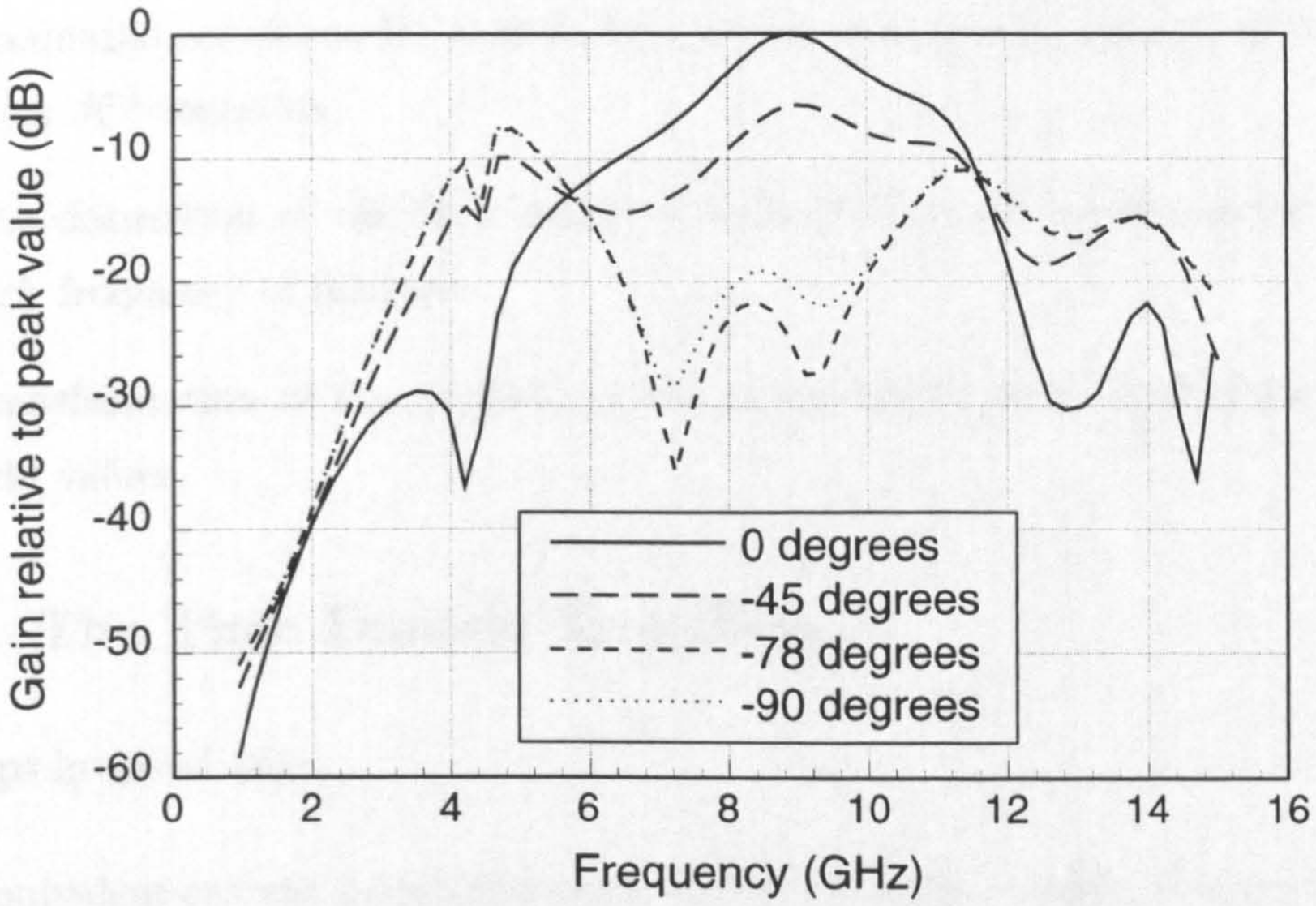

Figure 3.10: Broadband theoretical results.

3.5 Discussion of the Transform

The extra computation and memory storage required by both the frequency and time domain near far transforms clearly adds to the the overall demands of the FDTD method; it is desirable therefore that these additional overheads be relatively small. It is also important to understand whether in some circumstances the different computational overheads of either the frequency or time domain transform might lead to one or the other being preferred.

A detailed analysis of the computational overheads of the two methods is not presented here; and in fact such an analysis is difficult and to some extent machine and implementation dependent. Some appreciation of the merits of the two techniques can however be produced quite straightforwardly by considering the steps involved in each method.

3.5.1 The Frequency Domain Transform

The steps involved are;

i . Equivalent current calculation from the FDTD fields at each point on S at every K^{th} iteration.

ii . Accumulation of one DFT at each point on S at each frequency of interest at every K^{th} iteration.

iii . Transformation of the final result of each DFT to each observation point at each frequency of interest.

iv . Transformation of the far field vector potentials at each observation point to field values.

3.5.2 The Time Domain Transform

The steps involved are;

i . Equivalent current calculation from the FDTD fields at each point on S at every K^{th} iteration.

ii . Transformation of each equivalent current to each observation point at every K^{th} iteration.

iii . Transformation of the far field vector potentials at each observation point to field values at every K^{th} iteration.

3.5.3 Time vs. Frequency Domain Transforms

3.5.3.1 Amount of Computation

The actual amount of computation required by the two transforms is relatively small, particularly as in each case the value of K will be substantially greater than unity. Disregarding step (i) (the equivalent current calculation which is common to both methods), for the frequency domain transform the extra computation is mostly related to the accumulation of a DFT at each point on S (step (ii)) and for the time domain version it is entailed in the transformation of the currents to the far field (step (ii) – described in section 3.3.2). The major overheads for the frequency domain transform are therefore proportional to the number of frequency points required and for the time domain transform proportional to the number of far field observation points.

It was found that in the example of the printed dipole that a frequency domain transform at one spot frequency and a time domain transform increased the total

computation time by approximately the same proportion (around 10%). Clearly if more observation points had been required by the time domain method it would have become less attractive however the frequency domain method only provided one frequency of interest. The choice between the two methods on grounds of the amount of computation depends therefore on the application – if very high angular resolution is needed and there is one specific frequency of interest then the frequency domain method is the obvious choice, if however a moderate angular resolution is sufficient and a wider band characterisation is needed then the time domain method is to be preferred.

3.5.3.2 Amount of Memory

The second form of computational overhead is the amount of memory required by the transforms; it is clearly very desirable to keep the increase in memory useage to a minimum. The printed dipole example required 10 MBytes of memory for the FDTD analysis alone, the additional memory required for the accumulation of the frequency domain transform's DFT was 1.7 MBytes and, for the time domain method, 13 MBytes.

It is apparent then that the time domain transform's biggest drawback is its memory useage. This overhead arises because the algorithm must store the delay from each point on the extrapolation surface S to *each* observation point. Since the frequency domain transform's memory useage is simply that involved in accumulating a DFT (the time delay/phase information need not be stored as it is only used once, at the end of the FDTD computation) its memory overhead is independent of the number of observation points.

The total storage needed for the efficient time domain transformation of the currents $\mathbf{J}_{eq}$ and $\mathbf{M}_{eq}$ to the far field is one integer and two real numbers per current per observation point [3, chapter 6]. Since there will be many thousands of currents on S and at least 10–20 observation points, this very easily results in large demands on memory resources.

The amount of memory required by the time domain transform is therefore a significant drawback. Various techniques suggest themselves for the amelioration of this effect and are discussed in chapter 7.

3.6 Analysis of Resonant Structures

One of the disadvantages of any time domain analysis method is that the computational effort is proportional to the amount of time domain data required. In general, FDTD computations must proceed until the fields have died away to a negligibly low level; failure to observe this requirement will typically lead to an inaccurate characterisation of the structure when the Fourier transform of the time domain data is performed.

A particular problem occurs when the structure has a high Q factor (i.e. is highly resonant); in this case it may take tens or even hundreds of cycles at the frequency of interest before the fields decay sufficiently for the analysis to be terminated.

Most antennas have relatively high Q factors and this results in their FDTD analysis becoming a relatively lengthy process. This difficulty is more important when the additional computational overheads of the time domain near far transform are considered.

In the following section the system identification method is presented and its application to the time domain far field characterisation of a patch antenna is considered.

3.6.1 System Identification

Various techniques are available to reduce the computation associated with the time domain analysis of highly resonant structures with the perhaps best known example being Prony's method [8]. Prony's method, essentially a curve-fitting procedure, is widely used, although its robustness is not always satisfactory [9].

The system identification method provides an interesting, signal processing based, alternative to Prony's method and has previously been applied in the analysis of resonant structures with FDTD [10]. Its application to the time domain near far transform was first demonstrated by the author in [11].

3.6.1.1 The RLS System Identification Method

The techniques of system identification are well established in the fields of communications and control [12–14], one of the simplest and most popular techniques being

the Recursive Least Squares (RLS) method [14, chapter 9].

The discrete time system identification problem is shown by figure 3.11. A discrete time filter is shown operating in parallel with the FDTD and near far transform. The signal x represents the FDTD input (the excitation) and y is the output (in this case the response of the structure in the far field). The identification procedure consists of choosing the filter coefficients a_i and b_j such that the output of the filter $\hat{y}$ follows y with minimum error.

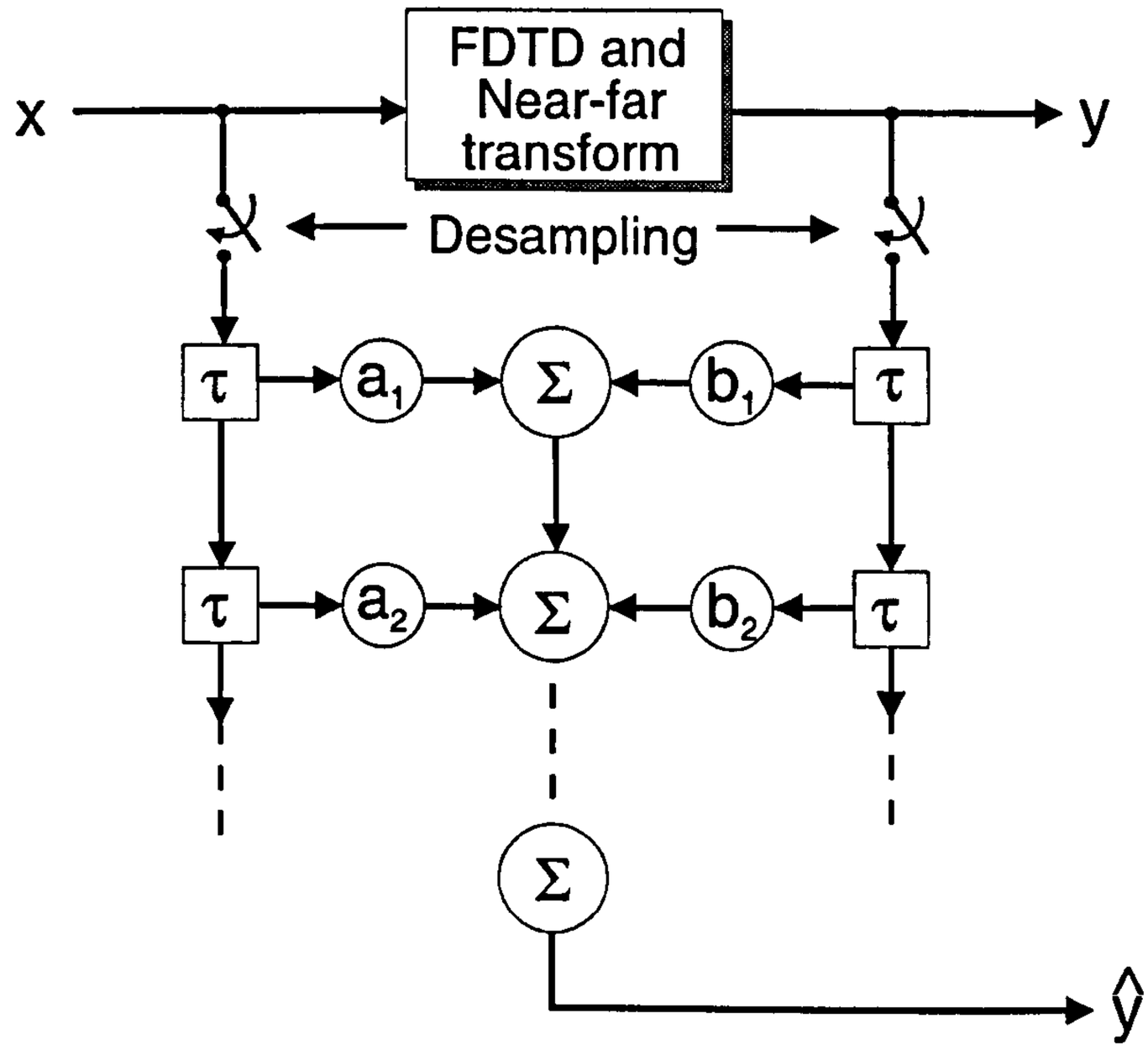

Figure 3.11: Principle of system identification

Combining the past values of x and y into a data vector $\mathbf{u}$, and $\mathbf{a}$ and $\mathbf{b}$ into the coefficient vector $\mathbf{w}$ of total length M, the output $\hat{y}$ at any time n (where n is a point in time $t = nD\Delta t$ with D a desampling factor) can be written:

$$\hat{y}[n] = \mathbf{w}^T[n]\,\mathbf{u}[n] \tag{3.5}$$

Minimising the mean-square difference between y and $\hat{y}$ with respect to $\mathbf{w}[n]$ yields a recursive expression for the optimum vector of filter coefficients:

$$\mathbf{w}[n] = \mathbf{w}[n-1] - \frac{\boldsymbol{\phi}^{-1}[n-1]\mathbf{u}[n](y[n] - \mathbf{u}^T[n]\mathbf{w}[n-1])}{1 + \mathbf{u}^T[n]\boldsymbol{\phi}^{-1}[n-1]\mathbf{u}[n]} \tag{3.6}$$

where $\boldsymbol{\phi}[n]$ is a $M \times M$ correlation matrix whose recursive definition is:

$$\boldsymbol{\phi}^{-1}[n] = \boldsymbol{\phi}^{-1}[n-1] - \frac{\boldsymbol{\phi}^{-1}[n-1]\mathbf{u}[n]\mathbf{u}^T[n]\boldsymbol{\phi}^{-1}[n-1]}{1 + \mathbf{u}^T[n]\boldsymbol{\phi}^{-1}[n-1]\mathbf{u}[n]} \tag{3.7}$$

These relations, requiring only matrix/vector multiplication, constitute a simple and reasonably efficient iterative determination of the optimum coefficients given the initial values $\mathbf{w}[0] = (0\ 0\ 0\ ..)^T$ and $\boldsymbol{\phi}^{-1}[0] = k\mathbf{I}$ where k is a large positive constant and $\mathbf{I}$ the identity matrix.

The oversampled nature of FDTD models (see section 2.7.2) necessitates desampling of the data by the factor D; in practice desampling to the Nyquist limit for the FDTD model yields an appropriate choice for D (this limit should take into account the bandwidth of the excitation and the low pass nature of the FDTD model).

At each (desampled) iteration of the RLS algorithm the filter coefficients are updated according to (3.6). This process is called the 'training period' for the algorithm – if the behaviour of y has predictable qualities (if, for example, it has a number of steady resonances) the coefficients will converge to a set of values. Once this is done, by transferring the filter's y input to its own output $\hat{y}$, the filter will produce the rest of the response with no further values of y.

The choice of model order M is dictated largely by the number of resonances of the structure under study. A suitable value may be determined for a particular type of structure either manually by a few trials, or by use of a formal order estimation method such as the Akaike information criterion [12].

3.6.1.2 Use of the RLS Method

The printed dipole described in section 3.4 is not a particularly high Q device – it is in fact designed to operate over a reasonably broad band, and its analysis does not therefore benefit greatly from the use of the system identification method. Where system identification does provide large computational savings is for devices such as the patch antenna shown in figure 3.12. Patch antennas are well known to be high Q radiators and the transient far field, produced by the near far transform described in this chapter, exhibits the slowly decaying resonances that would be expected from such a device – see figure 3.13.

The analysis of the patch by means of FDTD and the time domain near far transform requires many iterations (typically around 22,000) in order to accurately obtain the broadband response shown by figure 3.14 (the result shown is for one observation point at 60° of elevation in the antenna's E plane – the E plane indicated in figure 3.12 is

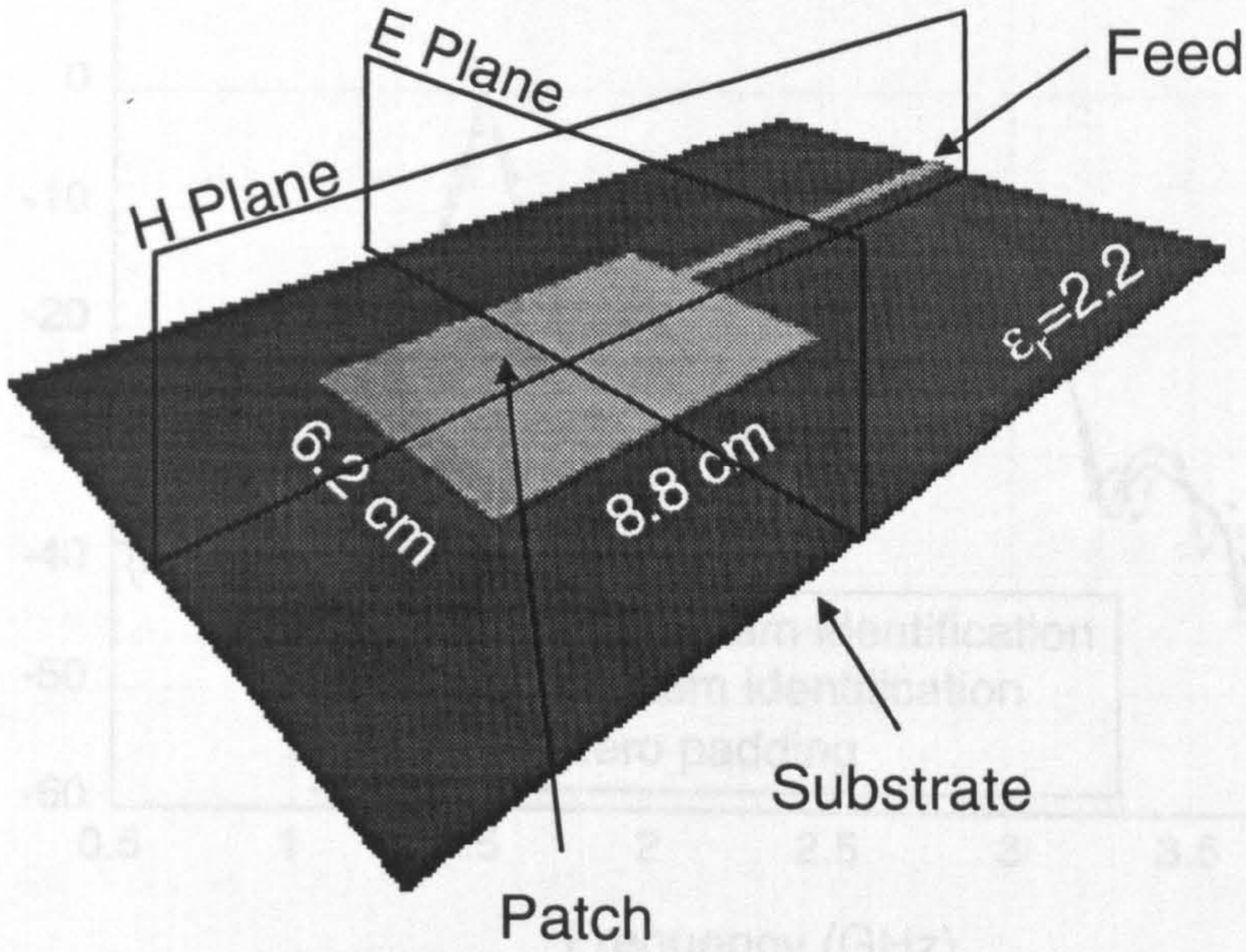

Figure 3.12: Edge fed patch antenna

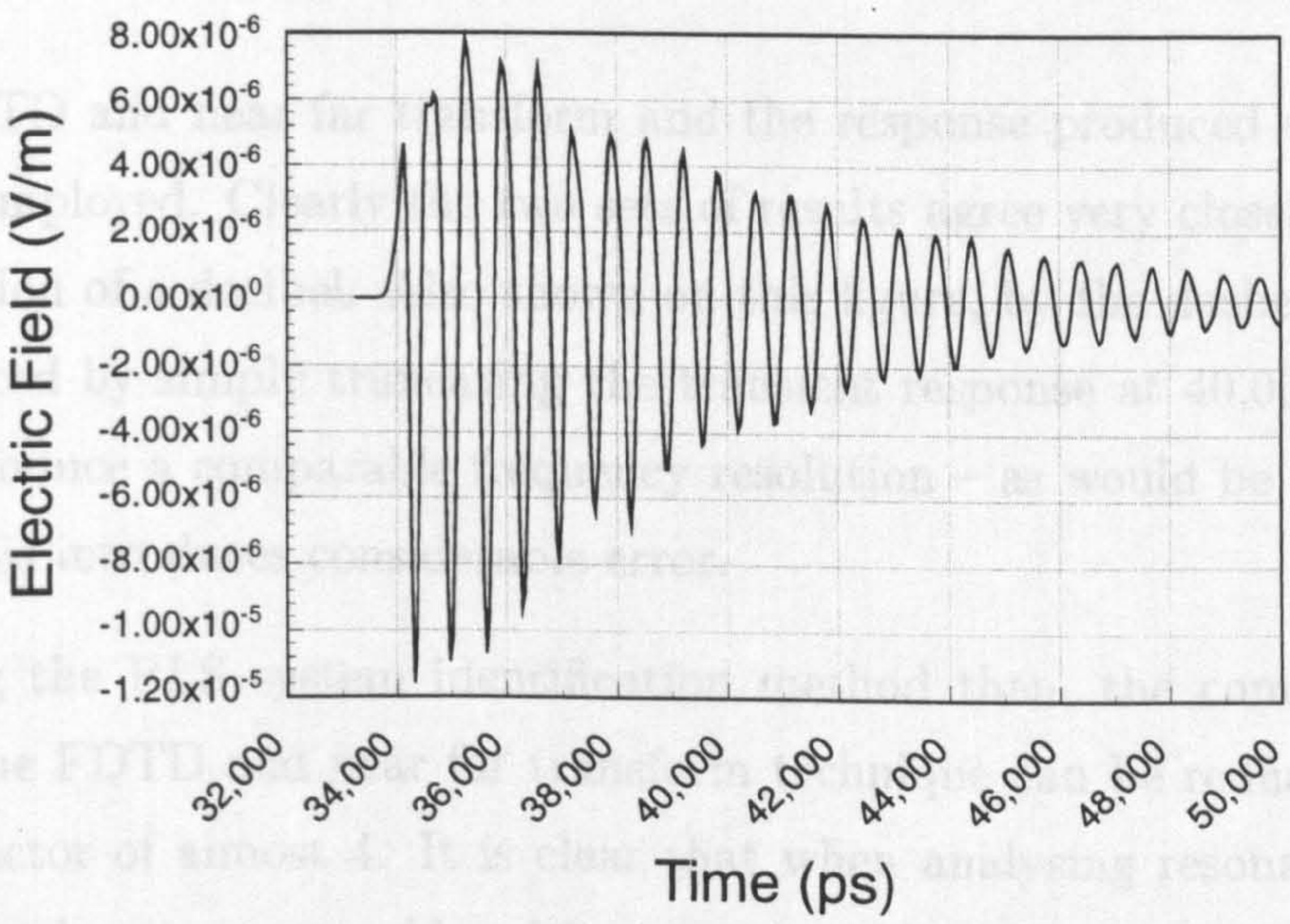

Figure 3.13: Transient far field of patch antenna.

referred to the device's dominant mode at 1.56 GHz).

An RLS model with 60 input and output filter coefficients (i.e. $M = 60$) was trained to the output of the near far transform, desampled by a factor of 40; convergence of the filter coefficients was produced by time=40,000ps (see figure 3.13) or 6000 FDTD iterations. From that time onwards the discrete time filter produced the remainder of the far field data without the FDTD model.

The solid lines in figure 3.14 shows the frequency domain far field response produced

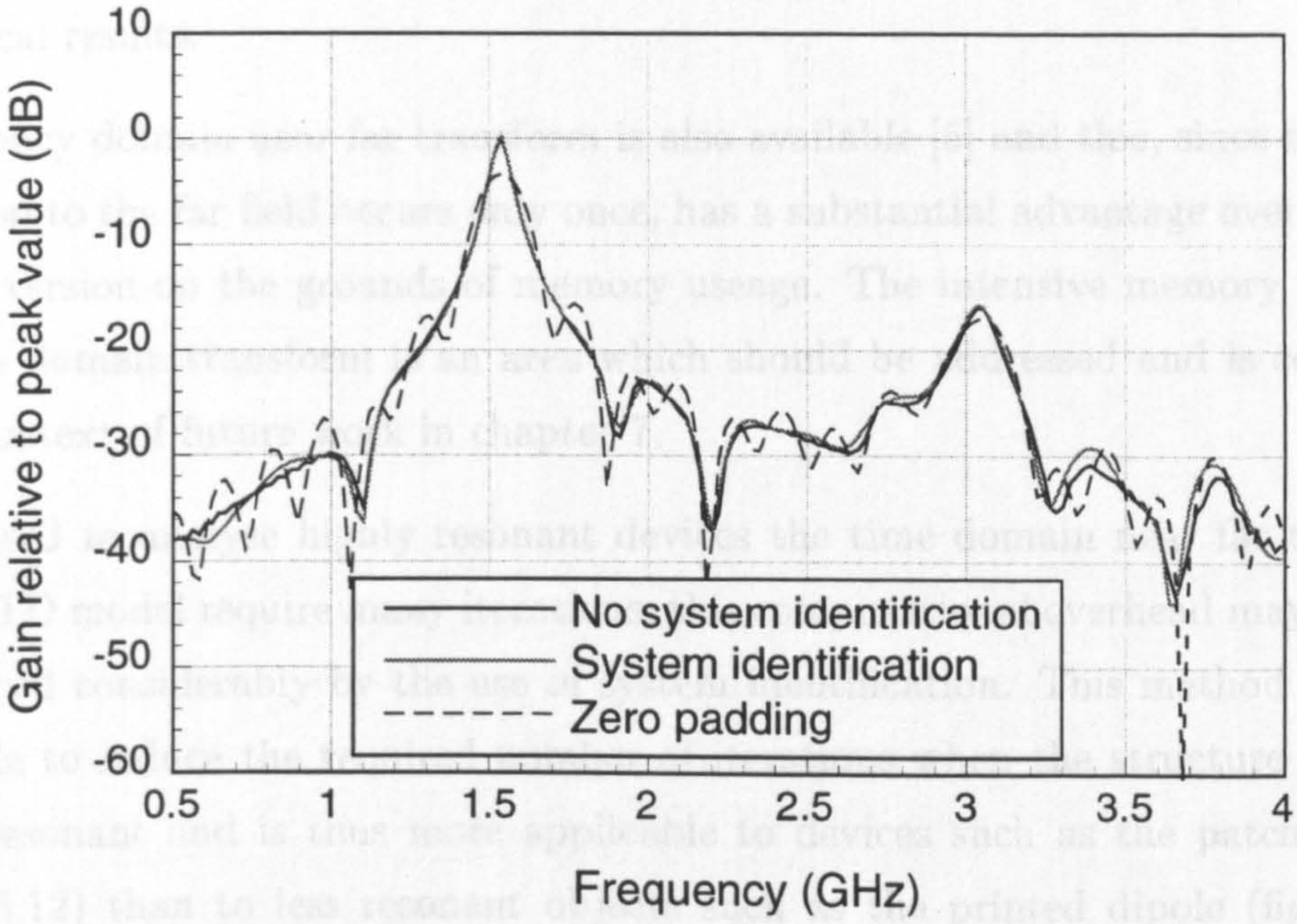

Figure 3.14: Broadband far field response of patch antenna

using the FDTD and near far transform and the response produced when the RLS method was employed. Clearly the two sets of results agree very closely, typically to within a fraction of a decibel. Also shown on this figure, by the dashed line, are the results produced by simply truncating the transient response at 40,000 ps and zero padding to produce a comparable frequency resolution – as would be expected from figure 3.13, this introduces considerable error.

By employing the RLS system identification method then, the computation time required by the FDTD and near far transform technique can be reduced in this example by a factor of almost 4. It is clear that when analysing resonant structures, such as the patch antenna considered here, system identification can provide a dramatic reduction in the required computation time without affecting the accuracy of the results.

3.7 Conclusions

This chapter has described and applied the time domain near far transform [1–3]. This method has been shown to be able to characterise the far field pattern of a complex printed antenna without requiring a very large computational domain; the accuracy of this characterisation has been evaluated by comparison with both measured and

theoretical results.

A frequency domain near far transform is also available [5] and this, since the transformation to the far field occurs only once, has a substantial advantage over the time domain version on the grounds of memory useage. The intensive memory useage of the time domain transform is an area which should be addressed and is considered in the context of future work in chapter 7.

When used to analyse highly resonant devices the time domain near far transform and FDTD model require many iterations, this computational overhead may however be reduced considerably by the use of system identification. This method is clearly only able to reduce the required number of iterations when the structure is indeed highly resonant and is thus more applicable to devices such as the patch antenna (figure 3.12) than to less resonant objects such as the printed dipole (figure 3.5). The system identification method is also of use in the near-field characterisation of resonant structures and has been successfully applied by the author to the analysis of a slot antenna, thin wire dipoles and a high Q microstrip filter.

References

[1] K. S. Yee, D. Ingham, and K. Schlager, "Time domain extrapolation to the far field based on FDTD calculations," *IEEE Transactions on Antennas and Propagation*, vol. AP-39, pp. 411–413, Mar. 1991.

[2] R. J. Luebbers, K. S. Kunz, M. Schneider, and F. Hunsberger, "A finite difference time domain near zone to far zone transformation," *IEEE Transactions on Antennas and Propagation*, vol. AP-39, pp. 429–433, Apr. 1991.

[3] E. M. Daniel, *The analysis and CAD of microwave and millimetre wave planar antennas.* PhD thesis, Universtity of Bristol, 1992.

[4] R. F. Harrington, *Time-Harmonic Electromagnetic Fields.* McGraw Hill, 1961.

[5] G. S. Hilton, C. J. Railton, G. J. Ball, A. L. Hume, and M. Dean, "Finite difference time domain analysis of a printed dipole antenna," in *Proceedings of IEE 9th International Conference on Antennas and Propagation*, (Eindhoven), pp. 172–175, Apr. 1995.

[6] G. S. Hilton, C. J. Railton, and J. P. McGeehan, "Finite difference time domain modelling of microwave antennas," *Fifth Report on DRA Research Agreement 2034/101*, Aug. 1993.

[7] S. A. Meade, G. S. Hilton, C. J. Railton, and J. P. McGeehan, "Finite difference time domain modelling of microwave antennas," *Sixth Report on DRA Research Agreement 2034/101*, May. 1994.

[8] W. L. Ko and R. Mittra, "A combination of FDTD and Prony's methods for analyzing microwave integrated circuits," *IEEE Transactions on Microwave Theory and Techniques*, vol. MTT-39, pp. 2176–2181, Nov. 1991.

[9] M. L. van Blaricum and R. Mittra, "Problems and solutions associated with Prony's method for processing transient data," *IEEE Transactions on Antennas and Propagation*, vol. AP-26, pp. 174–182, Jan. 1978.

[10] W. Kumpel and I. Wolff, "Digital signal-processing of time-domain field simulation results using the system-identification method," *IEEE Transactions on Microwave Theory and Techniques*, vol. MTT-42, pp. 667–671, Apr. 1994.

[11] I. J. Craddock, P. G. Turner, and C. J. Railton, "Reducing the computational overhead of the near field transform through system identification," *Electronics Letters*, vol. 30, pp. 1609–1610, Sept. 1994.

[12] P. Strobach, *Linear Prediction Theory.* Springer-Verlag, 1990.

Chapter 3, References

[13] T. Soderstrom and P. Stoica, *System Identification.* Prentice Hall, 1989.

[14] S. Haykin, *Adaptive Filter Theory.* Prentice Hall, 2 ed., 1991.

Chapter 4

Inclusion of *a Priori* Knowledge in FDTD

4.1 Introduction

In chapter 2, section 2.6.2, the widely accepted Yee FDTD algorithm [1] was introduced as a time domain Differential electromagnetic analysis method. The method has been applied to a wider range of electromagnetic problems than perhaps any other technique (with the possible exception of the related TLM method [2]), these applications include:

- Scattering from complex metallic geometries [3].
- Analysis of planar waveguides [4].
- Characterisation of complex and lossy dielectric structures [5].
- Modelling of frequency–dependent materials [6].

Two principal problems however still remain with the method – these are its treatment of geometrical detail and its characterisation of curved structures.

As discussed in chapter 2 the unit cell dimension (Δ) in the FDTD method must be small enough to characterise the smallest significant geometrical detail in the problem under consideration. A small Δ is disadvantageous since it implies a large number of unknown field components (giving overheads in terms of memory and computation time) and secondly, by virtue of the stability criterion given in section 2.7.2, a small value of the algorithm time step Δ_t (which gives rise in turn to further computational overheads).

The modelling of curved surfaces is achieved in the standard FDTD method by a 'staircase' approximation [7]. If the unit cell size is large with respect to the surface curvature (as shown in figure 4.1) a variety of undesirable effects occur [8] and the results become very poor; if however the mesh is refined, the small unit cell size poses the same problem as the characterisation of geometrical detail – namely the requirement for many unit cells and a small value for the time step Δ_t.

In this chapter the related problems of the treatment of geometrical detail and curved surfaces will be discussed. Consideration is subsequently given to a number of techniques which have been reported to improve the FDTD method in these situations. One such technique, the 'correction factor' method, is particularly attractive and its application to a number of examples is considered in some detail. The method

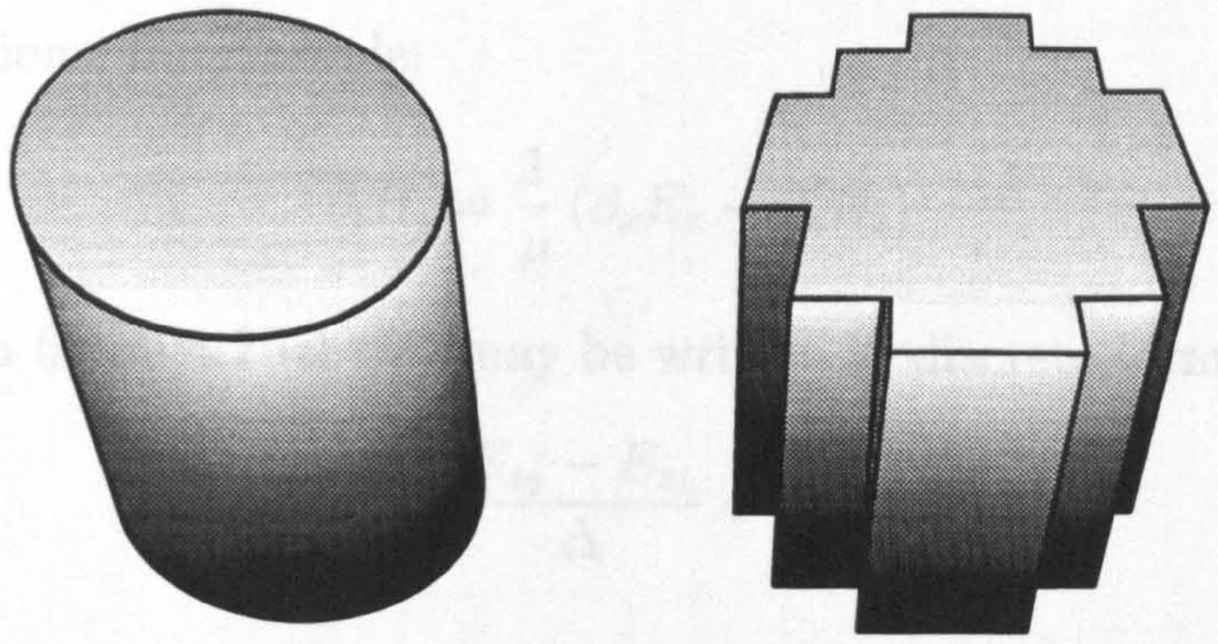

Figure 4.1: (i) Cylindrical body and (ii) its representation by a staircase approximation.

has however been limited in its application by concerns about stability and thus this chapter concludes with a discussion of the stability of the corrected FDTD algorithm.

4.2 Interpretations of the FDTD Method

In chapter 2 (section 2.6.2) it was shown that the FDTD algorithm may be derived by the approximation of Maxwell's partial differential equations. The derivatives in these equations are approximated by centred finite differences (or, equivalently, piecewise linear basis functions with delta test functions).

The improvement of the FDTD method is however frequently approached by an alternative interpretation of FDTD as being a discretisation of the integral form of Maxwell's equations (namely the Faraday and modified Ampère laws) [9]; the two complementary interpretations are illustrated by figures 4.2(i) and (ii) which show the section of the Yee cell relevant to the calculation of the H_y component.

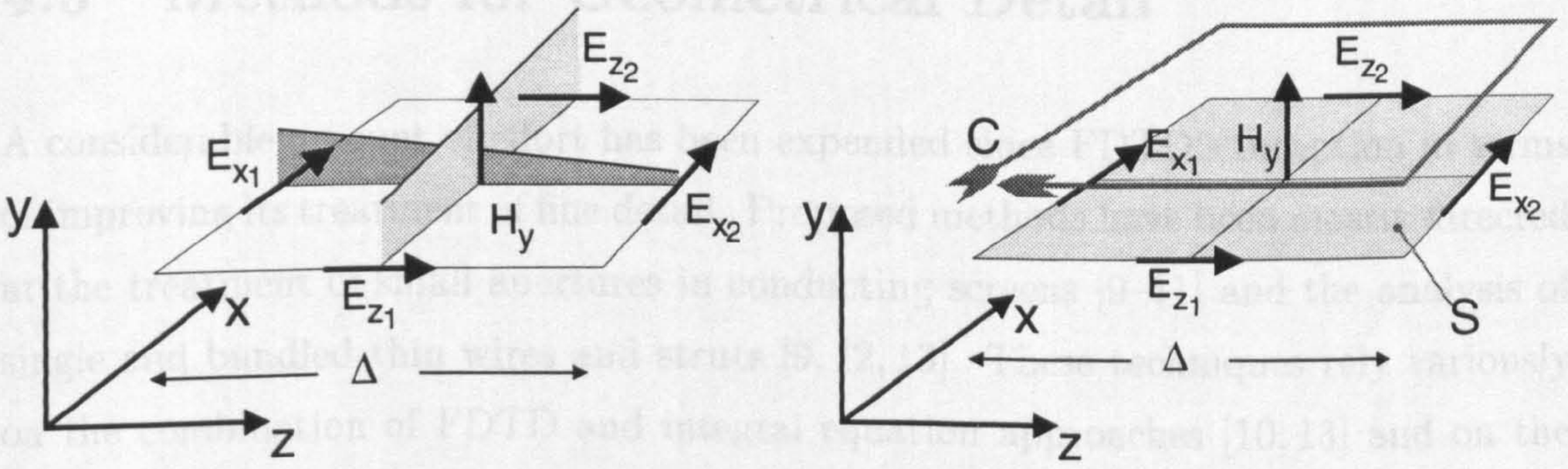

Figure 4.2: (i) Differential and (ii) Integral interpretations of FDTD.

The derivation of the FDTD equations from the differential point of view begins with

Maxwell's equations, for example:

$$\partial_t H_y = \frac{1}{\mu}\left(\partial_x E_z - \partial_z E_x\right) \tag{4.1}$$

with reference to figure 4.2 (i) this may be written in discrete form as:

$$\partial_t H_y = \frac{1}{\mu}\left(\frac{E_{z_2} - E_{z_1}}{\Delta} + \frac{E_{x_1} - E_{x_2}}{\Delta}\right) \tag{4.2}$$

Alternatively the integral form of Maxwell's curl equation (Faraday's law) may be considered for the surface S and closed contour C in figure 4.2 (ii), thus:

$$\partial_t \int_S \mathbf{H} \cdot d\mathbf{a} = \partial_t \iint_S H_y \, dx \, dz = \frac{1}{\mu} \oint_C \mathbf{E} \cdot d\mathbf{l} \tag{4.3}$$

assuming that the E field components are the average value of the field along their respective edges and that H_y is the average of the field across the surface S, these integrals evaluate to:

$$(\Delta)^2 \partial_t H_y = \frac{1}{\mu}\Delta\left(E_{z_2} - E_{z_1} + E_{x_1} - E_{x_2}\right) \tag{4.4}$$

Clearly the two approaches (integral and differential) both lead to exactly the same equation for H_y; this equivalence extends simply to the other electric and magnetic field components. As will be shown in the following sections either approach may be used when considering the improvement of the FDTD algorithm – in some cases the differential form is most suitable, in others the problem is more easily described from the surface–contour integral point of view.

4.3 Methods for Geometrical Detail

A considerable amount of effort has been expended since FDTD's inception in terms of improving its treatment of fine detail. Proposed methods have been mostly directed at the treatment of small apertures in conducting screens [9–11] and the analysis of single and bundled thin wires and struts [9, 12, 13]. These techniques rely variously on the combination of FDTD and integral equation approaches [10, 13] and on the modification of the FDTD update equations [9, 10] based on *a priori* knowledge of the fields in the vicinity of the small object.

Take, for example, the thin wire model of [9], illustrated by figure 4.3.

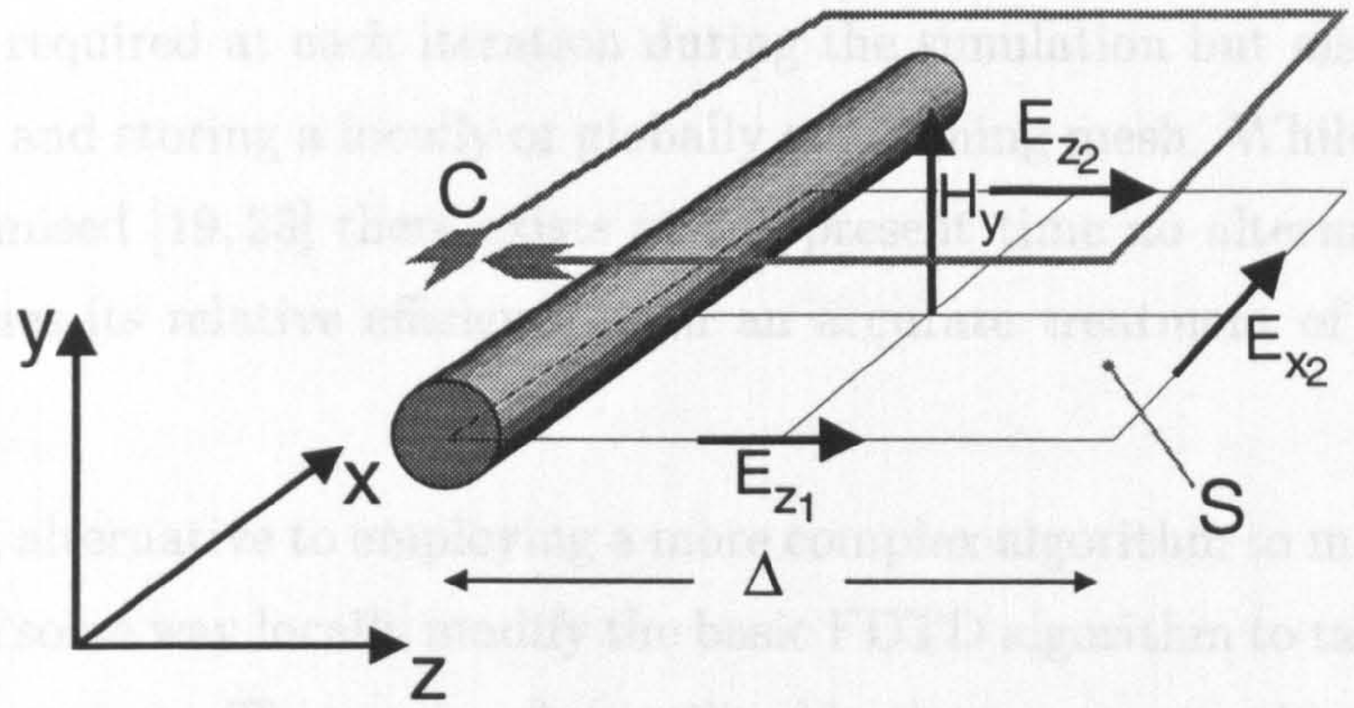

Figure 4.3: Thin wire in FDTD mesh

The variation of H_y and E_z close to the wire is known [9] to be proportional to r^{-1} where r is the radial distance from the centre of the wire (r_0 is the wire radius). If these functions are assumed when evaluating (4.3) the result (4.4) then becomes:

$$\partial_t H_y = \frac{(E_{z_2} - E_{z_1}) \ln\left(\frac{\Delta}{r_o}\right) - 2E_{x_2}}{\mu\Delta \ln\left(\frac{\Delta}{r_o}\right)} \tag{4.5}$$

This is a modified difference equation which, by including the effect of the known field distribution around a thin wire, enables the FDTD treatment of a region of fine geometry without the use of a small cell size.

At Bristol University the incorporation of known field variation has been extended considerably from that given in [9]. Thin metal strips [14, 15], slots [16], curved surfaces [17] and curved laminæ [18] as well as thin wires [16] have all been treated by means of a general technique which has become known as the 'correction factor' method.

4.4 Methods for Curved Surfaces

A number of approaches have been proposed for the accurate characterisation of curved surfaces [19–22]. As described in section 2.6 these methods all abandon FDTD when characterising curved surfaces and employ instead more sophisticated algorithms (at least in the immediate vicinity of the curved structure).

These new approaches have demonstrated large improvements in the characterisation of curved and angled objects [19–22] but at the same time introduce considerable computational overheads. These overheads concern not only the additional

computation required at each iteration during the simulation but also the necessity of generating and storing a locally or globally conforming mesh. While the overheads may be minimised [19, 23] there exists at the present time no alternative to FDTD which combines its relative efficiency with an accurate treatment of non-rectilinear geometry.

The principal alternative to employing a more complex algorithm to model the curved object is to in some way locally modify the basic FDTD algorithm to take into account the surface curvature. This approach is utilised in the 'contour path' method [24, 25].

The contour path technique relies on the interpretation of FDTD as being a discretisation of the integral form of Maxwell's equations (as shown in section 4.2). Consider the geometry shown by figure 4.4, where a curved metal surface intersects the FDTD mesh.

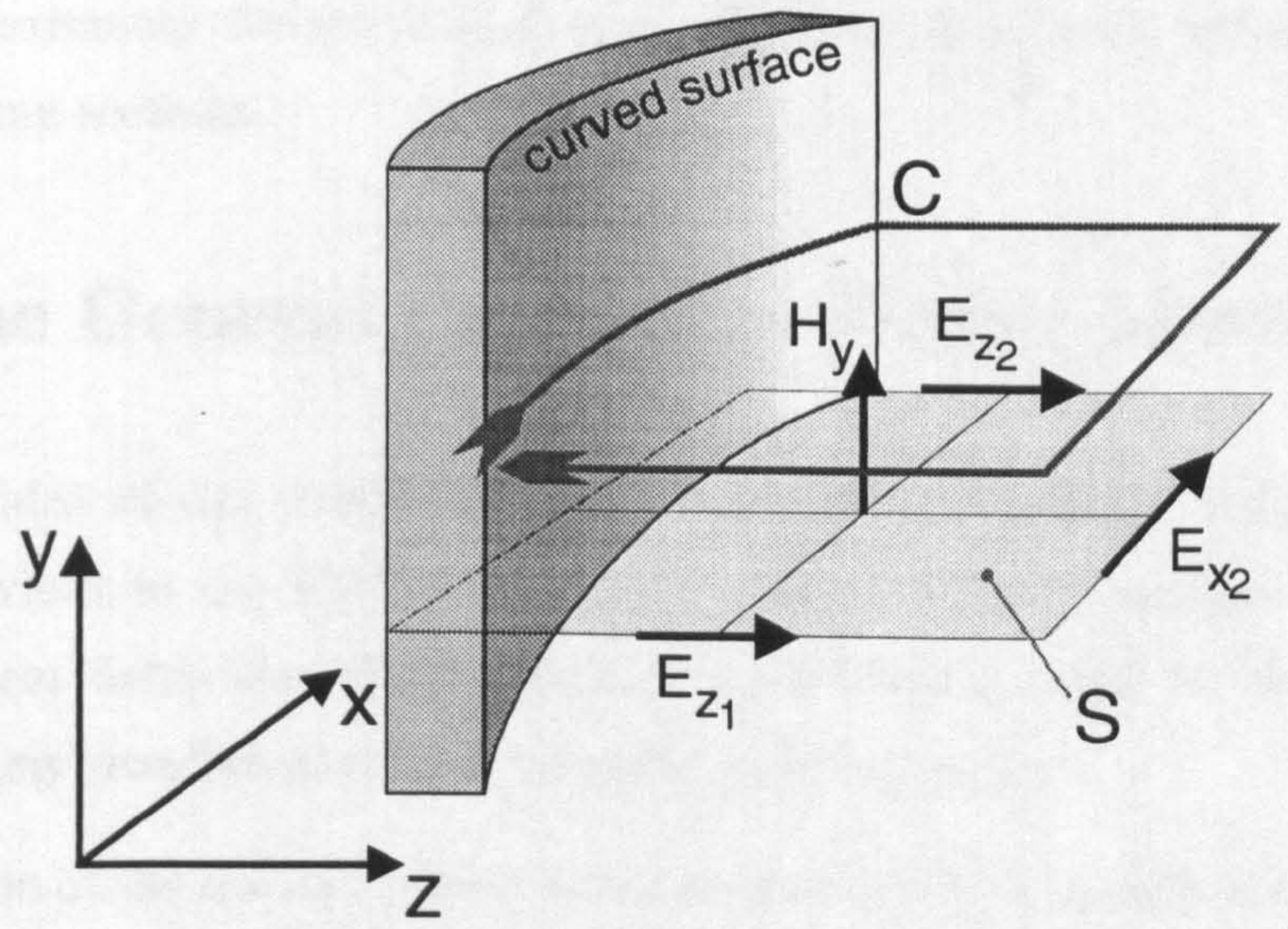

Figure 4.4: Curved surface and FDTD mesh.

The integral interpretation of FDTD states that:

$$\partial_t \int_S \mathbf{H} \cdot d\mathbf{a} = \partial_t \iint_S H_y \, dx \, dz = \frac{1}{\mu} \oint_C \mathbf{E} \cdot d\mathbf{l} \tag{4.6}$$

The contour path method assumes that H_y is the average value over S and that the electric field components are linear along their respective edges of the contour C. Along the curved edge of the contour the value of $\mathbf{E} \cdot \mathbf{l}$ is zero and thus (4.4) becomes:

$$A \partial_t H_y = \frac{1}{\mu} \left(L_2 E_{z_2} - L_1 E_{z_1} - \Delta E_{x_2} \right) \tag{4.7}$$

where A is the area of surface S, L_1 and L_2 are the lengths along the edges of the contour associated with E_{z_1} and E_{z_2} respectively.

The contour method has been used with some success, however in many cases the geometry of the problem prevents the method described above from calculating a number of the required field components. When this situation occurs the needed field is 'borrowed' from its nearest neighbour [25].

The nearest neighbour borrowing of fields is unappealing and approximate at best. Recent research directed at this problem, using the results of chapter 6 of this thesis, confirms that it can also induce numerical instability [26] (a disadvantage of the contour path method also alluded to in [23]).

The correction factor method referred to in section 4.3 for the treatment of geometric detail has also been applied to the characterisation of curved bodies [17]. The fact that the correction factor technique permits improved analysis of both sub-cellular details *and* curved surfaces, without introducing significant computational overheads, makes it an extremely attractive approach. The correction factor method is described in the following sections.

4.5 The General Correction Factor Method

The central idea of the correction factor method is to include *a priori* knowledge of field behaviour in the FDTD algorithm. This is done by replacing the assumed piecewise linear behaviour of the fields in the FDTD method by behaviour which more accurately matches known asymptotic field functions.

This alteration of the assumed field functions results in the modification or *correction* of the coefficients of the FDTD update equations; the method has therefore become known as the 'correction factor' technique.

Two approaches have been used in the development of correction factor schemes; the first relies upon the integral interpretation of FDTD and is illustrated here by its application to the characterisation of a microstrip line, the second is derived from FDTD's differential interpretation and, as an example, is applied to the analysis of a thin slot.

4.5.1 Integral Approach to Metal Edge Corrections [17]

Consider figure 4.5 showing a microstrip line intersecting a plane of the FDTD mesh. The transverse fields close to this object are well known to be singular – the behaviour of the fields being [15, 27]:

$$E_y(z,y) \propto H_z(z,y) \propto \Re\mathrm{e}\left\{\frac{1}{\sqrt{(\frac{w}{2})^2-(y+jz)^2}}\right\} = f_1(z,y) \tag{4.8}$$

$$E_z(z,y) \propto H_y(z,y) \propto \Im\mathrm{m}\left\{\frac{1}{\sqrt{(\frac{w}{2})^2-(y+jz)^2}}\right\} = f_2(z,y) \tag{4.9}$$

where the (z,y) origin is assumed to be the centre of the strip and w is its width.

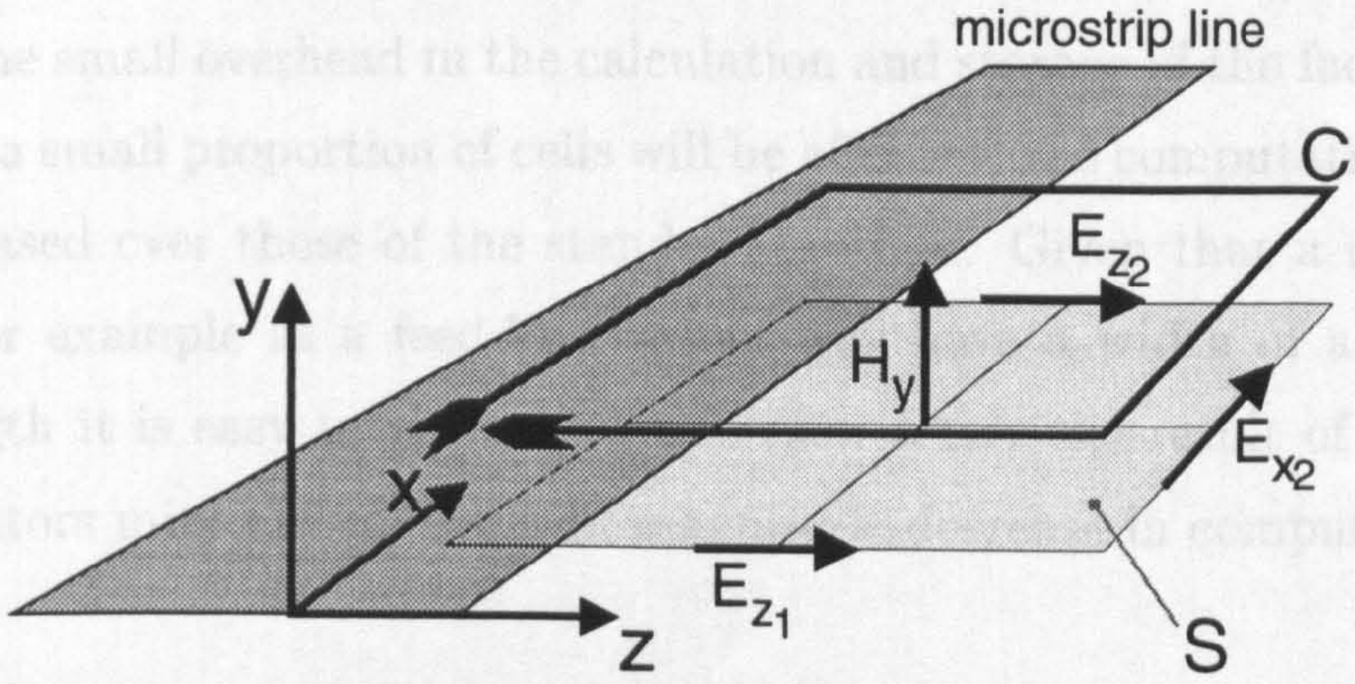

Figure 4.5: Microstrip line and FDTD mesh.

Assuming that the behaviour of the fields close to the edge is dominated by the static singularity, the function f_2 can be assumed to describe the behaviour of the E_z and H_y fields over the unit cell shown. This function is substituted into:

$$\iint_S \partial_t H_y \, dx \, dz = \frac{1}{\mu}\oint_C \mathbf{E} \, d\mathbf{l} \tag{4.10}$$

to give:

$$\partial_t H_y = \frac{1}{\mu}\frac{\left(\int_{z_1}^{z_2} f_2(z,y)\,dz\right)E_{z_2} - \Delta E_{x_2} - \left(\int_{z_1}^{z_2} f_2(z,y)\,dz\right)E_{z_1}}{\int_{z_1}^{z_2}\int_{x_1}^{x_2} f_2(z,y)\,dx\,dz} \tag{4.11}$$

where x_1, x_2, z_1, z_2 are the appropriate limits on the surface S (z_1 is the position where the strip intersects the surface S).

The integrals may be performed analytically and, on substitution of the limits, yield a corrected version of (4.2):

$$\partial_t H_y = \frac{1}{\mu\Delta}\left(k_1 E_{z_2} - k_2 E_{z_1} + k_3 E_{x_1} - k_4 E_{x_2}\right) \tag{4.12}$$

- the constants k are referred to as the 'correction factors' and are unity in the uncorrected FDTD algorithm.

A similar approach can be followed for the other field components and the resulting corrected FDTD method has been shown to produce an accurate characterisation of microstrip lines [15] even when employed with a unit cell size which would normally be far too large for modelling the strip.

The correction factor method then provides a rigorous technique for characterising microstrip lines without requiring a small cell size and subsequently small time step. Apart from the small overhead in the calculation and storage of the factors (considering that only a small proportion of cells will be affected) the computational overheads are not increased over those of the standard method. Given that a microstrip line, when used for example as a feed-line, might well have a width of a small fraction of a wavelength it is easy to envisage a situation where the result of employing the correction factors might be an order of magnitude decrease in computer run-time.

4.5.2 Differential Approach to Thin Slot Corrections [16]

The correction factor scheme for the microstrip line was produced by considering the integral interpretation of FDTD; correction methods have also been derived from the differential representation [16] and this approach is illustrated here by means of the example shown in figure 4.6.

Figure 4.6 depicts a narrow slot in a conducting plane that is to be modelled using FDTD by means of the correction factor method. Rather than formulating a correction factor scheme via the integral approach the differential form will be employed; specifically it is recalled from chapter 2 that FDTD can be viewed as a finite element method with piecewise linear basis functions $\phi_{i,j,k}$ and Dirac delta testing functions $\delta_{i,j,k}$.

The usefulness of the finite element concept for FDTD is now apparent; all that is needed to correct for the non-linear behaviour of the fields near the slot is a modification of the relevant basis functions. The functions which are modified are those for

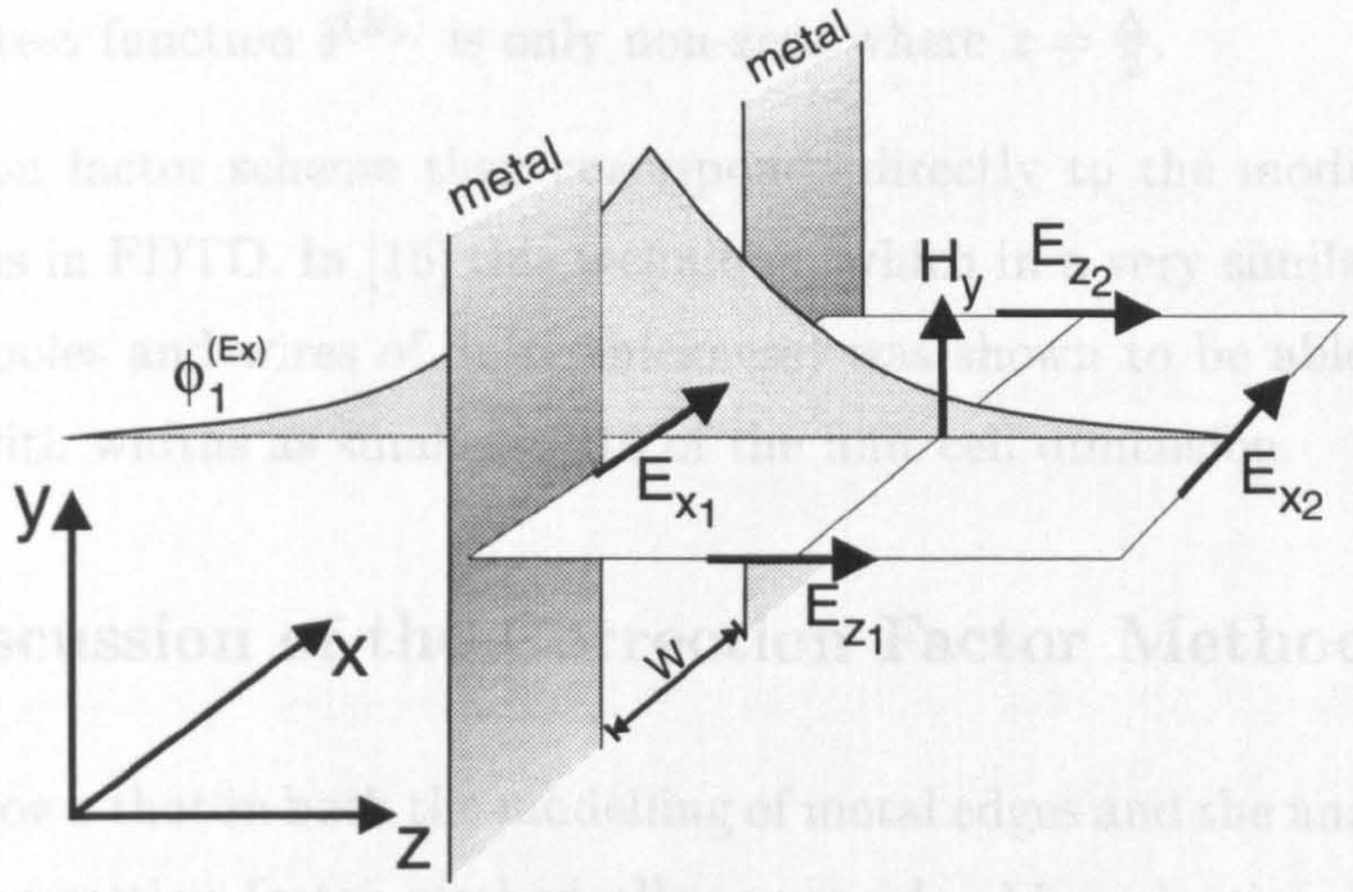

Figure 4.6: Slot and FDTD mesh.

the E_x component in the slot and the adjacent H_y fields. Considering as an example the illustrated H_y field:

$$\left\langle \delta^{(H_y)}, \phi^{(H_y)} \right\rangle \partial_t H_y(t) = -\frac{1}{\mu} \left\langle \delta^{(H_y)}, \left(\partial_x \left\{ \phi_2^{(E_z)} E_{z_2}(t) + \phi_1^{(E_z)} E_{z_1}(t) \right\} \right.\right.$$
$$\left.\left. -\partial_z \left\{ \phi_2^{(E_x)} E_{x_2}(t) + \phi_1^{(E_x)} E_{x_1}(t) \right\} \right) \right\rangle \tag{4.13}$$

where $\delta^{(H_y)}$ and $\phi^{(H_y)}$ are the test and basis functions associated with H_y. $\phi_1^{(E_x)}$, $\phi_2^{(E_x)}$, $\phi_1^{(E_z)}$ and $\phi_2^{(E_z)}$ are the basis functions belonging to the components E_{x_1}, E_{x_2}, E_{z_1} and E_{z_2} respectively.

If the basis functions are piecewise linear then the original FDTD equations are returned. In this case the known static field solution is employed for the basis function associated with E_{x_1}. If $z = 0$ is the position of the slot, the function has the form:

$$f_1(z) = \frac{1}{\sqrt{(\frac{w}{2})^2 + z^2}} \tag{4.14}$$

which describes the field in the plane through the centre of the slot (illustrated in figure 4.6). For the remaining three electric field components the standard piecewise linear function is retained.

Evaluation of the inner products gives:

$$\partial_t H_y = \frac{1}{\mu\Delta} \left(E_{z_2} - E_{z_1} + k_1 E_{x_1} - E_{x_2} \right) \tag{4.15}$$

where:

$$k_1 = \frac{\Delta}{f_1(\frac{\Delta}{2})} \partial_z f_1(\tfrac{\Delta}{2}) \tag{4.16}$$

since the H_y test function $\delta^{(H_y)}$ is only non-zero where $z = \frac{\Delta}{2}$.

This correction factor scheme then corresponds directly to the modification of the basis functions in FDTD. In [16] this technique (which in a very similar form may be applied to dipoles and wires of finite thickness) was shown to be able to accurately model slots with widths as small as 0.16 of the unit cell dimension.

4.5.3 Discussion of the Correction Factor Method

It has been shown that in both the modelling of metal edges and the analysis of curved surfaces the correction factor method allows considerable reduction in the required mesh density without sacrificing accuracy. If the method could be implemented reliably it would undoubtedly enable the efficient treatment of many common structures and greatly increase the applicability of the FDTD technique.

The principal drawback to the correction factor method has been numerical instability. In the majority of cases introduction of the correction factors has resulted in dramatic, non-physical, solution growth. When the growth is slow enough it is possible to complete the analysis before the instability becomes noticeable. In most situations however algorithmic instability is not tolerable.

The rest of this thesis is concerned almost entirely with the stability problems that have beset the correction factor method; to begin the consideration of this phenomenon, techniques for determining the stability of the FDTD method are examined. These techniques provide some insight into the stability issue and if a method can predict whether or not the algorithm will become unstable it is possible that the correction factors can be chosen to avoid the instability.

4.6 Discussion of Algorithm Stability

Two general methods are available for evaluating the stability of an explicit numerical algorithm; the first is the classical Fourier method and the second is the matrix technique. The following sections consider the application of both methods to the analysis of the correction factor stability problem.

4.6.1 The Fourier Method

The standard method for analysing the stability of finite difference algorithms is the Fourier, or von Neumann, method [28, p.92] [29, p.47]. In this method the spatial and temporal behaviour of the solution is expressed as a sum of complex exponentials of the form $e^{j\omega t+\beta x}e^{\alpha t}$ and the condition is sought for which $e^{\alpha t}$ does not grow with time.

This method is widely used and was the technique first employed to derive the Courant stability condition for FDTD in [7]. The method however does not extend to the treatment of difference algorithms where the coefficients are variable over space (algorithms that might be called 'non-uniform') and thus cannot yield a stability criterion for the corrected FDTD algorithm.

4.6.2 The Matrix Method

The matrix method, unlike the Fourier technique, provides a stability test for a non-uniform algorithm.

Consider the finite element formulation of FDTD as given by section 2.6.2:

$$\mathbf{M}_1\partial_t\mathbf{h}(t) = \mathbf{K}_1\mathbf{e}(t) \tag{4.17}$$

$$\mathbf{M}_2\partial_t\mathbf{e}(t) = \mathbf{K}_2\mathbf{h}(t) \tag{4.18}$$

where the mass matrices $\mathbf{M}$ are diagonal. This may be written for convenience as:

$$\partial_t\mathbf{e}(t) = \mathbf{A}\mathbf{h}(t) \tag{4.19}$$

$$\partial_t\mathbf{h}(t) = \mathbf{B}\mathbf{e}(t) \tag{4.20}$$

For ease of manipulation the solution vector $\mathbf{h}$ is eliminated to give the relation:

$$\partial_{tt}\mathbf{e}(t) = \mathbf{A}\mathbf{B}\mathbf{e}(t) \tag{4.21}$$

This equation describes the continuous time system represented by FDTD and intuitively it must itself be stable if the FDTD algorithm is to be stable – in this thesis this type of system is called the *equivalent* system for the algorithm.

The equation may be written in the standard (phase-variable) form:

$$\partial_t \begin{pmatrix} \dot{\mathbf{e}} \\ \mathbf{e} \end{pmatrix} = \begin{pmatrix} \mathbf{0} & \mathbf{AB} \\ \mathbf{I} & \mathbf{0} \end{pmatrix} \begin{pmatrix} \dot{\mathbf{e}} \\ \mathbf{e} \end{pmatrix} \text{ or } \partial_t \begin{pmatrix} \dot{\mathbf{e}} \\ \mathbf{e} \end{pmatrix} = \mathbf{C} \begin{pmatrix} \dot{\mathbf{e}} \\ \mathbf{e} \end{pmatrix} \tag{4.22}$$

It is well known that for this system to be stable, the eigenvalues of the system matrix $\mathbf{C}$ must have non-positive real parts (this result may also be considered as arising from taking the Laplace transform of (4.21) and evaluating the roots of the characteristic equation [30, chapter 8]).

FDTD however is a discrete time system and replaces the time derivatives of (4.21) with centred differences. This gives:

$$\mathbf{e}^{n+1} - 2\mathbf{e}^n + \mathbf{e}^{n-1} = \Delta_t^2 \mathbf{AB} \mathbf{e}^n \tag{4.23}$$

(eliminating the magnetic fields from the FDTD algorithm gives an effectively identical update equation which uses the intermediate $\mathbf{h}$ values instead of the past values of $\mathbf{e}$).

Equation (4.23) can be written as:

$$\begin{pmatrix} \mathbf{e}^{n+1} \\ \mathbf{e}^n \end{pmatrix} = \begin{pmatrix} (2\mathbf{I} + \Delta_t^2 \mathbf{AB}) & -\mathbf{I} \\ \mathbf{I} & 0 \end{pmatrix} \begin{pmatrix} \mathbf{e}^n \\ \mathbf{e}^{n-1} \end{pmatrix} \text{ or } \mathbf{D} \begin{pmatrix} \mathbf{e}^n \\ \mathbf{e}^{n-1} \end{pmatrix} \tag{4.24}$$

this matrix equation governs the evolution of $\mathbf{e}$ at each iteration.

It is apparent by repeated application of (4.24) that, given an initial condition:

$$\begin{pmatrix} \mathbf{e}^{n+1} \\ \mathbf{e}^n \end{pmatrix} = \mathbf{D}^n \begin{pmatrix} \mathbf{e}^1 \\ \mathbf{e}^0 \end{pmatrix} \tag{4.25}$$

and taking some vector norm $\|\cdot\|$ of both sides to be a measure of the magnitude of the solution,

$$\left\| \begin{pmatrix} \mathbf{e}^{n+1} \\ \mathbf{e}^n \end{pmatrix} \right\| = \left\| \mathbf{D}^n \begin{pmatrix} \mathbf{e}^1 \\ \mathbf{e}^0 \end{pmatrix} \right\| \tag{4.26}$$

thus:

$$\left\| \begin{pmatrix} \mathbf{e}^{n+1} \\ \mathbf{e}^n \end{pmatrix} \right\| \leq |||\mathbf{D}^n||| \left\| \begin{pmatrix} \mathbf{e}^1 \\ \mathbf{e}^0 \end{pmatrix} \right\| \leq |||\mathbf{D}|||^n \left\| \begin{pmatrix} \mathbf{e}^1 \\ \mathbf{e}^0 \end{pmatrix} \right\| \tag{4.27}$$

Thus the norm of the solution is bounded as n increases provided that $|||\mathbf{D}|||^n$ is bounded as $n \to \infty$. This implies that for stability:

$$\left\| \begin{pmatrix} (2\mathbf{I} + \Delta_t^2 \mathbf{AB}) & -\mathbf{I} \\ \mathbf{I} & 0 \end{pmatrix} \right\| \leq 1 \tag{4.28}$$

this matrix must therefore have a spectral radius that is less than or equal to unity [29, p.56] (this result may also be arrived at by considering the z-transform of (4.23)).

It has been shown then that a matrix representation of FDTD yields two stability criteria; the first specifies that the eigenvalues of the equivalent system modelled by FDTD must have real parts less than or equal to zero and the second specifies that the discrete time algorithm must have eigenvalues with a modulus less than or equal to unity.

The criterion for the equivalent system is a necessary one for FDTD stability and the criterion for the discrete time system is sufficient. In both cases however the stability test involves finding the eigenvalues of a matrix.

The size of the matrix will be the number of unknown field components in the FDTD model (a typical number would be around 1 million). It can be seen therefore that, while the matrix method can determine the stability of the FDTD algorithm both with and without correction factors, the computation is likely to be unfeasibly time consuming. No general stability test has been found for the corrected FDTD algorithm which can provide a practical evaluation of the stability of the method.

It might be thought that reducing the time step is one route to regaining the stability of the algorithm regardless of the imposed correction factors. In the following section the validity of this hypothesis is briefly investigated by means of a simple example which also helps to illustrate the stability theory given above.

4.6.3 FDTD Stability – Some Examples

The preceding theory is entirely valid for one, two or three dimensional FDTD algorithms. In order to minimise the required size of the matrices however the problem chosen for consideration here is a small, one-dimensional Yee FDTD algorithm. This simple example is quite complex enough however to exhibit identical instability phenomena to those exhibited by much larger three-dimensional algorithms.

The problem considered is illustrated by figure 4.7 and consists of 7 field components forming a one dimensional problem space. The outer electric field components are set equal to zero, imposing a perfectly electrically conducting (Dirichlet) boundary condition on the problem.

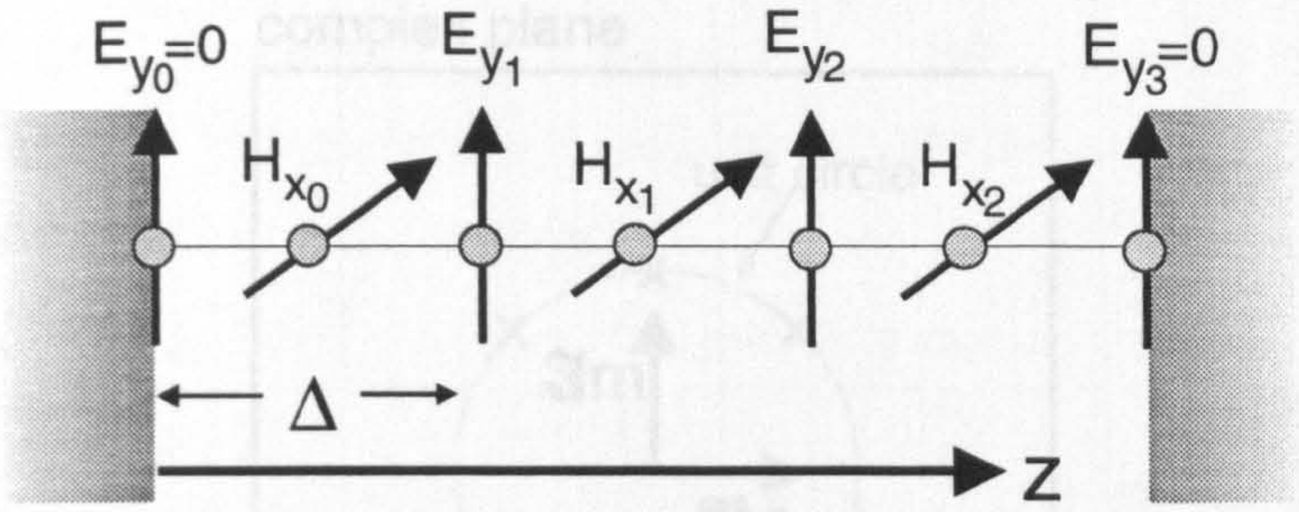

Figure 4.7: One dimensional FDTD problem.

The remaining free field components can be calculated by means of the standard FDTD method, for example:

$$H_{x_1}^{n+0.5} = H_{x_1}^{n-0.5} + \Delta_t \frac{E_{y_2}^n - E_{y_1}^n}{\Delta} \tag{4.29}$$

$$E_{y_1}^{n+1} = E_{y_1}^n + \Delta_t \frac{H_{x_1}^{n+0.5} - H_{x_0}^{n+0.5}}{\Delta} \tag{4.30}$$

where the physical space is assumed normalised to $\epsilon, \mu = 1$.

Once again the calculation of the H fields is omitted, giving:

$$E_{y_1}^{n+1} = -E_{y_1}^{n-1} + 2\left(1 - \frac{\Delta_t^2}{\Delta^2}\right) E_{y_1}^n + \frac{\Delta_t^2}{\Delta^2} E_{y_2}^n + \frac{\Delta_t^2}{\Delta^2} E_{y_0}^n \tag{4.31}$$

Assembling the nodal equations into the form of the matrix equation (4.24) gives:

$$\begin{pmatrix} E_{y_1}^{n+1} \\ E_{y_2}^{n+1} \\ E_{y_3}^{n+1} \\ E_{y_1}^{n} \\ E_{y_2}^{n} \\ E_{y_3}^{n} \end{pmatrix} = \begin{pmatrix} 2(1-a) & a & 0 & -1 & 0 & 0 \\ a & 2(1-a) & a & 0 & -1 & 0 \\ 0 & a & 2(1-a) & 0 & 0 & -1 \\ 1 & 0 & 0 & 0 & 0 & 0 \\ 0 & 1 & 0 & 0 & 0 & 0 \\ 0 & 0 & 1 & 0 & 0 & 0 \end{pmatrix} \begin{pmatrix} E_{y_1}^{n} \\ E_{y_2}^{n} \\ E_{y_3}^{n} \\ E_{y_1}^{n-1} \\ E_{y_2}^{n-1} \\ E_{y_3}^{n-1} \end{pmatrix} \tag{4.32}$$

where $a = (\frac{\Delta_t}{\Delta})^2$.

The Courant limit for this model is easily seen to be $a = 1$, for this value the eigenvalues of the system (as calculated by the analysis program Mathcad[1]) are shown in figure 4.8; the six eigenvalues lie on the perimeter of the unit circle showing that the system is stable and, indeed, non-dissipative.

The effect of adding some entirely arbitrary correction factors into the algorithm is easily demonstrated by introducing two factors k_1 and k_2 into the update matrix

[1] ©MathSoft Inc.

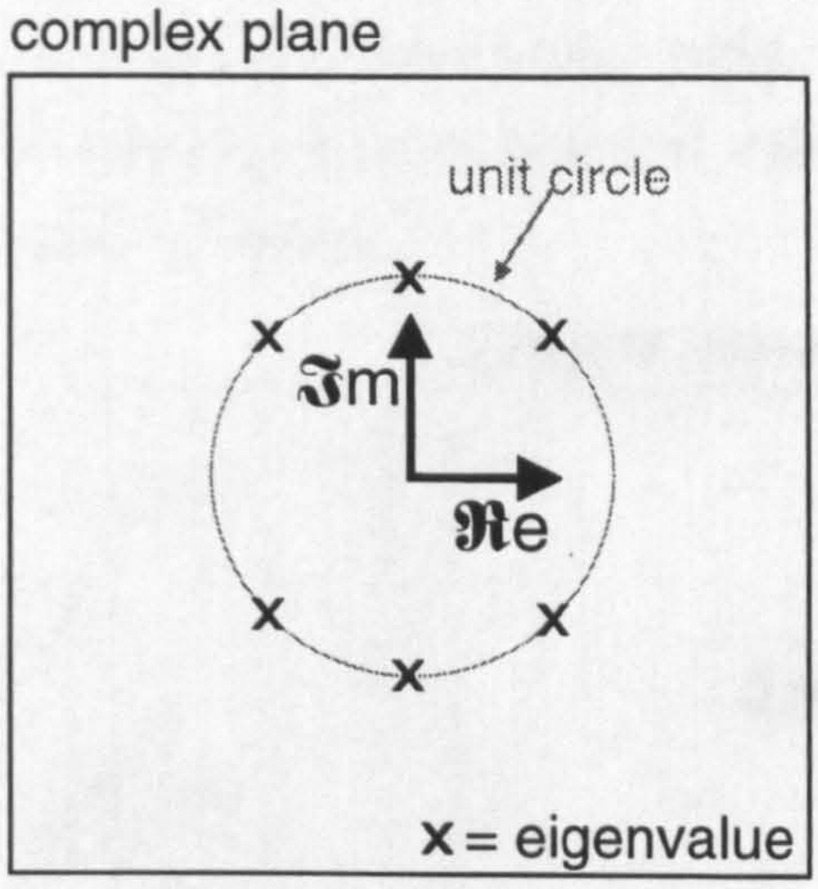

Figure 4.8: Eigenvalues for FDTD algorithm ($a = 1$)

of (4.32), thus:

$$\begin{pmatrix} 2(1-a) & k_1 a & 0 & -1 & 0 & 0 \\ k_2 a & 2(1-a) & t & 0 & -1 & 0 \\ 0 & a & 2(1-a) & 0 & 0 & -1 \\ 1 & 0 & 0 & 0 & 0 & 0 \\ 0 & 1 & 0 & 0 & 0 & 0 \\ 0 & 0 & 1 & 0 & 0 & 0 \end{pmatrix} \tag{4.33}$$

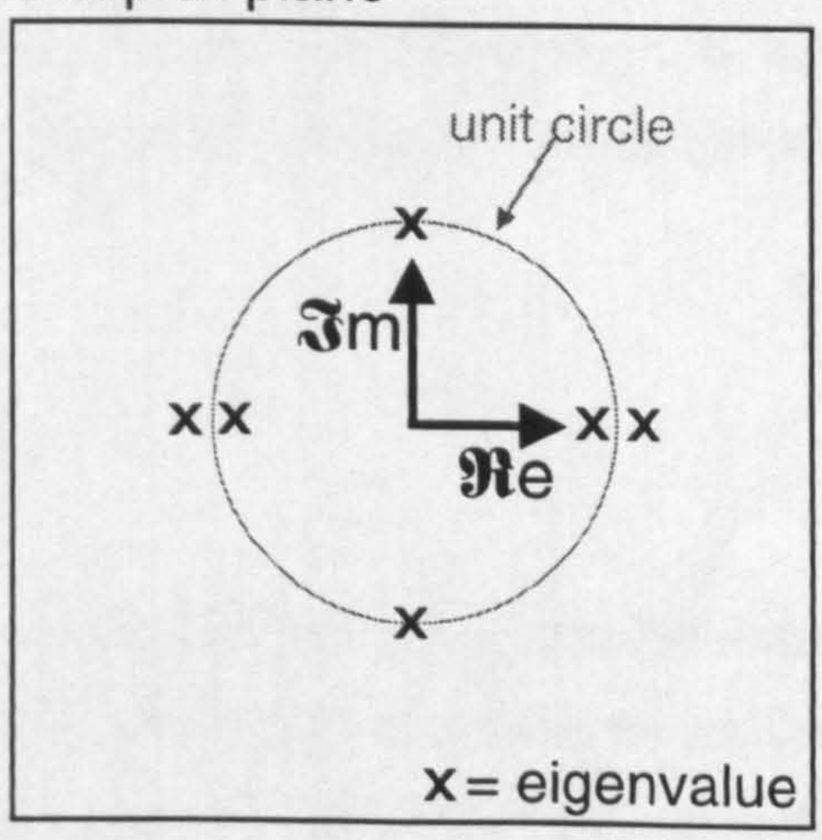

Figure 4.9: Eigenvalues for corrected FDTD algorithm ($a = 1$).

With $a = 1$ and $k_1 = k_2 = 1.75$ the eigenvalues are shown by figure 4.9 – clearly the system is unstable as there are two (real) eigenvalues outside the unit circle.

To test the hypothesis that stability may be regained by reducing the time step the eigenvalues are recalculated with $a = 0.5$ and $a = 0.1$, obtaining figures 4.10(i) and

(ii). It is seen that there remains one eigenvalue outside the unit circle even when the value of $a = 0.1$ – this corresponds to a choice of time step Δ_t only 32% of the value required by the Courant criterion.

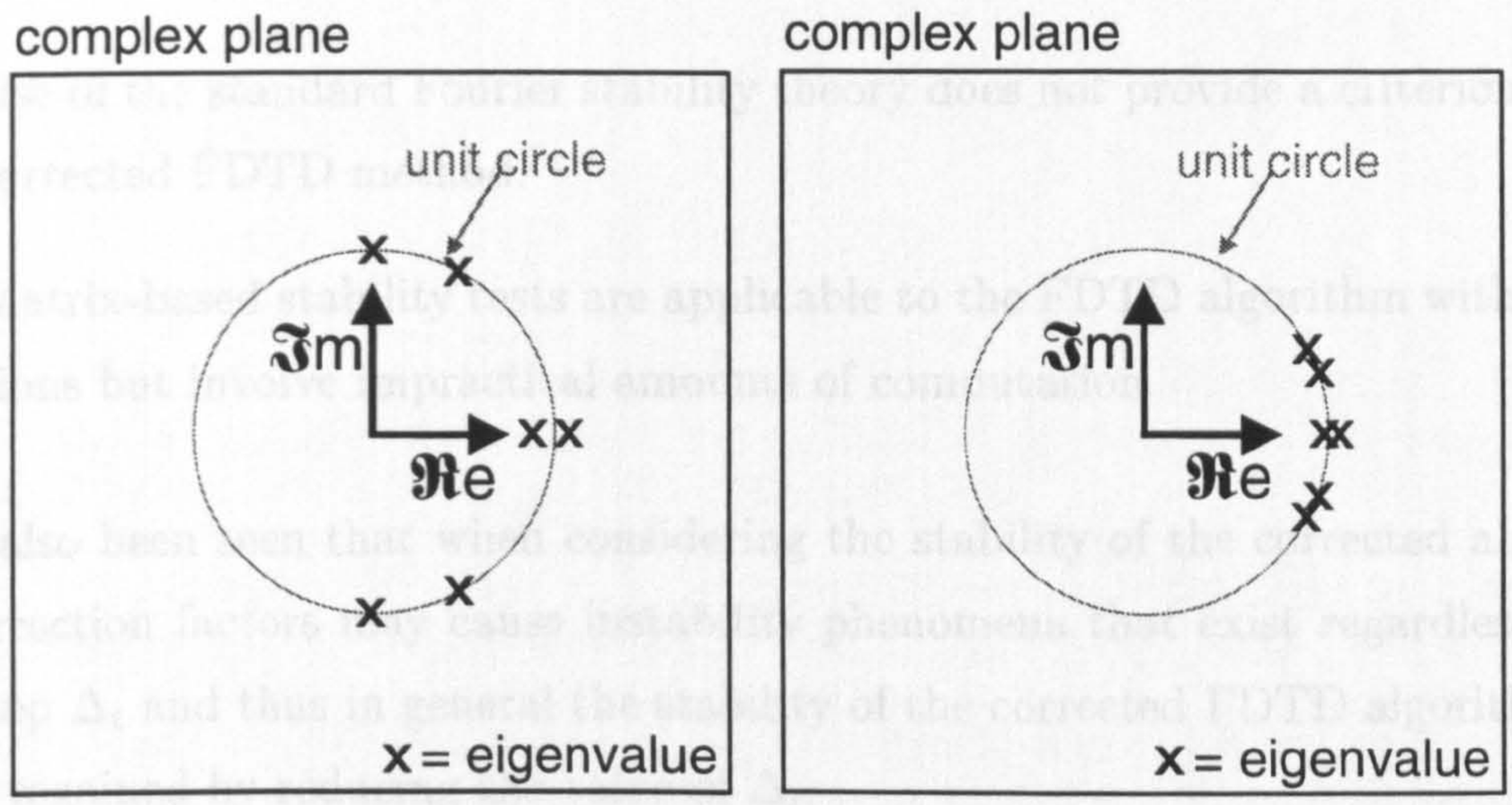

Figure 4.10: Eigenvalues for corrected FDTD algorithm (i) $a = 0.5$ (ii) $a = 0.1$.

As the ratio of time step to space step is reduced, the eigenvalues do not move inside the unit circle but instead move *around* it towards the point $1 + 0j$. This observation correlates with the observed manifestations of instability in the FDTD method with actual correction factors (rather than the arbitrary values used here) – in general reducing the time step may slow the increase in solution magnitude per time iteration but it does not solve the problem. It is in fact possible to show that the eigenvalues of this problem only reach the perimeter of the unit circle and achieve stability when $a = 0$.

4.7 Summary

This chapter has described some of the various methods that exist to improve FDTD's handling of fine geometrical detail and of curved structures. Of these techniques the correction factor technique is an attractive and general methodology by which *a priori* knowledge of the field behaviour may be included in FDTD.

A correction factor scheme can be introduced by consideration of either the differential or integral nature of the FDTD method - both approaches have been illustrated by means of examples.

While the correction factors are potentially a means to overcome the majority of

Section 4.7 : Summary

FDTD's shortcomings their use has been limited by the occurrence of numerical instability. Some sort of criterion is clearly required on the basis of which a stable set of correction factors can be chosen. This chapter however has shown that:

- Use of the standard Fourier stability theory does not provide a criterion for the corrected FDTD method.

- Matrix-based stability tests are applicable to the FDTD algorithm with corrections but involve impractical amounts of computation.

It has also been seen that when considering the stability of the corrected algorithm the correction factors may cause instability phenomena that exist regardless of the time step Δ_t and thus in general the stability of the corrected FDTD algorithm may not be regained by reducing the value of Δ_t.

Chapters 5 and 6 continue the investigation of the instability caused by the correction factors and draw upon many of the concepts introduced by this chapter (and by section 4.6 especially). One idea in particular is found to be of considerable utility, this being the "equivalent system" for the difference algorithm – the continuous-time system obtained by re-inserting the derivatives in place of the temporal difference approximations of the algorithm.

References

[1] K. S. Yee, "Numerical solution of initial boundary value problems involving Maxwell's equations in isotropic media," *IEEE Transactions on Antennas and Propagation*, vol. AP-14, pp. 302–307, May 1966.

[2] W. J. R. Hoefer, "Huygens and the computer – a powerful alliance in numerical electromagnetics," *Proceedings of the IEEE*, vol. 79, pp. 1459–1471, Oct. 1991.

[3] K. S. Kunz and K. M. Lee, "A three dimensional finite difference solution of the external response of an aircraft to a complex transient EM environment," *IEEE Transactions on Electromagnetic Compatibility*, vol. EMC-20, pp. 328–332, Feb. 1978.

[4] X. Zhang, J. Fang, K. K. Mei, and Y. Lui, "Calculation of the dispersive characteristics of microstrips by the time domain finite difference method," *IEEE Transactions on Microwave Theory and Techniques*, vol. MTT-36, pp. 263–267, Feb. 1988.

[5] D. M. Sullivan, O. P. Ghandi, and A. Taflove, "Use of the finite difference time domain method for calculating EM absorption in man models," *IEEE Transactions on Biomedical Engineering*, vol. BME-35, pp. 179–186, Mar. 1988.

[6] R. Luebbers, F. Hunsberger, K. S. Kunz, R. Standler, and M. Schneider, "A frequency dependent finite difference time domain formulation for dispersive materials," *IEEE Transactions on Electromagnetic Compatibility*, vol. EMC-32, pp. 222–227, Aug. 1990.

[7] A. Taflove and M. E. Brodwin, "Numerical solution of steady state electromagnetic scattering problems using the time dependent Maxwell's equations," *IEEE Transactions on Microwave Theory and Techniques*, vol. MTT-23, pp. 623–630, Aug. 1975.

[8] A. C. Cangellaris and D. B. Wright, "Analysis of the numerical error caused by the stair-stepped approximation of a conducting boundary in FDTD simulations of electromagnetic phenomena," *IEEE Transactions on Antennas and Propagation*, vol. AP-39, pp. 1518–1525, Oct. 1991.

[9] A. Taflove, K. R. Umashankar, F. Harfoush, and K. S. Yee, "Detailed FDTD analysis of elecromagnetic fields penetrating narrow slots and lapped joints in thick conducting screens," *IEEE Transactions on Antennas and Propagation*, vol. AP-36, pp. 247–257, Feb. 1988.

[10] A. Taflove and K. R. Umashankar, "A hybrid moment method/finite difference time domain approach to electromagnetic coupling and aperture penetration

into complex geometries," *IEEE Transactions on Antennas and Propagation*, vol. AP-30, pp. 617–627, July 1982.

[11] K. R. Demarest, "A finite difference time domain technique for modelling narrow apertures in conducting surfaces," *IEEE Transactions on Antennas and Propagation*, vol. AP-35, pp. 826–831, July 1987.

[12] R. Holland and L. Simpson, "Finite difference analysis of EMP coupling to thin struts and wires," *IEEE Transactions on Electromagnetic Compatibility*, vol. EMC-23, pp. 88–97, May. 1984.

[13] K. R. Umashankar, A. Taflove, and B. Beker, "Calculation and experimental validation of induced currents on coupled wires in an arbitrary shaped cavity," *IEEE Transactions on Antennas and Propagation*, vol. AP-35, pp. 1248–1257, Nov. 1987.

[14] D. B. Shorthouse and C. J. Railton, "Incorporation of static singularities into the finite difference time domain technique with application to microstrip structures," in *Proceedings of the 20th European Microwave Conference*, vol. 1, pp. 531–536, Sept. 1990.

[15] C. J. Railton, D. B. Shorthouse, and J. P. McGeehan, "Modelling of narrow microstrip lines using finite difference time domain method," *Electronics Letters*, vol. 28, pp. 1168–1170, June 1992.

[16] C. J. Railton, "The simple rigorous and effective treatment of thin wires and slots in the FDTD method," in *Proceedings of the 24th European Microwave Conference*, vol. 2, pp. 1541–1546, 1994.

[17] C. J. Railton, "Use of static field solutions in the FDTD method for the efficient treatment of curved metal surfaces," *Electronics Letters*, vol. 29, pp. 1466–1467, Aug. 1993.

[18] C. J. Railton, "An algorithm for the treatment of curved metallic laminas in the finite difference time domain method," *IEEE Transactions on Microwave Theory and Techniques*, vol. MTT-41, pp. 1429–1438, Aug. 1993.

[19] K. S. Yee, J. S. Chen, and A. H. Chang, "Conformal finite difference time domain (FDTD) with overlapping grids," *IEEE Transactions on Antennas and Propagation*, vol. AP-40, pp. 1068–1075, Sept. 1992.

[20] R. Holland, "Finite difference solutions of Maxwells equations in generalised non-orthogonal coordinates," *IEEE Transactions on Nuclear Science*, vol. NS-30, pp. 4589–4591, Dec. 1983.

[21] N. K. Madsen, "Divergence preserving discrete surface integral methods for Maxwell's curl equations using non-orthogonal unstructured grids," *Journal of Computational Physics*, pp. 34–45, 1995.

[22] J. J. Ambrosiano, S. T. Brandon, R. Lohner, and C. R. DeVore, "Electromagnetics via the Taylor Galerkin finite element method on unstructured grids," *Journal of Computational Physics*, vol. 110, pp. 310–319, 1994.

[23] N. K. Madsen, "Divergence preserving discrete surface integral methods for Maxwell's curl equations using non-orthogonal unstructured grids," *Journal of Computational Physics*, vol. 119, pp. 34–45, June 1995.

[24] T. G. Jurgens, A. Taflove, K. Umashankar, and T. G. Moore, "Finite difference time domain modelling of curved surfaces," *IEEE Transactions on Antennas and Propagation*, vol. AP-40, pp. 357–366, Apr. 1992.

[25] T. G. Jurgens and A. Taflove, "Three dimensional contour FDTD modelling of scattering from single and multiple bodies," *IEEE Transactions on Antennas and Propagation*, vol. AP-41, pp. 1703–1708, Dec. 1993.

[26] C. J. Railton, I. J. Craddock, and J. B. Schneider, "An improved locally distorted CPFDTD algorithm with provable stability," *Electronics Letters*, vol. 31, pp. 1585–1586, Aug. 1995.

[27] C. J. Railton and J. P. McGeehan, "A rigorous and computationally efficient analysis of microstrip for use as an electro-optic modulator," *IEEE Transactions on Microwave Theory and Techniques*, vol. MTT-37, pp. 1099–1104, Aug. 1989.

[28] G. D. Smith, *Numerical Solution of Partial Differential Equations: Finite Difference Methods.* Oxford University Press, 2 ed., 1978.

[29] W. F. Ames, *Numerical Methods for Partial Differential Equations.* Thomas Nelson and Sons, 1969.

[30] O. L. R. Jacobs, *Introduction to Control Theory.* Oxford University Press, 3 ed., 1993.

Chapter 5

A Novel Algorithm Incorporating *a Priori* Knowledge

5.1 Introduction

In chapter 4, section 4.5, the correction factor method [1–6] was introduced as an attractive concept for the improved characterisation of fine detail and curved surfaces in the FDTD method. The correction factor technique, approached by either the integral or differential interpretation of FDTD, is a very general method for the incorporation of *a priori* knowledge of the fields into the FDTD algorithm.

Section 4.6 introduced the stability problems that have to date prevented widespread use of the correction factor method – it was shown that the problem of determining whether or not an arbitrary set of correction factors results in instability essentially requires the evaluation of the eigenvalues of the algorithm's system matrix. The sheer size of the matrix involved however makes examination of these eigenvalues an impractical test for stable correction schemes. It was also shown that the corrected algorithms may be unstable regardless of the choice of time step – thus stability will not necessarily be regained by reducing Δ_t.

Correction factor schemes can be implemented for time domain finite difference algorithms other than FDTD and in this chapter an alternative difference algorithm and correction factor formulation is investigated. This new technique proves to be not only stable but capable of an accurate analysis of smooth perfectly conducting structures. Additionally however, by virtue of the very special form of its correction factor scheme, the new method provides an entirely new understanding of the stability issue.

5.2 Initial Investigations of Instability

The cause of the aforementioned instability problem is far from clear; one hypothesis which suggests itself is that, since in the FDTD algorithm both the electric and magnetic fields (**E** and **H**) are independently corrected, an inconsistency between the corrections to each field results in a physically unrealisable model and hence instability.

Since the magnetic fields can be eliminated from Maxwell's equations it is possible to formulate a difference algorithm, and thus a correction factor scheme, in which corrections for **H** are not required.

In order to examine this idea three different electric-field-only time domain difference algorithms were derived and implemented by the author. For each algorithm a suitable correction factor scheme for the modelling of curved surfaces was formulated and then implemented. In general however these algorithms were found to be as potentially unstable as the FDTD method – thus invalidating the hypothesis.

One algorithm, with one particular correction factor scheme, seemed however to have extremely favourable stability characteristics and was investigated further; this algorithm [7, 8] was denoted 'SFDTD' (for 'Second order Finite Difference Time Domain' as its formulation involved only second order spatial and temporal derivatives) in order to distinguish it from the Yee FDTD method.

5.3 The SFDTD Method

Eliminating the magnetic fields from Maxwell's curl equations is straightforward in a lossless medium and yields the well known double-curl equation:

$$\nabla \times (\nabla \times \mathbf{E}) = -c^{-2}\partial_{tt}\mathbf{E} \tag{5.1}$$

where $c = (\mu\epsilon)^{-\frac{1}{2}}$ is the propagation speed in the medium under consideration. This expression can be rewritten by means of a standard identity:

$$\nabla^2\mathbf{E} - \nabla(\nabla \cdot \mathbf{E}) = c^{-2}\partial_{tt}\mathbf{E} \tag{5.2}$$

At this point one of two possible directions can be taken; one in which the divergence $\nabla \cdot \mathbf{E}$ is assumed to be zero – leading to a pure wave equation, and another in which the divergence term is retained. The choice made here directly affects the spatial discretisation required by the algorithm and, while algorithms based on both choices were investigated, the discretisation used by the successful SFDTD method required $\nabla \cdot \mathbf{E} = 0$. The implications of neglecting the divergence is that the standard algorithm cannot model regions, such as metal edges, where the divergence is non zero.

Neglecting the divergence gives:

$$\nabla^2\mathbf{E} = c^{-2}\partial_{tt}\mathbf{E} \tag{5.3}$$

– the effect of assuming the divergence to be zero has been to *decouple* the field components. Equation (5.3) can, for example, be written for E_y:

$$\partial_{xx}E_y + \partial_{yy}E_y + \partial_{zz}E_y = c^{-2}\partial_{tt}E_y \tag{5.4}$$

with similar expressions available for the other field components.

Well known centred finite difference expressions [9, 10] such as:

$$\partial_{xx} E_y(x = i\Delta) = \frac{E_{y_{i+1}} - 2E_{y_i} + E_{y_{i-1}}}{\Delta^2} \tag{5.5}$$

may be employed for the solution of this equation on a non-staggered grid (one where all the field components are defined at the vertex of each unit cell rather than being displaced along each edge of the cell – as shown by figure 5.1).

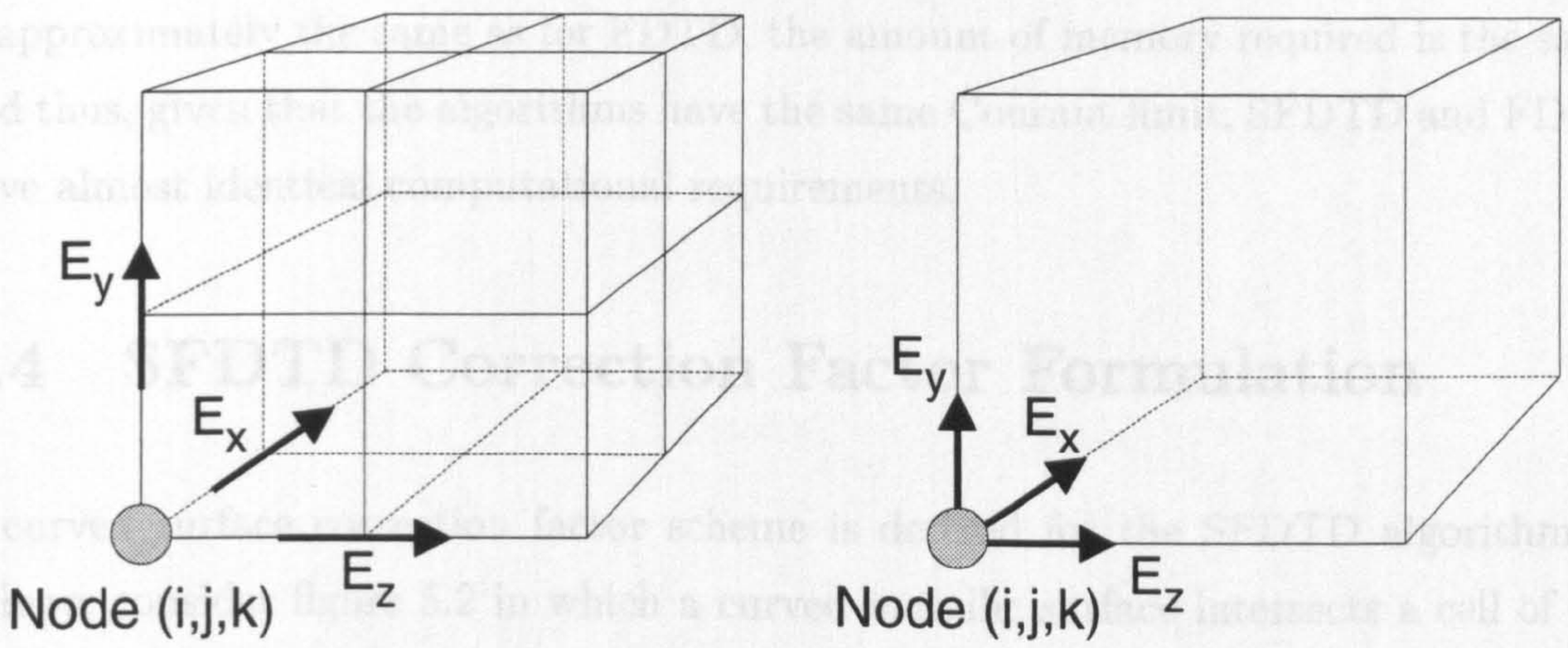

Figure 5.1: A comparison of FDTD (staggered) and SFDTD (non-staggered) meshes.

Given this discretisation of the **E** field components and using the notation $E^n_{y_{i,j,k}}$ to represent the E_y field coefficient in unit cell (i, j, k) an explicit update equation for E_y can be written:

$$E^{n+1}_{y_{i,j,k}} = -E^{n-1}_{y_{i,j,k}} + \left(2 - \frac{6c^2\Delta_t^2}{\Delta^2}\right) E^n_{y_{i,j,k}} + \left[E^n_{y_{i+1,j,k}} + E^n_{y_{i-1,j,k}} + E^n_{y_{i,j,k+1}} + E^n_{y_{i,j,k-1}} + E^n_{y_{i,j+1,k}} + E^n_{y_{i,j-1,k}}\right] \frac{c^2\Delta_t^2}{\Delta^2} \tag{5.6}$$

where the standard symbols for the space and time step have been employed; similar expressions are obtained for the other two electric components. The equation states that the value of E_y at iteration $(n+1)$ is calculated from the six surrounding values at step n and its own previous values at iterations n and $(n-1)$.

This algorithm is in itself not a particularly novel technique – essentially it is an extension of the two-dimensional difference algorithm given under the section 'Die Schwingungsgleichung in drei Variablen' of [11] to three spatial dimensions and three (uncoupled) field components. In electromagnetics similar electric-field-only algorithms have been investigated [12, 13] although these methods either use FDTD's

staggered spatial discretisation [12] or retain the divergence term in (5.2) [13] and thus differ substantially from SFDTD.

The Courant condition for SFDTD can be shown by means of the argument of section 2.7.2 to be the same as for FDTD, that is:

$$\Delta_t \leq \frac{\Delta}{c\sqrt{3}} \tag{5.7}$$

It is readily seen that the number of operations needed by SFDTD at each iteration is approximately the same as for FDTD, the amount of memory required is the same and thus, given that the algorithms have the same Courant limit, SFDTD and FDTD have almost identical computational requirements.

5.4 SFDTD Correction Factor Formulation

A curved surface correction factor scheme is derived for the SFDTD algorithm as follows; consider figure 5.2 in which a curved metallic surface intersects a cell of the SFDTD mesh; this surface is approximated over the SFDTD cell by the angled facet illustrated by the inset in figure 5.2.

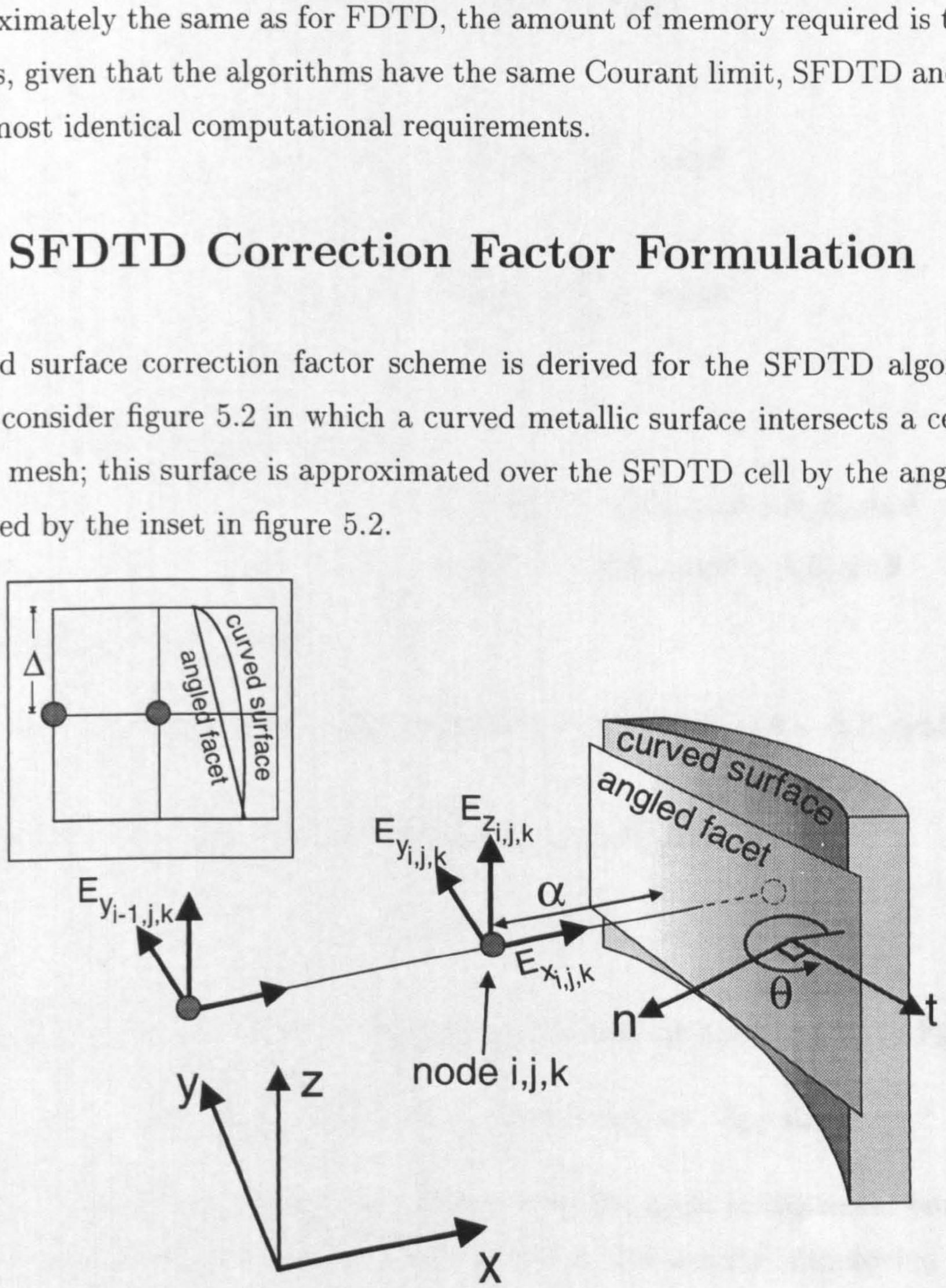

Figure 5.2: Curved surface and SFDTD mesh.

The behaviour of the normal and tangential fields near the angled plane is given by:

$$E_n = k_1 \qquad E_t = k_2 n \tag{5.8}$$

where n and t are the coordinates normal and tangential to the surface (see figure 5.2) and k_1, k_2 are unknown coefficients.

Take the first order spatial derivative of E_y:

$$\partial_x E_y = \left[\partial_n E_y \frac{\partial n}{\partial x} + \partial_t E_y \frac{\partial t}{\partial x}\right] \tag{5.9}$$

now:

$$n = x\sin\theta - y\cos\theta \Rightarrow \frac{\partial n}{\partial x} = \sin\theta \tag{5.10}$$

$$t = x\cos\theta + y\sin\theta \Rightarrow \frac{\partial t}{\partial x} = \cos\theta \tag{5.11}$$

and:

$$\begin{aligned} E_y &= -E_n\cos\theta + E_t\sin\theta \\ \Rightarrow \partial_n E_y &= -\partial_n E_n\cos\theta + \partial_n E_t\sin\theta \\ \Rightarrow \partial_t E_y &= -\partial_t E_n\cos\theta + \partial_t E_t\sin\theta \end{aligned} \tag{5.12}$$

Substitution into (5.9) yields:

$$\partial_x E_y = [-\partial_n E_n\cos\theta\sin\theta + \partial_n E_t\sin\theta\sin\theta - \partial_t E_n\cos\theta\cos\theta + \partial_t E_t\sin\theta\cos\theta] \tag{5.13}$$

employing the functions given by (5.8) for E_n and E_t gives:

$$\partial_x E_y = k_2\sin^2\theta \tag{5.14}$$

The value of k_2 can be found by considering the field at node (i, j, k) in figure 5.2:

$$E_t = E_{y_{i,j,k}}\sin\theta + E_{x_{i,j,k}}\cos\theta = k_2 n_0 = -k_2\alpha\sin\theta \tag{5.15}$$

where $n_0 = -\alpha\sin\theta$ is the normal distance from the node to the metal boundary (α is the distance along the x axis from the node to the metal). Employing this value of k_2 gives:

$$\partial_x E_y = -\frac{\sin^2\theta(E_{y_{i,j,k}}\sin\theta + E_{x_{i,j,k}}\cos\theta)}{\alpha\sin\theta} \tag{5.16}$$

The SFDTD method requires the second derivative ∂_{xx} which at node (i, j, k) is given by:

$$\partial_{xx}E_y(x = i\Delta) = \frac{\partial_x E_y(x = (i + \frac{1}{2})\Delta) - \partial_x E_y(x = (i - \frac{1}{2})\Delta)}{\Delta} \tag{5.17}$$

use of the standard centred differences for the two first order operators ∂_x gives the usual expression (5.5) however in this case the corrected approximation (5.16) is employed for $\partial_x E_y(x = (i + \frac{1}{2})\Delta)$. Writing β for α/Δ gives:

$$\partial_{xx}E_y(x = i\Delta) = \left(\frac{E_{y_{i-1,j,k}}}{\Delta^2} - \frac{E_{x_{i,j,k}}\cos\theta\sin\theta}{\Delta^2\beta}\right) - \frac{E_{y_{i,j,k}}}{\Delta^2}\left(1 + \frac{\sin^2\theta}{\beta}\right) \tag{5.18}$$

which is the required corrected approximation for the second derivative in the SFDTD algorithm close to the metal boundary. If $\theta = 3\pi/2$ and $\beta = 1$ the expression reduces to the standard centred difference expression for $\partial_{xx}E_y$ as would be expected.

Similar expressions to (5.18) are readily obtained for the other field components and the other spatial second derivatives; use of these expressions in the SFDTD algorithm results in a correction factor formulation which makes use of the known boundary conditions for the tangential and normal electric fields at a metal surface.

5.5 Validation of SFDTD

In order to validate the correction factor scheme and the SFDTD algorithm two test problems were considered, the first being the analysis of a closed cylindrical resonator and the second a closed square resonator angled with respect to the mesh.

By investigating closed structures, uncertainty over the effect of two necessarily different implementations of a radiating boundary condition does not arise; the simple geometries also allow analytic cavity resonance techniques to calculate the actual resonant frequencies.

5.5.1 Cylindrical Resonator

A metal-walled closed cylindrical resonator was modelled using the combination of SFDTD and the correction method described by section 5.4 and a *fixed* uniform mesh size Δ of 5cm. The problem was also analysed using the standard, staircased, FDTD technique. Both techniques were used to determine the resonant frequencies

of the structure and these were compared with results available in closed form. This comparison is given by figure 5.3.

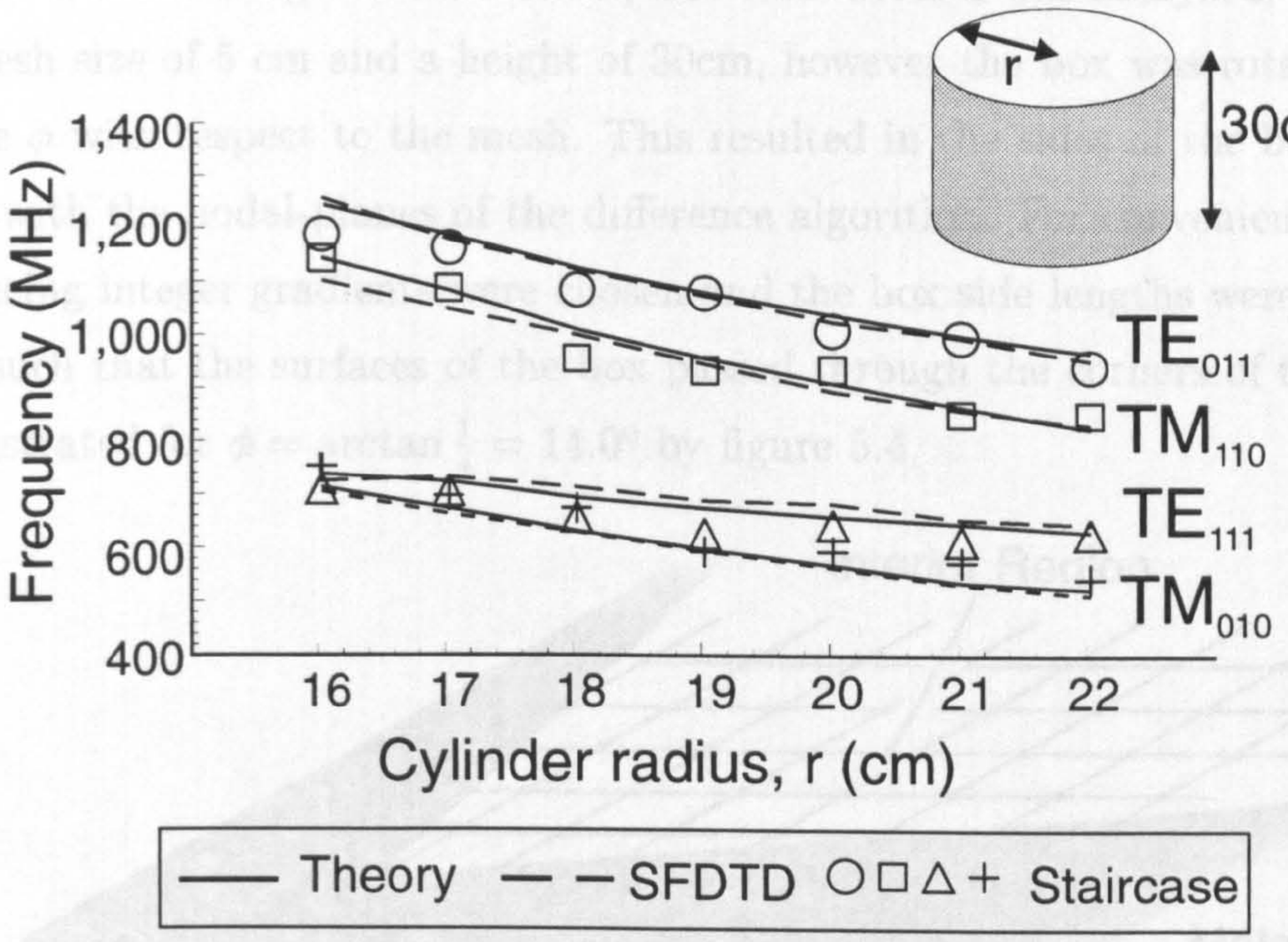

Figure 5.3: Cylinder resonant frequencies.

The solid line represents the (perfect) analytic solution and the dashed line the results produced by SFDTD. The marker points indicate the predictions of the staircased FDTD method.

Overall, given the coarseness of the mesh with respect to both frequency and surface curvature, the SFDTD results adhere well to the theoretical curves and are, as expected, considerably more accurate than the staircased FDTD technique. The TM_{010} mode in particular is excellently characterised, virtually independently of cylinder radius. The results for the TM_{110} mode are good for radii of greater than 18cm but become less accurate as the radius decreases (this is probably due to both a decrease in the number of field components available to describe the cylinder and to the increase in frequency of the mode). The most difficult mode to model is clearly the TE_{111} mode, the FDTD results for this are notably poor and while the SFDTD algorithm performs more consistently, the results may indicate potential for improvement in the technique.

5.5.2 Rectangular Resonator

A metal walled rectangular box with square cross-section was analysed, again with a fixed mesh size of 5 cm and a height of 30cm, however the box was rotated through an angle ϕ with respect to the mesh. This resulted in the sides of the box not being aligned with the nodal-planes of the difference algorithm. For convenience, values of ϕ producing integer gradients were chosen and the box side lengths were selected for each ϕ such that the surfaces of the box passed through the corners of the unit cells – as illustrated for $\phi = \arctan\frac{1}{4} = 14.0^{\circ}$ by figure 5.4.

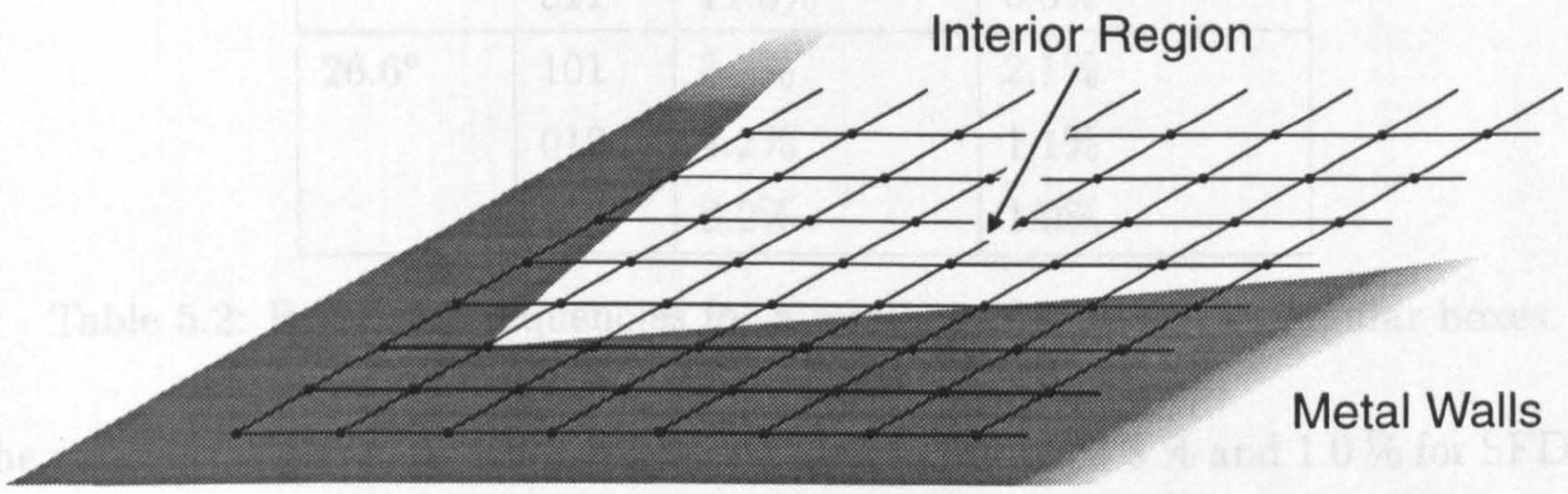

Figure 5.4: Segment of rotated rectangular box cross-section for $\phi = 14^{\circ}$.

The FDTD algorithm approximates the angled surfaces with a staircase and the SFDTD algorithm with the correction factors of section 5.4.

Table 5.1 shows the resonant frequencies for the box with angle $\phi = 14.0^{\circ}$ (it should be noted that due to the square cross-section of the structure each resonance may represent more than one mode). A summary of the results for four angles (arctan $\frac{1}{5}$,

Mode	Theory	FDTD	SFDTD	FDTD Error	SFDTD Error
101	633 MHz	620 MHz	622 MHz	2.1%	1.7%
012	869 MHz	648 MHz	870 MHz	2.4%	0.1%
011	549 MHz	575 MHz	545 MHz	4.7%	0.7%

Table 5.1: Resonant frequencies for rotated rectangular box.

arctan $\frac{1}{4}$, arctan $\frac{1}{3}$ and arctan $\frac{1}{2}$) is given by table 5.2. Once again the SFDTD results (with curved surface corrections) agree well with the analytic results, in the majority of cases the resonant frequencies are correct to within one percent. The FDTD algorithm, as might be expected, fares less well – although some modes are well characterised, most exhibit significant error.

Angle, ϕ	Mode	FDTD Error	SFDTD Error
11.3°	101	1.6%	0.6%
	012	0.1%	0.6%
	011	6.3%	0.9%
14.0°	101	2.1%	1.7%
	012	2.4%	0.1%
	011	4.7%	0.7%
18.4°	101	0.3%	1.8%
	012	0.6%	0.8%
	011	11.3%	0.5%
26.6°	101	3.7%	2.1%
	012	4.2%	1.1%
	011	8.2%	1.0%

Table 5.2: Resonant frequencies for a number of rotated rectangular boxes.

The mean error across all modes and all ϕ for FDTD was 3.8 % and 1.0 % for SFDTD, thus SFDTD's curved surface corrections reduce the modelling error in this case by around a factor of 4; this is a similar level of accuracy to that achieved when modelling the cylindrical cavity.

The SFDTD method incorporating the curved surface correction factor scheme is clearly able to characterise curved and angled surfaces with better accuracy than the Yee FDTD algorithm and yet retains the same level of efficiency. More importantly however, and unlike any corrected difference algorithm previously investigated by the author, all the models were stable given a suitable time step (usually slightly smaller than that stipulated by the Courant Criterion).

5.6 Stability Theory

The question arises then as to why the SFDTD correction factor scheme for curved and angled surfaces is stable while the FDTD schemes are almost invariably unstable. In this section the two dimensional SFDTD algorithm will be examined in an attempt to answer this question.

The approach taken toward studying the stability of SFDTD is to consider the continuous time system represented by SFDTD and its correction factor scheme. This

system is the algorithm's equivalent system – a concept introduced in section 4.6.2.

At a node (i, j) where the correction scheme is not applied the nodal equations for the equivalent system are:

$$\partial_{tt} E_{x_{i,j}} = -4\frac{c^2 E_{x_{i,j}}}{\Delta^2} + (E_{x_{i+1,j}} + E_{x_{i-1,j}} + E_{x_{i,j+1}} + E_{x_{i,j-1}})\frac{c^2}{\Delta^2} \tag{5.19}$$

$$\partial_{tt} E_{y_{i,j}} = -4\frac{c^2 E_{y_{i,j}}}{\Delta^2} + (E_{y_{i+1,j}} + E_{y_{i-1,j}} + E_{y_{i,j+1}} + E_{y_{i,j-1}})\frac{c^2}{\Delta^2} \tag{5.20}$$

Close to a curved boundary the SFDTD algorithm employs the correction factor scheme of section 5.4; in general the two dimensional method may require two independent corrections. Figure 5.5 shows this situation where two angled facets intersect the SFDTD mesh at angles of θ_x and θ_y.

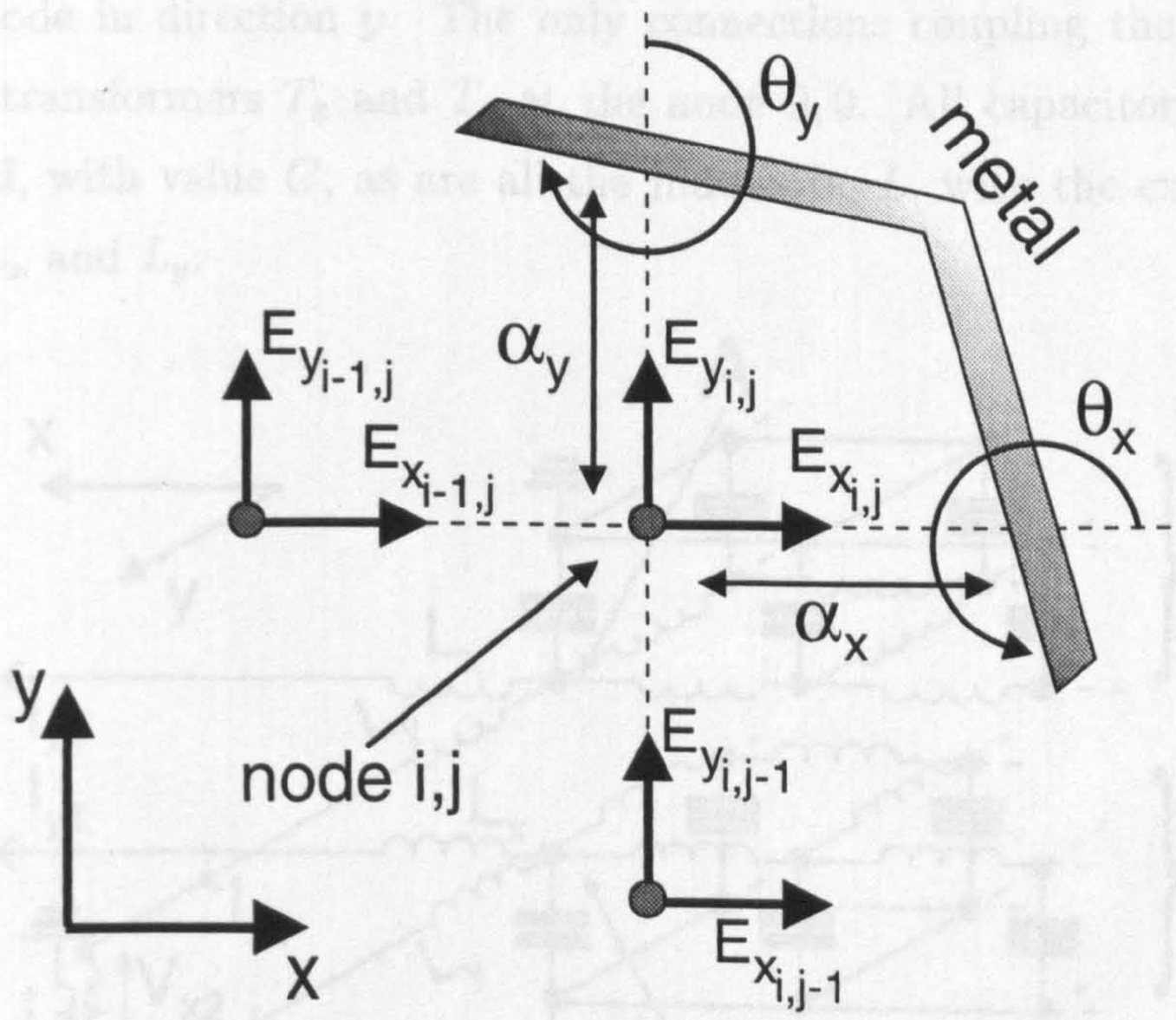

Figure 5.5: Intersection of a curved surface with SFDTD grid.

Using the notation of figure 5.5 the equivalent system's equations at a corrected node (i, j) are:

$$\partial_{tt} E_{x_{i,j}} = -\frac{c^2 E_{x_{i,j}}}{\Delta^2}\left(\frac{\cos^2\theta_x}{\beta_x} + \frac{\sin^2\theta_y}{\beta_y} + 1 + 1\right) + \frac{c^2 E_{x_{i,j-1}}}{\Delta^2} + \frac{c^2 E_{x_{i-1,j}}}{\Delta^2} - \frac{c^2 E_{y_{i,j}}}{\Delta^2}\left(\frac{\cos\theta_x \sin\theta_x}{\beta_x} + \frac{\cos\theta_y \sin\theta_y}{\beta_y}\right) \tag{5.21}$$

and for E_y:

$$\partial_{tt}E_{y_{i,j}} = -\frac{c^2 E_{y_{i,j}}}{\Delta^2}\left(\frac{\sin^2\theta_x}{\beta_x} + \frac{\cos^2\theta_y}{\beta_y} + 1 + 1\right) + \frac{c^2 E_{y_{i-1,j}}}{\Delta^2} + \frac{c^2 E_{y_{i,j-1}}}{\Delta^2} - \frac{c^2 E_{x_{i,j}}}{\Delta^2}\left(\frac{\cos\theta_x \sin\theta_x}{\beta_x} + \frac{\cos\theta_y \sin\theta_y}{\beta_y}\right) \quad (5.22)$$

where $\beta_x = \alpha_x/\Delta$ and $\beta_y = \alpha_y/\Delta$.

The nodal equations could be assembled into a matrix (as in chapter 4) however this is of little benefit as the task of finding the eigenvalues remains an impractical one. An alternative and more useful approach is to consider the electrical network of figure 5.6.

This circuit consists of two separate 2-D networks, one ('Network X') with nodal voltages represented by $V_{x_{i,j}}$ and the other ('Network Y') with voltages $V_{y_{i,j}}$. The co-ordinates i, j specify the voltage at the i^{th} node in the direction x in the network, and the j^{th} node in direction y. The only connections coupling the two networks are the ideal transformers T_x and T_y at the node $0, 0$. All capacitors are assumed to be identical, with value C, as are all the inductors, L, with the exception of the components L_x and L_y.

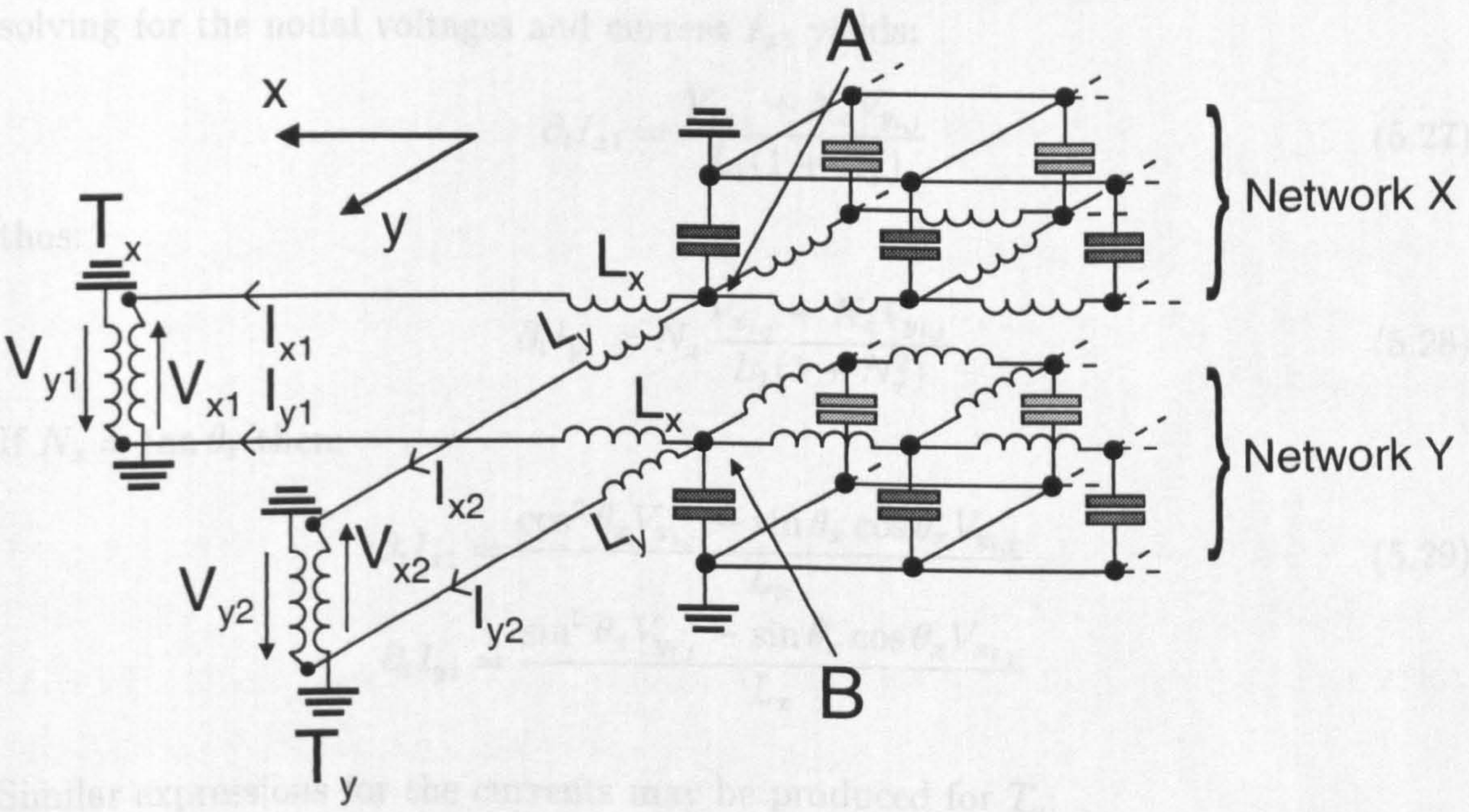

Figure 5.6: Passive electrical network.

Application of Kirchoff's current law at any node apart from those connected directly to a transformer gives for the capacitor voltage in each network:

$$\partial_{tt}V_{x_{i,j}} = -4\frac{V_{x_{i,j}}}{LC} + (V_{x_{i+1,j}} + V_{x_{i-1,j}} + V_{x_{i,j+1}} + V_{x_{i,j-1}})\frac{1}{LC} \quad (5.23)$$

$$\partial_{tt} V_{y_{i,j}} = -4\frac{V_{y_{i,j}}}{LC} + (V_{y_{i+1,j}} + V_{y_{i-1,j}} + V_{y_{i,j+1}} + V_{y_{i,j-1}})\frac{1}{LC} \tag{5.24}$$

if $C = \epsilon\Delta^2$ and $L = \mu$ these are the same equations as (5.19) and (5.20). Thus the equivalent system for the uncorrected SFDTD algorithm obeys exactly the same equations as a passive electrical network.

Now consider the behaviour at the nodes (i, j) (such as those labeled 'A' and 'B' in figure 5.6) which *are* connected directly to a transformer. Firstly the transformers are assumed to be ideal with winding ratios $1 : N_x$ and $1 : N_y$ respectively. Thus for T_x:

$$\begin{aligned} V_{y1} &= -\frac{V_{x1}}{N_x} \\ I_{y1} &= N_x I_{x1} \end{aligned} \tag{5.25}$$

since the transformer is ideal. Summing voltages around the loops containing the windings gives:

$$\begin{aligned} V_{x_{i,j}} - V_{x1} &= L_x \partial_t I_{x1} \\ V_{y_{i,j}} - V_{y1} &= L_x \partial_t I_{y1} \end{aligned} \tag{5.26}$$

solving for the nodal voltages and current I_{x1} yields:

$$\partial_t I_{x1} = \frac{V_{x_{i,j}} + N_x V_{y_{i,j}}}{L_1(1 + N_x^2)} \tag{5.27}$$

thus:

$$\partial_t I_{y1} = N_x \frac{V_{x_{i,j}} + N_x V_{y_{i,j}}}{L_1(1 + N_x^2)} \tag{5.28}$$

If $N_x = \tan\theta_x$ then:

$$\begin{aligned} \partial_t I_{x1} &= \frac{\cos^2\theta_x V_{x_{i,j}} - \sin\theta_x \cos\theta_x V_{y_{i,j}}}{L_x} \\ \partial_t I_{y1} &= \frac{\sin^2\theta_x V_{y_{i,j}} - \sin\theta_x \cos\theta_x V_{x_{i,j}}}{L_x} \end{aligned} \tag{5.29}$$

Similar expressions for the currents may be produced for T_y:

$$\begin{aligned} \partial_t I_{x2} &= \frac{\sin^2\theta_y V_{x_{i,j}} - \sin\theta_y \cos\theta_y V_{y_{i,j}}}{L_y} \\ \partial_t I_{y2} &= \frac{\cos^2\theta_y V_{y_{i,j}} - \sin\theta_y \cos\theta_y V_{x_{i,j}}}{L_y} \end{aligned} \tag{5.30}$$

where $N_y = \cot\theta_y$.

Using these currents in the evaluation of $\partial_{tt}V_x$ and $\partial_{tt}V_y$ gives:

$$\partial_{tt}V_{x_{i,j}} = -\frac{V_{x_{i,j}}}{C}\left(\frac{\cos^2\theta_x}{L_x}+\frac{\sin^2\theta_y}{L_y}+\frac{1}{L}+\frac{1}{L}\right)+ \frac{V_{x_{i,j-1}}}{LC}+\frac{V_{x_{i-1,j}}}{LC}-\frac{V_{y_{i,j}}}{C}\left(\frac{\sin\theta_x\cos\theta_x}{L_x}+\frac{\sin\theta_y\cos\theta_y}{L_y}\right) \tag{5.31}$$

$$\partial_{tt}V_{y_{i,j}} = -\frac{V_{y_{i,j}}}{C}\left(\frac{\sin^2\theta_x}{L_x}+\frac{\cos^2\theta_y}{L_y}+\frac{1}{L}+\frac{1}{L}\right)+ \frac{V_{y_{i-1,j}}}{LC}+\frac{V_{y_{i,j-1}}}{LC}-\frac{V_{x_{i,j}}}{C}\left(\frac{\sin\theta_x\cos\theta_x}{L_x}+\frac{\sin\theta_y\cos\theta_y}{L_y}\right) \tag{5.32}$$

given values $L_x = \mu\beta_x$ and $L_y = \mu\beta_y$ these are identical to the equations (5.21) and (5.22).

It has been shown therefore that the nodal equations for the equivalent system at both corrected and uncorrected SFDTD nodes are identical to the expressions for the nodal voltages in a passive electrical network; this electrical network is accordingly described as the *equivalent circuit* for SFDTD and its correction factor scheme.

It is a straightforward (although lengthy) process to show that the equivalent circuit concept extends to the full three dimensional SFDTD algorithm.

5.6.1 Continuous and Discrete Time Stability

If the equivalent system for the SFDTD algorithm and its correction factors is a passive circuit it is clear that the equivalent system must be energy conserving as there is no mechanism for gain in the network. The system must therefore have eigenvalues with real parts ≤ 0.

In this section further consideration is given to the concepts introduced in section 4.6.2. The theory presented here will concern the SFDTD algorithm rather than FDTD and thus some small changes in notation will be introduced. The results however are valid for *both* methods.

The equivalent system for SFDTD (and FDTD) may be written:

$$\partial_{tt}\mathbf{e}(t) = \mathbf{F}\mathbf{e}(t) \tag{5.33}$$

The assumptions that will be made are that the model is electrically loss-less and bounded by closed metal walls. The first point arises because (5.33) cannot describe

electrical loss as this would introduce a first order temporal derivative; with a mixture of first and second order temporal derivatives a true centred difference cannot be used to approximate the time derivatives and the following analysis becomes invalid. The second point arises in much the same manner since a Radiating Boundary Condition will normally introduce a first order time derivative.

In chapter 4 it was stated that intuitively the equivalent system must be stable if the time-discretised algorithm is to be stable. A more rigorous treatment of this concept may be obtained as follows:

Assuming that $\mathbf{F}$ is diagonalisable it has a set of linearly independent eigenvectors $\mathbf{f}_1 \dots \mathbf{f}_J$ with corresponding distinct eigenvalues $\lambda_1 \dots \lambda_J$. $\mathbf{e}(t)$ may thus be written:

$$\mathbf{e}(t) = \sum_{j=1}^{J} a_j(t)\mathbf{f}_j \tag{5.34}$$

thus:

$$\sum_{j=1}^{J} \partial_{tt} a_j(t)\mathbf{f}_j = \sum_{j=1}^{J} \lambda_j a_j(t) \tag{5.35}$$

and since the eigenvectors are linearly independent:

$$\partial_{tt} a_j(t) = \lambda_j a_j(t) \tag{5.36}$$

thus the poles of the continuous time system are given by the roots of $s^2 - \lambda_j = 0$ (either by writing (5.36) in phase-variable form or by taking the Laplace transform).

It can be seen that for any eigenvalue λ_j of $\mathbf{F}$ there are two eigenvalues μ_j of the continuous time system, where:

$$\mu_j = \pm\sqrt{\lambda_j} \tag{5.37}$$

if the continuous time system is passive (thus stable) its eigenvalues μ are in the negative real complex half-plane; in other words:

$$\frac{3\pi}{2} \geq \arg(\mu_j) \geq \frac{\pi}{2} \tag{5.38}$$

thus from (5.37):

$$\frac{3\pi}{2} \geq \frac{\arg(\lambda_j)}{2} \geq \frac{\pi}{2} \text{ and } \frac{3\pi}{2} \geq \frac{\arg(\lambda_j)}{2} + \pi \geq \frac{\pi}{2} \tag{5.39}$$

the only solution to this is in the range $0 \leq \arg(\lambda_j) \leq 2\pi$ is $\arg(\lambda_j) = \pi$, therefore the eigenvalues λ_j of $\mathbf{F}$ must lie exactly on the negative real axis if the continuous

time system is stable. For stability of the continuous time system then:

$$\begin{aligned} \Im\mathrm{m}(\lambda_j) &= 0 \\ \Re\mathrm{e}(\lambda_j) &\leq 0 \end{aligned} \tag{5.40}$$

Now consider the discrete time system produced by taking a centred difference approximation to the continuous time operator ∂_{tt} in (5.33):

$$\mathbf{e}^{n+1} - 2\mathbf{e}^n + \mathbf{e}^{n-1} = \Delta_t \mathbf{F}\mathbf{e}^n \tag{5.41}$$

where Δ_t is the time step (a positive real number). This relation represents either the SFDTD or FDTD algorithm depending on the form of $\mathbf{F}$.

Writing $\mathbf{e}^n$ once more in terms of the eigenvectors of $\mathbf{F}$:

$$\mathbf{e}^n = \sum_{j=1}^{J} a_j^n \mathbf{f}_j \tag{5.42}$$

thus for any one of the eigenvectors:

$$a_j^{n+1} - 2a_j^n + a_j^{n-1} = \Delta_t \lambda_j a_j^n \tag{5.43}$$

by employing a z-transform for example, the two poles of this discrete time system corresponding to each λ_j are the roots z_1, z_2 of the polynomial:

$$z^2 - (2 + \Delta_t \lambda_j) z + 1 = 0 \tag{5.44}$$

the sum of the roots is therefore:

$$z_1 + z_2 = 2 + \Delta_t \lambda_j \tag{5.45}$$

and the product of the roots is:

$$z_1 z_2 = 1 \tag{5.46}$$

writing $z = re^{j\theta}$ in (5.46) gives:

$$r_1 r_2 e^{j(\theta_1 + \theta_2)} = 1 \tag{5.47}$$

this implies that:

$$r_1 r_2 = 1 \text{ and } \theta_1 = -\theta_2 \tag{5.48}$$

If λ_j, the eigenvalue of $\mathbf{F}$, is written $\lambda_j = a + jb$ then the sum of roots expression (5.45) yields:

$$\Im\mathrm{m}(\lambda_1 + \lambda_2) = \Delta_t b \tag{5.49}$$

$$r_1 \sin\theta_1 + r_2 \sin\theta_2 = \Delta_t b \tag{5.50}$$

and, since $\theta_1 = -\theta_2$:

$$\sin\theta_1(r_1 - r_2) = \Delta_t b \tag{5.51}$$

thus $r_1 \neq r_2$ if $b \neq 0$. This implies that either r_1 or r_2 must be greater than unity if $b \neq 0$.

Similarly:

$$\Re\mathrm{e}(\lambda_1 + \lambda_2) = 2 + \Delta_t a \tag{5.52}$$

$$r_1 \cos\theta_1 + r_2 \cos\theta_2 = 2 + \Delta_t a \tag{5.53}$$

then:

$$\cos\theta_1(r_1 + r_2) = 2 + \Delta_t a \tag{5.54}$$

if $a > 0$ then this implies that $r_1 + r_2 > 2$ and hence that either r_1 or r_2 must be greater than unity.

If however $a \leq 0$ there is always a Δ_t such that:

$$\cos\theta_1(r_1 + r_2) = \cos\theta_1(2) = 2 + \Delta_t a \tag{5.55}$$

where $r_1 = r_2 = 1$.

To summarise the results presented above:

i . If the continuous time equivalent system is unstable, at least one eigenvalue λ_j of $\mathbf{F}$ will not be on the negative real axis and hence the discrete time algorithm must have a pole outside the unit circle for any $\Delta_t > 0$.

ii . If the continuous time system is stable all the eigenvalues λ_j of $\mathbf{F}$ must be on the negative real axis and hence there is always a value of time step Δ_t such that the discrete time algorithm is stable.

It has been shown therefore that if the equivalent system is passive and hence stable there must be a time step that results in stability of the discrete time system. If on the other hand the equivalent system is *un*stable there is no (non zero) value of time step that gives stability.

As already mentioned, the above analysis does not extend to algorithms with electrical loss or radiating boundary conditions; addition of either of these two phenomena provides a mechanism for dissipation in the algorithm. It is reasonable to suppose however that:

i . If a dissipation free algorithm is stable then adding dissipation is unlikely to result in instability.

ii . If a dissipation free algorithm is unstable then adding dissipation is unlikely to result in stability.

– these properties have been observed in practice. In extreme circumstances however, if for example the amount of added loss is very large, the two suppositions may become invalid.

5.6.2 Discussion of Equivalent Circuit Criterion

The equivalent system need not necessarily be passive to be stable – many common systems, electrical and otherwise, contain active components (i.e. ones which introduce gain into a system) and yet remain stable.

Since active circuits may also be stable it might then be thought that requiring that a corrected finite difference algorithm have a passive equivalent system is an unnecessarily strict criterion for stability. While not disputing this assertion consideration should be given to two points:

- A node in an algorithm like SFDTD or FDTD receives a time delayed influence from every other node in the problem space. There are then a multitude of feedback loops for each node and thus, given the presence of just one non-passive element, a high potential for instability.

- If a non-passive element exists it would expected that each feedback path would need to be examined in order to assess the stability of the system. In effect the

problem reduces once more to finding the eigenvalues of the system.

It seems clear then that the existence of the passive equivalent circuit is *likely* to be (i) A *virtually* necessary criterion for stability and (ii) The only means by which a requirement to examine all the millions of eigenvalues of the algorithm may be avoided.

Some further appreciation of these two points may be gained by consideration of two slight modifications to the SFDTD correction factor formulation that were investigated by the author; these are briefly described in the following sections.

5.6.2.1 Alternative Correction Factor Scheme #1

In [7] a slightly different correction factor formulation was proposed for SFDTD. In this formulation the only change was that the second spatial derivative is approximated by:

$$\partial_{xx} E_y = \frac{\partial_x E_y(x = (i + \frac{1}{2})\Delta) - \partial_x E_y(x = (i - \frac{1}{2})\Delta)}{0.5(\Delta + \alpha)} \tag{5.56}$$

rather than the expression (5.17) in an attempt to improve the calculation of the derivative. It can be shown that in the presence of more than one correction at a given node (the situation shown by figure 5.5) the correction factor scheme can no longer be represented by a passive circuit.

Despite the fact that the use of (5.56) as opposed to (5.17) makes only a small difference to the update algorithm and the fact that it is only for a proportion of the nodes that the scheme is has no passive representation (since many nodes will only need correcting in one direction) it was found that instability occurred in a number of cases. This finding lends credence to the idea that the existence of the passive circuit is in practice a virtually necessary condition for stability.

5.6.2.2 Alternative Correction Factor Scheme #2

A second alternative correction scheme was investigated in order to determine whether the results for the cylindrical resonator could be improved by expanding the normal fields close to the metal surface as:

$$E_n = k_1 + k_3 n^2 \tag{5.57}$$

rather than the simpler constant function of section 5.4.

The resulting correction factor scheme achieved some improvement in the characterisation of the cylinder's modes but, despite being based on the SFDTD algorithm, was found strongly unstable.

Since it is possible to demonstrate that this alternative correction factor formulation does not have a passive equivalent circuit, the investigation of this correction scheme further supports the contention that the existence of a passive equivalent circuit is a virtually necessary criterion for algorithmic stability.

5.7 Summary

In this chapter the SFDTD algorithm has been presented along with a suitable correction factor scheme for its treatment of curved boundaries. With the correction factor formulation described in section 5.4, SFDTD, unlike any previously implemented corrected algorithm, was found to be stable.

Further investigation of this fact shows that the corrected algorithm has a passive equivalent system and as a result must be stable given a sufficiently small time step. The existence of this passive circuit is not strictly necessary for stability of the discrete time system however investigation of alternative SFDTD correction factor schemes which do *not* possess a passive representation has shown that these schemes are almost invariably unstable.

The SFDTD algorithm has been shown not only to be stable but also to be particularly suitable for the analysis of curved metallic boundaries. In its present form it is unable to characterise dielectric interfaces and non-smooth perfectly conducting objects. It may be possible to introduce a correction factor scheme for these structures in which case, given a suitable radiating boundary condition, the scope of the algorithm could rival that of FDTD.

For the present however the SFDTD method has been most useful in shedding valuable light on the difficult stability issue. The question that is immediately raised is whether or not it is possible to employ a passive equivalent circuit for the original FDTD algorithm. It is with answering this question that chapter 6 is concerned.

References

[1] D. B. Shorthouse and C. J. Railton, "Incorporation of static singularities into the finite difference time domain technique with application to microstrip structures," in *Proceedings of the 20th European Microwave Conference*, vol. 1, pp. 531–536, Sept. 1990.

[2] C. J. Railton, D. B. Shorthouse, and J. P. McGeehan, "Modelling of narrow microstrip lines using finite difference time domain method," *Electronics Letters*, vol. 28, pp. 1168–1170, June 1992.

[3] C. J. Railton, "An algorithm for the treatment of curved metallic laminas in the finite difference time domain method," *IEEE Transactions on Microwave Theory and Techniques*, vol. MTT-41, pp. 1429–1438, Aug. 1993.

[4] C. J. Railton, "Use of static field solutions in the FDTD method for the efficient treatment of curved metal surfaces," *Electronics Letters*, vol. 29, pp. 1466–1467, Aug. 1993.

[5] C. J. Railton, "The simple rigorous and effective treatment of thin wires and slots in the FDTD method," in *Proceedings of the 24th European Microwave Conference*, vol. 2, pp. 1541–1546, 1994.

[6] D. B. Shorthouse, *The CAD and analysis of passive monolithic microwave integrated circuits by the finite difference time domain technique.* PhD thesis, University of Bristol, 1992.

[7] I. J. Craddock and C. J. Railton, "A novel finite difference algorithm incorporating correction coefficients for curved structures," in *Proceedings of the 24th European Microwave Conference*, vol. 2, pp. 1536–1540, 1994.

[8] I. J. Craddock and C. J. Railton, "Analysis of curved and angled surfaces on a Cartesian mesh using a novel finite difference time domain algorithm," *IEEE Transactions on Microwave Theory and Techniques*, vol. MTT-43, Oct. 1995. In press.

[9] W. F. Ames, *Numerical Methods for Partial Differential Equations.* Thomas Nelson and Sons Ltd, 1969.

[10] L. F. Richardson, "The approximate arithmetical solution by finite differences of physical problems involving differential equations, with an application to the stresses in masonry dams," *Philosophical Transactions*, vol. A210, pp. 307–357, 1910.

[11] R. Courant, K. Friedrichs, and H. lewy, "Über die partiellen Differenzengleichungen der mathematischen Physik," *Mathematische Annalen*, vol. 100, pp. 32–74, 1928.

[12] P. H. Aoyagi and R. Lee, J F Mittra, "A hybrid Yee algorithm/scalar wave equation approach," *IEEE Transactions on Microwave Theory and Techniques*, vol. MTT-41, pp. 1593–1600, Sept. 1993.

[13] D. V. Krupezevic, V. J. Brancovic, and F. Arndt, "The wave equation FDTD method for the efficient eigenvalue analysis and s-matrix computation of waveguide structures," *IEEE Transactions on Microwave Theory and Techniques*, vol. MTT-41, pp. 2109–2114, Dec. 1993.

Chapter 6

Stability Preserving Methods for Inclusion of *a Priori* Knowledge in FDTD

6.1 Introduction

Chapter 4 introduced the correction factor method as a means to overcome FDTD's inefficient modelling of curved surfaces and fine geometric detail. It was shown however that the inclusion of the correction factors in FDTD (and in general any arbitrary modification to a standard FDTD update equation coefficient) was likely to result in instability.

In chapter 5 however it was demonstrated that if an algorithm has a passive equivalent system then it is necessarily stable for some non-zero value of time step. The SFDTD algorithm and correction factor scheme described in chapter 5 satisfied this condition and as a result was indeed found to be stable.

The primary aim of this chapter is to present a passive equivalent system for FDTD (in the form once again of an electrical network) and to examine whether or not correction factor schemes may be formulated in such a way as to preserve the passive representation.

6.2 A Passive Equivalent Circuit for FDTD

The FDTD algorithm is more complex than the SFDTD method of chapter 5 and it is to be expected that the form of its equivalent circuit will be more complex than the simple LC network required for SFDTD.

In order to embody the required duality of the electric and magnetic fields it is firstly necessary to define the gyrator, or generalised impedance converter as it is sometimes known. This device is illustrated by figure 6.1 and its symbol includes an arrow which defines the direction of power flow through the device when the voltages at the ports are of the same sign (when the relationship between the circuit and the fields in the FDTD model emerges this can be understood in terms of the direction of the Poynting vector). The voltage–current relationships at ports 1 and 2 are [1, p.40]

$$V_2 = GI_1 \qquad V_1 = GI_2 \tag{6.1}$$

The ideal gyrator is a passive device since it can be shown that the power flowing into either port is exactly matched by power flowing out of the other (it is irrelevant that a practical and inevitably non-ideal implementation of a gyrator is usually achieved

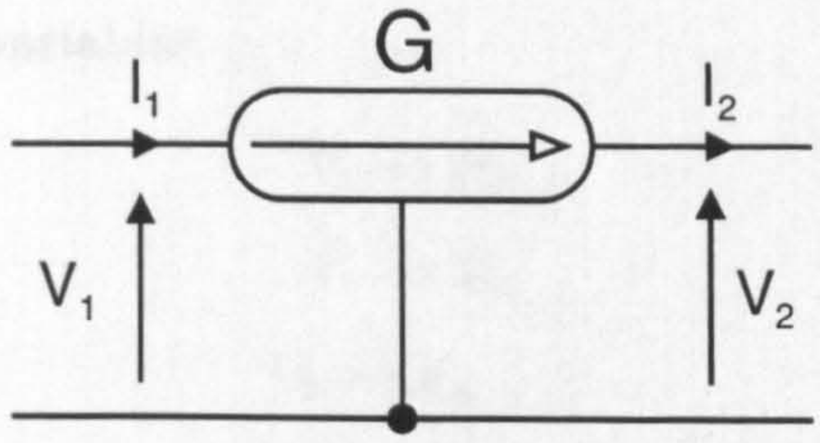

Figure 6.1: A gyrator.

with active components [2, p.281]).

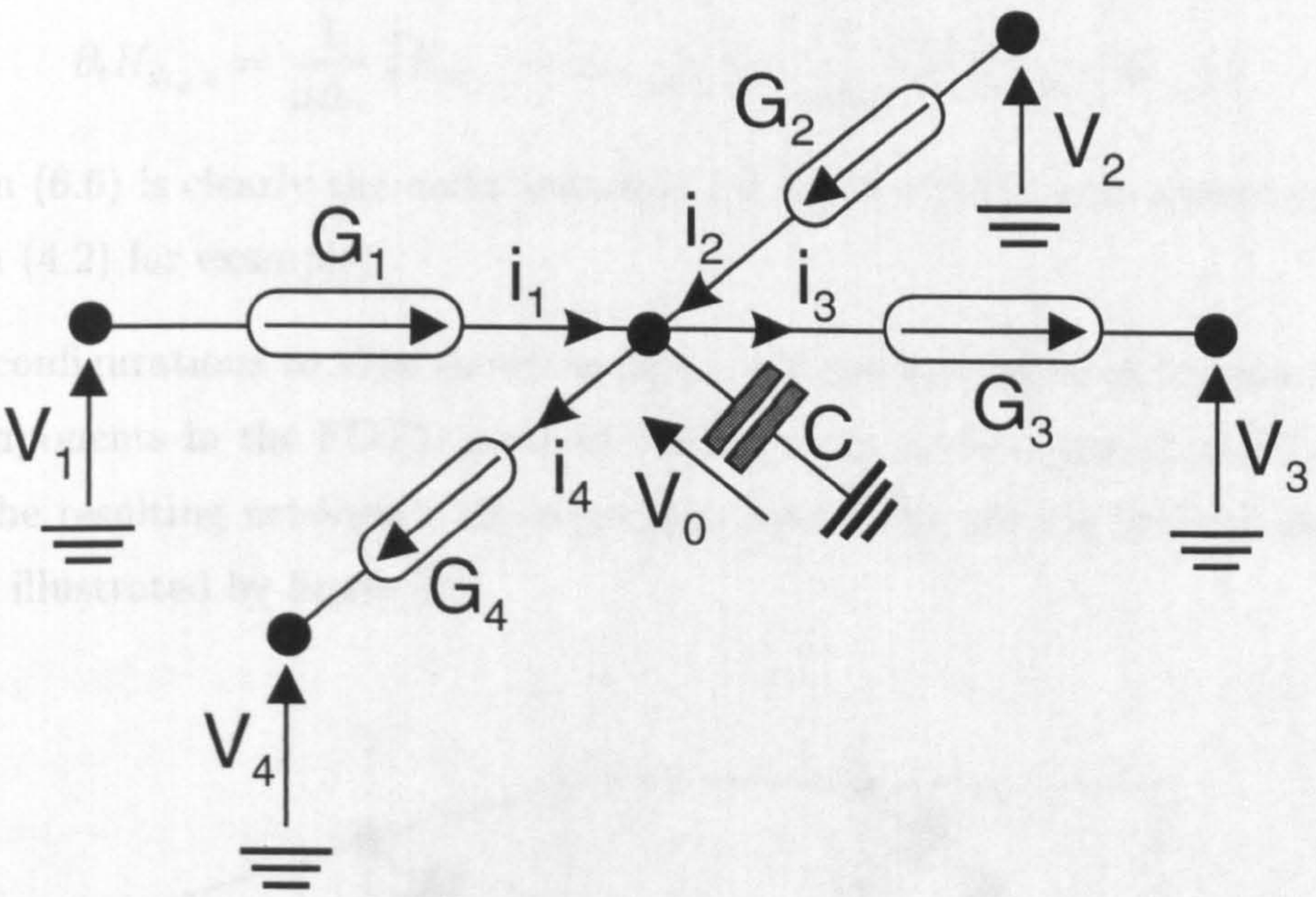

Figure 6.2: Interconnection of gyrators and a capacitor.

Now consider figure 6.2 in which four gyrators are connected to a central capacitor; at the junction of the gyrators application of Kirchoff's current law yields:

$$C\partial_t V_0 = i_1 - i_3 + i_2 - i_4 \tag{6.2}$$

use of the gyrator relationships of (6.1) gives:

$$C\partial_t V_0 = G_1 V_1 - G_3 V_3 + G_2 V_2 - G_4 V_4 \tag{6.3}$$

with the following substitutions:

$$\begin{aligned} C &= \mu \Delta_x \Delta_y \Delta_z \\ G_1 = G_3 &= \Delta_x \Delta_y \\ G_2 = G_4 &= \Delta_z \Delta_y \end{aligned} \tag{6.4}$$

and with the change of variables:

$$\begin{aligned} V_0 &\rightarrow H_{y_{i,j,k}} \\ V_1 &\rightarrow E_{x_{i,j,k}} \\ V_2 &\rightarrow E_{z_{i+1,j,k}} \\ V_3 &\rightarrow E_{x_{i,j,k+1}} \\ V_4 &\rightarrow E_{z_{i,j,k}} \end{aligned} \tag{6.5}$$

equation (6.3) becomes:

$$\partial_t H_{y_{i,j,k}} = \frac{1}{\mu\Delta_z}\left(E_{x_{i,j,k}} - E_{x_{i,j,k+1}}\right) + \frac{1}{\mu\Delta_x}\left(E_{z_{i+1,j,k}} - E_{z_{i,j,k}}\right) \tag{6.6}$$

Equation (6.6) is clearly the nodal equation for H_y in FDTD's equivalent system (cf equation (4.2) for example).

Similar configurations to that shown in figure 6.2 can be produced for the other five field components in the FDTD method. When these circuits are properly interconnected the resulting network is the equivalent system for all the fields in the FDTD method, illustrated by figure 6.3.

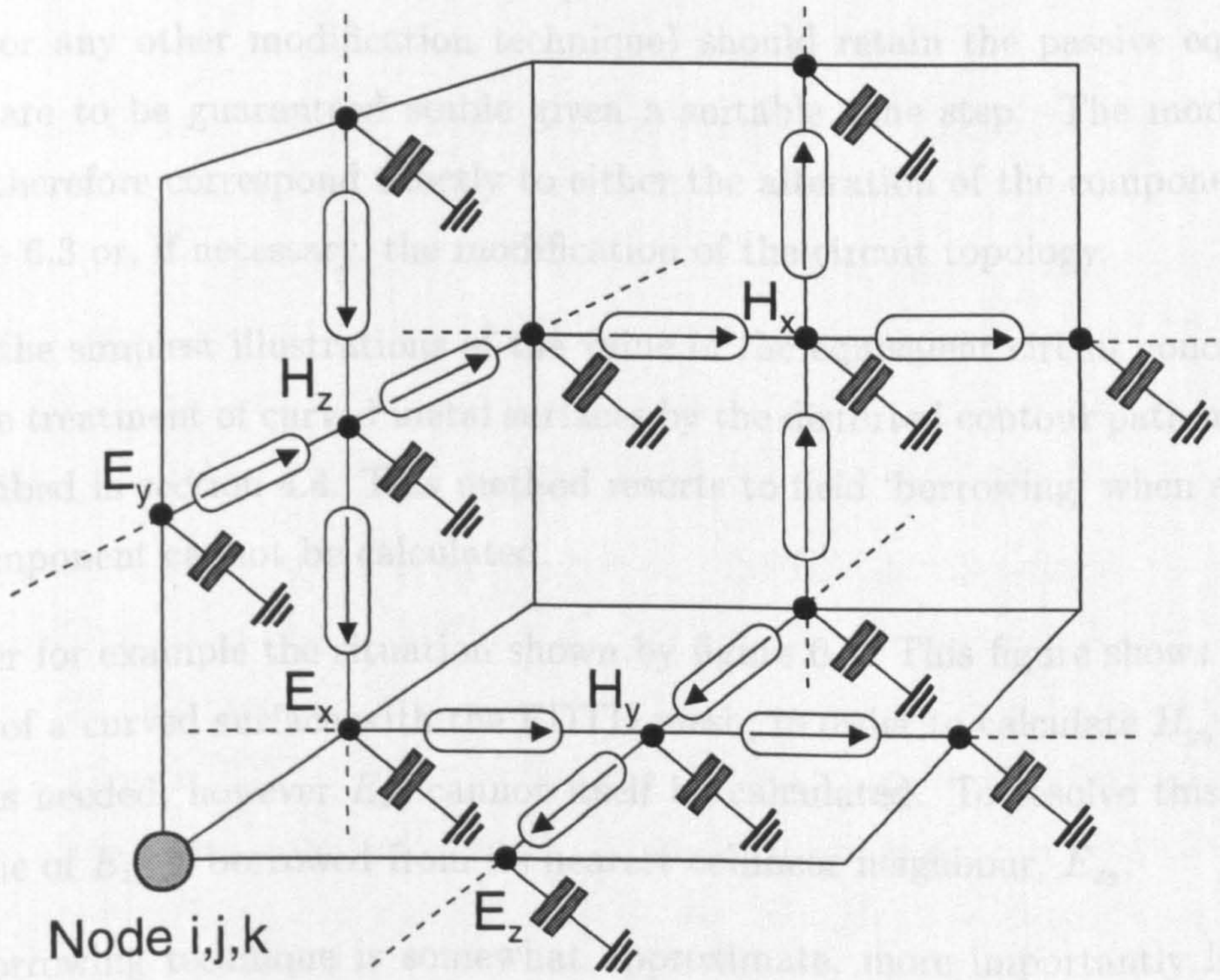

Figure 6.3: Equivalent circuit for FDTD.

The values of the components in figure 6.3 are given by:

$$\begin{aligned} C_e = \epsilon_0 \Delta_x \Delta_y \Delta_z \qquad C_h = \mu_0 \Delta_x \Delta_y \Delta_z \\ G_x = \Delta_y \Delta_z \qquad G_y = \Delta_x \Delta_z \qquad G_z = \Delta_x \Delta_y \end{aligned} \tag{6.7}$$

where all the gyrators whose arrows are parallel to the x, y and z directions are assumed to have values G_x, G_y and G_z repectively and the capacitors at the position of each field component have value C_h if the component is magnetic and C_e if it is electric.

The equivalent circuit of figure 6.3 is entirely passive; as shown in chapter 5 therefore, a discrete time algorithm derived from centred difference approximations to the time derivatives in the circuit is necessarily stable for some value of time step.

While the network of figure 6.3 was developed independently by the author for the stability analysis of the FDTD algorithm, an electrically identical (but very different) circuit was proposed by Kron in [3] as a model of Maxwell's equations.

6.2.1 Implications of the Equivalent Circuit

Any modifications to the FDTD algorithm (whether these arise from the correction factors or any other modification technique) should retain the passive equivalence if they are to be guaranteed stable given a suitable time step. The modifications should therefore correspond exactly to either the alteration of the component values in figure 6.3 or, if necessary, the modification of the circuit topology.

One of the simplest illustrations of the value of the equivalent circuit concept arises from the treatment of curved metal surfaces by the distorted contour path method [4, 5] described in section 4.4. This method resorts to field 'borrowing' when a required field component cannot be calculated.

Consider for example the situation shown by figure 6.4. This figure shows the intersection of a curved surface with the FDTD mesh; in order to calculate H_{y0} the value of E_{z_1} is needed, however E_{z_1} cannot itself be calculated. To resolve this difficulty the value of E_{z_1} is borrowed from its nearest collinear neighbour, E_{z_2}.

This borrowing technique is somewhat approximate, more importantly however it cannot be represented in terms of a passive circuit since it requires that H_{y0} be a function of E_{z_2} and yet E_{z_2} is *not* a function of H_{y0}. It is found in practice that in many situations this loss of the passive representation may easily result in instability [6].

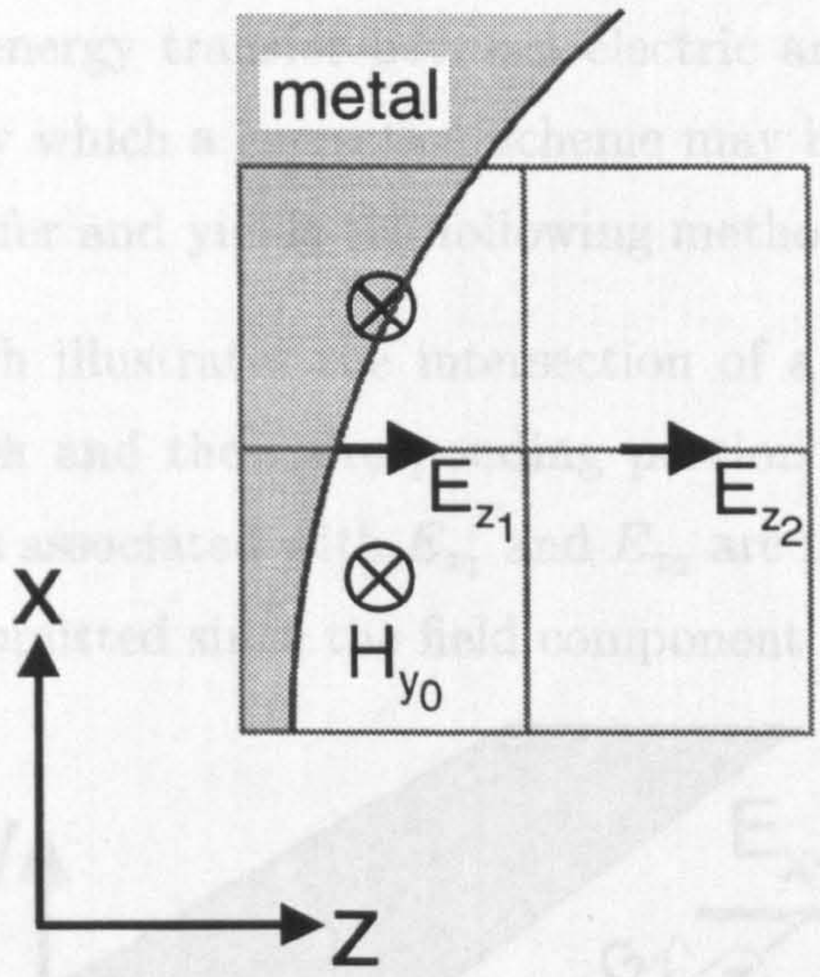

Figure 6.4: Field borrowing required by distorted contour method.

In [6] a modification to the borrowing procedure is presented which corresponds exactly to the addition of an extra gyrator to the passive equivalent circuit. This revised borrowing procedure is found to be entirely stable. Further discussion of the implications of the equivalent circuit for the distorted contour path algorithm may be found in [7, 8].

6.3 Correction Scheme for Metal Strips

As seen in chapter 4, one application for the correction factors was the characterisation of narrow microstrip lines without the need for a very fine mesh [9, 10]. The aim of this section is to determine whether or not a correction scheme may be formulated for this problem while retaining the passive equivalent circuit representation.

To formulate a correction factor method which satisfies the existence of the equivalent circuit one of the existing techniques [9, 10] might be employed. A set of capacitors and gyrators could then be selected in order to match as closely as possible the desired coefficients of each FDTD update equation. This is an unappealing method since each electrical component necessarily affects more than one field update equation and as a result the selection process is likely to be difficult except in simple cases.

An alternative approach is to examine the physical significance of the capacitors and gyrators in the equivalent circuit. It is clear that the capacitors represent the mechanism of energy storage associated with each field component and the gyrators

represent the means of energy transfer between electric and magnetic components. This suggests a means by which a correction scheme may be approached in terms of energy storage and transfer and yields the following method.

Consider figure 6.5 which illustrates the intersection of a microstrip line with one plane of the FDTD mesh and the corresponding portion of the equivalent circuit. For clarity the capacitors associated with E_{x_1} and E_{x_2} are not shown and the gyrator between H_{y_1} and E_{z_1} is omitted since the field component is in the metal.

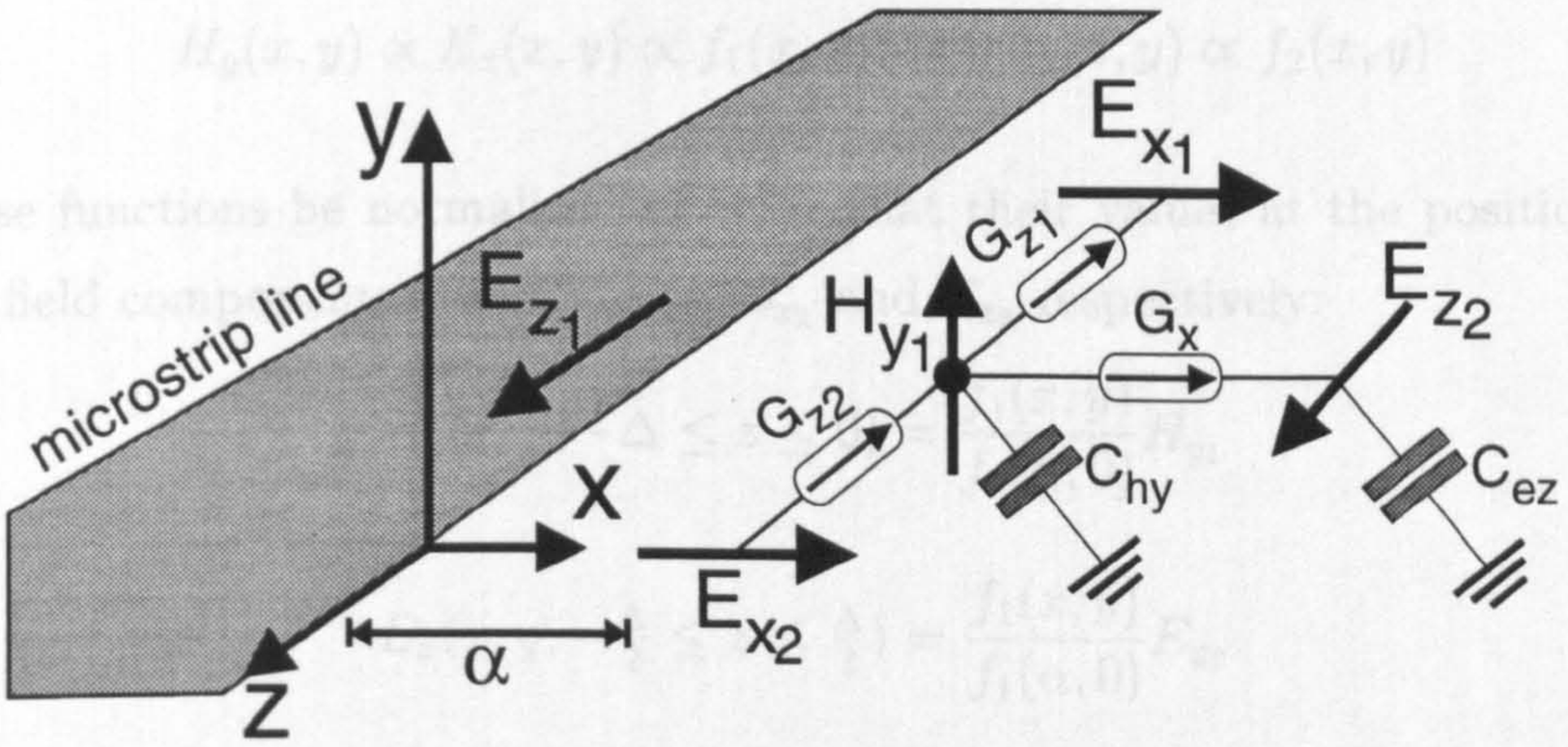

Figure 6.5: Microstrip line and FDTD mesh.

In the equivalent circuit the energies stored in the two illustrated capacitors are:

$$\mathcal{E}_{H_{y_1}} = \frac{1}{2} C_{hy} H_{y_1}^2 \tag{6.8}$$

$$\mathcal{E}_{E_{z_2}} = \frac{1}{2} C_{ez} E_{z_2}^2 \tag{6.9}$$

and the power flow $\mathcal{P} = VI$ through G_{z1}, G_{z2} and G_x is given by:

$$\mathcal{P}_{G_{z1}} = G_{z1} E_{x_1} H_{y_1} \tag{6.10}$$

$$\mathcal{P}_{G_{z2}} = G_{z2} E_{x_2} H_{y_1} \tag{6.11}$$

$$\mathcal{P}_{G_x} = G_x E_{z_2} H_{y_1} \tag{6.12}$$

Now assume that the transverse behaviour of the fields close to the edge is given by the functions [11] [12, p.142]:

$$\begin{aligned} f_1(r,\theta) &= \frac{1}{r^{\frac{1}{2}}} \cos\left(\frac{\theta}{2}\right) \\ f_2(r,\theta) &= r^{\frac{1}{2}} \cos\left(\frac{\theta}{2}\right) \end{aligned} \tag{6.13}$$

where r is the radial distance from the edge, and θ is the angle of elevation from the plane of the strip. These functions, unlike those of section 4.5.1, only take into account the static field resulting from an isolated edge and hence are not strictly valid for very narrow strips; they are, however, somewhat easier to manipulate.

Given f_1 and f_2 and changing to a Cartesian coordinate system where the x, y origin is taken to be at the edge of the strip, the field components have the following behaviour close to the edge:

$$H_y(x,y) \propto E_x(x,y) \propto f_1(x,y) \qquad E_z(x,y) \propto f_2(x,y) \tag{6.14}$$

Let these functions be normalised in order that their values at the positions of the defined field components are H_{y_1}, E_{x_1}, E_{x_2} and E_{z_2} respectively:

$$H_y(x,y,-\Delta \leq z \leq 0) = \frac{f_1(x,y)}{f_1(\alpha,0)} H_{y_1} \tag{6.15}$$

$$E_x(x,y,-\tfrac{\Delta}{2} \leq z \leq \tfrac{\Delta}{2}) = \frac{f_1(x,y)}{f_1(\alpha,0)} E_{x_2} \tag{6.16}$$

$$E_x(x,y,-\tfrac{3\Delta}{2} \leq z \leq -\tfrac{\Delta}{2}) = \frac{f_1(x,y)}{f_1(\alpha,0)} E_{x_1} \tag{6.17}$$

$$E_z(x,y,-\Delta \leq z \leq 0) = \frac{f_2(x,y)}{f_2(\alpha+\frac{\Delta}{2},0)} E_{z_2} \tag{6.18}$$

The *a priori* knowledge of the field behaviour yields the power flow and storage in the physical fields. This knowledge can be used to modify the values of capacitors and gyrators in the equivalent circuit, as shown in the following sections.

6.3.1 Capacitor Modification

The magnetic energy stored in the $\Delta \times \Delta \times \Delta$ volume of space with H_{y_1} at its centre is the volume integral of the energy density $\frac{1}{2}\mu H^2$ [13, p.233], thus:

$$\mathcal{E}_{H_{y_1}} = \mu \frac{1}{2} \int_{-\Delta}^{0} \int_{-\frac{\Delta}{2}}^{\frac{\Delta}{2}} \int_{\alpha-\frac{\Delta}{2}}^{\alpha+\frac{\Delta}{2}} H_y^2(x,y,z)\, dx\, dy\, dz \tag{6.19}$$

therefore:

$$\mathcal{E}_{H_{y_1}} = \mu \frac{1}{2} \left(\frac{\int_{-\Delta}^{0} \int_{-\frac{\Delta}{2}}^{\frac{\Delta}{2}} \int_{\alpha-\frac{\Delta}{2}}^{\alpha+\frac{\Delta}{2}} f_1^2(x,y)\, dx\, dy\, dz}{f_1^2(\alpha,0)} \right) H_{y_1}^2 \tag{6.20}$$

It is clear then that if (6.20) and (6.8) are to be equal then the value of the capacitor C_{hy} must be:

$$C_{hy} = \mu \left(\frac{\int_{-\Delta}^{0} \int_{-\frac{\Delta}{2}}^{\frac{\Delta}{2}} \int_{\alpha-\frac{\Delta}{2}}^{\alpha+\frac{\Delta}{2}} f_1^2(x,y)\, dx\, dy\, dz}{f_1^2(\alpha,0)} \right) \tag{6.21}$$

By consideration of the energy storage in the electric field [13, p.77] it can be shown by similar arguments that:

$$C_{ez} = \epsilon \left(\frac{\int_{-\Delta}^{0} \int_{-\frac{\Delta}{2}}^{\frac{\Delta}{2}} \int_{\alpha}^{\alpha+\Delta} f_2^2(x,y)\, dx\, dy\, dz}{f_2^2(\alpha+\frac{\Delta}{2},0)} \right) \tag{6.22}$$

It should be noted that if the fields are assumed to vary in a linear fashion within the respective volumes then the values yielded for the two components are:

$$C_{hy} = \mu\Delta^3 \qquad C_{ez} = \epsilon\Delta^3 \tag{6.23}$$

and as expected these are the values used in the uncorrected FDTD equivalent circuit.

6.3.2 Gyrator Modification

The power flow in an electromagnetic field is given by the integral of the Poynting vector [13, p.465]. Considering the power being transferred across an imaginary surface at $x = x_1$ between E_{z_2} and H_{y_1}:

$$\mathcal{P}_{G_x} = \int_{-\Delta}^{0} \int_{-\frac{\Delta}{2}}^{\frac{\Delta}{2}} E_z(x_1,y,z) H_y(x_1,y,z)\, dy\, dz \tag{6.24}$$

A simple approximation to this expression, which was found to give good results, is:

$$\mathcal{P}_{G_x} = \left(\frac{\int_{-\Delta}^{0} \int_{-\frac{\Delta}{2}}^{\frac{\Delta}{2}} f_1(\alpha,y) f_2(\alpha+\frac{\Delta}{2},y)\, dy\, dz}{f_1(\alpha,0) f_2(\alpha+\frac{\Delta}{2},0)} \right) E_{z_2} H_{y_1} \tag{6.25}$$

section 6.5.2 describes how an alternative expression for the gyrator might be preferred.

It is apparent then from (6.25) and (6.12) that G_x is given by:

$$G_x = \left(\frac{\int_{-\Delta}^{0} \int_{-\frac{\Delta}{2}}^{\frac{\Delta}{2}} f_1(\alpha,y) f_2(\alpha+\frac{\Delta}{2},y)\, dy\, dz}{f_1(\alpha,0) f_2(\alpha+\frac{\Delta}{2},0)} \right) \tag{6.26}$$

Repeating the above procedure for the other two gyrators yields:

$$G_{z1} = \left(\frac{\int_{-\frac{\Delta}{2}}^{\frac{\Delta}{2}} \int_{\alpha-\frac{\Delta}{2}}^{\alpha+\frac{\Delta}{2}} f_1(\alpha, y) f_1(\alpha, y)\, dx\, dy}{f_1(\alpha, 0) f_1(\alpha, 0)} \right) \tag{6.27}$$

$$G_{z2} = \left(\frac{\int_{-\frac{\Delta}{2}}^{\frac{\Delta}{2}} \int_{\alpha-\frac{\Delta}{2}}^{\alpha+\frac{\Delta}{2}} f_1(\alpha, y) f_1(\alpha, y)\, dx\, dy}{f_1(\alpha, 0) f_1(\alpha, 0)} \right) \tag{6.28}$$

If the field variations are considered linear these expressions reduce to:

$$G_x = G_{z1} = G_{z2} = \Delta^2 \tag{6.29}$$

which, as would be expected, are the uncorrected values used by the standard FDTD.

The insertion of modified gyrators and capacitors in the equivalent circuit gives rise in turn to modified update equation coefficients. The values of these coefficients are are obtained as follows.

6.3.3 Coefficient Correction

The update equation for H_{y_1} arises from the discrete time approximation to :

$$C_{hy} \partial_t H_{y_1} = G_x E_{z_2} + G_{z1} E_{x_1} - G_{z2} E_{x_2} \tag{6.30}$$

Thus the corrected coefficients (from left to right in the above equation) are given by:

$$\frac{G_x}{C_{hy}} = \left(\frac{f_1^2(\alpha, 0) \int_{-\Delta}^{0} \int_{-\frac{\Delta}{2}}^{\frac{\Delta}{2}} f_1(\alpha, y) f_2(\alpha + \frac{\Delta}{2}, y)\, dy\, dz}{\mu f_1(\alpha, 0) f_2(\alpha + \frac{\Delta}{2}, 0) \int_{-\Delta}^{0} \int_{-\frac{\Delta}{2}}^{\frac{\Delta}{2}} \int_{\alpha-\frac{\Delta}{2}}^{\alpha+\frac{\Delta}{2}} f_1^2(x, y)\, dx\, dy\, dz} \right) \tag{6.31}$$

$$\frac{G_{z1}}{C_{hy}} = \frac{G_{z2}}{C_{hy}} = \frac{1}{\mu \Delta} \tag{6.32}$$

The special form of the coefficients relating H_{y_1} to the neighbouring E_x components arises from the fact that the static solutions f_1 and f_2 are not functions of z since

the strip is considered uniform in the longitudinal direction. As a result the integrals cancel out to give no alteration to the standard algorithm in the z direction.

The preceding discussion demonstrates how a correction factor formulation can be constructed from the point of view of the equivalent circuit. The correction factor values for the calculation the H_y field in the plane of the microstrip have been provided. Since it is the capacitor and gyrator values themselves that are being corrected, as opposed to the coefficients in the update equations, stability problems will not arise.

In addition to the H_y component shown, a correction factor scheme should alter the update equations of the other field components adjacent to the strip. Figure 6.6 shows the field components on and below the plane of the strip for which corrected capacitors and gyrators are introduced. The corrections are symmetrical with respect to the vertical position of the strip and hence the corresponding fields above the strip will also be corrected (although they are not shown in figure 6.6 for clarity). For each capacitor associated with the illustrated field components and for every gyrator between two such components, the value of C or G may be calculated by straightforward adaptations to the method described by sections 6.3.1 and 6.3.2.

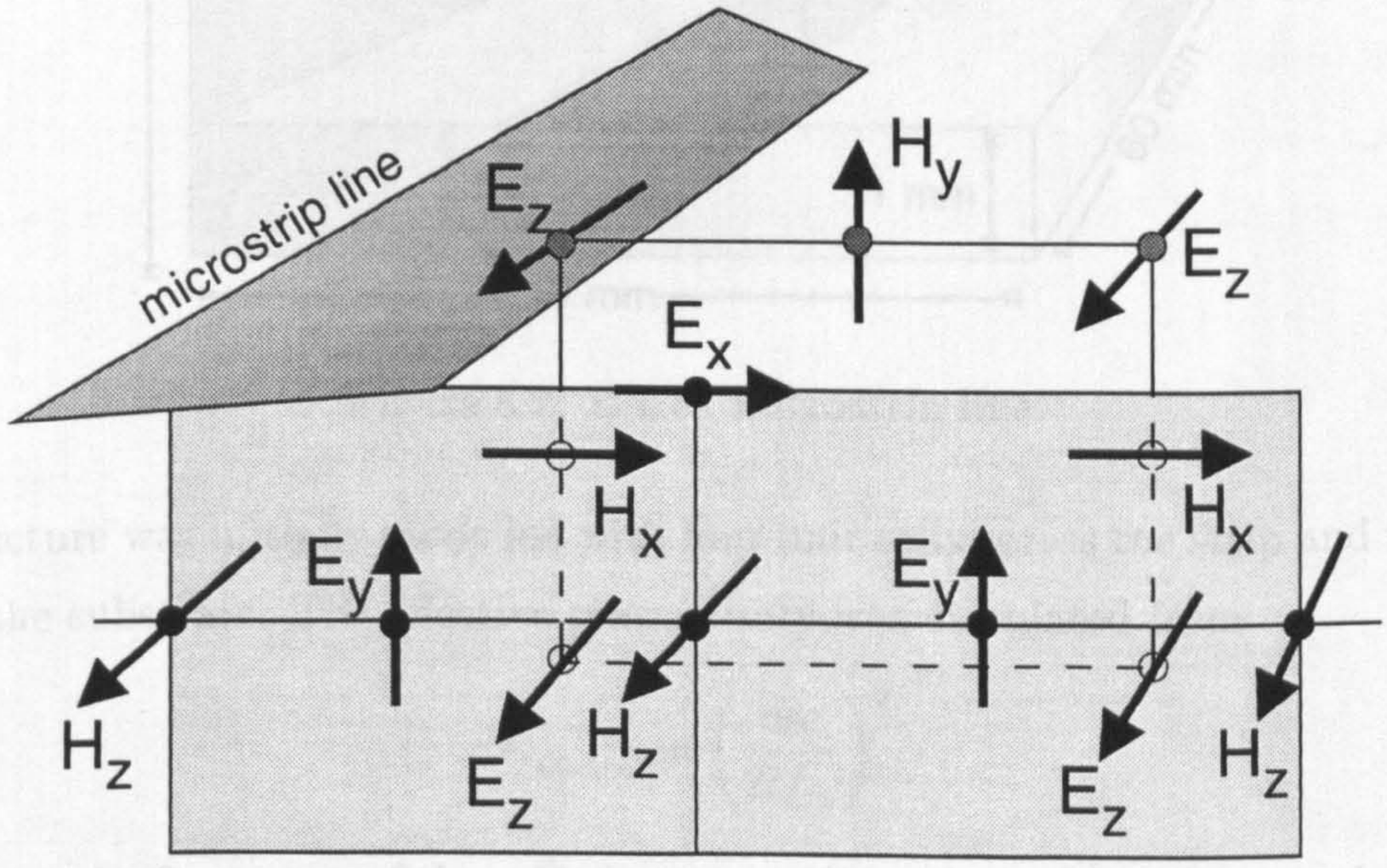

Figure 6.6: Corrected field components.

6.4 Validation of Correction Scheme

While the correction factor scheme described above is guaranteed to be stable given an appropriate time step it bears little resemblance to the (unstable) methods used

in [9, 10]. Clearly it is important that the method, in addition to being stable, remains capable of improving the standard FDTD method's characterisation of microstrip lines.

In this section the simple boxed microstrip structure illustrated by figure 6.7 was analysed using the FDTD algorithm and the equivalent circuit based correction method. Results were sought for the effective permittivity of the line as this parameter is known to be very sensitive to modelling accuracy. For comparison the Spectral Domain Method (SDM) [14], in the form described in [15], was employed to analyse the same structure – this method is known to be capable of highly accurate characterisations of microstrip structures.

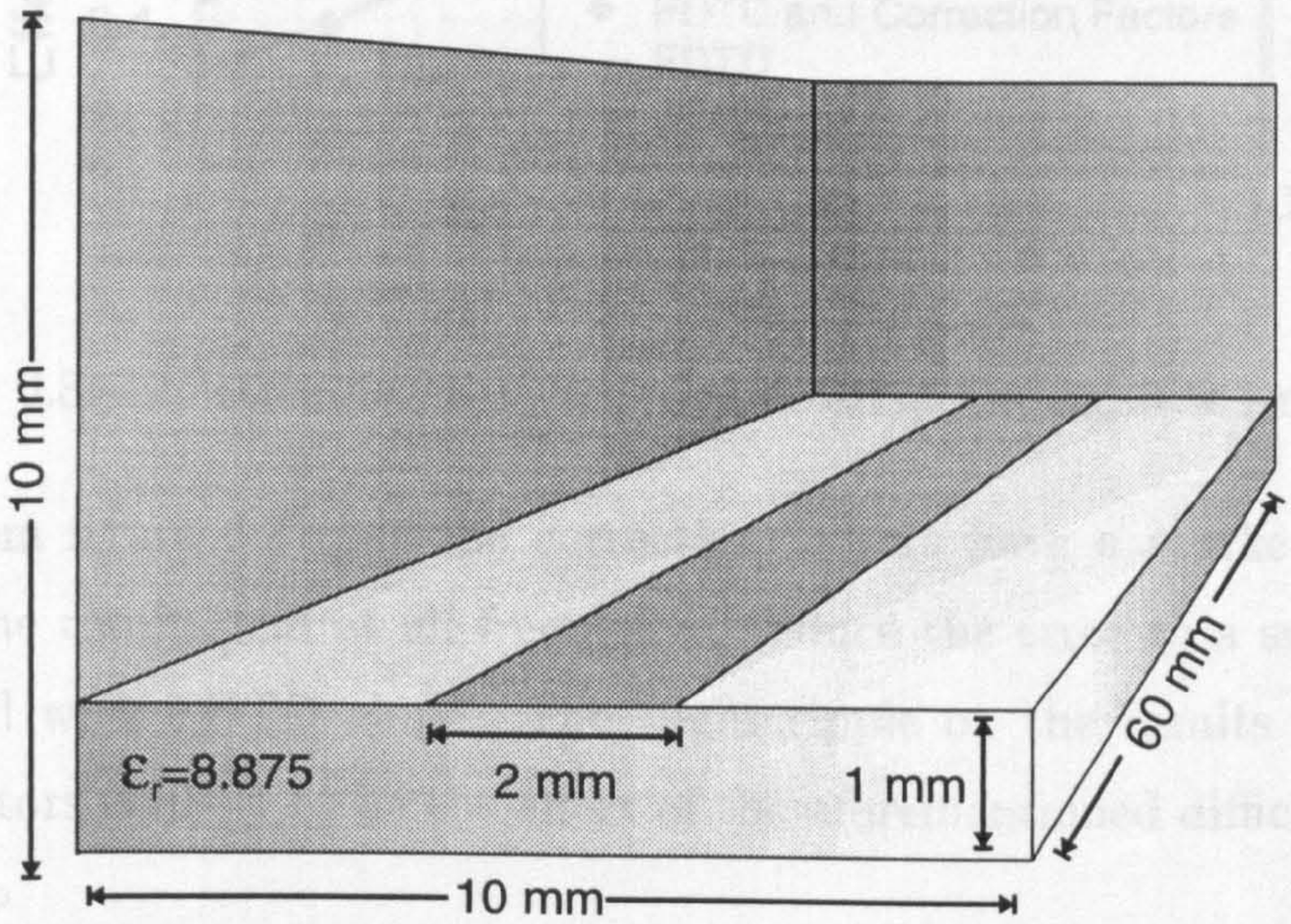

Figure 6.7: Boxed microstrip line.

The structure was initially modelled with four unit cells across the strip and four unit cells in the substrate. The effective permittivity was calculated from

$$\epsilon_{r_{\text{effective}}} = \left(\frac{mc}{2lf_m}\right)^2 \tag{6.33}$$

where f_m is the frequency of the m^{th} resonance of the shorted line (as calculated from FDTD), $l = 60\text{mm}$ is the length of the line and c is the speed of light in vacuum.

It was found to be difficult to establish a mode on the microstrip as there seemed to be an unwanted interaction between the excitation and the correction factors; it was for this reason that the effective permittivity was calculated from the resonant frequencies of the line as this technique is relatively insensitive to the nature of the excitation.

Figure 6.8 shows the variation in the effective permittivity of the microstrip against frequency as calculated by SDM (the solid line), and the standard FDTD method (the dashed line). The correction factor results were only available at the resonant frequencies of the line and are therefore indicated by marker points.

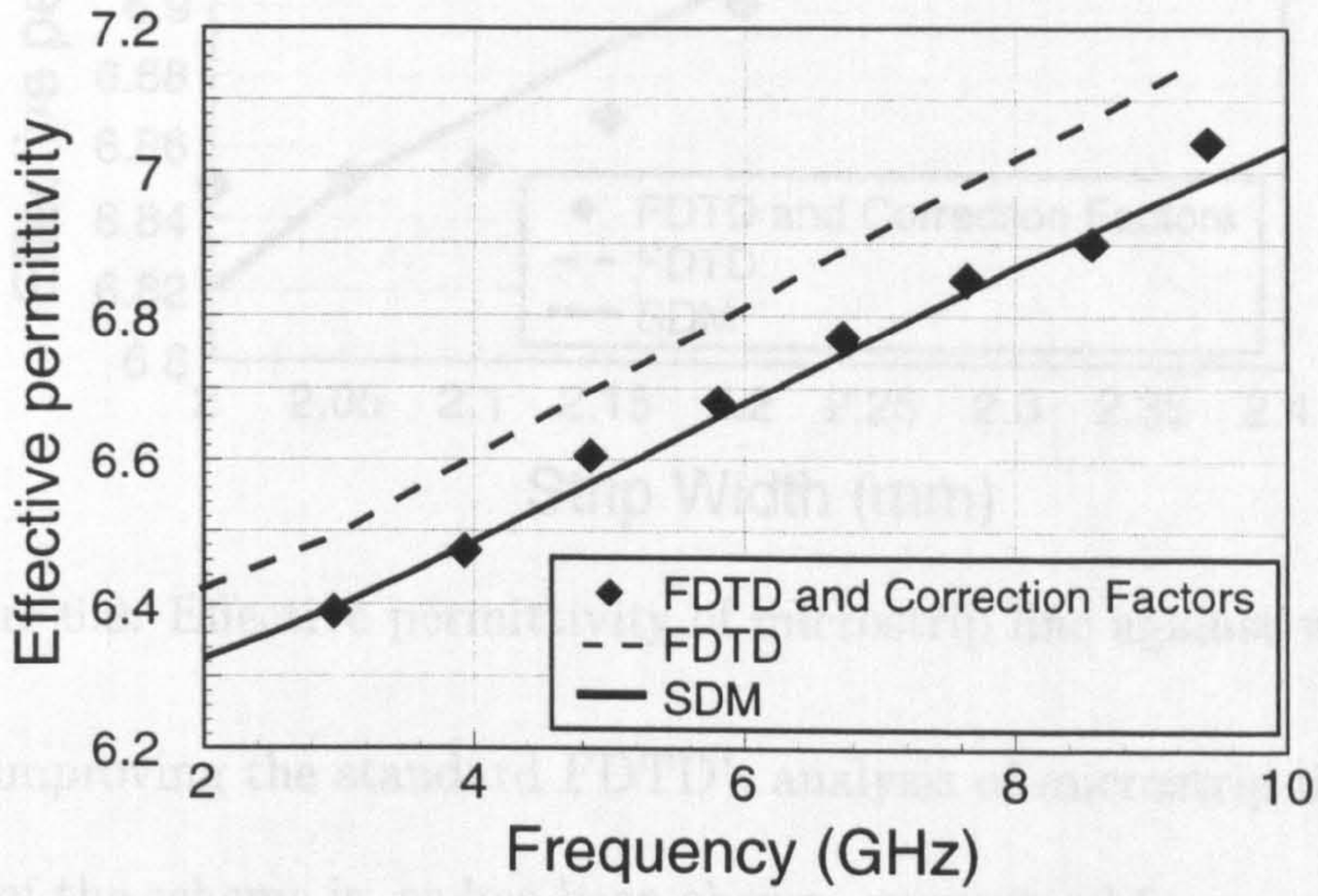

Figure 6.8: Effective permittivity of microstrip line against frequency.

It is clear from figure 6.8 that the correction factors have a marked effect on the accuracy of the results and at all frequencies reduce the error to a small fraction of that produced with FDTD alone. The slight ripple on the results obtained using correction factors is likely to be the effect of the aforementioned difficulty in exciting the microstrip.

As a second test the FDTD mesh was kept fixed while the width of the microstrip was gradually increased. The standard FDTD algorithm is not affected at all by changes in dimensions of less than the unit cell size and this is apparent in figure 6.9 which shows the variation in effective permittivity at one of the frequencies for which correction factor results were available (7.6 GHz) as the width is changed[1].

Once again the correction factor results are in excellent agreement with those of SDM. The difference between the two curves is largest for small widths however at its worst this disagreement is less than 0.5 %.

The results presented above show that the correction factor formulation based upon principles of energy storage and transfer and the equivalent circuit is capable of

[1]7.6 GHz is the nominal frequency. The correction factor results were obtained at the actual resonant frequency which varies slightly as the permittivity changes – the error this introduces in the results is however < 0.005 in the permittivity value.

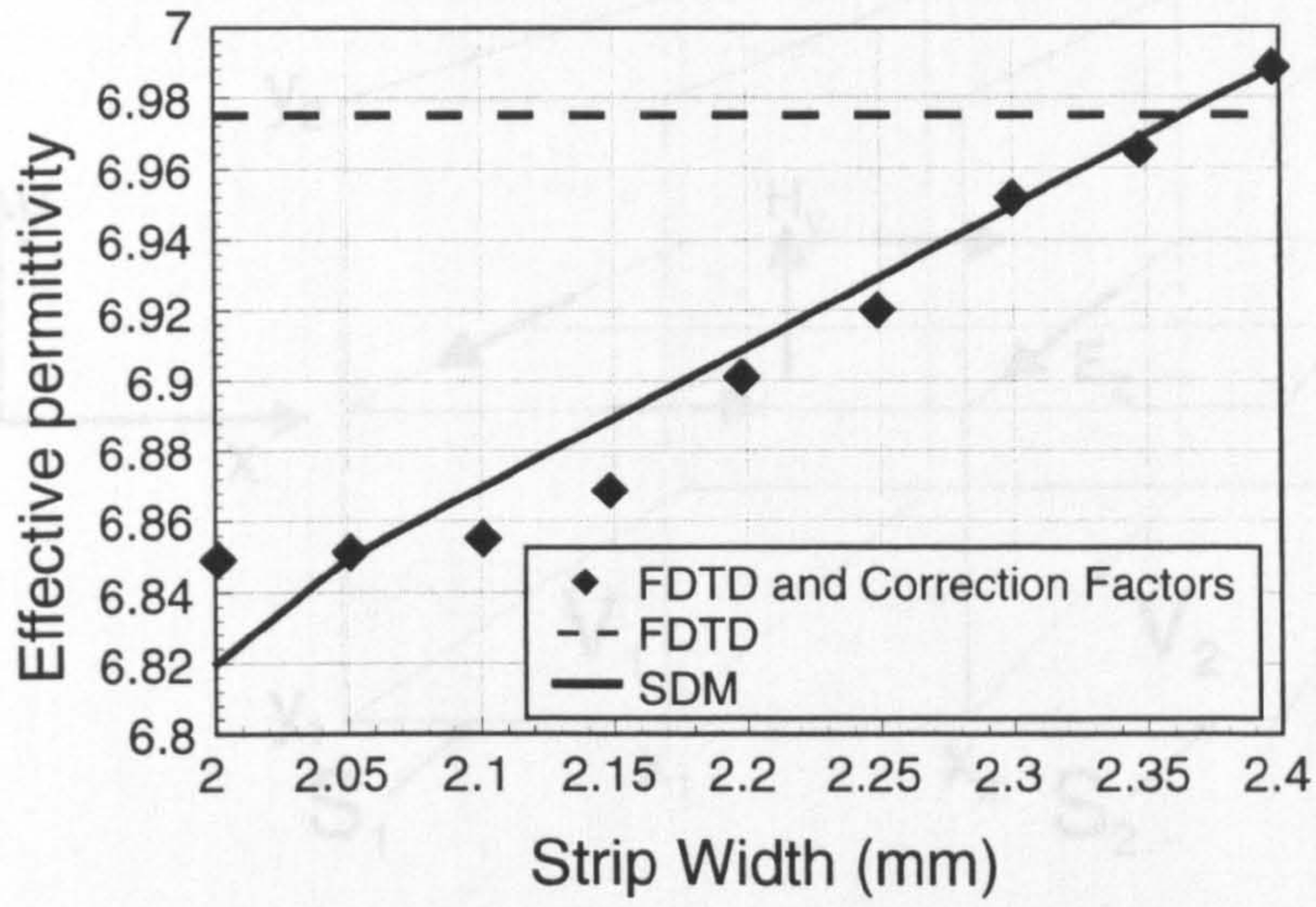

Figure 6.9: Effective permittivity of microstrip line against width.

dramatically improving the standard FDTD's analysis of microstrip lines.

The stability of the scheme is, as has been shown, guaranteed for a non-zero value of time step; it might be expected that the necessary value of time step be somewhat smaller than that required by the uncorrected algorithm. It was found, however, that the microstrip line geometry described above was stable, regardless of the strip width used, even when the time step employed was *unchanged* from the Courant limit. This property of an equivalent circuit based correction scheme was also found in the modified distorted contour path algorithms described in [6–8].

The only problem which occurred relates to the excitation of the microstrip line. It is believed that this arises from the fact that the corrected algorithm is locally not divergence conserving; further investigation of this problem is certainly required.

6.5 Further Investigation

Throughout this thesis the relationship between the FDTD method and the finite element method has been emphasized. In chapter 2 the reasonably well known fact that FDTD corresponds precisely to a collocation method was presented and in chapter 4 it was shown that the correction factor technique could be considered a modification of the piecewise linear basis functions.

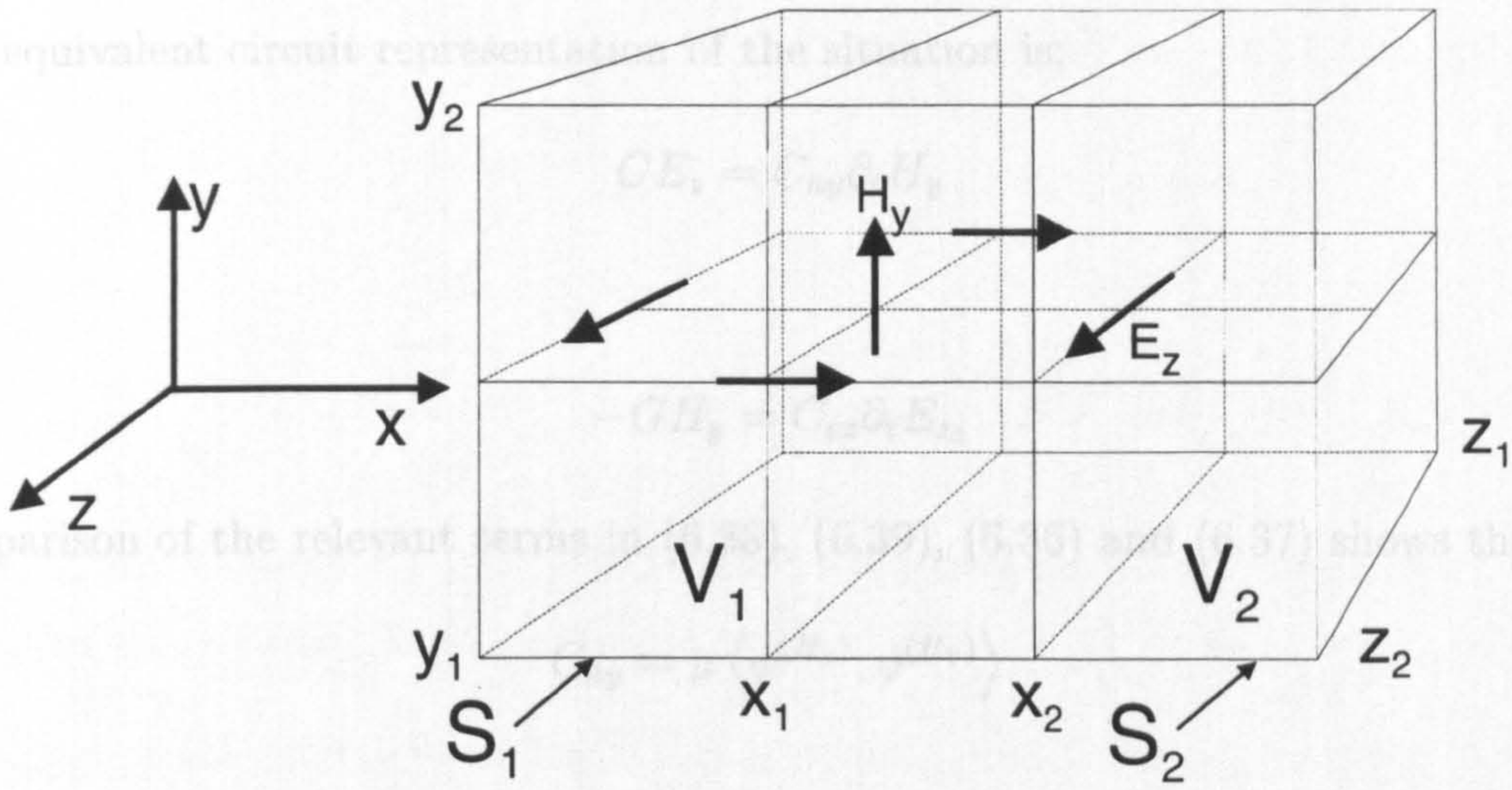

Figure 6.10: Field components in FDTD method.

Consider the general finite element formulation:

$$\left\langle \boldsymbol{\psi}^H_{i,j,k}, \sum^{i,j,k} \nabla \times \boldsymbol{\phi}^E_{i,j,k} \right\rangle \mathbf{E}_{i,j,k}(t) = -\mu \left\langle \boldsymbol{\psi}^H_{i,j,k}, \boldsymbol{\phi}^H_{i,j,k} \right\rangle \partial_t \mathbf{H}_{i,j,k}(t) \quad \forall i,j,k \tag{6.34}$$

where $\boldsymbol{\psi}^H$ and $\boldsymbol{\psi}^E$ are the dyadic test functions (for convenience labeled according to which field type they are associated with). $\boldsymbol{\phi}^H$ and $\boldsymbol{\phi}^E$ are the dyadic basis functions. It has already been assumed that basis functions associated with a given field type (either electric or magnetic) do not overlap another basis function associated with the same type.

Furthermore the discussion is restricted to the Galerkin finite element methods in which the test and basis functions are identical, thus:

$$\left\langle \boldsymbol{\phi}^H_{i,j,k}, \sum^{i,j,k} \nabla \times \boldsymbol{\phi}^E_{i,j,k} \right\rangle \mathbf{E}_{i,j,k}(t) = -\mu \left\langle \boldsymbol{\phi}^H_{i,j,k}, \boldsymbol{\phi}^H_{i,j,k} \right\rangle \partial_t \mathbf{H}_{i,j,k}(t) \quad \forall i,j,k \tag{6.35}$$

Consider figure 6.10 in which two overlapping cubical volumes are shown; one, V_1, has component H_y at its centre and is bounded by the closed surface S_1, the other, V_2 is centred on the position of the component E_z and has S_2 as its boundary.

Consider now the finite element formulation for the two components labeled H_y and E_z only:

$$\left\langle \mathbf{j}\phi^{(H_y)}, \nabla \times \mathbf{k}\phi^{(E_z)} \right\rangle E_z(t) = -\mu \left\langle \phi^{(H_y)}, \phi^{(H_y)} \right\rangle \partial_t H_y(t) \tag{6.36}$$

$$\left\langle \mathbf{k}\phi^{(E_z)}, \nabla \times \mathbf{j}\phi^{(H_y)} \right\rangle H_y(t) = \epsilon \left\langle \phi^{(E_z)}, \phi^{(E_z)} \right\rangle \partial_t E_z(t) \tag{6.37}$$

The equivalent circuit representation of the situation is;

$$GE_z = C_{hy}\partial_t H_y \tag{6.38}$$

and:

$$-GH_y = C_{ez}\partial_t E_{z_2} \tag{6.39}$$

comparison of the relevant terms in (6.38), (6.39), (6.36) and (6.37) shows that:

$$C_{hy} = \mu \left\langle \phi^{(H_y)}, \phi^{(H_y)} \right\rangle \tag{6.40}$$

$$C_{ez} = \epsilon \left\langle \phi^{(E_z)}, \phi^{(E_z)} \right\rangle \tag{6.41}$$

and the gyrator connecting to the two field components is:

$$G = \left\langle \mathbf{j}\phi^{(H_y)}, \nabla \times \mathbf{k}\phi^{(E_z)} \right\rangle = \left\langle \mathbf{k}\phi^{(E_z)}, \nabla \times \mathbf{j}\phi^{(H_y)} \right\rangle \tag{6.42}$$

the final result arising from the fact that curl is a self-adjoint operator [16].

This analysis can be applied to all the other field components in a similar manner and yields the general conclusion that a Galerkin finite element formulation of this type is exactly equivalent to the passive circuit for FDTD (although it is interesting that the converse is not necessarily true). This finding is in contrast to the situation for the point matched finite element form of FDTD (described in section 2.6.2) which does not in general possess the properties of the passive circuit. It is for this reason that correction factor schemes based upon modification of the point matched finite element formulation's basis functions (see for example section 4.5.2) were usually unstable.

6.5.1 Galerkin FDTD Formulation

To recover the standard form of the FDTD algorithm the basis functions should be chosen to be piecewise constant functions:

$$\phi^{H_y}(\mathbf{r}) = \begin{cases} A & \mathbf{r} \text{ in } V_1 \\ 0 & \text{otherwise} \end{cases} \tag{6.43}$$

$$\phi^{E_z}(\mathbf{r}) = \begin{cases} B & \mathbf{r} \text{ in } V_2 \\ 0 & \text{otherwise} \end{cases} \tag{6.44}$$

When these functions are introduced into equations (6.36) and (6.37) they yield:

$$-E_z(t) \iiint_{V_1} \phi^{(H_y)} \partial_x \phi^{(E_z)} \, dx \, dy \, dz = -\mu \Delta^3 A^3 \partial_t H_y(t) \tag{6.45}$$

$$H_y(t) \iiint_{V_2} \phi^{(E_z)} \partial_x \phi^{(H_y)} \, dx \, dy \, dz = \epsilon \Delta^3 B^3 \partial_t E_z(t) \tag{6.46}$$

where the inner products on the left hand sides have reduced to integrals over $V_{1,2}$ and those on the right hand side to integrals over either V_1 or V_2.

The appropriate limits (see figure 6.10) may now be introduced, however (6.45) has a discontinuity at x_1 and (6.46) has one at x_2. Treatment of these discontinuities is facilitated by introducing the points $x_1^- = x_1 - \delta_x$, $x_1^+ = x_1 + \delta_x$, $x_2^- = x_2 - \delta_x$ and $x_2^+ = x_2 + \delta_x$. as shown in figure 6.11. The behaviour of $\partial_x \phi^{(E_z)}$ and $\partial_x \phi^{(H_y)}$ at x_1 and x_2 respectively may be considered as $\delta_x \to 0$.

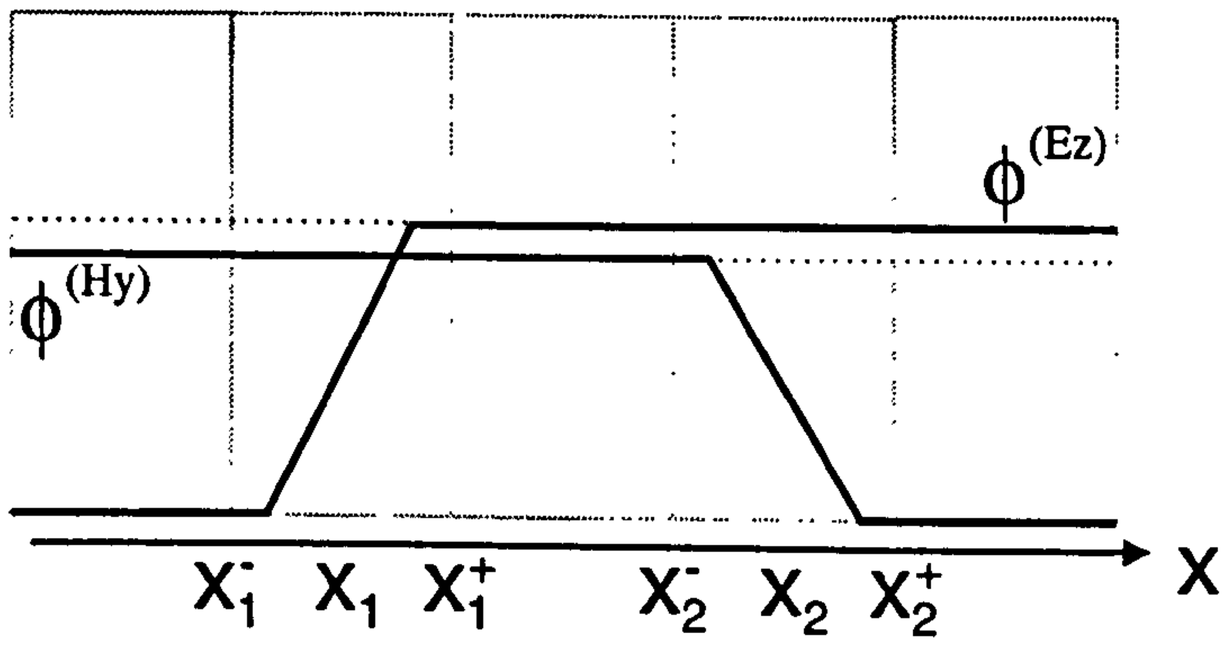

Figure 6.11: Treatment of discontinuities at x_1 and x_2.

The expressions (6.45) and (6.46) become:

$$E_z(t) \int_{y_1}^{y_2} \int_{z_1}^{z_2} \int_{x_1^-}^{x_2^+} \phi^{(H_y)} \partial_x \phi^{(E_z)} \, dx \, dy \, dz = \mu \Delta^3 A^3 \partial_t H_y(t) \tag{6.47}$$

and:

$$H_y(t) \int_{y_1}^{y_2} \int_{z_1}^{z_2} \int_{x_1^-}^{x_2^+} \phi^{(E_z)} \partial_x \phi^{(H_y)} \, dx \, dy \, dz = \epsilon \Delta^3 B^3 \partial_t E_z(t) \tag{6.48}$$

Splitting the required integrals into two parts yields:

$$E_z(t) \int_{y_1}^{y_2} \int_{z_1}^{z_2} \left(\int_{x_1^-}^{x_1^+} \phi^{(H_y)} \partial_x \phi^{(E_z)} \, dx \right) + \left(\int_{x_1^+}^{x_2^+} \phi^{(H_y)} \partial_x \phi^{(E_z)} \, dx \right) dy \, dz = \mu \Delta^3 A^3 \partial_t H_y(t) \tag{6.49}$$

$$H_y(t)\int_{y_1}^{y_2}\int_{z_1}^{z_2}\left(\int_{x_1^-}^{x_2^-}\phi^{(E_z)}\partial_x\phi^{(H_y)}\,dx\right)+\left(\int_{x_2^-}^{x_2^+}\phi^{(E_z)}\partial_x\phi^{(H_y)}\,dx\right)dy\,dz=$$
$$\epsilon\Delta^3B^3\partial_tE_z(t) \tag{6.50}$$

the derivative of the step discontinuity in $\phi^{(E_z)}$ at x_1 is given, for example, by:

$$\partial_x\phi^{(E_z)}(x)=\delta(x,x_1)(\phi^{(E_z)}(x_1^+)-\phi^{(E_z)}(x_1^-)) \tag{6.51}$$

where $\delta(x,x_1)$ is a Dirac delta function with unity weight.

Application of this result to (6.49) and (6.50) gives:

$$E_z(t)\int_{y_1}^{y_2}\int_{z_1}^{z_2}(AB)+\left(\int_{x_1^+}^{x_2^+}\phi^{(H_y)}\partial_x\phi^{(E_z)}\,dx\right)dy\,dz=\mu\Delta^3A^3\partial_tH_y(t) \tag{6.52}$$

$$H_y(t)\int_{y_1}^{y_2}\int_{z_1}^{z_2}\left(\int_{x_1^-}^{x_2^-}\phi^{(E_z)}\partial_x\phi^{(H_y)}\,dx\right)+(-BA)\,dy\,dz=\epsilon\Delta^3B^3\partial_tE_z(t) \tag{6.53}$$

It is straightforward to show that, given that the derivatives of the piecewise constant basis functions are zero over the range of the remaining integrations with respect to x, equations (6.52) and (6.53) yield:

$$E_z(t)\int_{y_1}^{y_2}\int_{z_1}^{z_2}AB\,dy\,dz=\mu\Delta^3A^3\partial_tH_y(t) \tag{6.54}$$

$$H_y(t)\int_{y_1}^{y_2}\int_{z_1}^{z_2}(-BA)\;dy\,dz=\epsilon\Delta^3B^3\partial_tE_z(t) \tag{6.55}$$

which, if the basis functions are assumed to have unity amplitude (ie $A=B=1$), gives:

$$E_z(t)\Delta^2=\mu\Delta^3\partial_tH_y(t) \tag{6.56}$$

$$-H_y(t)\Delta^2=\epsilon\Delta^3\partial_tE_z(t) \tag{6.57}$$

these are recognised as the appropriate parts of the standard FDTD algorithm.

The results given above may in fact be achieved with considerably less effort given the simple form of the basis functions in this case, however the derivation given above readily extends to the case when the basis functions are more elaborate functions.

In is interesting to note that the fact that FDTD may be derived from a Galerkin finite element approach with piecewise constant basis functions has recently and independently confirmed in [17].

6.5.2 Correction Factors in the Galerkin Method

While the correction factor scheme based on the equivalent circuit was developed before the existence of the Galerkin form of FDTD was perceived it is immediately apparent that the correction scheme used, based on the energy storage and transfer within the algorithm is almost exactly equivalent to the modification of the basis functions in the Galerkin method.

The corrected capacitance for H_y from (6.21) was:

$$C_{hy} = \mu \left(\frac{\int_{-\Delta}^{0} \int_{-\frac{\Delta}{2}}^{\frac{\Delta}{2}} \int_{\alpha-\frac{\Delta}{2}}^{\alpha+\frac{\Delta}{2}} f_1^2(x,y)\, dx\, dy\, dz}{f_1^2(\alpha,0)} \right) \tag{6.58}$$

where f_1 and f_2 were the assumed behaviour of the fields over the unit cell, this is exactly the same expression as (6.40) apart from the normalisation terms in the denominator.

The expression used for the gyrator (6.26) was:

$$G_x = \left(\frac{\int_{-\Delta}^{0} \int_{-\frac{\Delta}{2}}^{\frac{\Delta}{2}} f_1(\alpha,y) f_2(\alpha+\frac{\Delta}{2},y)\, dy\, dz}{f_1(\alpha,0) f_2(\alpha+\frac{\Delta}{2},0)} \right) \tag{6.59}$$

this is similar to (6.42) but not in fact identical. Whether or not modifying the gyrator calculation to that suggested by the finite element method will produce an improved correction factor formulation is open to question and the matter is addressed in chapter 7 in the context of suggestions for future work.

It is proposed therefore that the Galerkin FDTD formulation provides an entirely general method of including *a priori* knowledge of the field behaviour into the algorithm without any possibility of instability. Since the Galerkin formulation may always be viewed as an equivalent circuit the modification of the FDTD algorithm can be viewed from either viewpoint; depending on the problem under consideration one interpretation or the other may prove more attractive.

6.6 Summary

In this chapter an equivalent passive electrical circuit has been presented for the FDTD algorithm. A correction factor formulation for metal edges which retains this

passive representation has been derived and it has been shown that the formulation is both accurate and stable even with a time step equal to the Courant limit; the fact that it is not divergence preserving presents a slight problem which may need to be resolved.

The equivalent circuit is not only useful in assuring the stability of correction factor schemes; an example of its application to the deformed contour path method has been presented in this chapter and further applications are expected.

The equivalent circuit also points the way to a new finite element perspective on FDTD; this finite element method must always have a passive circuit representation and is therefore always stable given a suitable time step. This alternative approach gives a method for selecting correction factor schemes based on *a priori* knowledge of the field behaviour and also provides an important new understanding of the FDTD method.

References

[1] A. S. Sedra and K. C. Smith, *Microelectronic Circuits.* CBS College Publishing, 1987.

[2] P. Horowitz and H. Winfield, *The Art of Electronics.* Cambridge University Press, 2 ed., 1989.

[3] G. Kron, "Equivalent circuit of field equations of Maxwell – I," *Proceedings of the IRE*, vol. 32, pp. 289–299, 1944.

[4] T. G. Jurgens, A. Taflove, K. Umashankar, and T. G. Moore, "Finite difference time domain modelling of curved surfaces," *IEEE Transactions on Antennas and Propagation*, vol. AP-40, pp. 357–366, Apr. 1992.

[5] T. G. Jurgens and A. Taflove, "Three dimensional contour FDTD modelling of scattering from single and multiple bodies," *IEEE Transactions on Antennas and Propagation*, vol. AP-41, pp. 1703–1708, Dec. 1993.

[6] C. J. Railton, I. J. Craddock, and J. B. Schneider, "Improved locally distorted CPFDTD algorithm with provable stability," *Electronics Letters*, vol. 31, pp. 1585–1586, Aug. 1995.

[7] C. J. Railton and I. J. Craddock, "Analysis of general 3D PEC structures using an improved CPFDTD algorithm," *Electronics Letters*, vol. 31, pp. 1753–1754, Sept. 1995.

[8] C. J. Railton, I. J. Craddock, and J. B. Schneider, "The analysis of general 2D PEC structures using a modified CPFDTD algorithm," *IEEE Transactions on Microwave Theory and Techniques.* submitted.

[9] D. B. Shorthouse and C. J. Railton, "Incorporation of static singularities into the finite difference time domain technique with application to microstrip structures," in *Proceedings of the 20th European Microwave Conference*, vol. 1, pp. 531–536, Sept. 1990.

[10] C. J. Railton, D. B. Shorthouse, and J. P. McGeehan, "Modelling of narrow microstrip lines using finite difference time domain method," *Electronics Letters*, vol. 28, pp. 1168–1170, June 1992.

[11] R. E. Collin, *Field Theory of Guided Waves.* McGraw Hill, 1960.

[12] D. B. Shorthouse, *The CAD and analysis of passive monolithic microwave circuits by the finite difference time domain technique.* PhD thesis, University of Bristol, 1992.

[13] J. D. Kraus, *Electromagnetics.* McGraw–Hill, 3 ed., 1984.

[14] T. Itoh and R. Mittra, "A technique for computing dispersion characteristics of shielded microstrip lines," *IEEE Transactions on Microwave Theory and Techniques*, vol. MTT-22, pp. 896–898, Oct. 1974.

[15] C. J. Railton and T. Rozzi, "Complex modes in boxed microstrip," *IEEE Transactions on Microwave Theory and Techniques*, vol. MTT-26, pp. 865–874, May 1988.

[16] Z. Yoshida, "Discrete eigenstates of plasmas described by the Chandrasekhar-Kendal functions," *Progress of Theoretical Physics*, vol. 86, July 1991.

[17] M. Krumpholtz, C. Huber, and P. Russer, "A field theoretical comparison of FDTD and TLM," *IEEE Transactions on Microwave Theory and Techniques*, vol. MTT-43, pp. 1935–1950, Aug. 1995.

Chapter 7

Conclusions and Future Work

7.1 Summary

The behaviour of the electromagnetic waves upon which so many human activities depend is described by Maxwell's equations [1]. These equations are simple in form however in realistic situations their solution requires the use of sophisticated numerical methods and hours or even days of computer time.

Numerical methods are used throughout engineering and science and, while their evolution can be traced from the pioneering work of the early twentieth century [2], their range of application is such that their use and development remains to this day a focus of great attention.

This thesis has been concerned entirely with the application and improvement of numerical methods in the field of electromagnetics. Commencing with an illustrative account of an early use of numerical methods in chapter 1 and, in chapter 2, a review of some of the techniques currently used in electromagnetics, later chapters progressed to consider new enhancements and adaptations pioneered at the University of Bristol and by the author personally.

In chapter 3 the time domain near far transform was presented. While being well known in the field of time domain electromagnetic analysis [3, 4] its applications have not been numerous and its application here to a printed dipole represents to the authors' knowledge the most sophisticated example of its use to date. Some consideration was given to the computational costs of the method and to what extent the use of system identification [5] can reduce these costs.

The correction factor method [6] is a technique which alters the update equations in a finite difference algorithm by the consideration of *a priori* knowledge of the field behaviour. Chapter 4 presented the general correction factor technique and also described the stability problems that have prevented this invaluable method from gaining wider use.

The author's main contributions to the enhancement of time domain numerical methods were described in chapters 5 and 6. In chapter 5 a new method (the SFDTD technique) was presented and found to have a stable correction factor formulation [7]. With the insight provided into stability by examination of the SFDTD method, a scheme was presented in chapter 6, based on energy conservation, for ensuring stability of the FDTD algorithm [8]. By employing this method a stable correction factor

scheme for metal edges was derived and shown to produce considerable improvement in the accuracy of the FDTD characterisation of a microstrip line. The final results of chapter 6 examined the relationship between energy based stability theory and the Galerkin finite element approach.

7.2 Future Work

The following avenues for future work are suggested by the research described in chapters 3, 5 and 6 of this thesis:

7.2.1 The Time Domain Near Far Transform

In chapter 3 the time domain near far algorithm was presented. This algorithm was shown to be able to accurately characterise the far field of a printed dipole antenna and clearly its ability to perform this characterisation over a broad band is of considerable importance given the wide band nature of the antenna. It was shown however that the memory requirements for the algorithm in some applications can become excessive (a greater than 100% overhead on the FDTD method) and this may limit its future application.

It is frequently the case that memory usage and speed in an algorithm are to some extent traded off against each other and that is the case for the time domain extrapolation method. The implementation considered in chapter 3 saved computation time by storing extra parameters (in the manner described by [9, p.165]) with the result that 4 floating point and 2 integer variables are stored per point on the extrapolation surface for each observation point; the minimum storage that is in fact necessary is 2 floating point numbers but this is at the expense of considerable extra computation.

A second approach which sacrifices very little computation time is to not store separate delay times for the M and J currents – the only reason this is done is to take into account their displacement in time of $\Delta_t/2$; this fact may be accounted for instead by staggering the accumulation of the two integrals in the far zone (equations (3.3)) by this half time step. A small amount of extra computation will be required at each observation point to interpolate the vector potentials but the storage requirements will drop by 50%.

In summarising the time domain transform it may be said that, in the example given of the printed dipole, the memory overhead may easily be reduced from 13 MBytes to 7.5 MBytes or even as little as approximately 2 MBytes – the latter figure achieved at a considerable increase in computation time. If future work can demonstrate that a reduction in memory requirements of this order can be made without sacrificing too much in terms of computation time, the applicability of the transform will be greatly widened.

7.2.2 The SFDTD Technique

The SFDTD method of chapter 5 employs, unlike FDTD, a non staggered field discretisation (figure 5.1). This discretisation allows an easier treatment of curved surfaces since the resolution of the field components into tangential and normal directions is straightforward. The greatest disadvantage of the SFDTD method (which fundamentally arises from the adoption of a non-staggered discretisation) is its neglection of the field divergence term (see section 5.3).

The consequences of neglecting the divergence in Maxwell's equations is that the treatment of dielectric interfaces and metal edges is not (as it is in FDTD) simple. In order to solve these problems correction factor methods (such as the technique for curved surfaces described in section 5.4) may be derived for each of these circumstances or alternatively a combination of the SFDTD and FDTD methods could be achieved by interpolation at a common interface. Either of these possibilities would merit further investigation.

7.2.3 The FDTD Equivalent Circuit

Having seen the utility of an equivalent passive circuit for the SFDTD method, an equivalent circuit for FDTD was shown in chapter 6 (figure 6.3). The equivalent circuit provides a means by which stable modification schemes for the algorithm (for example correction factor and contour path schemes [10]) may be selected.

It was shown in section 6.3 that by considering the energy stored and transferred in the electromagnetic fields and relating these quantities to the elements of the equivalent circuit, a correction factor scheme for microstrip lines may be produced. Application of this method yielded a stable and extremely accurate characterisation

of the effective permittivity of the microstrip geometry of figure 6.7.

The correction factor formulation may easily be applied to more complex microstrip geometries and is likely to greatly reduce the computational overheads of including narrow microstrip feedlines, for example, in FDTD models. Future work on the method will need to address the issue of the conservation of divergence in the algorithm mentioned in section 6.4; it is anticipated that careful consideration of the correction formulation should produce a solution to this difficulty.

A second area of the correction factor formulation of chapter 6 that would benefit from further investigation is the fact that the method does not correspond exactly to the Galerkin finite element formulation of section 6.5. This correspondence is not a required property of the algorithm, however it would be illuminating to evaluate whether recasting the gyrator evaluation in terms of the finite element method (section 6.5.2) yielded an even more accurate technique.

The equivalent circuit representation and the finite element formulation (section 6.5) are perhaps the most significant aspects of this thesis and potentially enable an extremely wide range of developments. It is likely that, in addition to yielding schemes for curved surfaces [10] and microstrip lines, the guaranteed stable inclusion of *a priori* knowledge for narrow wires, narrow slots, curved dielectric boundaries, angled microstrip lines and dielectric wedges are all possibilities. If successful these applications would entirely remove the most common causes of large computational overheads in the FDTD method.

7.3 Concluding Remarks

With the advent of digital electronic computers in the 1940's, numerical algorithms have become widespread in engineering and the sciences. In electromagnetics in particular their use has become increasingly popular since the 1970's and methods such as the Yee FDTD algorithm [11] have been applied to many situations where any other form of analysis is impossible.

Fully three dimensional solutions, particularly those which operate in the time domain, require very large amounts of computation and the availability and expense of computers has provided, and always will provide, a fundamental limit on the applicability of techniques such as the Yee method.

Section 7.3 : Concluding Remarks

In this thesis three methods for reducing the required computation resources in a time domain electromagnetic analysis have been presented; the near far transform (chapter 3), the system identification technique (chapter 3) and the correction factor method (chapters 4, 5 and 6). In particular the final results of a careful investigation of the correction factor method, presented in chapter 6, provide the means for a large reduction in computational overheads in many situations and hence a considerable widening of the applicability of the FDTD technique. With the ever increasing use of the electromagnetic spectrum any such increase in the usefulness of the FDTD method is likely to be widely beneficial.

References

[1] J. C. Maxwell, *A Treatise on Electricity and Magnetism.* Dover Publications, 3 ed., 1954. Work originally published in 1873.

[2] L. F. Richardson, *Weather Prediction by Numerical Process.* Cambridge University Press, 1922. Re-printed in 1965 by Dover Publications.

[3] K. S. Yee, D. Ingham, and K. Schlager, "Time domain extrapolation to the far field based on FDTD calculations," *IEEE Transactions on Antennas and Propagation*, vol. AP-39, pp. 411–413, Mar. 1991.

[4] R. J. Luebbers, K. S. Kunz, M. Schneider, and F. Hunsberger, "A finite difference time domain near zone to far zone transformation," *IEEE Transactions on Antennas and Propagation*, vol. AP-39, pp. 429–433, Apr. 1991.

[5] T. Soderstrom and P. Stoica, *System Identification.* Prentice Hall, 1989.

[6] D. B. Shorthouse and C. J. Railton, "Incorporation of static singularities into the finite difference time domain technique with application to microstrip structures," in *Proceedings of the 20th European Microwave Conference*, vol. 1, pp. 531–536, Sept. 1990.

[7] I. J. Craddock and C. J. Railton, "Analysis of curved and angled surfaces on a Cartesian mesh using a novel finite difference time domain algorithm," *IEEE Transactions on Microwave Theory and Techniques*, vol. MTT-43, Oct. 1995. In press.

[8] I. J. Craddock and C. J. Railton, "Derivation and application of an equivalent circuit for FDTD," *Microwave and Guided Wave Letters*, vol. 6, Jan. 1996. In press.

[9] E. M. Daniel, *The analysis and CAD of microwave and millimetre wave planar antennas.* PhD thesis, Universtity of Bristol, 1992.

[10] C. J. Railton, I. J. Craddock, and J. B. Schneider, "Improved locally distorted CPFDTD algorithm with provable stability," *Electronics Letters*, vol. 31, pp. 1585–1586, Aug. 1995.

[11] K. S. Yee, "Numerical solution of initial boundary value problems involving Maxwell's equations in isotropic media," *IEEE Transactions on Antennas and Propagation*, vol. AP-14, pp. 302–307, May 1966.

Copy of Publications

Derivation and Application of a Passive Equivalent Circuit for the Finite Difference Time Domain Algorithm.

I. J. Craddock, C. J. Railton and J. P. McGeehan
Centre for Communications Research, University of Bristol, UK.

Abstract

The widely used Finite Difference Time Domain (FDTD) algorithm in its standard form is *conditionally stable*, the condition being the well known Courant criterion. Much research has focussed on modifying the standard algorithm to improve its characterisation of geometrical detail and curved surfaces; these modified algorithms however may easily be *unconditionally unstable* – there is no value of time step which stabilizes the algorithm. This contribution presents a passive electrical circuit which, by virtue of its formal equivalence with FDTD, provides a criterion by which unconditionally unstable algorithms may be avoided. As an example the passive circuit criterion is used to remove the instability from a Contour-Path FDTD algorithm.

It is emphasized that the circuit presented here is not a lumped equivalent to some discontinuity or other physical feature to be included in the FDTD algorithm – it is an equivalent to the algorithm itself.

It is necessary to define the generalised gyrator shown in figure 1 whose symbol includes an arrow which serves to set a reference direction for the currents at ports 1 and 2; with the reference shown, the relationships at ports 1 and 2 are $V_2 = GI_1$ and $V_1 = GI_2$.

Now consider the circuit given by figure 2 consisting of a network of gyrators wth capacitors attached to each junction of the circuit (for clarity only one capacitor is shown). Considering power flow in the circuit it is simple to show that the circuit is entirely passive. Summing currents at the node labelled V_0 gives, for example;

$$C_h \partial_t V_0 = G_x(V_2 - V_4) - G_z(V_3 - V_1) \tag{1}$$

With the following change of variables; $C_h \to \mu_0 \Delta_x \Delta_y \Delta_z$, $G_x \to \Delta_y \Delta_z$, $G_z \to \Delta_x \Delta_y$, $V_0 \to H_y(i + 0.5, j, k + 0.5)$ and transforming $V_1 \ldots V_4$ to the four corresponding electric components in the algorithm, the FDTD equation for $\partial_t H_y(i + 0.5, j, k + 0.5)$ is recovered.

The relationships for all the fields in the FDTD algorithm can be derived in this manner from the circuit; the only aspect of the FDTD algorithm not represented in the circuit is the discrete time approximation of the continuous time derivative ∂_t.

The main theorem is:

§ *An FDTD algorithm cannot be unconditionally unstable if it arises from the centred-difference discrete-time approximation to the passive circuit.*

the proof of this intuitive result is given in [7, Ch.5] but is too lengthy to be included here.

It can be seen therefore that, if the FDTD method is to be modified, the modification should be based on a modification of the passive circuit. In this way unconditionally unstable schemes will not arise and there will always be a value of time step which guarantees stability – this point is illustrated by the following example.

3 Application of Equivalent Circuit

As a simple example of a situation where the equivalent circuit provides an invaluable insight into the stability of a modified FDTD algorithm, consider using the deformed Contour method [1] to model the interior of a perfectly conducting cylinder (radius 19 cm) on a two-dimensional uniform mesh (mesh spacing $\Delta = 5$ cm). A portion of this model is shown by figure 3; E_x and E_z fields are indicated by arrows, the H_y components by crosses.

The CP method is employed (as described in [1]) to alter the FDTD algorithm close to the curved surface. When calculating $H_y(0.5, 0.5)$ however the algorithm requires the value of

$E_z(1, 0.5)$ - which itself cannot be calculated from its surrounding H components. In this case the technique 'borrows' the nearest collinear E field - $E_z(1, 1.5)$.

This results in the situation where $H_y(0.5, 0.5)$ is updated from $E_z(1, 1.5)$ but not *vice-versa*. In terms of an equivalent circuit this situation *cannot* be achieved with passive components and must be avoided, instead an extra gyrator is introduced between $H_y(0.5, 0.5)$ and $E_z(1, 1.5)$ as shown in figure 4. The only change to the algorithm is the updating of $E_z(1, 1.5)$ which *is* now a function of $H_y(0.5, 0.5)$:

$$\begin{aligned} \epsilon_0(\Delta + \Delta_1)\Delta\partial_t E_z(1, 1.5) = (\Delta + \Delta_1)H_y(1.5, 1.5) \\ -\Delta H_y(0.5, 1.5) - \Delta_1 H_y(0.5, 0.5) \end{aligned} \tag{2}$$

The CP method involving field borrowing exhibited instability after a few hundred iterations even with greatly reduced values of time step and results were unavailable. The new technique, derived using the equivalent circuit, exhibited no instability even with an unmodified time step of $\Delta/c\sqrt{2}$ and produced the first two TE resonant frequencies of the cylinder within 1% of analytic results.

4 Conclusions

This contribution has shown the existence of an equivalent passive circuit for the FDTD method. Such a passive representation ensures that the algorithm (given an appropriate limit on the time-step) is stable.

The equivalent circuit concept is shown to stabilize the field 'borrowing' procedure widely used in the Contour Path method. The usefulness of the equivalent circuit is not limited however to this problem; it has also been applied to stabilize other variants of the CP method and the SFS method [2]. Further applications of the circuit are under investigation.

Acknowledgements

This work was supported by DRA Malvern and EPSRC UK.

References

[1] T. Jurgens and A. Taflove, "Three dimensional contour modelling of scattering from single and multiple bodies," *IEEE Trans. Antennas and Propagat.*, vol. AP-41, pp. 1703–1708, Dec. 1993.

[2] C. J. Railton, "An algorithm for the treatment of curved metallic laminas in the finite difference time domain method," *IEEE Trans. Microwave Theory Tech.*, vol. MTT-41, p. 1429, Aug. 1993.

[3] G. Smith, *Numerical Solution of Partial Differential Equations.* Clarendon Press, 2 ed., 1978.

[4] A. Taflove and M. Brodwin, "Numerical solution of steady-state electromagnetic scattering problems using the time-dependent Maxwell's equations," *IEEE Trans. Microwave Theory Tech.*, vol. MTT-23, pp. 623–630, Aug. 1975.

[5] C. R. Brewitt-Taylor and P. B. Johns, "On the construction and numerical solution of transmission line and lumped network models of Maxwell's equations," *International Journal for Numerical Methods in Engineering*, vol. 15, pp. 13–30, 1980.

[6] W. K. Gwarek, "Analysis of an arbitrarily-shaped planar circuit – a time-domain approach," *IEEE Trans. Microwave Theory Tech.*, vol. MTT-33, pp. 1067–1072, Oct. 1985.

[7] I. J. Craddock, *Enhanced numerical methods for time domain electromagnetic analysis.* PhD thesis, University of Bristol, 1995.

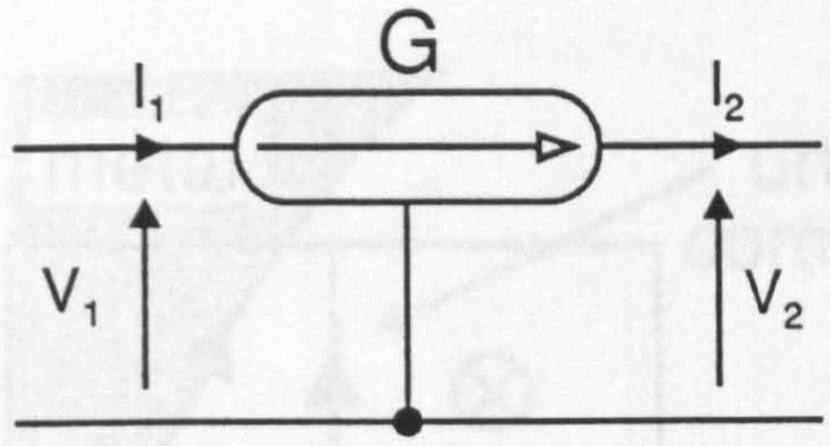

Figure 1: A gyrator

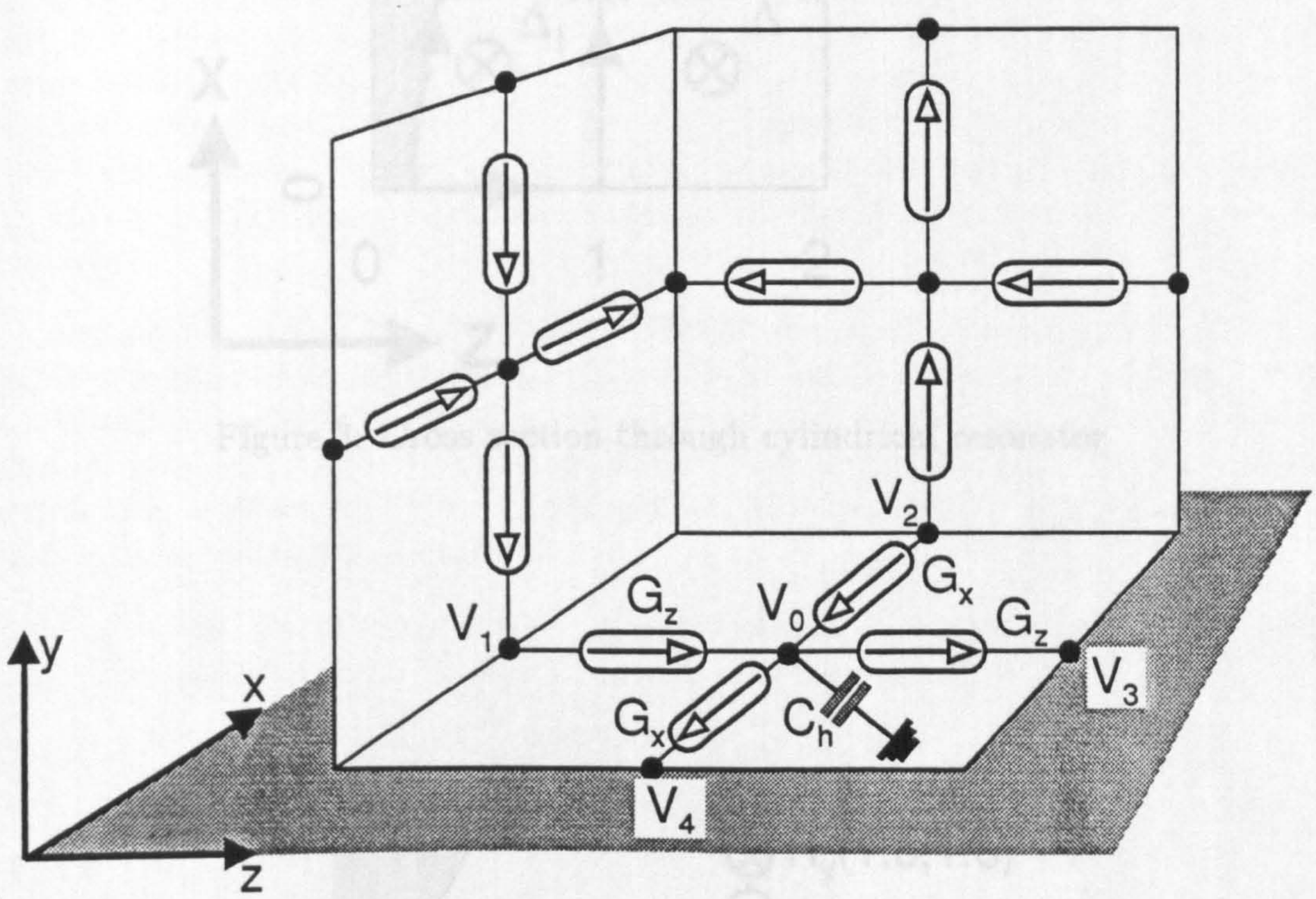

Figure 2: Yee algorithm equivalent circuit

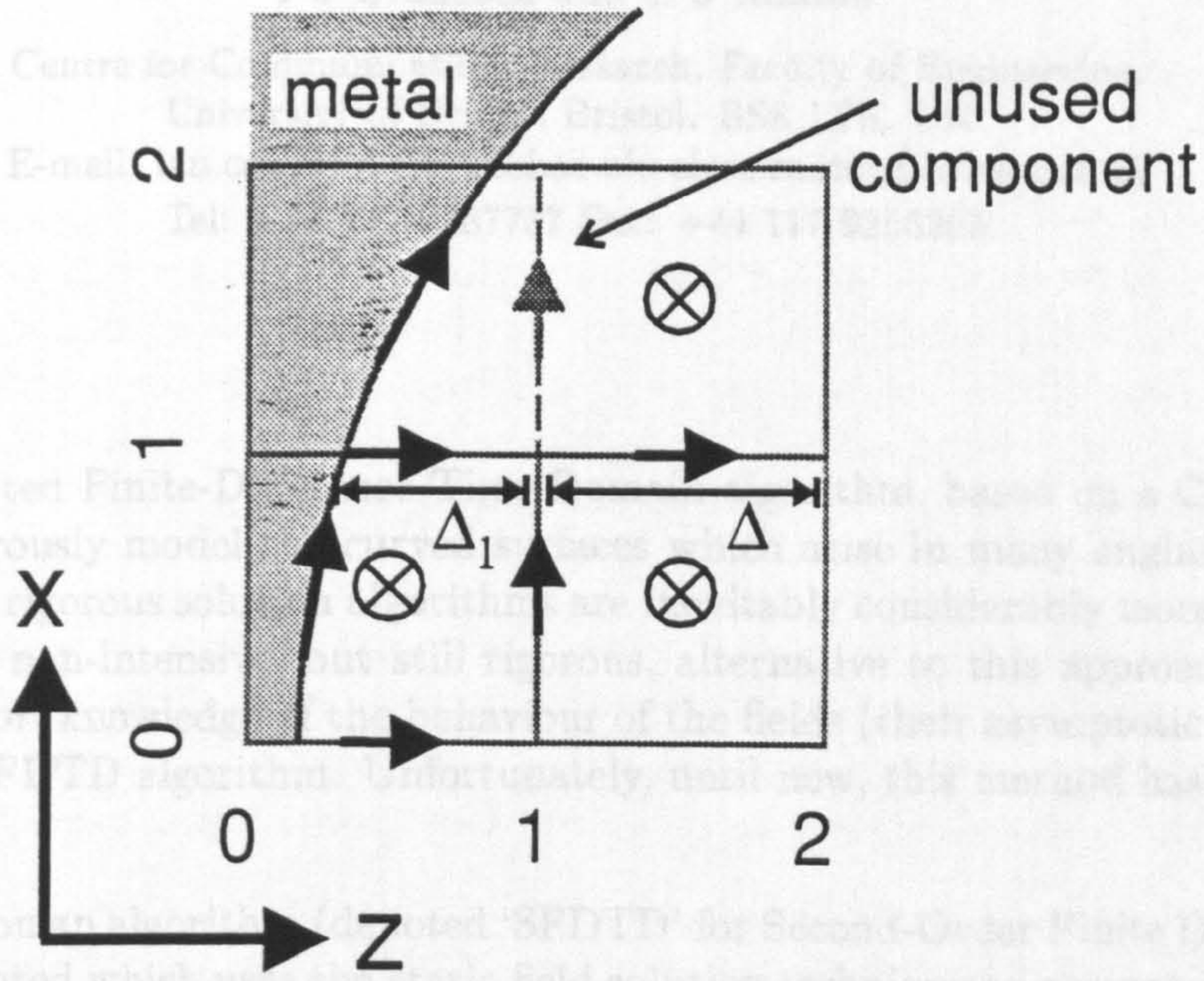

Figure 3: Cross section through cylindrical resonator

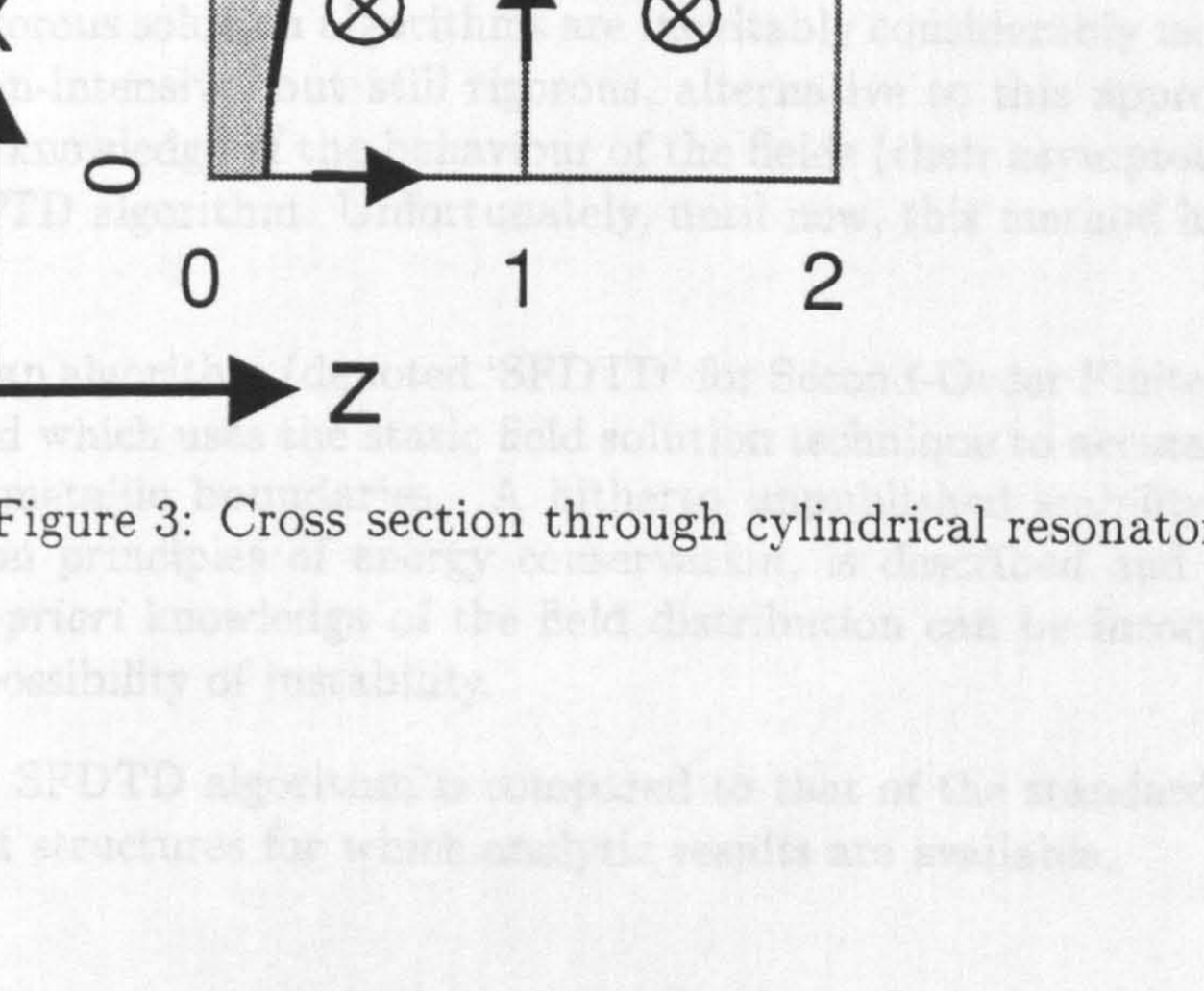

Figure 4: Modified equivalent circuit

Analysis of Curved and Angled Surfaces on a Cartesian Mesh Using a Novel Finite-Difference Time-Domain Algorithm.

I J Craddock and C J Railton

Centre for Communications Research, Faculty of Engineering,
University of Bristol, Bristol. BS8 1TR. UK.
E-mail: ian.craddock@bristol.ac.uk, chris.railton@bristol.ac.uk
Tel: +44 117 9287737 Fax: +44 117 9255265

Abstract

The widely accepted Finite-Difference Time-Domain algorithm, based on a Cartesian mesh, is unable to rigorously model the curved surfaces which arise in many engineering applications, while more rigorous solution algorithms are inevitably considerably more computationally intensive. A non-intensive, but still rigorous, alternative to this approach has been to incorporate *a priori* knowledge of the behaviour of the fields (their asymptotic static field solutions) into the FDTD algorithm. Unfortunately, until now, this method has often resulted in instability.

In this contribution an algorithm (denoted 'SFDTD' for Second-Order Finite Difference Time Domain) is presented which uses the static field solution technique to accurately characterise curved and angled metallic boundaries. A hitherto unpublished stability theory for this algorithm, relying on principles of energy conservation, is described and it is found that for the first time *a priori* knowledge of the field distribution can be incorporated into the algorithm with no possibility of instability.

The accuracy of the SFDTD algorithm is compared to that of the standard FDTD method by means of two test structures for which analytic results are available.

1 Introduction

The Finite-Difference Time-Domain (FDTD) technique is widely accepted as an efficient, reliable and flexible method for the electromagnetic analysis of a wide variety of structures. Perhaps the most fundamental limitation of FDTD is that in its usual form, first suggested by Yee in 1966 [1], the method represents the modelled object as a Cartesian-based mesh of field components. This spatial discretisation prevents the standard FDTD method from accurately characterising the curved structures which arise frequently in engineering applications.

In [2] the authors first presented a finite-difference time-domain algorithm (Second-Order Finite Difference Time Domain or 'SFDTD') which facilitated the treatment of curved metallic structures. The algorithm utilised the static field solution technique, originally described in [3], to rigorously model the curved surfaces. Employing static field solutions when attempting to analyse curved bodies with the well-known Yee algorithm (FDTD) often resulted in instability; SFDTD however appeared not to suffer from this problem.

For clarity we initially review some of the background pertaining to the modelling of curved structures and then describe a modification of the SFDTD correction factor scheme given in [2]. This modification results in it being possible to show, by means of a previously unpublished stability theory, that the stability of the corrected algorithm is assured. Further

validation of the SFDTD algorithm is then given for the case of angled and curved metal structures.

2 Modelling Curved Structures with Finite-Methods

The conventional approach to modelling curved surfaces with FDTD is to employ a finely staircased mesh [4], this approach is unattractive as it requires a large number of FDTD unit cells and a correspondingly small time-step. An alternative approach is to locally deform the integration contours of the FDTD algorithm [5] in the vicinity of the curved surface; this method yields improved accuracy but may require non-physical nearest neighbour 'borrowing' of field components. For planar circuits the locally conforming method of Gwarek [6] may be employed.

There are rigorous approaches to the time-domain characterisation of curved bodies - those recently proposed include finite-volume [7], hybrid finite-volume/finite-difference [8] and vector finite element methods [9]. These techniques yield much improved accuracy at the expense of increased numbers of operations at each time-step and extra memory requirements.

A different approach has been followed at the Centre for Communications Research, University of Bristol, whereby the normal FDTD method is utilised with correction factors, based on the static field solutions, introduced into the standard difference equations in the vicinity of the curved surface. These factors are calculated by assuming the variation of the field close to a metal object to be dominated by its asymptotic static behaviour [10].

This approach can be briefly summarised as follows: A section of the standard Yee mesh, describing the spatial discretisation of the electric and magnetic fields, is shown in figure 1.

If a metallic boundary intersects the surface of integration of a field component as shown, the standard difference equations for the affected component are modified by the inclusion of altered coefficients (or 'correction factors') which are calculated from the field's static behaviour.

If the standard FDTD method is viewed as a moment method with delta test functions and piecewise linear basis functions, the static field solution theory can be interpreted as the local modification of the linear basis functions to a form which more closely resembles the expected spatial behaviour of the fields [10]. This is a standard technique in finite-element analysis where higher accuracy and reduced numbers of basis functions can be achieved in this manner.

Static field solutions have been very successful in permitting the accurate analysis of a number of curved [10] and small-scale features [11]. In addition to its accuracy, the technique requires no increase in computational effort over the standard model, apart from a short initialisation procedure within which the correction factors are calculated.

The drawback to this potentially invaluable technique is that instability may result from the introduction of the correction factors into the FDTD algorithm. The problem of whether or not an arbitrary set of correction factors will result in instability does not appear to be amenable to either an analytic or a practical numerical solution and the problem of how that set should be modified to avoid the instability is even more intractable.

3 A New Finite-Difference Algorithm

In an attempt to solve the instability problem a model based on the electric field vector wave equation was employed, as first described in [2]; in this algorithm the magnetic fields are eliminated. In addition it becomes possible to employ a co-located field discretisation (ie one where all the field components in a given unit cell are placed at the cell's vertices) which leads to a much more elegant correction factor formulation.

Eliminating the magnetic field H from Maxwell's curl equations in a lossless medium gives:

$$\nabla \times (\nabla \times \mathbf{E}) = -c^{-2}\partial_{tt}\mathbf{E} \qquad \text{or} \qquad \nabla^2\mathbf{E} - \nabla(\nabla \cdot \mathbf{E}) = c^{-2}\partial_{tt}\mathbf{E} \tag{1}$$

where $\mathbf{E}$ is the electric field, c is the velocity of propagation and t is time. In *uniform media* ($\nabla \cdot \mathbf{E} = 0$) this simplifies to :

$$\nabla^2\mathbf{E} = c^{-2}\partial_{tt}\mathbf{E} \tag{2}$$

(In the case of metallic boundaries the field divergence is non-zero but, in effect, the correction factor scheme described in the next section re-introduces the electric field divergence term).

Using an electric field discretisation scheme where all field components are co-located and assuming a regular spatial mesh, the second-order partial derivatives may be replaced by centred difference approximations. For example, the update equation for a field component E_y may be written:

$$\begin{aligned} E_y^{n+1}(i,j,k) &= -E_y^{n-1}(i,j,k) + (2 - \frac{6c^2\Delta_t^2}{\Delta^2})E_y^n(i,j,k) \\ &+ \Big[E_y^n(i+1,j,k) + E_y^n(i-1,j,k) + \\ &\quad E_y^n(i,j,k+1) + E_y^n(i,j,k-1) + \\ &\quad E_y^n(i,j+1,k) + E_y^n(i,j-1,k)\Big]\frac{c^2\Delta_t^2}{\Delta^2} \end{aligned} \tag{3}$$

where Δ is the space-step, Δ_t is the time-step, and $^n(i,j,k)$ represents a point in space $(i\Delta, j\Delta, k\Delta)$ at time $t = n\Delta_t$.

Update equations for the other electric field components may be derived similarly, yielding a Second-order Finite Difference Time Domain algorithm (or 'SFDTD' for convenience) as opposed to the standard FDTD algorithm which involves only first-order derivatives. This discretisation of the wave equation is well known, being nothing more than, for example, the extension to three dimensions of the one dimensional algorithm of [12]. Other, similar, algorithms are those of [13] and [14]. The new aspects of this contribution are the modifications, described in section 4, which enable the rigorous treatment of curved surfaces and the stability theory developed in section 5 .

It can be shown that the Courant stability criterion (which relates the maximum time step Δ_t to the minimum space step Δ) is identical to that required for FDTD. The extra amount of memory required by SFDTD to store the past value of each electric field component (E_y^{n-1} in (3)) is balanced by that needed for the storage of the magnetic fields in FDTD. The computational effort associated with SFDTD in terms of the number of numerical operations is slightly lower than that of FDTD.

4 SFDTD Correction Factor Technique

A curved metal surface may be accurately approximated on a small scale by an angled planar surface as shown in figure 2. The behaviour of the electric field close to a metal boundary is well known to converge to the static solution [15] and hence, in this case, may be described by two functions

$$E_n = k_1 \qquad E_t = k_2 n \tag{4}$$

where n and t are co-ordinates normal and tangential, respectively, to the surface.

Taking as an example the first-order spatial derivative,

$$\partial_x E_y = \left[\partial_n E_y \frac{\partial n}{\partial x} + \partial_t E_y \frac{\partial t}{\partial x}\right] \tag{5}$$

since

$$\begin{aligned} n &= x\sin\theta - y\cos\theta \\ t &= -x\cos\theta - y\sin\theta \end{aligned} \tag{6}$$

and

$$E_y = -E_n\cos\theta - E_t\sin\theta \tag{7}$$

we produce an expression within which (4) may be substituted, yielding the following improved expression for the derivative at the metal boundary :

$$\partial_x E_y|_{\text{improved}} = -(\sin^2\theta)k_2 \tag{8}$$

However

$$E_t = -E_{y2}\sin\theta - E_x\cos\theta = k_2 n_0 \tag{9}$$

where n_0 is the normal distance from the position of E_{y2} and E_x to the metal boundary (see figure 2). Thus

$$\partial_x E_y|_{\text{improved}} = \frac{(\sin^2\theta)(E_{y2}\sin\theta + E_x\cos\theta)}{n_0} \tag{10}$$

the approximation used to the second-order derivative is

$$\partial_{xx} E_y(i,j,k) = \frac{\partial_x E_y(i+1/2,j,k) - \partial_x E_y(i-1/2,j,k)}{\Delta} \tag{11}$$

equation (11) represents a modification of the expression (9) in [2], where the denominator used was $\frac{1}{2}(\Delta+\alpha)$ in an attempt to centre the derivatives at the point (i,j,k). In fact doing this makes little difference to the accuracy of the results and prevents the use of the stability theory given in the following section.

Replacing $\partial_x E_y(i+1/2,j,k)$ with (10), and $\partial_x E_y(i-1/2,j,k)$ with the usual centred difference approximation, the required expression for the second-order derivative is

$$\partial_{xx} E_y(i,j,k) = \left(\frac{E_{y1}}{\Delta^2} - \frac{E_x\cos\theta\sin\theta}{\Delta^2\beta}\right) - \frac{E_{y2}}{\Delta^2}\left(1 + \frac{(\sin\theta)^2}{\beta}\right) \tag{12}$$

where β is defined as α/Δ and E_{y1}, E_{y2} and E_x are field components neighbouring the boundary (see figure 2).

Again, (12) differs slightly from that given in [2] for the reasons described above.

This corrected discrete approximation may be utilised instead of the standard difference form in the SFDTD algorithm. If β is unity and $\theta = 270^\circ$ then the original difference form is returned and, unless $\sin\theta$ is 0 or 1, energy will couple between orthogonal field components (as expected).

The approximations which have been made are that the boundary may be approximated over the unit cell by a planar surface (a considerable improvement over its approximation by a staircase) and that the fields will assume their static forms over a distance $\leq \Delta$ from the boundary (which is reasonable if Δ is a small fraction of a wavelength).

5 Stability Theory for the New Algorithm

In [2] it was stated that the SFDTD algorithm with its curved surface correction factors was an inherently more stable algorithm than the corrected FDTD algorithm. At the time of publication, however, the reasons for this were not well understood.

A necessary criterion for the stability of a numerical model is that it is a model of a stable physical process - this is intuitively clear and need not be discussed further except to say that this criterion is not by itself sufficient, as shown by the well known limit on the FDTD time-step Δ_t [16] which, when violated, results in algorithmic instability despite the energy conservation implicit in Maxwell's equations. We now show that the aforementioned criterion is met by the corrected SFDTD algorithm in two spatial dimensions - the extension to three dimensions being trivial.

In finite-difference form the uncorrected 2-D SFDTD algorithm for any given field component can be written:

$$\begin{aligned} E^{n+1}(i,k) = -E^{n-1}(i,k) + (2 - k(1+1+1+1))E^n(i,k) \\ +kE^n(i-1,k) + kE^n(i+1,k) + kE^n(i,k-1) + kE^n(i,k+1) \end{aligned} \tag{13}$$

with the stability factor $k = (\frac{c\Delta_t}{\Delta})^2$ (≤ 0.5 for stability). In equation (13) as elsewhere in this section, some terms have not been collected together in order to help make clear the correspondences between terms in the update equations and features of the physical problem.

In general two curved surface corrections may be required as shown, for example, at node (0,0) in figure 3, with the angles of the two tangents to the curved boundary being θ_1 and θ_2 and the distances from node (0,0) to the boundary being $\alpha_1 = \beta_1\Delta$ and $\alpha_2 = \beta_2\Delta$ in the x and z directions respectively. The update equations for E_x and E_z at the point $(0,0)$ then become:

$$\begin{aligned} E_x^{n+1}(0,0) = -E_x^{n-1}(0,0) + \left(2 - k\left(\frac{\sin^2\theta_1}{\beta_1} + \frac{\sin^2\theta_2}{\beta_2} + 1 + 1\right)\right) E_x^n(0,0) + \\ kE_x^n(1,0) + kE_x^n(0,1) - k\frac{\sin\theta_1\cos\theta_1}{\beta_1}E_z^n(0,0) - k\frac{\sin\theta_2\cos\theta_2}{\beta_2}E_z^n(0,0)) \end{aligned} \tag{14}$$

and

$$\begin{aligned} E_z^{n+1}(0,0) = -E_z^{n-1}(0,0) + \left(2 - k\left(\frac{\cos^2\theta_1}{\beta_1} + \frac{\cos^2\theta_2}{\beta_2} + 1 + 1\right)\right) E_z^n(0,0) + \\ kE_z^n(1,0) + kE_z^n(0,1) - k\frac{\sin\theta_1\cos\theta_1}{\beta_1}E_x^n(0,0) - k\frac{\sin\theta_2\cos\theta_2}{\beta_2}E_x^n(0,0)) \end{aligned} \tag{15}$$

Now consider the passive network shown by figure 4; this circuit consists of two separate 2-D networks, one with nodal voltages represented by $V_x(i,k)$ and the other, $V_z(i,k)$, where the co-ordinates (i,k) specify the voltage at the i^{th} node in the direction x in the network, and the k^{th} node in direction z. The only connections coupling the two networks are the ideal transformers T_1 and T_2 at the node $(0,0)$. All capacitors are assumed to be identical, with value C, as are all the inductors, L, with the exception of the components L_1 and L_2.

At, for example, the node $(1,1)$ (not connected to the transformer) simple analysis shows that:

$$\partial_{tt}V(1,1) = \left(\frac{V(2,1)-V(1,1)}{CL} + \frac{V(1,2)-V(1,1)}{CL} + \frac{V(0,1)-V(1,1)}{CL} + \frac{V(1,0)-V(1,1)}{CL}\right) \tag{16}$$

Replacing the *temporal* derivative of V with the appropriate centred difference expression yields:

$$V^{n+1}(1,1) = -V^{n-1} + \left(2 - \frac{\Delta_t^2}{C}\left(\frac{1}{L}+\frac{1}{L}+\frac{1}{L}+\frac{1}{L}\right)\right)V^n(1,1) \tag{17}$$
$$+\frac{\Delta_t^2}{CL}\left(V^n(2,1)+V^n(1,2)+V^n(0,1)+V^n(1,0)\right)$$

Thus, the nodal equations in the region *not* connected to the transformer are identical in form to the SFDTD update equations (13) in free space with the following substitutions:

$$\begin{aligned} C &= \epsilon\Delta^2 \\ L &= \mu \end{aligned} \tag{18}$$

It should be noted that the components in the network are analogs of the assumed spatial dependence of the fields in the SFDTD algorithm (ie: piecewise linear) and that, in the region not connected to the transformer, this two dimensional lumped equivalent circuit is the same as the planar FDTD equivalent circuit presented in [6].

The analysis of the nodal voltages at the node $(0,0)$, where two of the branch connections are to transformers rather than adjacent nodes, is more involved. Firstly we assume the transformers are ideal and have winding ratios $1:N_1$ and $1:N_2$ respectively. Thus for T_1:

$$\begin{aligned} V_{z1} &= -\frac{V_{x1}}{N_1} \\ I_{z1} &= N_1 I_{x1} \end{aligned} \tag{19}$$

since the transformer is ideal. Summing voltages around the loops containing the windings gives:

$$V_x(0,0) - V_{x1} = L_1\partial_t I_{x1} \tag{20}$$
$$V_z(0,0) - V_{z1} = L_1\partial_t I_{z1}$$

solving for the nodal voltages and current I_{x1} yields:

$$\partial_t I_{x1} = \frac{V_x(0,0) + N_1 V_z(0,0)}{L_1(1+N_1^2)} \tag{21}$$

thus

$$\partial_t I_{z1} = -N_1\frac{V_x(0,0) + N_1 V_z(0,0)}{L_1(1+N_1^2)} \tag{22}$$

If we now let $N_1 = \cot\theta_1$

$$\partial_t I_{x1} = \frac{\sin^2\theta_1 V_x(0,0) - \sin\theta_1\cos\theta_1 V_z(0,0)}{L_1} \tag{23}$$

$$\partial_t I_{z1} = \frac{-\cos^2\theta_1 V_z(0,0) + \sin\theta_1\cos\theta_1 V_x(0,0)}{L_1}$$

Identical expressions (but with θ_2 and L_2) can be produced for the other transformer. These currents can be used to derive:

$$V_x^{n+1}(0,0) = -V_x^{n-1}(0,0) + \left(2 - \frac{\Delta_t^2}{C}\left(\frac{\sin^2\theta_1}{L_1} + \frac{\sin^2\theta_2}{L_2} + \frac{1}{L} + \frac{1}{L}\right)\right) V_x^n(0,0) + \tag{24}$$

$$\frac{\Delta_t^2}{CL} V_x(1,0) + \frac{\Delta_t^2}{CL} V_x(0,1) - \frac{\Delta_t^2 \sin\theta_1\cos\theta_1}{CL_1} V_z^n(0,0) - \frac{\Delta_t^2 \sin\theta_2\cos\theta_2}{CL_2} V_z^n(0,0)$$

and it is now clear that substitution of

$$L_1 = \mu\beta_1 \tag{25}$$
$$L_2 = \mu\beta_2$$

yields the SFDTD update-equation (14) with the curved surface corrections.

It has now been shown that the SFDTD model both with and without the curved surface correction factors is exactly equivalent to a representation of a passive network. Energy conservation is guaranteed in such a network, and so therefore is stability. It is if course possible to have a stable *active* network but in such a case stability can only be assured by examination of all possible feedback paths within the network, this corresponds to the impractical task of evaluating all the eigenvalues of the difference algorithm.

Here it should be noted that if the denominator of (11) is that given by equation (9) in [2] it is not possible to produce a passive circuit equivalent to the corrected algorithm. This implies that the slightly different algorithm given in [2] may exhibit instability, and for a few structures this has proved to be the case.

6 Validation of the New Algorithm

6.1 Test case 1 : Cylindrical resonator

A metal-walled closed cylindrical resonator identical to that described in [10], was modelled using the combination of SFDTD and the correction method described above and a *fixed* uniform mesh size of 5cm. The simple geometry allows analytic cavity resonance techniques to predict the resonant frequencies with high accuracy for comparison.

Figure 5 shows the variation in the cylinder's resonant frequencies as a function of radius. The solid line represents the (perfect) analytic solution and the dashed line the results produced by the new algorithm, SFDTD. The marker points indicate the predictions of the standard, staircased, FDTD method (employing the same mesh size). Comparison of these results with those given in [2] using the slightly different, and potentially unstable, scheme shows that the modification to the correction factors introduced in section 4 of this contribution has had little effect on the results. Indeed, particularly for the model with radius 16cm, some improvement in accuracy can be noted.

Overall, given the coarseness of the mesh with respect to both frequency and surface curvature, the SFDTD results adhere well to the theoretical curves and are, as expected, considerably more accurate than the staircased FDTD technique. The TM_{010} mode in particular is excellently characterised, virtually independently of cylinder radius. The results for the TM_{110} mode are good for radii of $>$ 18cm but become less accurate as the radius decreases (this is probably due to both a decrease in the number of field components available to describe the cylinder and to the increase in frequency of the mode). The most difficult mode to model is clearly the TE_{111} mode, the FDTD results for this are notably poor and while the SFDTD algorithm performs more consistently, the results may indicate potential for improvement in the technique.

6.2 Test case 2 : Rotated rectangular box

A metal walled rectangular box with square cross-section was analysed, again with a fixed mesh size of 5 cm and a height of 15cm, however the box was rotated through an angle ϕ with respect to the mesh. This resulted in the sides of the box not being aligned with the nodal-planes of the difference algorithm. For convenience, values of ϕ producing integer gradients were chosen and the box side lengths were selected for each ϕ such that the surfaces of the box passed through the corners of the unit cells - as illustrated for $\phi = \arctan\frac{1}{4} = 14.0°$ by figure 6.

The FDTD algorithm approximates the angled surfaces with a staircase and the SFDTD algorithm with the correction factors described above.

Table 1 shows the resonant frequencies for the box with angle $\phi = 14.0°$ (it should be noted that due to the square cross-section of the structure each resonance may represent more than one mode). A summary of the results for four angles ($\arctan\frac{1}{5}$, $\arctan\frac{1}{4}$, $\arctan\frac{1}{3}$ and $\arctan\frac{1}{2}$) is given by table 2. Once again the SFDTD results (with curved surface corrections) agree well with the analytic results, in the majority of cases the resonant frequencies are correct to within one percent. The FDTD algorithm, as might be expected, fares less well - although some modes are well characterised, most exhibit significant error.

Mode	Theory	FDTD	SFDTD	FDTD Error	SFDTD Error
101	633 MHz	620 MHz	622 MHz	2.1%	1.7%
012	869 MHz	648 MHz	870 MHz	2.4%	0.1%
011	549 MHz	575 MHz	545 MHz	4.7%	0.7%

Table 1: Resonant frequencies for rotated rectangular box

The mean error across all modes and all ϕ for FDTD was 3.8 % and 1.0 % for SFDTD, thus SFDTD's curved surface corrections reduce the modelling error in this case by around a factor of 4; this being a similar figure to that achieved when modelling the cylindrical cavity described in the previous section.

As expected, neither the cylindrical nor the rotated-box geometries exhibited any form of numerical instability.

Angle, ϕ	Mode	FDTD Error	SFDTD Error
11.3°	101	1.6%	0.6%
	012	0.1%	0.6%
	011	6.3%	0.9%
14.0°	101	2.1%	1.7%
	012	2.4%	0.1%
	011	4.7%	0.7%
18.4°	101	0.3%	1.8%
	012	0.6%	0.8%
	011	11.3%	0.5%
26.6°	101	3.7%	2.1%
	012	4.2%	1.1%
	011	8.2%	1.0%

Table 2: Resonant frequencies for a number of rotated rectangular boxes

7 Summary and Conclusions

This contribution has shown how an alternative finite-difference time-domain algorithm can be derived. This algorithm, SFDTD, can be simply modified to rigorously model both curved and angled metal surfaces. The algorithm's stability is assured as the behaviour of the field components in the algorithm is an exact analog of the voltages in a passive electrical network.

The SFDTD algorithm is, in the authors' opinions, far better suited to the analysis of curved and angled boundaries than the FDTD method. This fact arises because the co-location of the field components enables a simple resolution into the normal and tangential components in terms of which the boundary conditions are specified.

Future development of this algorithm is expected to include its application to problems containing dielectric interfaces and sharp metallic boundaries (for example microstrip). For each of these cases a specific correction must be introduced into the algorithm by means of the appropriate static field solution, in order to compensate for the loss of the field divergence term, just as has been done here for smooth conducting boundaries. If this can be achieved SFDTD may prove in the future a superior alternative to the established FDTD algorithm.

8 Acknowledgements

The authors would like to thank Prof. J. P. McGeehan for provision of facilities at the Centre for Communications Research, both EPSRC and DRA Malvern for financial support and the present and past members of the Centre for Communications Research for their assistance in developing the FDTD program.

The authors are grateful to the reviewers for their extremely detailed and helpful comments on this contribution.

References

[1] K. S. Yee, "Numerical solution of initial boundary value problems involving Maxwell's equations in isotropic media," *IEEE Trans. Antennas and Propagat.*, vol. AP-14, no. 3, pp. 302-307, May 1966.

[2] I. J. Craddock and C. J. Railton, "A novel finite-difference algorithm incorporating correction coefficients for curved structures," *24th European Microwave Conf. Proc.*, Cannes, France, 1994, pp. 1536-1540.

[3] D. B. Shorthouse and C. J. Railton, "The incorporation of static field solutions into the finite difference time domain algorithm," *IEEE Trans. Microwave Theory Tech.*, vol. MTT-40, no. 5, pp. 986-994, May 1992.

[4] R. Holland, "Pitfalls of staircase meshing," *IEEE Trans. EMC*, vol. EMC-35, no. 4, pp. 434-439, Nov. 1993.

[5] T. Jurgens and A. Taflove, "Three dimensional contour FDTD modelling of scattering from single and multiple bodies," *IEEE Trans. Antennas and Propagat.*, vol. AP-41, no. 12, pp. 1703-1708, Dec. 1993.

[6] W. K. Gwarek, "Analysis of arbitrarily shaped two dimensional microwave circuits by finite difference time domain method," *IEEE Trans. Microwave Theory and Tech.*, vol. MTT-36, no. 4, pp. 738-744, Apr. 1988.

[7] N. K. Madsen and R. W. Ziolkowski, "A three dimensional modified finite volume technique for Maxwell's equations," *Electromagnetics*, Vol. 10, No. 1-2, pp. 147-161, 1990.

[8] K. S. Yee and J. S. Chen, "Conformal hybrid finite difference time domain and finite volume time domain," *IEEE Trans. Antennas and Propagat.*, vol. AP-42, no. 10, pp. 1450-1454, Oct. 1994.

[9] C. H. Thng and R. C. Booton, "Edge element time domain method for solving Maxwell's equations," *1994 IEEE MTT-S Int. Symp. Dig.*, pp. 693-696.

[10] C. J. Railton, "Use of static field solutions in the FDTD method for the efficient treatment of curved metal structures," *Electron. Lett.*, vol. 29, no. 16, pp. 1466-1467, Aug. 5, 1993.

[11] C. J. Railton, "The simple rigorous and effective treatment of thin wires and slots in the FDTD method," *24th European Microwave Conf. Proc.*, Cannes, France, 1994, pp. 1541-1546.

[12] W. F. Ames, *Numerical methods for partial differential equations.* Thomas Nelson and Sons, 1969. p. 193.

[13] P. H. Aoyagi, J. F. Lee and R. Mittra, "A hybrid Yee algorithm/scalar wave equation approach," *IEEE Trans. Microwave Theory and Tech.*, vol. MTT-41, no. 9, pp. 1593-1600, Sept. 1993.

[14] D. V. Krupezevic, V. J. Brancovic and F. Arndt, "The wave equation FDTD method for the efficient eigenvalue analysis and S-matrix computation of waveguide structures," *IEEE Trans. Microwave Theory and Tech.*, vol. MTT-41, no. 12, pp. 2109-2114, Dec. 1993.

[15] J. van Bladel, *Electromagnetic Fields.* Hemisphere publishing corporation, 1976.

[16] A. Taflove and M. E. Brodwin, "Numerical solution of steady state electromagnetic problems using the time dependent Maxwell's equations," *IEEE Trans. Microwave Theory Tech.*, vol. MTT-23, no. 8, pp. 623-630, Aug. 1975.

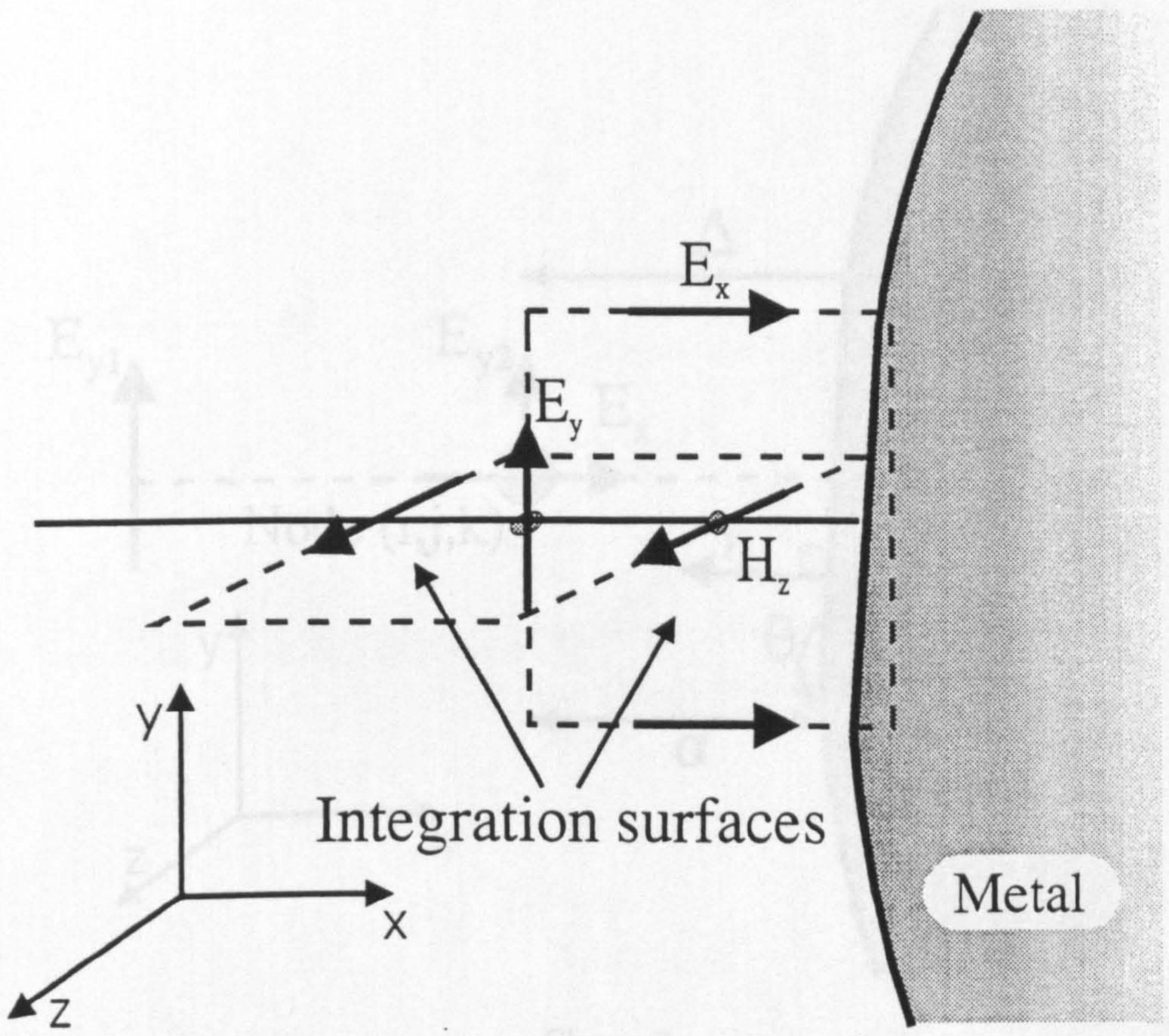

Figure 1:

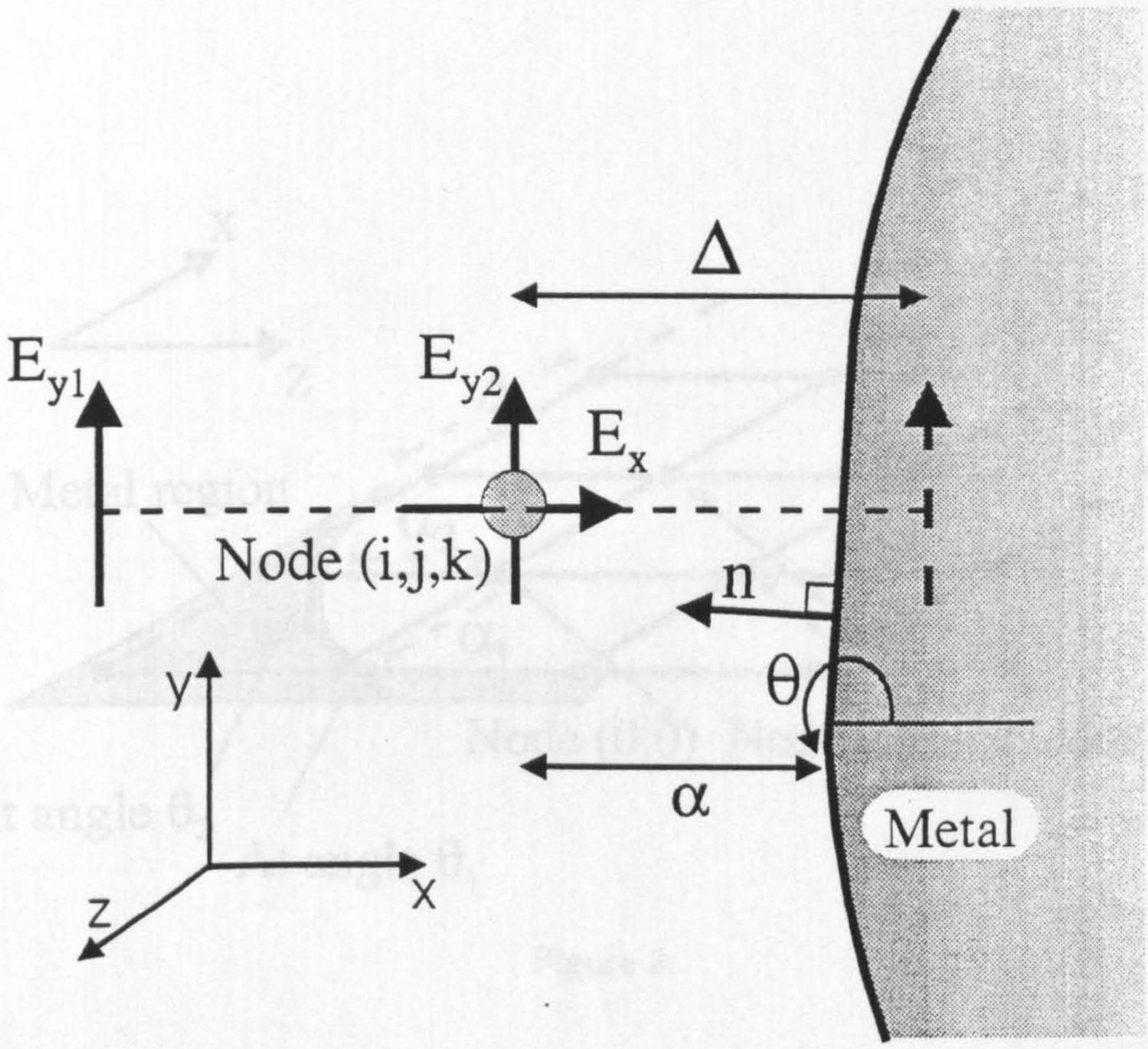

Figure 2:

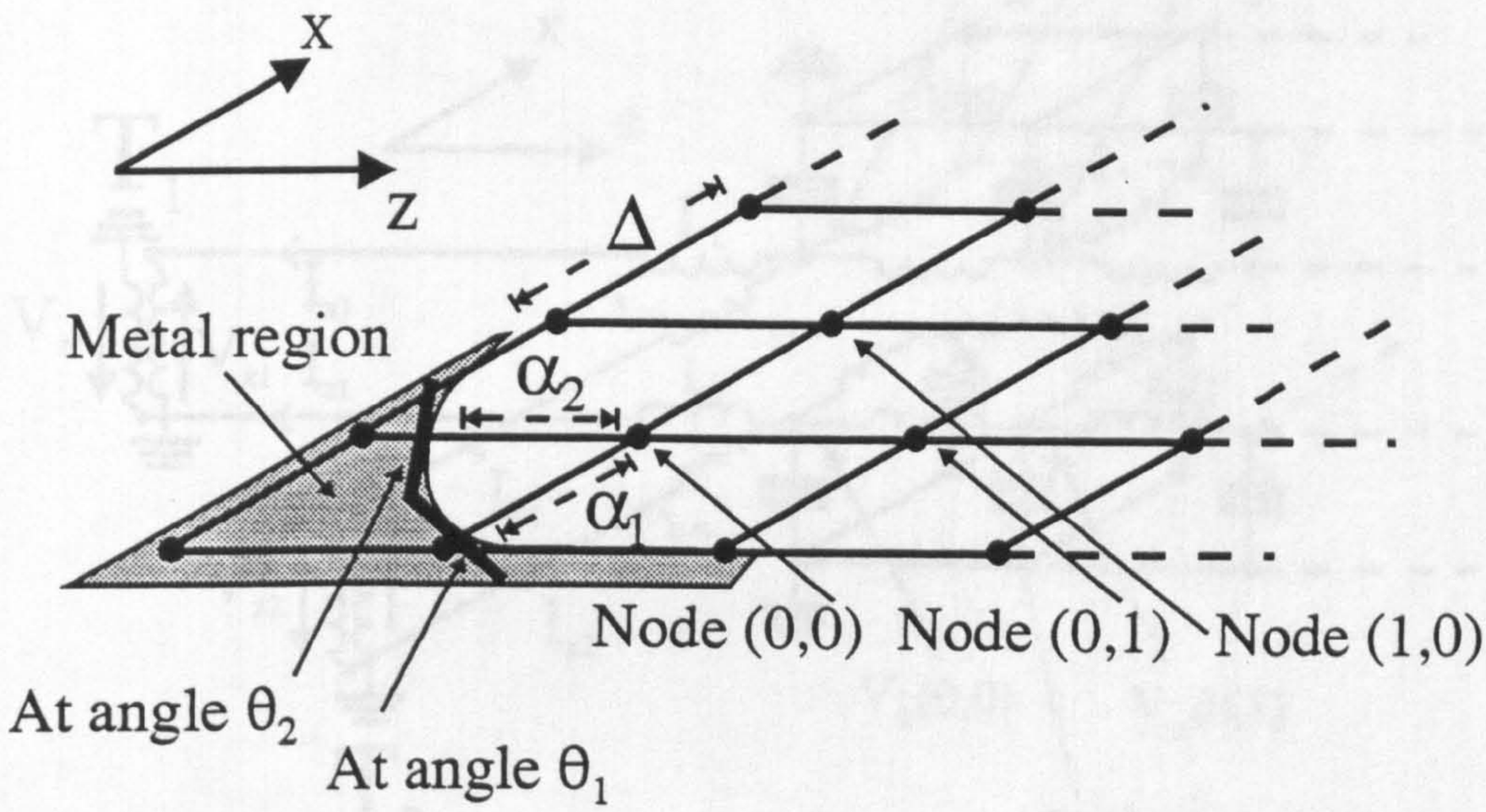
x
z
Δ
Metal region
α_2
α_1
Node (0,0)
Node (0,1)
Node (1,0)
At angle θ_2
At angle θ_1

Figure 3:

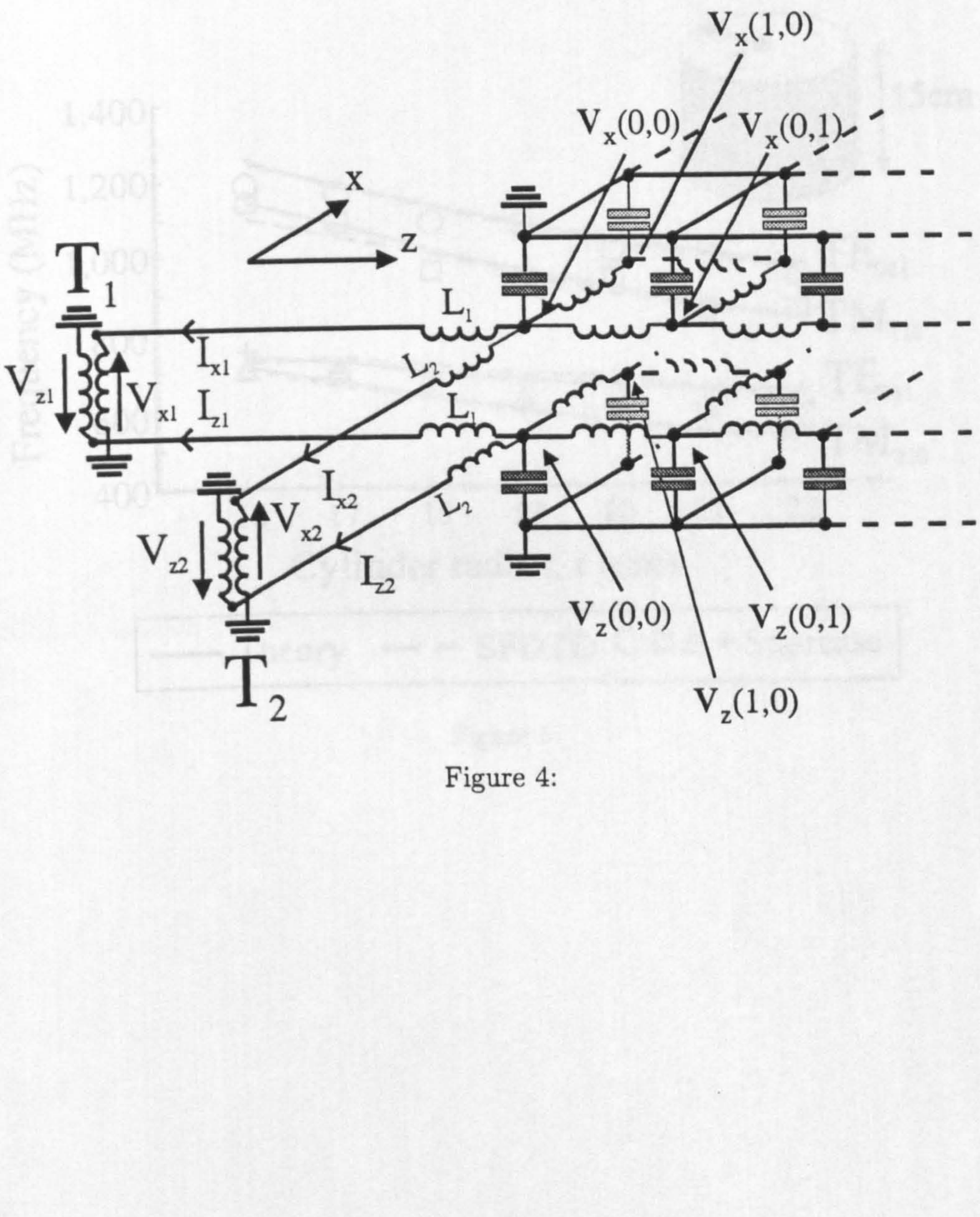
V_x(1,0)
V_x(0,0)
V_x(0,1)
x
z
T_1
L_1
I_x1
L_2
V_z1
V_x1
I_z1
L_1
I_x2
L_2
V_x2
V_z2
L_z2
V_z(0,0)
V_z(0,1)
V_z(1,0)
T_2

Figure 4:

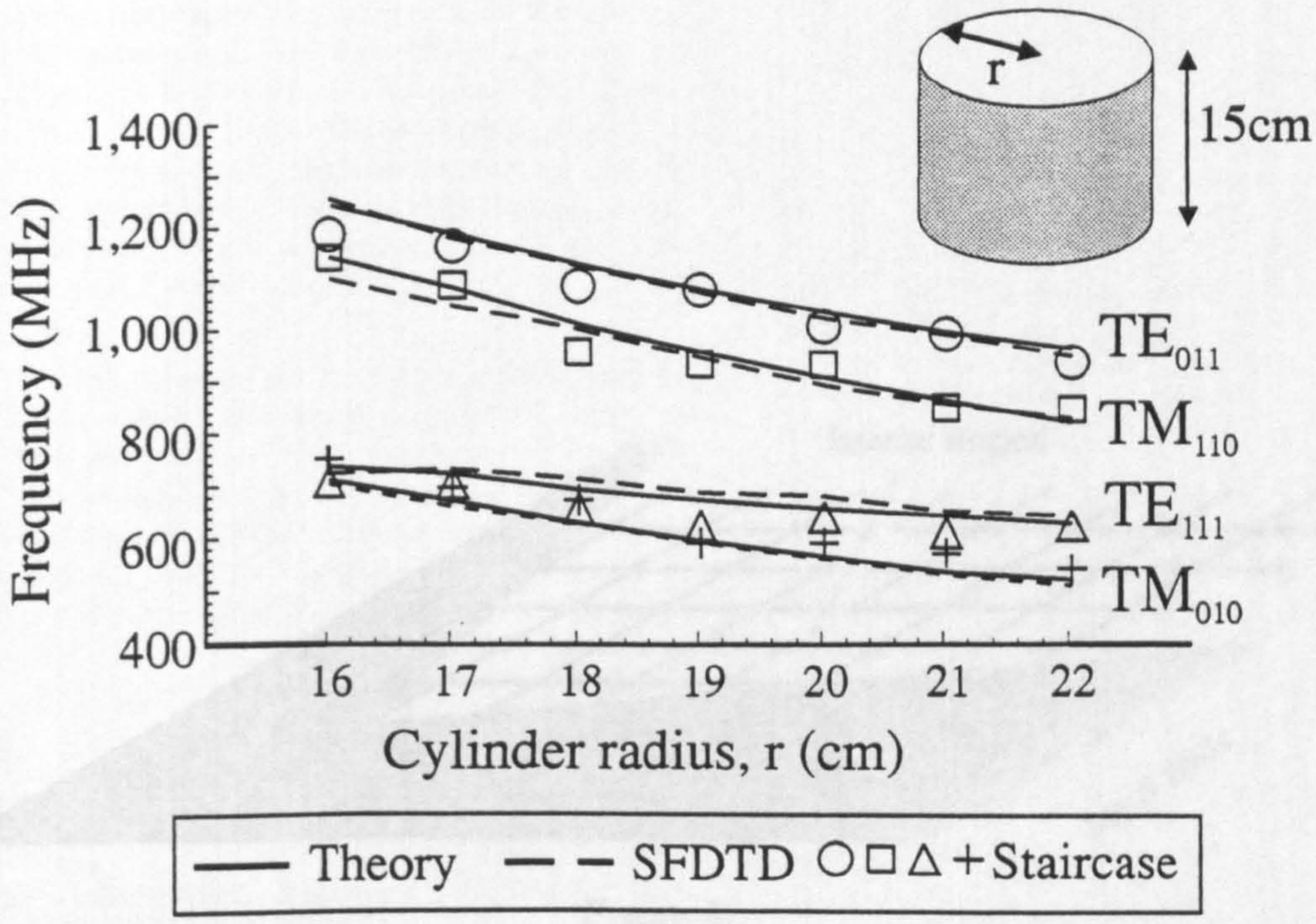
r
15cm
1,400
1,200
1,000
800
600
400
Frequency (MHz)
16
17
18
19
20
21
22
Cylinder radius, r (cm)
TE011
TM110
TE111
TM010
Theory
SFDTD
Staircase

Figure 5:

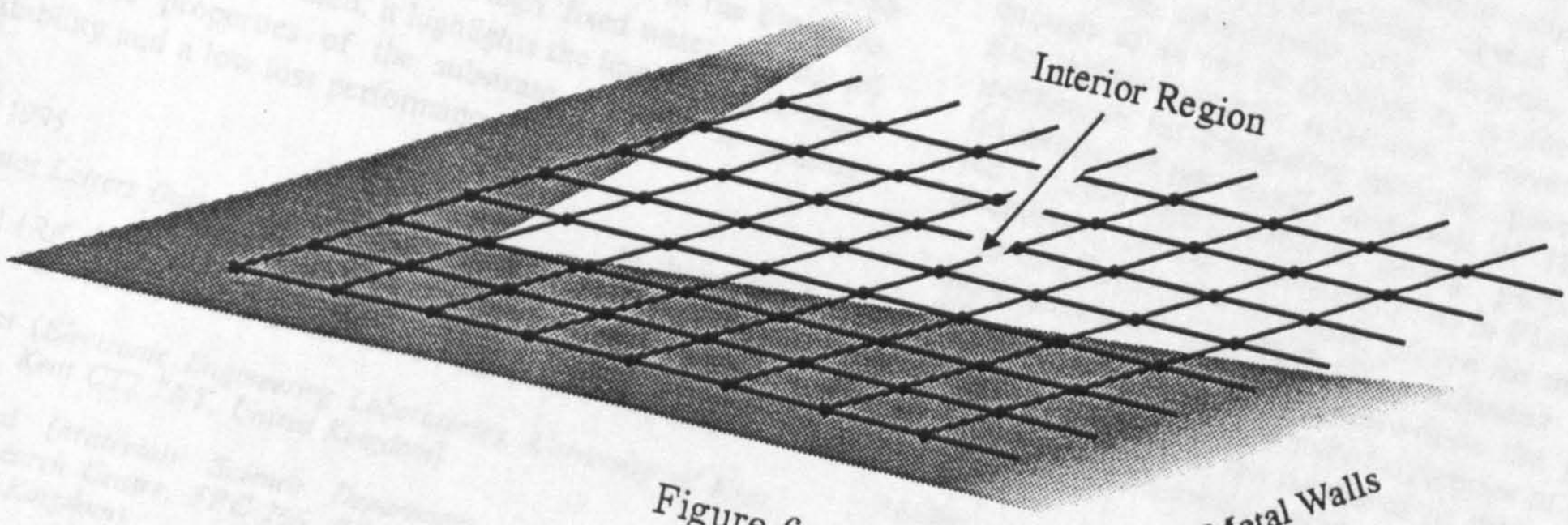

Figure 6:

two-layer FSS excites a passband of width 11.5%, which peaks at 355GHz to give an edge of band separation (where the loss in both bands is less than 0.5dB) of 1.07:1. The design of the four-layer semi-air spaced FSS permits the use of the interference effects between the two dichroic wafers to increase the roll-off rate to 1.05:1 (Fig. 3). In addition, the partially transmitting lobe centred at 450GHz is suppressed from –6dB to below –16dB, broadening the reflection bandwidth to 31%. Simultaneously, the passband width is increased to 19% by the excitation of a secondary peak at 315GHz. Figs. 2 and 3 show that the shape of the frequency response curves is predicted accurately. However, the measured loss, which for the four-layer FSS is less than 1dB in the range 300 – 355GHz but increases to 1.5dB at the specified band edge (362GHz), is somewhat higher than expected. The value of tanδ that was used in the initial design was found to be too low, and better agreement with measurements was obtained using a value of 157×10^{-4}, as indicated by the open circles in Figs. 2 and 3. This observation is consistent with comparisons made with measured results in the TE15°, TE45° and TM15° orientations.

In the design of rapid roll-off multilayer FSS, the passband is excited close to the edge of or even within the inherent reflection band of individual layers. However, the computer model predicts that there is no mismatch loss at the transmission band centre and very little loss at the band edge. The Fabry-Pérot concept points to the origin of this frequency dependent excess loss. The reflectivity of the individual arrays is high in this passband region, so the path length through the substrate which results from the multiple reflections between the screens is very large. The absorption component of the FSS insertion loss is therefore critically dependent on the substrate material properties.

Conclusions: The tanδ value for the fused silica wafers that were used to support a four-layer rapid roll-off submillimetre-wave FSS was found to be higher than previously reported in the literature. Although this may be attributed to a high 'fixed water' content [6] in the samples that were used, it highlights the importance of characterising the properties of the substrate material to achieve repeatability and a low loss performance.

15 August 1995

Electronics Letters Online No: 19951197

R. Cahill (*RF Systems and Technology Group, Matra Marconi Space, FPC 320, PO Box 16, Filton, Bristol BS12 7YB, United Kingdom*)

E.A. Parker (*Electronic Engineering Laboratories, University of Kent, Canterbury, Kent CT2 7NT, United Kingdom*)

I.M. Sturland (*Materials Science Department, British Aerospace Sowerby Research Centre, FPC 266, PO Box 5, Filton, Bristol BS12 7QW, United Kingdom*)

References

1 TR0109 'Limbsounder pre-phase. A study report'. Prepared by MMS (UK) for ESTEC, 10611/93/NL/SF, 1995

2 CAHILL, R., and PARKER, E.A.: 'Design of multilayer frequency selective surfaces for diplexing two closely spaced channels', *Microw. Opt. Technol. Lett.*, 1995, 8, (6), pp. 293–296

3 PARKER, E.A., ANTONOPOULOS, C., and DE C. LIMA, A.C.: 'Multiple layer FSS design and diagnostics using the Fabry Perot concept'. Proc. 4th Int. Conf. Electromagnetics in Aerospace Applications, Turin, Italy, September 1995, to be published

4 CAHILL, R., HALL, W.J., MARTIN, R.J., PARKER, E.A., and ANTONOPOULOS, C.: 'Development of FSS beamsplitting devices for millimeter and submillimeter wave ratiometers'. Proc. 4th Int. Conf. Electromagnetics in Aerospace Applications, Turin, Italy, September 1995, to be published

5 ASFAR, M.N., and BUTTON, K.J.: 'Millimeter wave dielectric measurement of materials', *Proc. IEEE*, 1985, 73, (1), pp. 131–153

6 PARSHIN, V.V.: 'Dielectric materials for gyrotron output windows', *Int. J. Infrared Millim. Waves*, 1994, 15, (2), pp. 339–348

Analysis of general 3-D PEC structures using improved CPFDTD algorithm

C.J. Railton and I.J. Craddock

Indexing terms: Finite-difference time domain method

The contour path finite difference time domain (CPFDTD) method, employing locally distorted integration contours, has been shown to give accurate results for curved three-dimensional metal structures. The numerical stability of this scheme is not, however, guaranteed and significant skill is required to generate an appropriate grid. The authors present a modification to the three-dimensional CPFDTD method which ensures stability and which permits simple generation of the locally distorted grid. The accuracy of the scheme is demonstrated through the calculation of the resonant frequencies of circular cylindrical and spherical resonators.

Introduction: The contour path finite difference time domain (CPFDTD) method has been shown to provide an accurate and efficient method for analysing smooth curved metal structures [1, 2]. A major advantage of this approach when compared with other conformal techniques is that the simplicity and efficiency of the Cartesian mesh is retained throughout the majority of the problem space and only those nodes which are adjacent to the curved surface need he given special attention. Despite the fact that this type of algorithm appears to allow the efficient analysis of very complex structures, comparatively little use of the method has been reported. Some researchers have called into question the stability of the original CPFDTD scheme since it employs a non-causal and nonreciprocal 'nearest neighbour' approximation [3]. Despite the fact that stability cannot be guaranteed, it appears that, with appropriate grid selection, the instability is weak enough so as not to preclude its use for open-domain problems. For lossless resonant structures, however, for which there is no mechanism for dissipating spuriously generated energy, meaningful results are not usually obtainable [4]. These difficulties prevent the scheme being used in general purpose codes which are intended to be used by nonspecialists in FDTD.

In this Letter, the technique, proven for the stabilisation of the two-dimensional CPFDTD [5], is extended and applied to the three-dimensional case. To demonstrate the performance of the scheme, the calculated resonant frequencies of circular cylindrical and spherical cavities are compared to those obtained using the staircased FDTD method and to analytical results.

Modification: All the instability mechanisms which were described in [5] and which resulted from nearest-neighbour borrowing or from the overlapping of integration surfaces also exist in the three-dimensional case and can be remedied using similar techniques. The modification to the algorithm used in [5] can be applied independently in each of the three orthogonal planes but, in addition, there are a number of complications peculiar to the three-dimensional formulation which need to be addressed. First, an edge which is not used in one plane may be required in the other. For example, the edge associated with an E_x node may be needed to calculate an adjacent H_y node but not used for the adjacent H_z node. This presents no problem in principle but more care is required when setting up the mesh.

A second situation, unique to the three-dimensional case, can occur when an H node is outside the metal but one or more of the surrounding E nodes are unavailable. Whereas in the two-dimensional case this situation is resolved by 'borrowing' the value of the unavailable E node from the adjacent collinear cell, in the three-dimensional case the nearest available collinear E field node may be a great distance away. This situation occurs when the metal object makes a glancing angle with the grid. To avoid the undesirable situation of long distance borrowing, we set the values of E field nodes to zero, which would require borrowing from a distance greater than one unit cell. With these provisions, it is possible, as in the two-dimensional case, to construct a mesh whose update equations are formally identical to those of a passive electrical circuit which is, therefore, guaranteed to be energy conserving. In the examples which follow, no instability was seen when using the modified scheme, even though the time step was not

reduced below that used in standard FDTD. Without the modification, however, they all exhibited severe instability even with very small time steps.

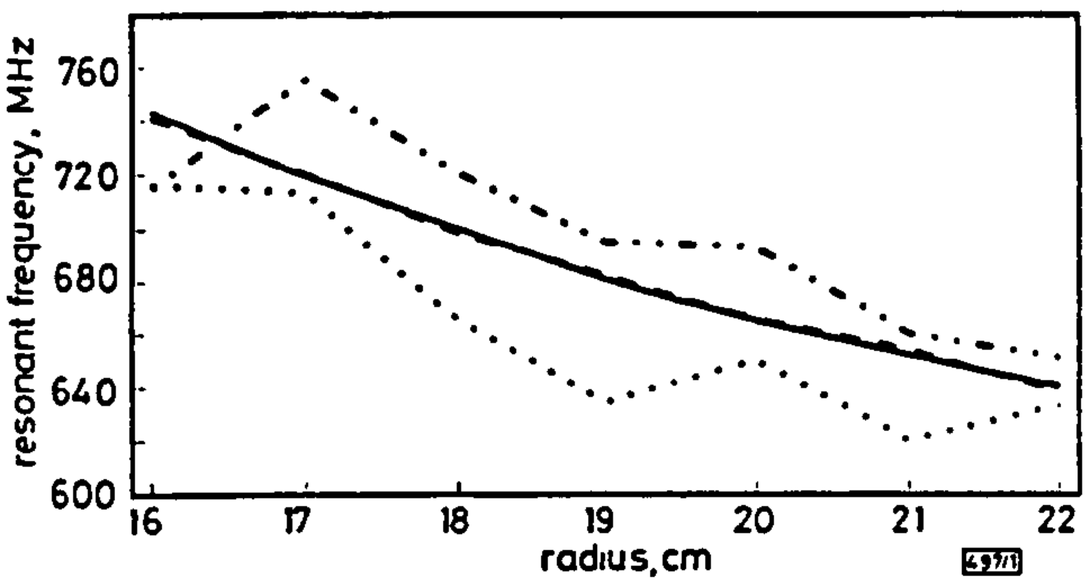

Fig. 1 *Calculated resonant frequency of first TE mode (TE111) of circular cylindrical cavity of height 30cm*

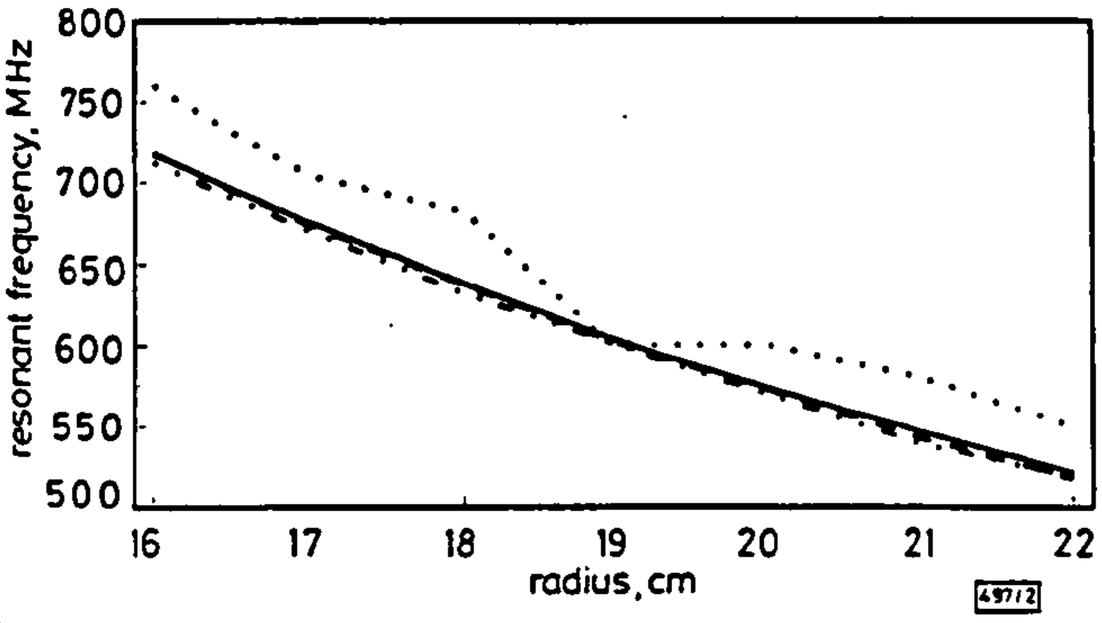

Fig. 2 *Calculated resonant frequency of first TM mode (TM010) of circular cylindrical cavity of height 30cm*

Application to circular cylindrical resonator: To verify the accuracy of the scheme, the resonant frequencies of a range of circular cylindrical cavities, having heights of 30cm and radii varying between 16 and 22cm, were calculated. The results for the first TE mode are shown in Fig. 1 and the results for the first TM mode are shown in Fig. 2, where they are compared to results obtained using the staircase approximation, the SFDTD method described in [6] and to analytical results. It can be seen that in both cases there is excellent agreement between the stabilised CPFDTD results and the analytical results. The results are clearly superior to those obtained using the staircase approximation and are at least as accurate as those obtained using the SFDTD method.

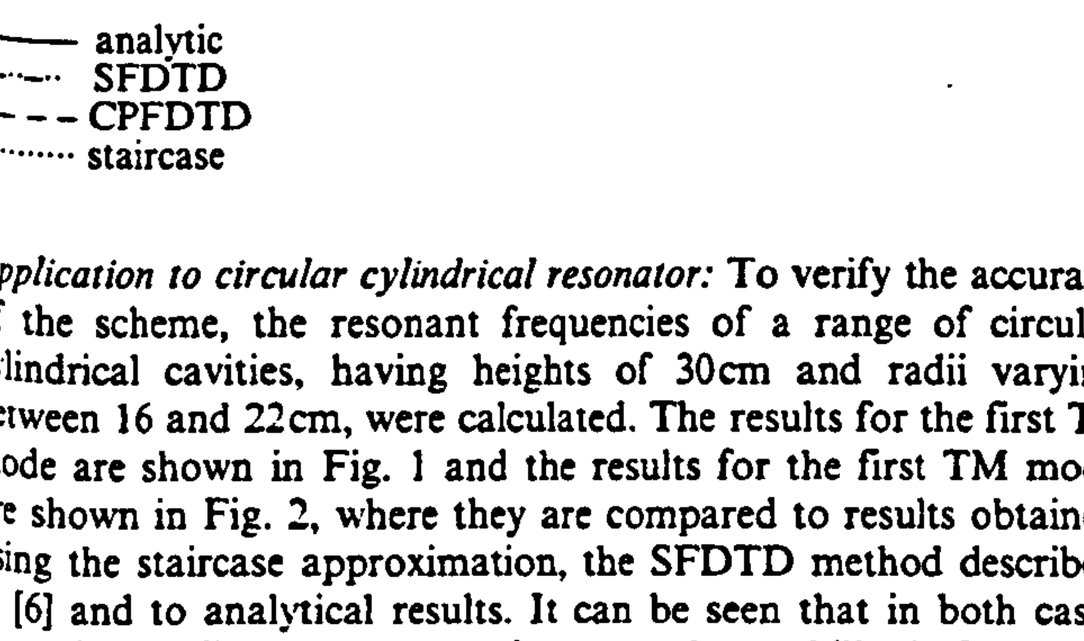

Fig. 3 *Calculated resonant frequencies of spherical cavity of radius 20cm against number of unit cells used*

Application to spherical cavity resonator: As a further example, the spherical cavity with a radius of 20cm was investigated. The sphere was placed in a cubic computational domain with sides of 50cm and unit cell sizes ranging from 1.25 to 10cm. Unlike the cylinder, this is a fully three-dimensional structure. The calculated resonant frequencies for the first four nondegenerate modes are shown in Fig. 3, where they are plotted against the number of unit cells used in each direction and compared with results obtained using the staircase approximation. It can be seen that accurate results are obtained for the modified CPFDTD method even with very coarse meshes, especially for the first two modes. As before, the results are clearly superior to those obtained using the staircase approximation.

Conclusion: It has been shown that the modification previously demonstrated for the two-dimensional CPFDTD scheme, which ensures that the spatial discretisation is energy conserving, can be successfully extended and applied to the general three-dimensional case. The accuracy of the method has been demonstrated for the case of circular cylindrical and spherical cavities. At no time did the algorithm exhibit numerical instability, even though the time step used was no less than that used for standard FDTD and the algorithm was run for many thousands of iterations. Without the modification, the algorithm often showed instability, sometimes after only a few hundred iterations, irrespective of the time step.

Acknowledgments: We thank J. McGeehan for the provision of facilities within the Centre for Communications Research. We also thank J. B. Schneider of Washington State University for many helpful discussions.

14 August 1995
Electronics Letters Online No: 19951221

C.J. Railton and I.J. Craddock (*Centre for Communications Research, Faculty of Engineering, University of Bristol, Bristol, BS8 1TR, United Kingdom*)

References

1 JURGENS, T.G., TAFLOVE, A., UMASHANKAR, K., and MOORE, T.G.: 'Finite-difference time-domain modeling of curved surfaces (EM scattering)', *IEEE Trans.*, 1992, **AP-40**, pp. 357–366
2 JURGENS, T.G., and TAFLOVE, A.: 'Three-dimensional contour FDTD modeling of scattering from single and multiple bodies', *IEEE Trans.*, 1993, **AP-41**, pp. 1703–1708
3 MADSEN, N.K.: 'Divergence preserving discrete surface integral methods for Maxwell's curl equations using non-orthogonal unstructured grids'. Report UCRL-JC-109787, Lawrence Livermore National Laboratory, 1992
4 OKONIEWSKI, M., ANDERSON, J., MROZOWSKI, M., and STUCHLY, S.S.: 'Arbitrarily located metal surfaces in FDTD technique'. Progress in Electromagnetics Research Symp., July 1995, (Seattle, WA, USA), pp. 178
5 RAILTON, C.J., CRADDOCK, I.J., and SCHNEIDER, J.B.: 'Improved locally distorted CPFDTD algorithm with provable stability', *Electron. Lett.*, 1995, **31**, (18), pp. 1585–1586
6 CRADDOCK, I.J., and RAILTON, C.J.: 'A novel FDTD algorithm incorporating correction coefficients for curved boundaries'. Proc. 24th European Microwave Conf., September 1994, (Cannes, France), pp. 1536–1540

Millimetre-wave signal generation by optical filtering of frequency modulated laser spectra

P.A. Davies, A.P. Foord and K.E. Razavi

Indexing terms: Distributed feedback lasers, Optical control of microwaves

Optical mixing on fast photodiodes is a potentially convenient method for generating millimetre-wave signals in fibre radio applications. The authors describe multiplication of the modulation frequency of a DFB laser using a periodic optical filter to enable mixing between FM sidebands, and report experimental generation of a 19.2GHz signal.

Improved Locally Distorted CPFDTD Algorithm with Provable Stability

Chris J. Railton, Ian J. Craddock
Centre for Communications Research, Faculty of Engineering,
University of Bristol, Bristol, BS8 1TR, UK

John B. Schneider
School of Electrical Engineering and Computer Science
Washington State University, Pullman, WA 99164-2752, USA

Abstract

The Contour Path Finite Difference Time Domain (CPFDTD) method has been shown to give accurate results for curved metal structures. However, the numerical stability of this scheme is not guaranteed and significant skill is required in order to generate an appropriate grid. In this contribution, we present a modification to the two-dimensional CPFDTD method which ensures stability and which permits simple generation of the locally distorted grid. The accuracy of the scheme is demonstrated through the calculation of the resonant frequencies of circular cylindrical resonators.

Introduction

The Contour Path Finite Difference Time Domain (CPFDTD) method has been shown to provide an accurate and efficient way to analyse smooth curved metal structures [1],[2]. Unfortunately the use of the "nearest neighbour" approximation or the use of extended contours which are allowed to overlap is likely to produce a system which violates the law of conservation of energy, regardless of the size of the time step. In this contribution we present a modified form of the CPFDTD algorithm which overcomes this problem without sacrificing accuracy. This modification recasts the "nearest neighbour" approximation, employed in standard CPFDTD, such that reciprocal interaction of nodes is obtained. It can be demonstrated that the modified system is equivalent to a passive network consisting only of capacitors and gyrators which must necessarily conserve energy [3]. The modified

The modified scheme has been tested on a variety of resonant structures including S bends, waveguides of complex cross-section and rotated rectangles. In each case the modified scheme has been found reliable and accurate.

The Nature of the Instability

Consider the cross-section of a circular cylindrical resonator, a quarter of which is shown in Figure 1. Here, the grid for the TE problem is shown where the H_z nodes are indicated by circles and are located at the centre of each undistorted cell. The E_x and E_y nodes are marked by crosses or arrows and are found along the edges of cells. The magnetic field is assumed to be constant over the area of a given cell while electric fields are assumed to be constant over the length of the edge corresponding to a given node. Dashed lines indicate edges which are not used in the scheme. The E nodes represented by arrows cannot be calculated directly using the FDTD scheme because one or both of the H_z nodes required in the corresponding update equation is in the metal. Following [1] these nodes borrow their value from the nearest available collinear E field component. The numbers in the centre of each square are the areas of the Faraday contours and the numbers next to the edges are the lengths of straight sections of the associated contour. In each case the values are normalised so that values of 100 correspond to an unmodified cell. Although the grid shown in Figure 1 appears to be the most obvious way of implementing the CPFDTD algorithm, it is not difficult to show that such an implementation leads to numerical instability, even using very small time steps.

The root of the problem, in this case, can be traced to those E nodes whose values are borrowed from neighbouring cells. This causes an influence on an H node from the borrowed E node without any corresponding influence on the E node from the H node. For instance, referring to Figure 1, the update equation for $H_z(1.5,0.5)$ is given by

$$H_z^{n+1}(1.5,0.5) = H_z^n(1.5,0.5) + \frac{\delta t}{\mu\delta}\left(\frac{100}{76}E_y^{n+1/2}(2,0.5) + \frac{80}{76}E_x^{n+1/2}(1.5,0) - \frac{67}{76}E_x^{n+1/2}(2.5,1)\right) \quad (1)$$

where $E_x(2.5,1)$ is the borrowed node, δt is the time step and δ is the space step.

The update equation for $E_x(2.5,1)$ is given by

$$E_x^{n+1/2}(2.5,1) = E_x^{n-1/2}(2.5,1) + \frac{\delta t}{\epsilon\delta}\left(H_z^n(2.5,1.5) - H_z^n(2.5,0.5)\right) \quad (2)$$

It can be seen that no corresponding inclusion of $H_z(1.5,0.5)$ exists. This scheme represents an unphysical situation which, therefore, cannot be guaranteed to behave in an energy conserving manner.

In order to remedy the situation, we must modify this equation to include the missing term as follows:

$$E_x^{n+1/2}(2.5,1) = E_x^{n-1/2}(2.5,1) + \frac{\delta t}{\epsilon \delta}\left(H_z^n(2.5,1.5) - \frac{67}{167}H_z^n(1.5,0.5) - \frac{100}{167}H_z^n(2.5,0.5)\right) \quad (3)$$

Here we have taken a weighted average of the two H_z nodes which have a dependence on $E_x(2.5,1)$ with the weights being in the same ratio as the strengths of the corresponding dependencies. As well as being intuitively more reasonable, the resulting scheme is directly equivalent to a passive circuit consisting entirely of capacitors and gyrators [3]. The system must, therefore, conserve energy.

Numerical Results

In order to demonstrate both the stability and accuracy of the scheme, the resonant frequencies of the TE modes of a circular cylinder have been calculated. (The TM case requires no modification to the standard CPFDTD scheme since, in this case, the scheme can be shown to be physically realisable.) Calculations were carried out for cylinders of radii 15cm - 24cm and, in each case, the space step, δ, was 5cm. Clearly this is a very coarse mesh and is a stringent test for the algorithm. The calculated results for the first three TE modes are shown in Figure 2 where they are compared with analytical results and with standard staircased FDTD. The agreement between the modified CPFDTD results and the analytic results is excellent for the first two modes. Furthermore, the modified CPFDTD results are clearly superior to the staircased results. For the third mode, some discrepancy between the analytic and the modified CPFDTD results are evident. This discrepancy is, however, only observed for frequencies corresponding to a discretisation of less than six cells per wavelength. For finer discretisations the excellent agreement is again obtained. In no case did the use of this algorithm cause numerical instability even though trials were carried out in all cases with 8000 iterations and in some cases 16000 iterations. All tests were performed using a time step which was 90% of the CFL limit for standard FDTD. With the unmodified algorithm most of the cylinders led to unstable systems. In many cases this became apparent after only a few hundred iterations even with time steps of 10% of the CFL limit.

Conclusions

We have described a simple and effective modification to the well known locally distorted CPFDTD. We have shown that, with this modification, the scheme is stable and we have verified this for circular cylindrical resonators of arbitrary radius. In addition, the good accuracy of the modified scheme has been shown. Trials have also been performed using different objects including rectangles whose edges are at an angle to the mesh, and on S bends in parallel plate waveguide. In all cases the algorithm remained stable and accurate. It is anticipated that the added robustness which the modification provides will facilitate more widespread use of the CPFDTD algorithm.

References

1. T.G. Jurgens, A. Taflove, K. Umashankar and T.G. Moore "Finite-Difference Time-Domain Modeling of Curved Surfaces," IEEE Trans. AP-40, April 1992, pp. 357-366.

2. T.G. Jurgens and A. Taflove "Three-Dimensional Contour FDTD Modeling of Scattering from Single and Multiple Bodies," IEEE Trans. AP-41, December 1993, pp. 1703-1708.

3. I. Craddock and C. J. Railton "Derivation and Application of a Passive Equivalent Circuit for the FDTD Algorithm," Submitted to Microwave and Guided Wave Letters May 1995.

Figure Captions

1. The CPFDTD method applied to a cylinder
2. Calculated resonant frequencies for circular cylindrical resonators

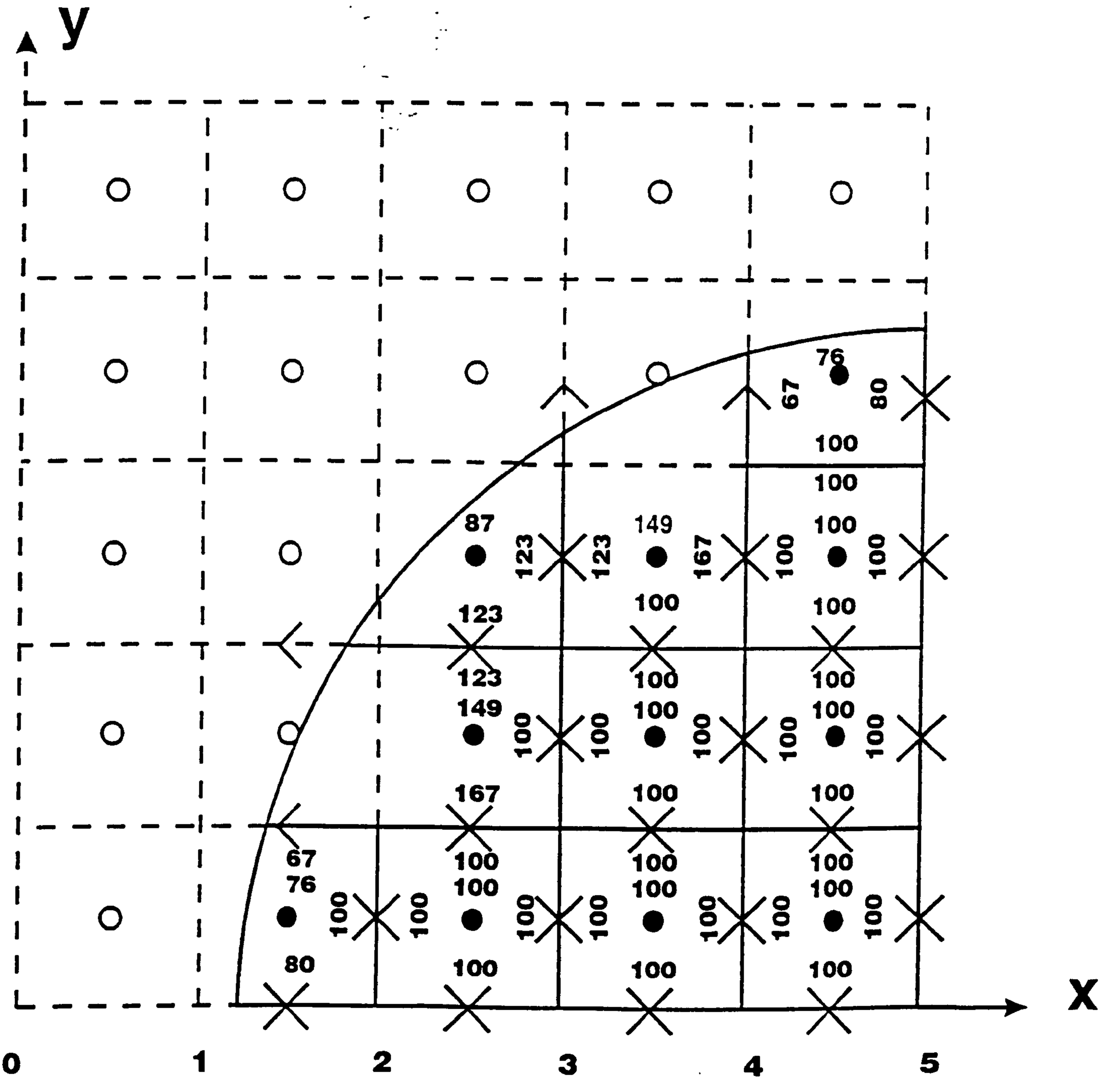
y
x
0
1
2
3
4
5
76
67
80
100
100
87
149
123
123
167
100
100
100
123
100
100
123
100
100
149
100
100
100
100
100
100
100
100
167
100
100
100
100
67
100
100
76
100
100
100
100
100
100
100
100
100
80
100
100
100
100

Fig 1

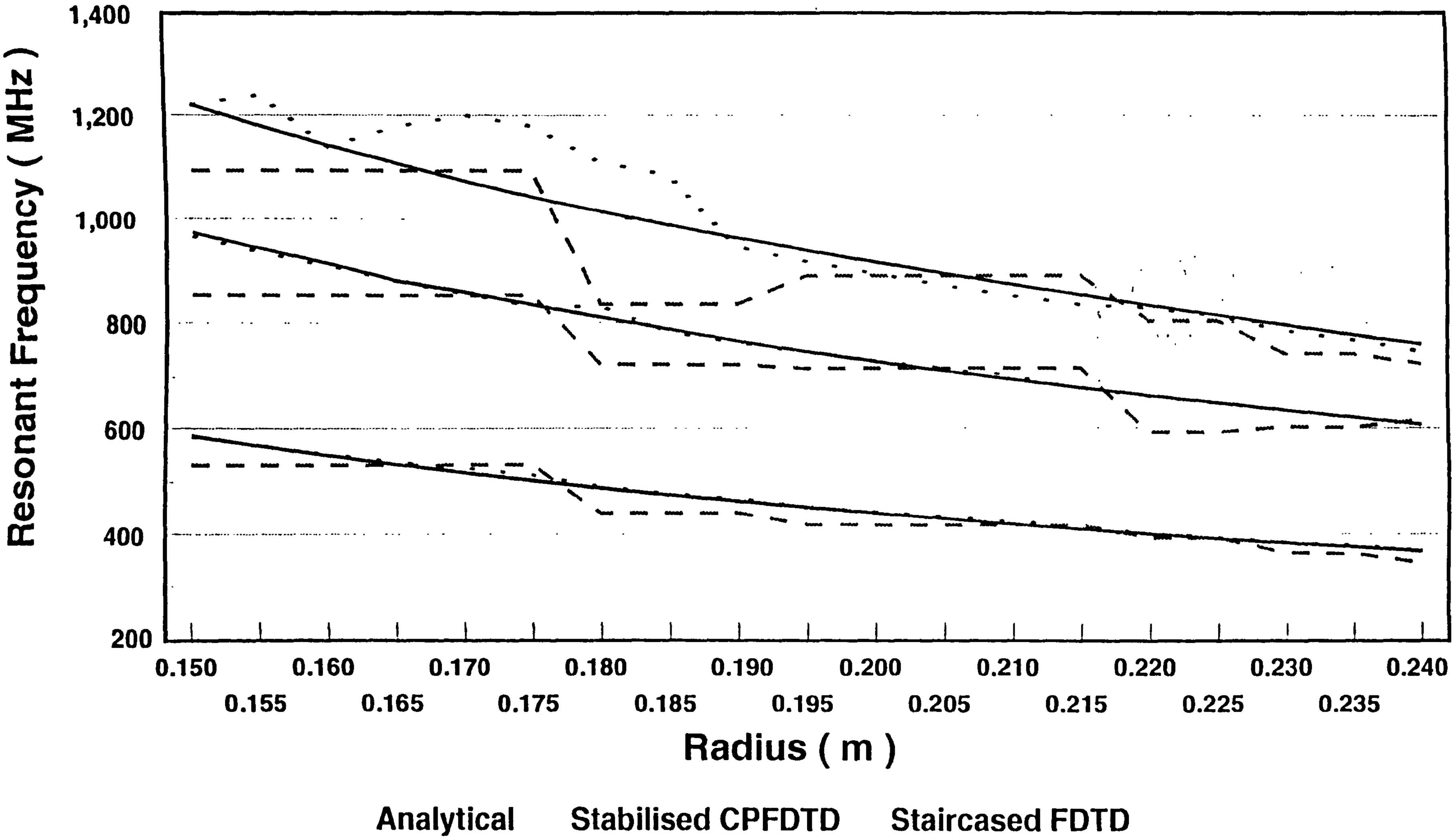
Resonant Frequency (MHz)
1,400
1,200
1,000
800
600
400
200
0.150
0.155
0.160
0.165
0.170
0.175
0.180
0.185
0.190
0.195
0.200
0.205
0.210
0.215
0.220
0.225
0.230
0.235
0.240
Radius (m)
Analytical
Stabilised CPFDTD
Staircased FDTD

A novel Finite-Difference Time-Domain algorithm incorporating correction coefficients for curved boundaries.

I J Craddock and C J Railton

Centre for Communications Research, Faculty of Engineering,
University of Bristol, Bristol. BS8 1TR. England. Tel: 0272 303727 Fax: 0272 255265

Abstract

This contribution describes research undertaken into a new finite-difference implementation of the equations of electromagnetism which is designed to facilitate the inclusion of static field solutions for the treatment of curved conducting surfaces. The new method's derivation is shown, the theory behind the use of the static field solutions in the algorithm is outlined and modelled results for a typical curved structure are compared to those produced analytically.

INTRODUCTION

The Finite-Difference Time-Domain (FDTD) technique is widely accepted as an efficient, reliable and flexible method for the electromagnetic analysis of a wide range of structures. Possibly the most fundamental disadvantage of FDTD is that the method represents the modelled object as a cartesian-based mesh of field components, usually arranged in the configuration first suggested by Yee [1] in 1966 (illustrated by figure 1).

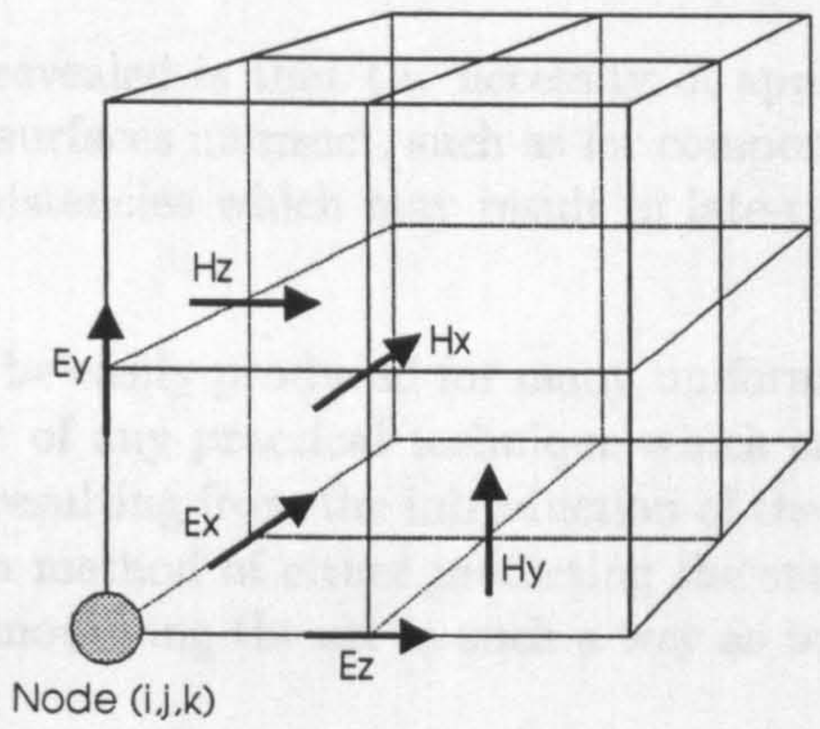

Figure 1: Yee field discretisation

This discretisation prevents the standard FDTD method from accurately characterising the curved structures which arise frequently in engineering applications. Simply increasing the spatial resolution of the algorithm is not generally effective, as shown by Holland in [2] and is also computationally expensive, and while conforming the mesh in the manner proposed by Holland *et al* [3] is an option, this necessitates a considerable increase in computational overheads.

A different approach has been followed at the Centre for Communications Research, University of Bristol, whereby the normal FDTD method is utilised with correction factors introduced into the standard difference equations in the vicinity of the curved surface. These factors are calculated by assuming the variation of field close to a metal object to be dominated by its static functions in the manner proposed by Railton [4]. In order to properly put this contribution into context this approach is briefly described in the following section.

FDTD CORRECTION FACTOR TECHNIQUE

A section of the standard Yee cell, describing the spatial discretisation of the electric and magnetic fields, is shown in figure 2.

If a metallic boundary intersects the surface of integration of a field component as shown, the standard difference equations for the affected component are modified by the inclusion of coefficients (or 'correction factors') which have been calculated from the field's static behaviour.

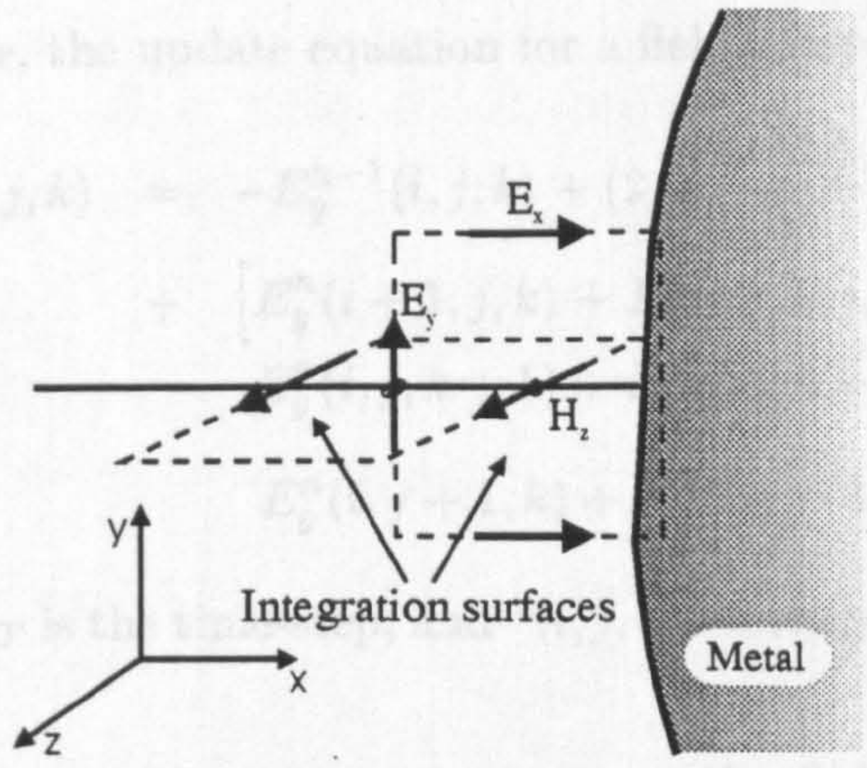

Figure 2: FDTD correction scheme

This method has permitted the accurate analysis of both curved structures, as in [4], and other objects in which the static field solution may be exploited, such as those investigated by Shorthouse and Railton in [5]. In addition to its accuracy, the technique requires no increase in computational effort over the standard model, apart from a short initialisation procedure within which the correction factors are calculated.

One problem which has been revealed is that the necessity of applying correction factors to field components whose integration surfaces intersect, such as for components Hx and Ey in figure 2, can cause apparent physical inconsistencies which may result in late-time numerical instability of the algorithm.

Analytic stability criteria may be easily produced for many uniform finite-difference schemes, however the authors are not aware of any practical technique which can rigorously take into account the effects of non-uniformities resulting from the introduction of the correction factors into an algorithm. There is then no known method of either predicting the stability characteristics of a given set of correction factors, or of modifying the set in such a way as to guarantee stability.

A NEW FDTD ALGORITHM

One solution to this difficulty is to employ a model based on the electric field vector wave equation. The algorithm is formulated entirely in terms of electric field which removes the necessity of correcting the magnetic fields, reducing or hopefully eliminating the aforementioned possibility of instability.

More than one implementation of such a model is possible, depending on the field discretisation employed, and several have been investigated by the authors. The model found most suitable, which also led to the simplest correction factor formulation, was based on a co-located field discretisation (ie one where all the field components are placed at the node (i, j, k) shown in figure 1).

The derivation is as follows:

Eliminating the magnetic field $\mathbf{H}$ from Maxwell's curl equations gives:

$$\nabla \times \nabla \times \mathbf{E} = c^2 \frac{\partial^2}{\partial t^2}\mathbf{E} \qquad \text{or} \qquad \nabla^2\mathbf{E} - \nabla(\nabla \cdot \mathbf{E}) = c^2 \frac{\partial^2}{\partial t^2}\mathbf{E} \tag{1}$$

where $\mathbf{E}$ is the electric field, c is the velocity of propagation and t is time. In *free space* ($\nabla \cdot \mathbf{E} = 0$) this simplifies to :

$$\nabla^2\mathbf{E} = c^2 \frac{\partial^2}{\partial t^2}\mathbf{E} \tag{2}$$

Using an electric field discretisation scheme where all field components are co-located and assuming a regular spatial mesh, the second-order partial derivatives may be replaced by centred difference

approximations. For example, the update equation for a field component E_y may be written:

$$\begin{aligned} E_y^{n+1}(i,j,k) &= -E_y^{n-1}(i,j,k) + (2 - \frac{6c^2\Delta_T^2}{\Delta^2})E_y^n(i,j,k) \\ &+ \Big[E_y^n(i+1,j,k) + E_y^n(i-1,j,k) + \\ &\quad E_y^n(i,j,k+1) + E_y^n(i,j,k-1) + \\ &\quad E_y^n(i,j+1,k) + E_y^n(i,j-1,k)\Big] \frac{c^2\Delta_T^2}{\Delta^2} \end{aligned} \tag{3}$$

where Δ is the space-step, Δ_T is the time-step, and $^n(i,j,k)$ represents a point in space $(i\Delta, j\Delta, k\Delta)$ at time $t = n\Delta_T$.

Update equations for the other electric field components may be derived similarly, yielding a Second-order Finite Difference Time Domain algorithm (or 'SFDTD' for convenience) as opposed to the standard FDTD algorithm which involves only first-order derivatives.

It can be shown that the stability criterion (which relates the maximum time step Δ_T to the minimum space step Δ) is identical to that required for FDTD. The extra amount of memory required by SFDTD to store the past value of each electric field component (E_y^{n-1} in (3)) is balanced by that needed for the storage of the magnetic fields in FDTD. The computational effort associated with SFDTD in terms of the number of numerical operations is slightly lower than that of FDTD.

SFDTD CORRECTION FACTOR TECHNIQUE

A curved metal surface may be accurately approximated on a small scale by an angled planar surface as shown in figure 3. The behaviour of the electric field close to a metal boundary is well known to converge to its static form, as described by Rayleigh in [6], and hence in this case may be characterised by two functions

$$E_n = k_1 \qquad E_t = k_2 n \tag{4}$$

where n and t are co-ordinates normal and tangential, respectively, to the surface.

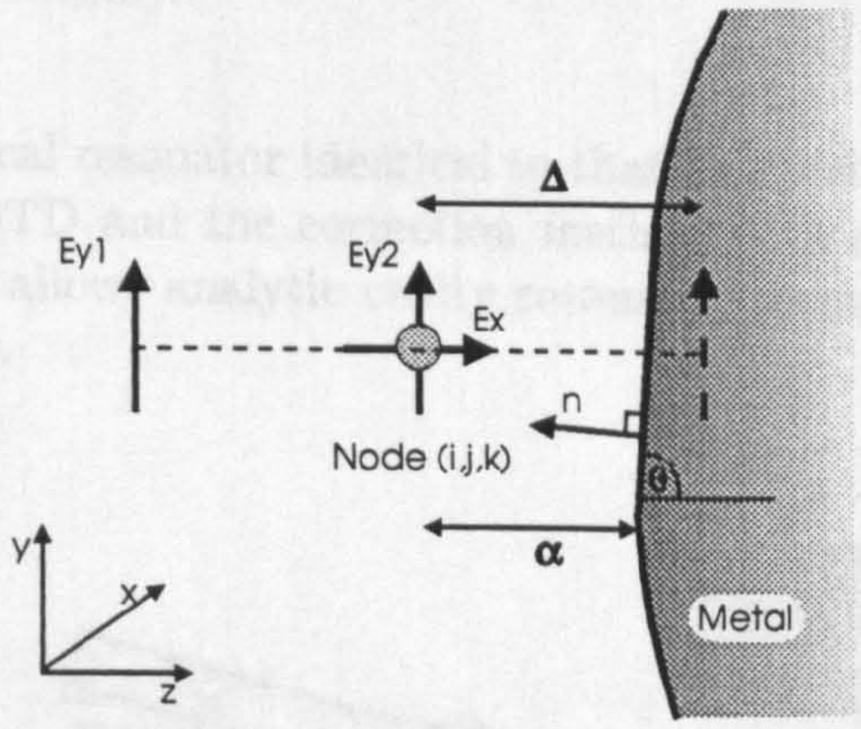

Figure 3: SFDTD correction scheme

Taking as an example the first-order spatial derivative,

$$\frac{\partial}{\partial x}E_y = \left[\frac{\partial E_y}{\partial n}\frac{\partial n}{\partial x} + \frac{\partial E_y}{\partial t}\frac{\partial t}{\partial x}\right] \tag{5}$$

Substituting functions in x and y for n and t, and expressing E_y as a rotation of E_t and E_n we produce an expression within which (4) may be substituted.

This yields the following improved expression for the derivative at the metal boundary :

$$\left.\frac{\partial E_y}{\partial x}\right|_{\text{improved}} = (\sin^2\theta)k_2 \tag{6}$$

However

$$E_t = E_{y2}\sin\theta + E_x\cos\theta = k_2 n_0 \tag{7}$$

where n_0 is the normal distance from the position of E_{y2} and E_x to the metal boundary (see figure 3). Thus

$$\left.\frac{\partial E_y}{\partial x}\right|_{\text{improved}} = -\frac{(\sin^2\theta)(E_{y2}\sin\theta + E_x\cos\theta)}{n_0} \tag{8}$$

the centred-difference second-order derivative is

$$\frac{\partial^2 E_y(i,j,k)}{\partial x^2} = \frac{\frac{\partial E_y(i+1/2,j,k)}{\partial x} - \frac{\partial E_y(i-1/2,j,k)}{\partial x}}{\frac{1}{2}(\Delta+\alpha)} \tag{9}$$

replacing the derivative closest to the boundary with (8), and the other derivative with the standard difference approximation, the required expression for the second-order derivative is

$$\frac{\partial^2 E_y(i,j,k)}{\partial x^2} = \left(\frac{E_{y1}}{\frac{1}{2}\Delta^2(\beta+1)} + \frac{E_x\cos\theta\sin\theta}{\frac{1}{2}\Delta^2\beta(\beta+1)}\right) - \frac{E_{y2}}{\frac{1}{2}\Delta^2(\beta+1)}\left(1+\frac{(\sin\theta)^2}{\beta}\right) \tag{10}$$

where β is defined as α/Δ and E_{y1}, E_{y2} and E_x are field components neighbouring the boundary (see figure 3).

This corrected discrete approximation may be utilised instead of the standard difference form in the SFDTD algorithm. If β is unity and $\theta = 90$ then the original difference form is returned and, unless $\sin\beta$ is 0 or 1, energy will couple between orthogonal field components (as expected). Note that by removing the magnetic fields and co-locating the field components, the resulting correction scheme is considerably more simple than that which was obtained when using FDTD.

The only assumptions which have been made are that the boundary may be approximated over the unit cell by a planar surface (an improvement over its approximation by a staircase) and that the fields will assume their static forms over a distance $\leq \Delta$ from the boundary (which is reasonable if Δ is a small fraction of a wavelength).

AN EXAMPLE PROBLEM

A metal-walled closed cylindrical resonator identical to that analysed by Railton [4], was modelled using the combination of SFDTD and the correction method with a *fixed* uniform mesh size (Δ) of 5cm. The simple geometry allows analytic cavity resonance techniques to predict the resonant frequencies with high accuracy.

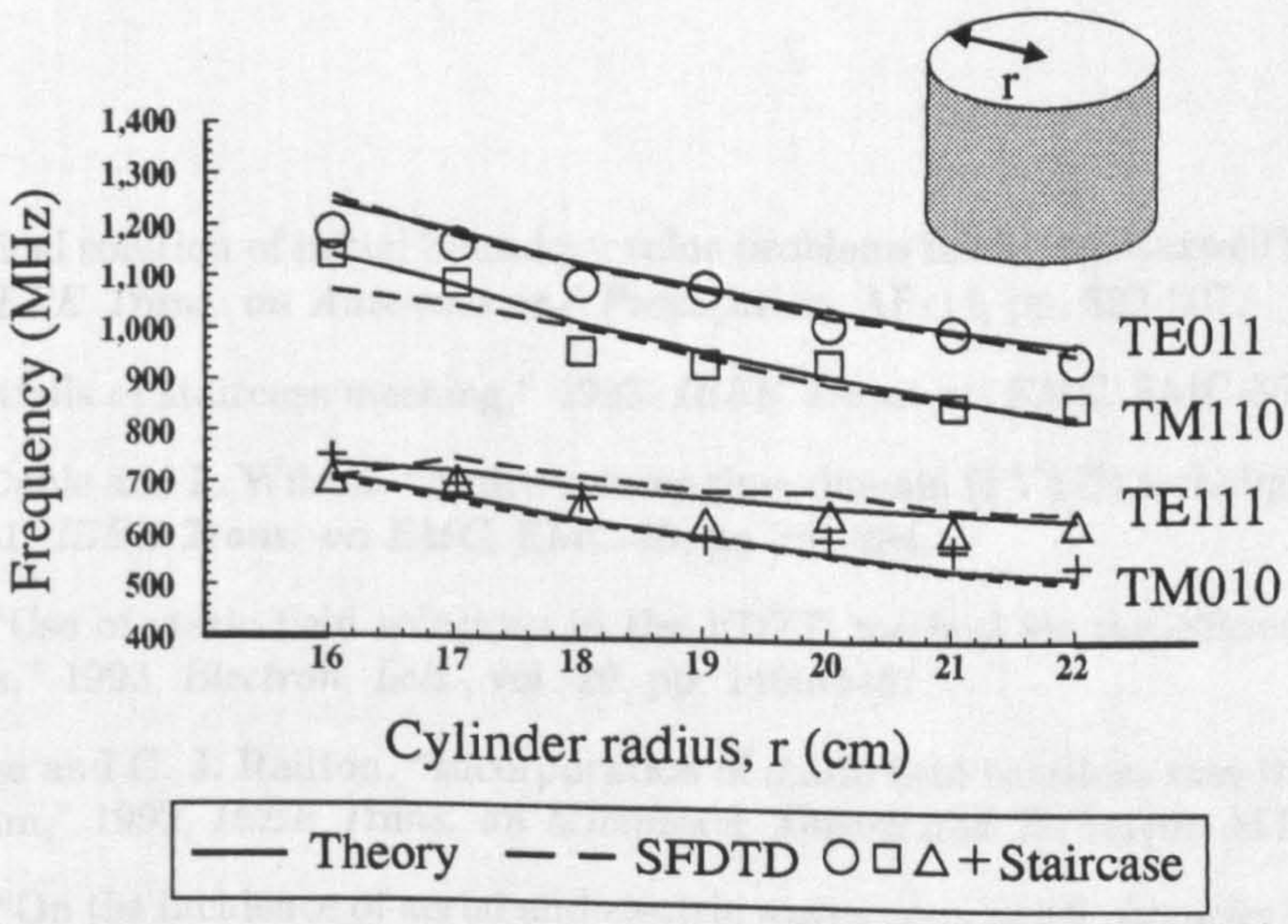

Figure 4: Cylinder resonant frequencies

Figure 4 shows the variation in the cylinder's resonant frequencies as a function of radius. The solid line represents the (perfect) analytic solution and the dashed line the results produced by the new algorithm, SFDTD. The marker points indicate the predictions of the standard, staircased, FDTD method.

Overall, given the coarseness of the mesh with respect to both frequency and surface curvature, the SFDTD results adhere well to the theoretical curves and are, as expected, considerably more accurate than the staircased FDTD technique. The TM010 mode in particular is excellently characterised, virtually independently of cylinder radius. The results for the TM110 mode are good for radii of > 18cm but become less accurate as the radius decreases (this is probably due to both the number of field components available to describe the cylinder decreasing and to the increasing frequency of the mode). The most difficult mode to model is clearly the TE111 mode, the stair-stepped FDTD results for this are notably poor and while the SFDTD algorithm performs more consistently, the results may indicate potential for improvement in the technique.

No evidence of any numerical instability was exhibited by the method even over runs of 20,000 iterations, except in a very small proportion of the test cases where it was found that the curved metal boundary passed very close to a field node; deforming the geometry slightly at these points or reducing the time-step were found to be suitable solutions to this problem. This is a not unexpected finding as the effect of the correction scheme is to effectively introduce an image node whose spacing from its neighbouring nodes should not violate the standard stability criterion.

CONCLUSION

The new algorithm, SFDTD, presented in this report, can be simply modified to include correction factors which enable the rigorous treatment of metallic curved boundaries. The method has been shown to provide a high degree of accuracy when analysing a cylindrical resonator even when employing a coarse mesh, while not exhibiting the numerical instability which may result from the modification of other difference algorithms.

The authors are continuing to investigate this technique and intend to both validate the method by further experiment and to generalise it to dielectric and open structures.

ACKNOWLEDGMENTS

The authors would like to thank Prof. J. P. McGeehan for provision of facilities at the Centre for Communications Research and both SERC and DRA Malvern for financial support. They are also grateful to present and past members of the Microwave and Mathematical Modelling Group for their rôle in developing the FDTD program.

References

[1] K. Yee, "Numerical solution of initial boundary value problems involving Maxwell's equations in isotropic media," 1966, *IEEE Trans. on Antennas and Propagation*, AP-14, pp. 302-307.

[2] R. Holland, "Pitfalls of staircase meshing," 1993, *IEEE Trans. on EMC*, EMC-35, pp. 434-439.

[3] R. Holland, V. Cable and L. Wilson, "Finite-volume time-domain (FVTD) techniques for Electromagnetic scattering," 1991, *IEEE Trans. on EMC*, EMC-23, pp 281-294.

[4] C. J. Railton, "Use of static field solutions in the FDTD method for the efficient treatment of curved metal structures," 1993, *Electron. Lett.*, vol. 29, pp. 1466-1467.

[5] D. B. Shorthouse and C. J. Railton, "Incorporation of static field solutions into the finite difference time domain algorithm," 1992, *IEEE Trans. on Microwave Theory and Technique*, MTT-40, pp. 986-994.

[6] Lord Rayleigh, "On the incidence of aerial and electric waves upon small obstacles in the form of ellipsoids or elliptic cylinders and on the passage of electric waves through a circular aperture in a conducting screen," 1897, *Philosophical Mag.*, vol 44, pp 28-52.

value, normalised to Z_m, and renormalised to Z_{def} (= 50Ω). The error bars represent the estimated measurement uncertainty to a 95% confidence level.

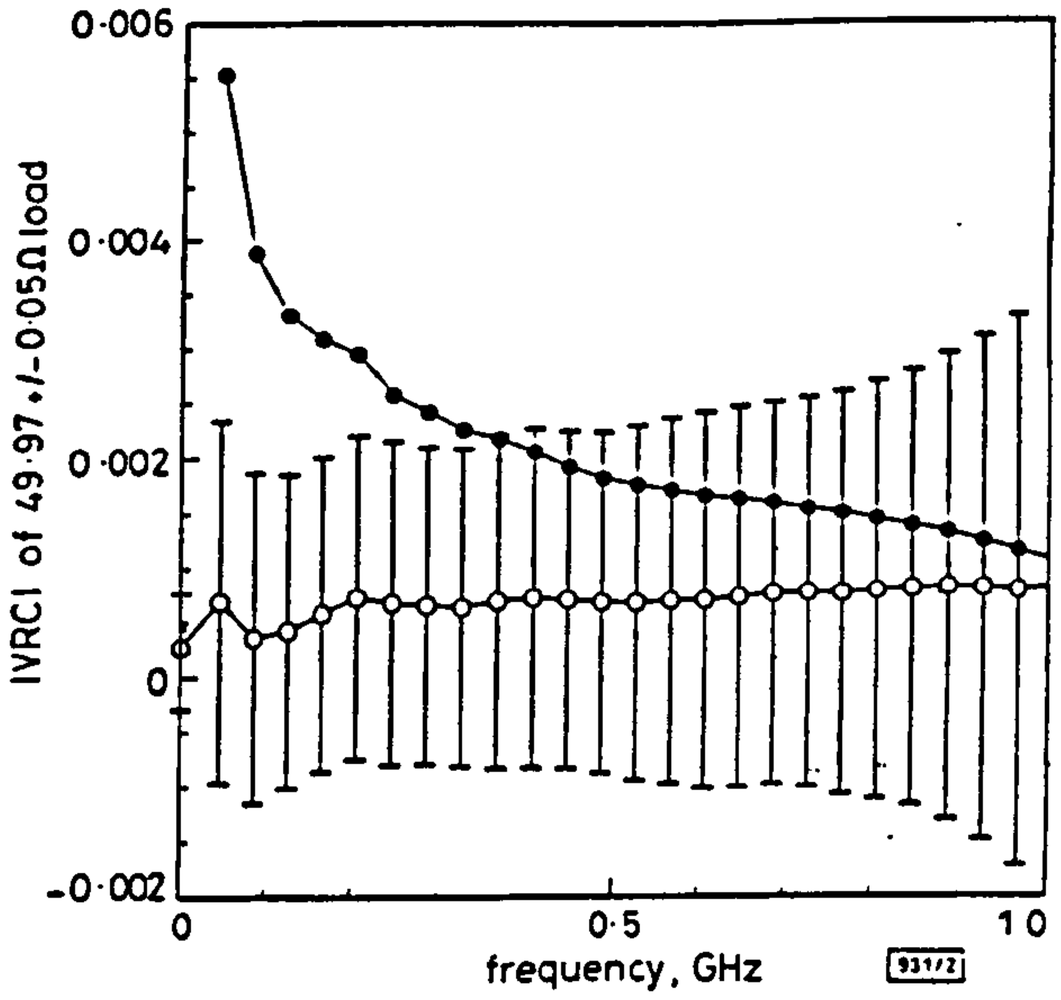

Fig. 2 *|r| for nominal 50Ω load, referenced to Z_m and normalised to 50Ω*

○ referenced to 50Ω
● referenced to Z_m

Comment: For the results of S measured in terms of Z_m to be renormalised to Z_{def}, the conditions at the junction between a lossy and an ideal lossless line must be considered (see [6]). It has been shown by calculation [5] that at a junction between lossy and lossless inner conductors of coaxial line the capacitance per unit length of the lossy line is independent of frequency below 500MHz. It can also be shown [2, 3] that even for ρ an order larger than those shown in Fig. 1. $(G/\omega C)<10^{-6}$. With those approximations, the perturbation to the field that would exist at the junction of a practical standard line with an ideal line is negligible. This condition is sufficient for the renormalisation process to be valid (at least to the extent that the method has given similar results to those shown in Fig. 2 when applied to a number of nominal 50Ω lines of different sizes and lengths).

Conclusion: A method of calibrating a VANA in terms of the nominal 50Ω defined for a lossless standard line at frequencies for which conductor loss is significant has been reported. The results of its use have been shown to be consistent with the DC resistance of a nominal 50Ω termination within the estimated measurement uncertainty.

Acknowledgments: This work is part of the Electrical Science programme at NPL sponsored by the National Measurement Standards Policy Unit of the DTI.

19 July 1994
Electronics Letters Online No: 19941105

E. J. Griffin (*RF and Microwave Guided-Wave Standards Branch, National Physical Laboratory, c/o DRA, St Andrews Road, Malvern, Worcs WR14 3PS, United Kingdom*)

References

1 HODGETTS, T.E., and GRIFFIN, E.J.: 'A unified treatment of the theory of six-port reflectometer calibration using the minimum of standards'. RSRE Report No 83003, Royal Signals and Radar Establishment, August 1983
2 DAYWITT, W.C.: 'First-order symmetric modes for a slightly lossy coaxial transmission line', *IEEE Trans.*, 1990, MTT-38, (11), pp. 1644–1650
3 DAYWITT, W.C.: 'Exact principal mode field for a lossy coaxial line', *IEEE Trans.*, 1991, MTT-39, (8), pp. 1313–1322
4 WOODS, D.: 'Multiport-network analysis by matrix renormalisation employing voltage wave S-parameters with complex normalisation', *Proc. IEE*, 1977, 124, (3), pp. 198–204
5 WILLIAMS, W.E., and CHAKRABARTI, A.: 'Reflection at a discontinuity in a transmission line', *IMA J. Appl. Math.*, 1982, 28, pp. 185–195
6 MARKS, R.B., and WILLIAMS, D.F.: 'A general waveguide circuit theory', *J. Res NIST*, 1992, 97, pp. 533–561

Reducing the computational overhead of the near-field transform through system identification

I.J. Craddock, P.G. Turner and C.J. Railton

Indexing terms: Finite-difference time domain method

The system identification technique is applied to the output of a time-domain near to far-field transform employed with the FDTD algorithm. The technique is used to characterise the far field of a microstrip antenna, the accuracy of the results is evaluated, and the computational savings and overheads involved are discussed.

Introduction: The current and predicted future high level of demand for mobile communications systems has stimulated research in the modelling of microwave antennas. One popular numerical technique is the finite difference time domain (FDTD) method.

The recent development of time-domain field extrapolation techniques [1] (or 'near-far' transforms) has enabled the wideband FDTD analalysis of the radiation processes inherent in antenna and EMC problems [2] by calculating the field level at a number of observation points outside the FDTD domain.

The computational overhead associated with the near-far transform is in general a small proportion of the overall requirement and in many cases may be disregarded. Unfortunately, this overhead rises in proportion to the number of observation points in the far-field and when characterising, for example, an antenna radiation pattern; achieving sufficient angular resolution requires this number to be large.

The resulting increase in run time makes the computation of an antenna's far-field on a modest-sized computer with reasonable angular resolution an almost prohibitively long process. It is shown in this Letter, however, that employing system idenitification to exploit the resonant nature of typical antennas achieves a major reduction in run-time without incurring any loss of accuracy. Neither this drawback of the near-far algorithm, nor the proposed solution have, to the authors' knowledge, been previously examined.

System identification theory: A detailed study of system identification techniques can be found in [3]; the application of one such technique to this particular problem may be briefly summarised as follows:

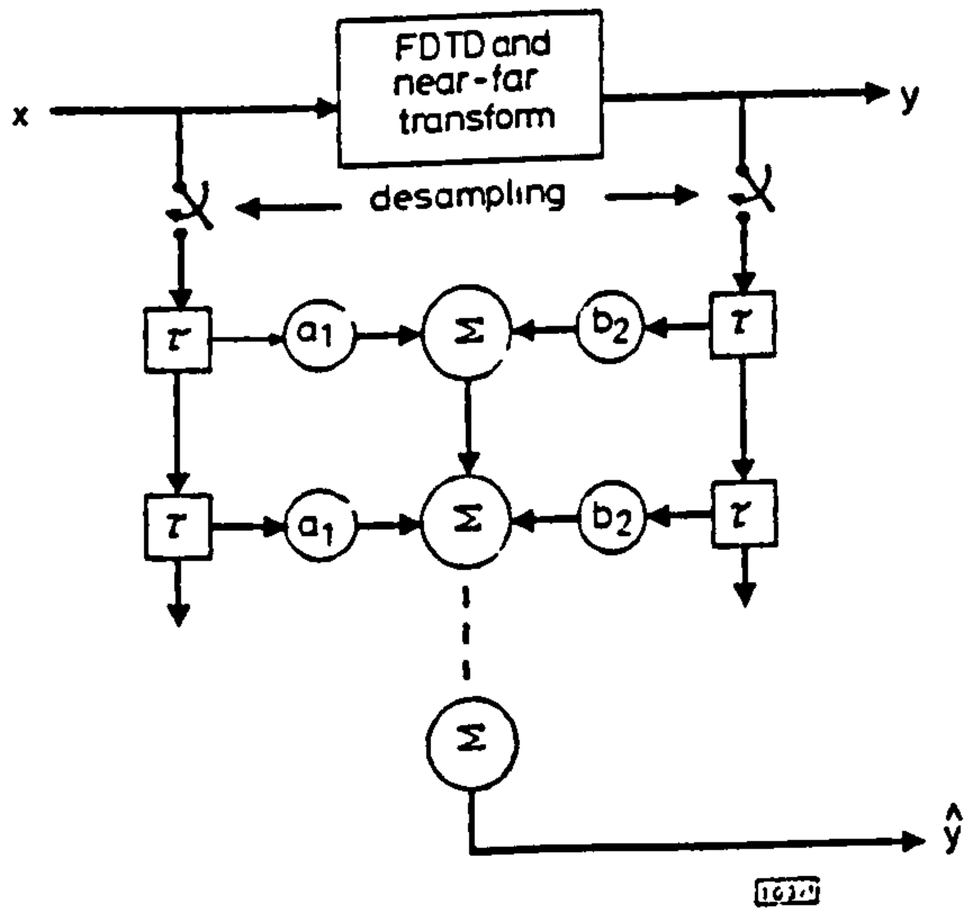

Fig. 1 *Principle of system identification*

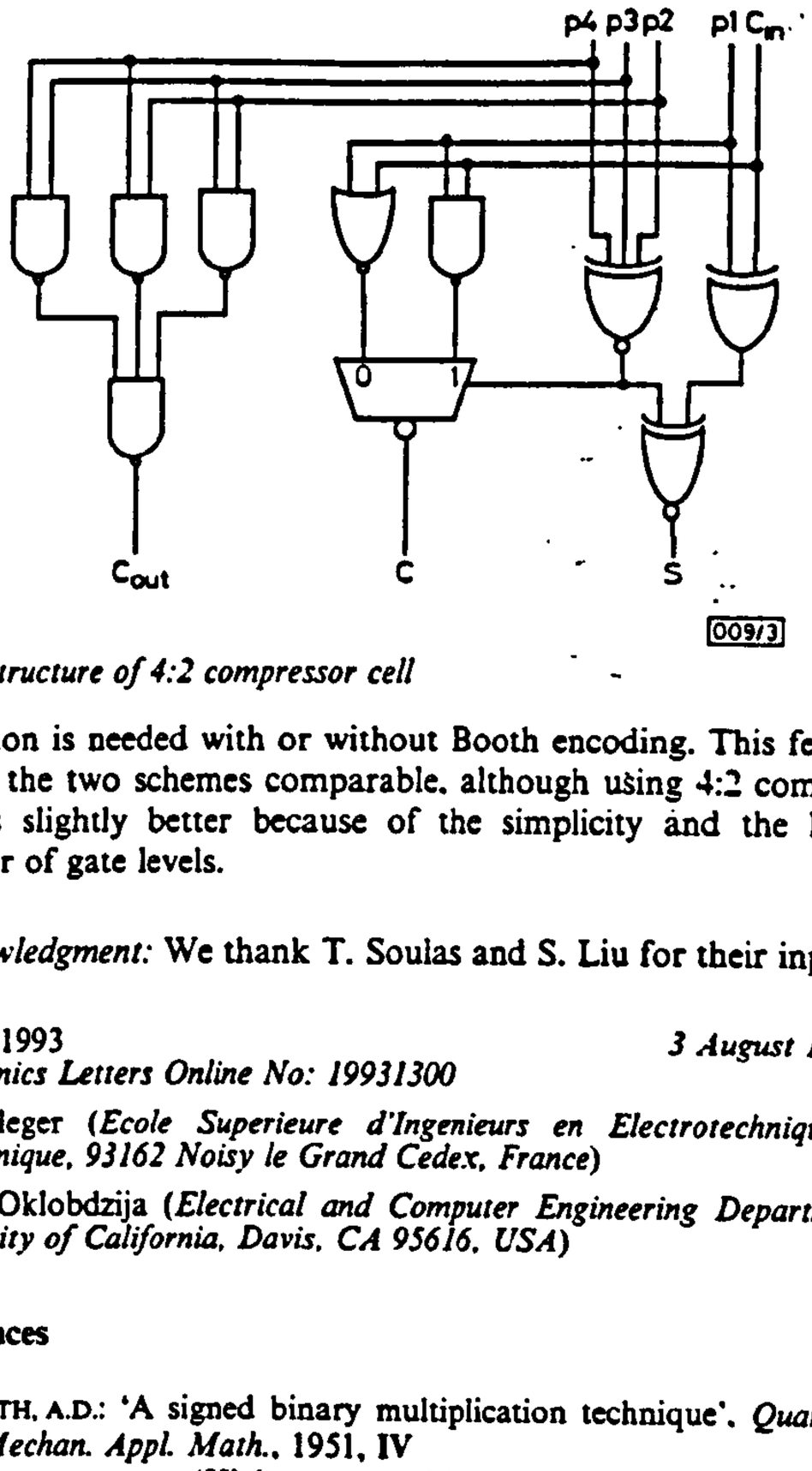

Fig. *Structure of 4:2 compressor cell*

extension is needed with or without Booth encoding. This feature makes the two schemes comparable, although using 4:2 compressors is slightly better because of the simplicity and the lower number of gate levels.

Acknowledgment: We thank T. Soulas and S. Liu for their input.

3 August 1993
Electronics Letters Online No: 19931300

D. Villeger (*Ecole Superieure d'Ingenieurs en Electrotechnique et Electronique, 93162 Noisy le Grand Cedex, France*)

V. G. Oklobdzija (*Electrical and Computer Engineering Department, University of California, Davis, CA 95616, USA*)

References

1 BOOTH, A.D.: 'A signed binary multiplication technique', *Quarterly J. Mechan. Appl. Math.*, 1951, IV
2 MACSORLEY, O.L.: 'High speed arithmetic in binary computers', *Proc. IRE*, 1961, 49, (1)
3 WEINBERGER, A.: '4:2 carry-save adder module', *IBM Tech. Disclosure Bulletin*, 1981, 23
4 MORI *et al.*, J.: 'A 10ns 54 × 54-b parallel structured full array multiplier with 0.5-u CMOS technology', *IEEE J. Solid State Circuits*, 1991, 26, (4)
5 SOULAS, T., VILLEGER, D., and OKLOBDZIJA, V.G.: 'An ASIC multiplier for complex numbers'. Proc. EURO-ASIC-93, 22–25 February 1993, (Paris, France)

Application of the FDTD method and a full time-domain near-field transform to the problem of radiation from a PCB

I.J. Craddock and C.J. Railton

Indexing terms: Finite-difference time domain method, Electromagnetic compatibility

The finite-difference time-domain method is combined with a full time-domain near-field transform to yield accurately and efficiently the radiated field levels measured at a distance of 3m from a printed circuit board.

Introduction: With the introduction of stringent new EC electromagnetic compatibility (EMC) standards the problem of quantifying and then minimising unwanted emissions from equipment assumes a new importance in hardware design. Solutions to this type of problem would be easier and cheaper to achieve if there existed a method of simulating the emissive characteristics of the proposed design. The development of simulation techniques suitable for application to realistic problems is accordingly the subject of much research.

This Letter describes the application of a well known electromagnetic analysis technique (the finite-difference time-domain, or FDTD method), along with new extensions to this technique, to the efficient analysis of a simple but realistic EMC problem for which measured data exist.

Trial problem: The field strength produced by the structure shown in Fig. 1 has been measured between 50 and 600MHz at a distance of 3m in a 10m semi-anechoic chamber (a typical EMC test configuration) [1]. The structure consists of a 2.8mm wide 50Ω track on a large PCB terminated at one end by a 50Ω load and driven at the other by a CMOS IC, powered by a shielded battery. This eliminates the need for power cables which would themselves cause radiation. In [1] the radiated field levels were predicted using the FDTD technique with a large computational domain, the aim of the work described within this Letter is to show that the measured results can be predicted far more efficiently by using a near-field transform in conjunction with a smaller domain.

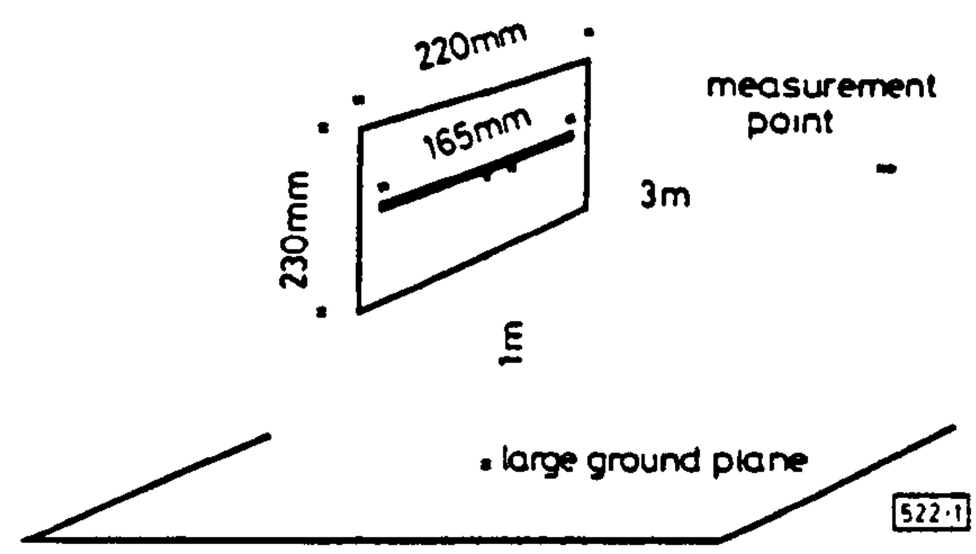

Fig. 1 *Geometry of trial problem*

FDTD method: This numerical technique has been applied with success to the analysis of a range of electromagnetic problems and uses the widely accepted discretisation of the Maxwell curl equations in space and time proposed by Yee in 1966 [2]. The electromagnetic behaviour of the structure of interest is modelled with full rigour (unlike many commercial analysis tools), the method imposes no restrictions on the geometry of the structure and the results are available over a wide frequency band.

The computational effort associated with the FDTD algorithm increases linearly with the electrical size of the structure and the spatial resolution required to describe the structure adequately (i.e. the size of its smallest feature). One method used to reduce the computational requirement is the employment of a non-uniform spatial discretisation of the Maxwell equations, whereby high spatial resolution is used in regions of fine geometrical detail or rapid field variation but in, for example, free space, the resolution may be decreased.

Near-field transformations: Although the FDTD method could be used to model the entire problem space (basically a 1.5 × 3 × 0.5m³ volume) under consideration, this is, for the reasons given above, a computationally expensive option. In this Letter FDTD is used to solve for only the fields on and enclosing the PCB, and a different time-domain technique is used to extend the FDTD results to a point 3m away.

This second technique is commonly known as a near-field transformation and may be briefly described as follows; The equivalence principle is used to replace the fields within a closed surface S, which encloses all the field sources of interest, by equivalent electric and magnetic currents, J and M, on S. Vector potential theory allows the calculation of the fields induced by these currents at any point P, in the volume outside S, from relations such as

$$\mathbf{E}_P(t) = \frac{1}{4\pi}\int_S \left(\frac{\mu}{r}\frac{\partial \mathbf{J}(t-\tau)}{\partial t} - \frac{1}{r^2}\hat{\mathbf{R}}\times\mathbf{M}(t-\tau)\right.$$
$$\left. -\frac{1}{cr}\hat{\mathbf{R}}\times\frac{\partial \mathbf{M}(t-\tau)}{\partial t}\right) dS$$

where $\mathbf{E}_P(t)$ is the electric field at P at time t, r is the distance to the point P, $\hat{\mathbf{R}}$ is the unit vector in the direction of P, τ is the time-delay to the point, c is the speed of light and μ is the permeability of the medium.

The combination of FDTD and a time-domain near-field transform has been described elsewhere, for example [3–5], but the application has been to the determination of the far-field charac-

teristics of regular-shaped metallic scatterers or arrays of Hertzian dipoles, where, because the point P is in the structure's far-field, the second term in the integral ($\alpha\ 1/r^2$) is neglected. The problem considered here cannot be thus simplified because the distance to P is not electrically large, so for this case the full transform is used.

In the case of a PCB modelled in free space, a suitable choice of S would be a closed rectangular box around the PCB (dimensions of 30cm × 6mm × 30cm would be appropriate). In this example, however, the PCB is situated above a large ground plane on which currents will flow whose contributions would not be included in the model, as S does not enclose them. To include the ground plane effect a second closed surface, S', is also considered, centred 1m below the ground plane, supporting the images of M and J, M' and J'.

Results: In [1] Railton *et al.* considered the radiation from the above PCB, and predicted the field values by using FDTD to model the whole problem space out to a distance of 3m from the PCB. Because details as fine as the 1.6mm thickness of the PCB had to be included in the model, even with the benefits of a non-uniform spatial discretisation the problem took 24h to solve on an HP9000 series 730 workstation. Using an FDTD model (with a finer discretisation on the PCB than that used by Railton) in conjunction with the near-field transform, the size of the problem domain is reduced from 230000 to 38000 of Yee's FDTD unit cells and the results shown by Fig. 2 were produced in just 3 h on the aforementioned workstation.

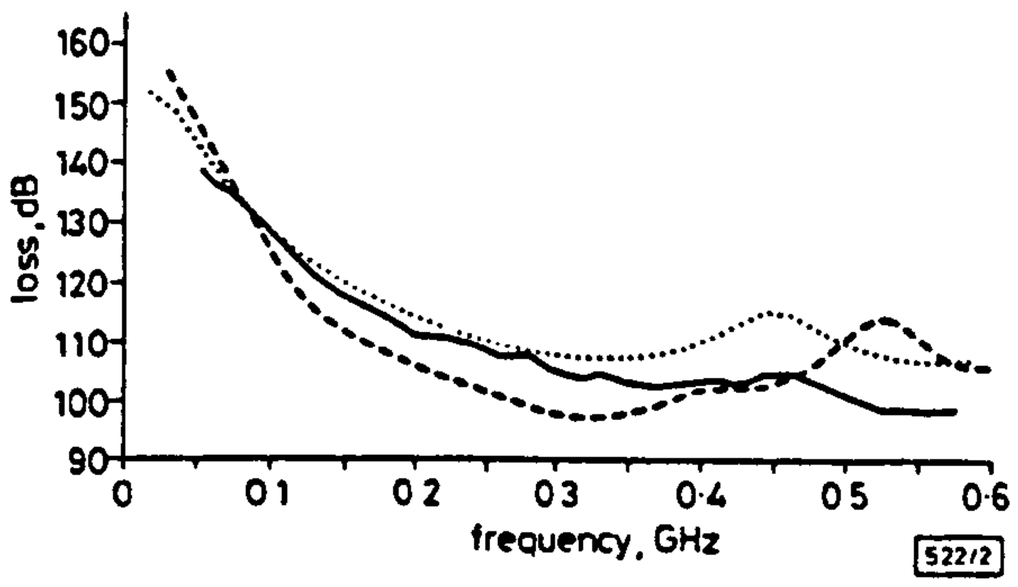

Fig. 2 *Comparison of measured and calculated data for the radiated field from a PCB*

——— measured
– – – – full FDTD
. . . . . FDTD and near-field transform

Fig. 2 shows the ratio between the field levels on the PCB and those 3m from it following an FFT of the model's time-domain data, compared with the values found by measurement and those found using the full FDTD method of [1]. Examination of Fig. 2 shows that the new results are extremely close to the measured values for much of the frequency range, and follow the form of the measured data more faithfully than those of [1], due to the finer discretisation of the PCB. Appreciable error does occur in both models around 400MHz as it was found that the results in this region (where the track length is approximately a half wavelength) were highly sensitive to the representation of the source impedance; this, being due to an active device, was not included in the FDTD model.

Conclusions: We have shown that for the problem of predicting the radiation levels from a simple PCB the combination of the FDTD method and a near-field transform provides accurate results over a wide band in a small fraction of the time required for a full FDTD analysis.

PCB layouts far more complex than the example given here could be analysed by FDTD without much penalty in terms of computer time, particularly if *a priori* knowledge of field behaviour at metal edges were included in the FDTD model [6]. The reduction in computational effort resulting from use of the FDTD method with the near-field transform makes it reasonable to expect that the accurate prediction of radiation from realistically complex PCB layouts is now a practical proposition.

Acknowledgments: The authors would like to thank J. P. McGeehan for provision of facilities at the Centre for Communications Research, and both SERC and DRA Malvern for financial support. They are also grateful to the members of the Microwave and Mathematical Modelling Group for their work in developing the FDTD program and in particular to E. Daniel for her work on near-field transformations.

20 September 1993
Electronics Letters Online No: 19931344

I. J. Craddock and C. J. Railton (*Centre for Communications Research, Faculty of Engineering, University of Bristol, BS8 1TR, United Kingdom*)

References

1 RAILTON, C.J., RICHARDSON, K.M., MCGEEHAN, J.P., and ELDER, K.F.: 'Modelling electromagnetic radiation from digital electronic systems by means of the finite-difference time-domain method'. IEEE Int. Symp. Dig. on EMC, 1991, (Anaheim, CA),pp. 38-44
2 YEE, K.S.: 'Numerical solution of initial boundary value problems involving Maxwell's equations in isotropic media', *IEEE Trans.*, 1966, AN-14, pp. 302–307
3 YEE, K.S., INGHAM, D., and SCHLAGER, K.: 'Time-domain extrapolation to the far-field based on FDTD calculations', *IEEE Trans*, 1991, AP-39, pp. 411–413
4 LUEBBERS, R.J., KUNZ, K.S., SCHNEIDER, M., and HUNSBERGER, F.: 'A finite-difference time-domain near zone to far zone transformation', *IEEE Trans.*, 1991, AN-39, pp. 429–433
5 BART, M.J., MCLEOD, R.R., and ZIOLKOWSKI, R.W.: 'A near and far-field projection algorithm for finite-difference time-domain codes', *J. Electromagnetic Waves and Applications*, 1992, 6, (1), pp. 5–18
6 SHORTHOUSE, D.B., and RAILTON, C.J.: 'Incorporation of static singularities into the finite-difference time-domain technique with application to microstrip'. Proc. 20th European Microwave Conf., 1990, (Budapest), pp. 531–536

Higher order formulation of absorbing boundary conditions for finite-difference time-domain method

P.Y. Wang, S. Kozaki, M. Ohki and T. Yabe

Indexing terms: Finite-difference time-domain method, Electromagnetic waves

A simple formulation of absorbing boundary conditions with higher order approximation is proposed for the finite-difference time-domain (FD-TD) method. Although this formulation is based on the third order approximation of the one-way wave equations, the authors have succeeded in reducing it to an equation in a form quite similar to the second order approximation.

Introduction: The FD-TD method for the solution of the Maxwell equations was first proposed by Yee [1]. It has been applied to various electromagnetic problems. Clearly, we can only simulate these problems in a limited computational domain. For unbounded problems, the absorbing boundary conditions (ABCs) must be applied to simulate the extension of the computational domain to infinity. In recent years, there have been many papers discussing the ABCs with several efficacious methods proposed. The formulation presented by Mur is the most popular method [2]; it uses a second order approximation of the one-way wave equations proposed by Engquist and Majda [3]. With increases in the number of applications of the FD-TD method, means of reducing the reflection error of the ABCs have recently received much attention [4–6]. Here, we introduce a formulation in which we use a third order approximation of one-way wave equations without third derivatives; it therefore possesses smaller reflection errors and has simpler expressions.

Principle and formulation: We consider the 2-D solution domain as shown in Fig. 1. The H_x, H_y, and E_z nodes are positioned in the